

Preliminary ILAW Formulation Algorithm Description, 24590 LAW RPT-RT-04-0003, Rev. 1

Prepared for the U.S. Department of Energy
Assistant Secretary for Environmental Management

The logo for the Office of River Protection features the text "Office of River Protection" in a bold, sans-serif font. The text is set against a background of a stylized, wavy river or water surface, rendered in shades of gray and white.

**P.O. Box 450
Richland, Washington 99352**

Preliminary ILAW Formulation Algorithm Description, 24590 LAW RPT-RT-04-0003, Rev. 1

D. S. Kim
Pacific Northwest National Laboratory
J. D. Vienna
Pacific Northwest National Laboratory

A. A. Kruger
Department of Energy - Office of River Protection

Date Published
November 2012

Prepared for the U.S. Department of Energy
Assistant Secretary for Environmental Management

Office of River Protection

P.O. Box 450
Richland, Washington 99352

APPROVED

By Julia Raymer at 11:14 am, Dec 03, 2013

Release Approval

Date

**Approved for Public Release;
Further Dissemination Unlimited**

TRADEMARK DISCLAIMER

Reference herein to any specific commercial product, process, or service by tradename, trademark, manufacturer, or otherwise, does not necessarily constitute or imply its endorsement, recommendation, or favoring by the United States Government or any agency thereof or its contractors or subcontractors.

This report has been reproduced from the best available copy.

Printed in the United States of America



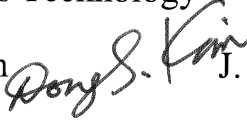
Preliminary ILAW Formulation Algorithm Description

Document title:

Document number: 24590-LAW-RPT-RT-04-0003, Rev 1

Contract number: DE-AC27-01RV14136

Department: Process Technology

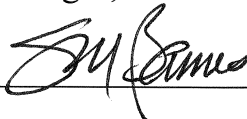

Author(s): D. Kim  J. D. Vienna

Checked by: J. L. Nelson 

Issue status: Approved

Approved by: S. M. Barnes

Approver's position: Manager, Process Technology

Approver's signature:  Signature  Date

History Sheet

Rev	Reason for revision	Revised by
0	Initial Issue	JD Vienna
1	Major rewrite to incorporate all the changes since Rev 0 including new glass property models, additional glass formulation rules, updated constraints, new method of uncertainty calculation, revised process conditions, and revised glass formulation steps with example calculations based on updated waste compositions. The report was also reorganized to make it consistent with the IHLW formulation algorithm report.	D Kim

Contents

History Sheet ii

Executive Summary vii

Abbreviations and Acronyms viii

Key Definitions ix

1 Introduction1

2 Symbols and Notation5

3 Description of Process Steps23

4 Description of Property Predictions, Uncertainties, and Constraints25

 4.1 Property Predictions25

 4.2 Uncertainties for Predicted Properties33

 4.3 Constraints41

5 Calculation Steps45

 5.1 Step 1 – Glass Formulation and Calculation of LAW Transfer Volume45

 5.2 Step 2 – Calculation of GFC Masses and Dilution Water Volume 79

 5.3 Step 3 – Calculation of Final Glass Composition and Properties with Uncertainties 82

 5.4 Step 4 – Comparison of Final Composition and Properties with Constraints 93

 5.5 Step 5 – Completion of Production Records 93

6 Calculation Examples108

 6.1 Example Step 1 – Glass Formulation and Calculation of LAW Transfer Volume 108

 6.2 Example Step 2 – Calculation of GFC Masses and Dilution Water Volume 134

 6.3 Example Step 3 – Calculation of Final Glass Composition and Properties with
 Uncertainties 136

 6.4 Example Step 4 – Comparison of Final Composition and Properties with Constraints 140

 6.5 Example Step 5 – Completion of Production Records 140

7 Summary and Recommendations147

8 References148

 8.1 Project Documents 148

 8.2 Codes and Standards 149

 8.3 Other Documents 149

Appendices

Appendix A –Inputs Used in Calculations..... A-1
Appendix B –Results of Example CalculationsB-1
Appendix C –Summary of Data Requirements..... C-1
Appendix D –Uncertainties for Waste Transfer Volume Measurements..... D-1
Appendix E –Uncertainties for GFC Mass Measurements.....E-1
Appendix F –GFC and Sucrose Volume Contributions.....F-1
Appendix G –PERT Distribution G-1

Tables

Table 1. LAW Process Vessel Sizes (L)..... 2
Table 2. Summary of LAW Glass and Melt Constraints Used in ILAW Algorithm^(a) 3
Table 3. Summary of Notations used in this Report 5
Table 4. List of Symbols 8
Table 5. PCT Release-Composition Model Coefficients and Selected Statistical Parameters 27
Table 6. VHT Alteration Depth-Composition Model Coefficients and Selected Statistical Parameters..... 29
Table 7. Viscosity-Composition Model Coefficients and Selected Statistical Parameters..... 31
Table 8. Electrical Conductivity-Composition Model Coefficients and Selected Statistical Parameters..... 33
Table 9. Summary of Uncertain Input Values that Are Generated for Mass Balance Equations 38
Table 10. LAW Glass and Melt Constraints Used in ILAW Algorithm^(a) 41
Table 11. Model Validity Range for $\tilde{g}_{ij}^{oxide\ in\ MFPV}$ (Single Component Constraints in Mass Fraction) 43
Table 12. Model Validity Constraints for Glass and Melt Properties..... 44
Table 13. Model Validity Multiple Component Constraints (in Mass Fraction) 44
Table 14. CRV-MFPV Line and Sampling Line Flush Nominal Volumes (L)..... 62
Table 15. Long Lived Radionuclides Class C Limits 71
Table 16. Short Lived Radionuclides Class C Limits 72
Table 17. Summary of Production Records Related Waste Form Specifications (24590-WTP-PL-RT-03-001) 94
Table 18. Preliminary Target Mass ($\ddot{M}_{k,A101}^{GFC\ in\ MFPV,pre}$) and Target Mass ($\ddot{M}_{k,A101}^{GFC\ in\ MFPV,target}$) of Each GFC per g Glass for the A101th MFPV Batch 116

Table 19. Masses of GFCs and Sucrose from Step 1 Calculation for the A101th MFPV Batch 121

Table 20. Example Calculation for Predicted PCT Normalized B Release, $P_{A101}^{pctB, Step1}$ in ln[g/L]..... 122

Table 21. Predicted Properties, Uncertainties, and UCCI/LCCI Values for the A101th MFPV Batch Compared with the Corresponding Limits 125

Table 22. Model Validity Constraints for the A101th MFPV Batch Compared with the Corresponding Limits..... 125

Table 23. Calculation of Sum of Fractions for Long Lived Radionuclides Class C Limits in the A101th MFPV batch 127

Table 24. Calculation of SD for Sum of Fractions for Long Lived Radionuclides Class C Limits in the A101th MFPV batch..... 127

Table 25. Calculation of Sum of Fractions for Short Lived Radionuclides Class C Limits in the A101th MFPV batch 128

Table 26. Calculation of SD for Sum of Fractions for Short Lived Radionuclides Class C Limits in the A101th MFPV batch..... 128

Table 27. Preliminary Target and Target Masses of Each GFC per g Glass for the A101th MFPV Batch after Target Glass Composition Adjustment 130

Table 28. Masses of GFCs and Sucrose from Step 1 Calculation for the A101th MFPV Batch after Target Composition Adjustment..... 131

Table 29. Predicted Properties, Uncertainties, and UCCI/LCCI Values for the A101th MFPV Batch Compared with the Corresponding Limits (After Formulation Adjustment)..... 132

Table 30. Additional Constraints for the A101th MFPV Batch after Composition Adjustment Compared with the Corresponding Limits 133

Table 31. Masses of GFCs and Sucrose from Step 2 Calculation for the A101th MFPV Batch 134

Table 32. Assumed Values for the Measured Masses of GFCs and Sucrose in Step 3 Calculation and Calculated GFC/Sucrose Masses per g Glass for the A101th MFPV Batch..... 136

Table 33. Predicted Properties, Uncertainties, and UCCI/LCCI Values for Final Composition from Step 3 Calculation of the A101th MFPV Batch Compared with the Corresponding Limits..... 138

Table 34. Additional Constraints for the Step 3 composition of the A101th MFPV Batch Compared with the Corresponding Limits..... 139

Table 35. Calculation of Waste Na₂O loading for the A501th and B501th Canisters 141

Table 36. Chemical Composition of Glass in the A501th and B501th Canisters 142

Table 37. Specific Activities of Radionuclides in the A501th and B501th Canisters 144

Table 38. Results of Calculating the Quantities for Radionuclide Concentration Limitations in the A501th and B501th Canisters 145

Table 39. Summary of PCT and VHT Results for the ILAW in the A501th and B501th Canisters 146

Figures

Figure 1. Schematic of the LAW Vitrification Process..... 1

Figure 2. Preliminary ILAW Product Qualification Process Flow Diagram 23

Figure 3. Block Diagram Showing the Sources of Uncertainties Applied To Glass Formulation..... 34

Figure 4. Process Flow Diagram for Algorithm Steps 1 through 5 45

Figure 5. Process Flow Diagram for Algorithm Step 1 Calculations 46

Figure 6. Schematic of Na₂O-SO₃-K₂O Rules for $g_{Na_2O,j}^{oxide\ in\ MFPV,\ pre-1}$ 55

Figure 7. Schematic of Cl-F-SO₃ Rules for $g_{Na_2O,j}^{oxide\ in\ MFPV,\ pre-2}$ [H (wt%) = Cl (wt%) + 0.3*F (wt%)] 56

Figure 8. Schematic of Cr₂O₃-K₂O-P₂O₅ Rules for $g_{Na_2O,j}^{oxide\ in\ MFPV,\ pre-3}$ 56

Figure 9. Relationship between Sodium Molarity and Waste Loading for Successful Melter Feed 65

Figure 10. Schematic of Glass Composition Averaging over MFPV Batches and ILAW Containers..... 95

Figure 11. Schematics of Glass Formulation Rules Showing the Initial Glass Composition for the A101th MFPV Batch [H (wt%) = Cl (wt%) + 0.3*F (wt%)] 114

Figure 12. Example Histogram of 5000 Random $V_{A11,1}^{transwaste\ CRV}$ Values (L) for Monte Carlo Simulation..... 124

Figure 13. Histogram of 5000 Predicted $P_{A101}^{pctB,\ Step1}$ Values (ln[g/L]) from Monte Carlo Simulation..... 124

Executive Summary

This report documents the initial algorithm for use by Hanford Tank Waste Treatment and Immobilization Plant (WTP) in batching low-activity waste (LAW) and glass-forming chemicals (GFCs) in the LAW melter feed preparation vessel (MFPV). Algorithm inputs include the chemical analyses of the pretreated LAW in the concentrate receipt vessel (CRV), the volume of the MFPV heel, and the compositions of individual GFCs. In addition to these inputs, uncertainties in the LAW composition and processing parameters are included in this algorithm.

Using the above inputs, the algorithm calculates the following outputs: 1) the volume of LAW to be transferred from the CRV to the MFPV, 2) the volume of any required dilution water, 3) the mass of each GFC for addition to the MFPV batch, 4) the composition of the glass that will be produced, and 5) the predicted properties, with associated uncertainties, of the resulting immobilized low-activity waste (ILAW) on a batch and lot scale.

The GFC additions are determined using a glass-formulation correlation (Muller et al. 2004) that produces an interpolation using glasses that were successfully demonstrated at pilot scale. Developing the ILAW correlation entailed fitting functions to glasses that met all property constraints and were demonstrated in the Duratek LAW pilot melter (DM3300). Many glass oxide components have constant concentrations in the ILAW glass; i.e., (Al_2O_3 [6.1 wt%], B_2O_3 [10], Fe_2O_3 [5.5], TiO_2 [1.4], ZnO [3.5], and ZrO_2 [3]). The concentrations of other components (CaO , Li_2O , and MgO) were determined from fitted curves as functions of alkali content of the glass. These glass formulation rules were supplemented by two set of additional rules (*Halide, Chromate, and Phosphate Impacts on LAW Glass Salt Limits*, CCN 150795), with one set based on the mass fractions of Cl, F, and SO_3 and the other based on the mass fractions of Cr_2O_3 , K_2O , and P_2O_5 in the CRV waste transferred to MFPV.

The algorithm also incorporates process measurement and property prediction uncertainties. Estimates of the various process and measurement uncertainties that affect glass compositions and predicted glass properties have been previously estimated (Piepel et al. 2005) and the impact of these estimated uncertainties on the product quality and processing-related properties were evaluated.

The details of work performed to date to develop this preliminary GFC addition and batching algorithm are summarized along with a statement of the required work to achieve a final operational control algorithm. This document will be updated as needed, as new data are available or changes to approaches/constraints are made.

Abbreviations and Acronyms

BNI	Bechtel National, Inc.
BOF	balance of facilities
CCN	correspondence control number
CFR	code of federal regulations
CI	confidence interval
CRV	concentrate receipt vessel
DM3300	LAW pilot-scale melter (designed, built, and operated by Duratek in Columbia, MD)
DOE	U.S. Department of Energy
EC	electrical conductivity
EPA	Environmental Protection Agency
FSO	full scale output
G2	WTP dynamic flowsheet model
GFC	glass forming chemical
GFSF	glass former storage facility
HLW	high-level waste
ILAW	immobilized low-activity waste
ISARD	integrated sampling and analysis requirements document
LAW	low-activity waste
LCCI	lower combined confidence interval
LL	lower limit
MDL	method detection limit
SQL	minimum quantification limit
MFPV	melter feed preparation vessel
MFV	melter feed vessel
ORP	Office of River Protection
PCT	product consistency test
PQR	product qualification report
PT	pretreatment facility
QAM	quality assurance manual
QAP	quality assurance program
RMSE	root mean squared error
RPD	relative percent difference
RSD	relative standard deviation
SD	standard deviation
SPC	statistical process control
SUCI	simultaneous upper confidence interval
T	temperature
TCP	treated LAW concentrate storage process system
TRU	transuranic
UCCI	upper combined confidence interval
UL	upper limit
VHT	vapor hydration test
VSL	Vitreous State Laboratory at the Catholic University of America
WAC	Washington Administrative Code
WQR	waste form qualification report
WTP	Hanford Tank Waste Treatment and Immobilization Plant

Key Definitions

Algorithm – a term “algorithm” used in this report signifies the process control methodology to formulate processable and compliant glass composition and generate data for production records.

CL% – a confidence level percent. This term is used in combination with other terms such as “CL% confidence interval (CL% CI)”, which is an interval that includes the true mean value of a quantity with CL% confidence.

ec – electrical conductivity. The “ec” notation is used as a superscript for various symbols to specify that the symbols are for electrical conductivity, e.g., U_{pred}^{ec} is the prediction uncertainty for electrical conductivity.

GFC – glass forming chemical(s), solid materials added to the LAW to form a suitable glass when melted and solidified in an ILAW container. Current GFCs include mined minerals (kyanite, wollastonite, olivine, silica, zincite, and zircon) and processed chemicals (boric acid, hematite, sodium carbonate, lithium carbonate, rutile, and sucrose).

GFC components – 11 glass components that are supplied from GFCs by design, Al_2O_3 , B_2O_3 , CaO , Fe_2O_3 , Li_2O , MgO , Na_2O , SiO_2 , TiO_2 , ZnO , and ZrO_2 . Every GFC component has one corresponding source GFC although some GFCs may contain additional GFC component(s) as major constituents (e.g., kyanite is a source for Al_2O_3 with roughly 57wt% Al_2O_3 but also contains 41 wt% SiO_2 supplying a portion of SiO_2 , which is primarily supplied by silica sand). **Non-GFC components** include all glass oxide components other than 11 GFC components and are originated from the waste (not intentionally added) although some components are supplied as impurities from GFCs (e.g., Cr_2O_3 , K_2O).

Glass oxides – a method or convention for reporting the composition of a glass, also called “oxides” in short. The notation used in this report to identify glass composition is to assume single element oxides that are represented in their most prevalent oxidation state (e.g., Fe_2O_3 , Na_2O , SO_3). Halogens are represented as single, neutrally charged, elements (e.g., Cl, F). This notation is used not to imply structure or local bonding of elements within the glass/melt, but rather, to give a simple, standardized method to identify glass or melter feed composition.

ILAW formulation algorithm – a set of steps to develop a successful LAW MFPV batch composition. A successful MFPV batch composition is one that is processable and results in an acceptable glass when vitrified. The algorithm also produces the data necessary for the glass composition related production records.

MFPV batch – a batch of material, consisting of the waste transferred from the CRV and the glass forming chemicals added, in either of the two melter feed preparation vessels. The Melter Feed Preparation Vessel (MFPV) batch becomes the smallest identifiable batch of melter feed. The MFPV does not completely drain and leaves behind some of the previous MFPV batch, which is called the heel.

Monte Carlo – Monte Carlo methods are a class of computational methods that rely on repeated random sampling to compute their results. Monte Carlo method is often used when simulating physical and mathematical systems; it is used here to estimate the distribution of possible solutions.

pct – product consistency test (PCT). The “pct” notation is used as a superscript for various symbols to specify that the symbols are for PCT releases, e.g., U_{pred}^{pctB} and U_{pred}^{pctNa} are the prediction uncertainties for PCT-B and Na normalized releases.

Processing property – those properties that are used as measures of the ability to process a given glass melt and/or melter feed. These properties typically include melter feed rheology, melt viscosity, melt electrical conductivity, and salt formation.

Product compliance – the activities performed during production to ensure and document compliance with contract and disposal system requirements for the ILAW waste form.

Product quality – those properties that are used as measures of the ability to dispose of the glass once it has been fabricated. These properties typically include chemical durability, regulatory compliance, and related contract requirements.

Production lot – as stated in WTP contract Specification 13, the certification and acceptance of ILAW product will be done on a lot basis. Currently, the proposed lot size is the amount of glass contained in three canisters as discussed in Section 5.5.

R² (after Hrma et al. 1994) – R² estimates the fraction of the variability in the property data accounted for by the fitted model. **R² Adjusted** adjusts R² to the number of terms in the model and the number of data points used to fit the model. It is useful for comparing models fitted with a different number of model terms. **R² Prediction** is the R² where each data point is left out of the fit in evaluating how well the model predicts that data point (one-point-at-a-time). It is useful in estimating the fraction of variability that would be explained in predicting new observations drawn from the same model composition region. **R² Validation** is the R² calculated using data not used to fit the model. In this report it is taken as the average R² Validation from 5 individual R² Validation values calculated from five separate modeling and validation subsets of data. Each modeling and validation subset of data was obtained by taking every fifth data point out of the model fit data set and using them for model validation.

Relative standard deviation – a relative standard deviation (RSD) is a standard deviation divided by a mean value. %RSD = 100×RSD.

Retention factor – a fraction of component mass retained in glass after melting to the mass in the feed that entered the melter.

Root Mean Squared Error – a root mean squared error (RMSE) is the square root of the mean square for error in a model. It estimates the standard deviation of the model random error.

Selected – “Selected” used in the property model equations means that only some of the model terms are included in the model.

Transformed – a term “transformed” used in this report has two meanings. (1) “transformed” property means that the property unit was converted to the natural logarithm of the property unit used by the property models, i.e., g/L to ln(g/L) for PCT, mg/L to ln(mg/L) for TCLP, P to ln(P) for viscosity and S/cm to ln(S/cm) for electrical conductivity, (2) a “transformed” value of component mass fractions means the calculated value of component mass fractions according to the appropriate basis for the specific model terms such as Al₂O₃×Al₂O₃, Al₂O₃×SiO₂, Al₂O₃/(T/1000)².

Validity range – component concentration range or property value range within which property models are valid.

Variance-covariance matrix – a variance-covariance matrix is calculated for the estimated coefficients of a model fitted by regression according to, $\Sigma^{prop} = \left(s_{prop}^{rmse\ of\ model} \right)^2 \left[(\mathbf{X}^{prop})^T \mathbf{X}^{prop} \right]^{-1}$ where Σ^{prop} is the variance-covariance matrix for the “prop” model, $s_{prop}^{rmse\ of\ model}$ is the RMSE for the “prop” model, and \mathbf{X}^{prop} is the matrix of glass composition vectors for all the data points (glasses) used to fit the “prop” model.

Vector/matrix notation used in this report – the notation in bold face is used in this report to represent vectors and matrices. Vectors are treated as column vectors (a matrix consisting of a single column of elements) in this report. An example of a vector is \mathbf{x}^{pct} in Equation (8), which represents the vector form of the component mass fraction in glass or transformed value of component mass fractions to the appropriate basis for the model terms in the PCT models. An example of a matrix is Σ^{pct} in Equation(8), which represents the variance-covariance matrix for the PCT normalized release models given in Tables A-7 and A-8.

vis – viscosity. The “vis” notation is used as a superscript for various symbols to specify that the symbols are for viscosity, e.g., U_{pred}^{vis} is the prediction uncertainties for viscosity.

Waste glass – a non-crystalline (i.e., vitreous) solid containing waste components chemically bound within the structure of the solid – thereby immobilizing the waste. Typically an alkali-alumino-borosilicate glass is used. The waste is initially dissolved in molten glass that is cooled quickly enough to prevent crystallization. However, some minor amounts of crystals may be present in the glass.

Waste loading - the mass fraction of the glass that originated as waste (e.g., mass of calcined glass oxides originated from waste divided by the glass mass).

Waste sodium – the sodium delivered to the WTP in waste batches from the tank farm system, plus the sodium used in the pretreatment process to perform leaching of the waste solids.

1 Introduction

The U.S. Department of Energy (DOE), Office of River Protection (ORP), has contracted with Bechtel National, Inc. (BNI) to design, construct, and commission the Hanford Tank Waste Treatment and Immobilization Plant (WTP) at the Hanford Site (DOE 2000). This plant is designed to operate for 40 years and treat roughly 50 million gallons of mixed hazardous high-level waste (HLW) stored in 177 underground tanks at the Hanford Site. The process involves separating the high-level and low-activity waste (LAW) fractions through filtration, leaching, Cs ion exchange, and precipitation. Each fraction will be separately vitrified into borosilicate waste glass.

Figure 1 shows a schematic of the LAW vitrification process. The LAW is transferred from the treated LAW concentrate storage process system (TCP) in the pretreatment facility (PT) to one of two concentrate receipt vessels (CRVs) in the LAW vitrification facility. The CRVs are sampled, and samples are analyzed at the WTP laboratory. These analyses are required for batching of glass-forming chemicals (GFCs), and for production records. LAW is transferred from the CRVs to the melter feed preparation vessels (MFPVs) in batches where GFCs are added, and the melter feed is blended. The blended melter feed is then transferred in batches to the melter feed vessels (MFVs), which continuously provide melter feed to the melters. The melt is cast into containers where it cools and solidifies into LAW glass, which is referred to as immobilized LAW (ILAW).

Figure 1. Schematic of the LAW Vitrification Process

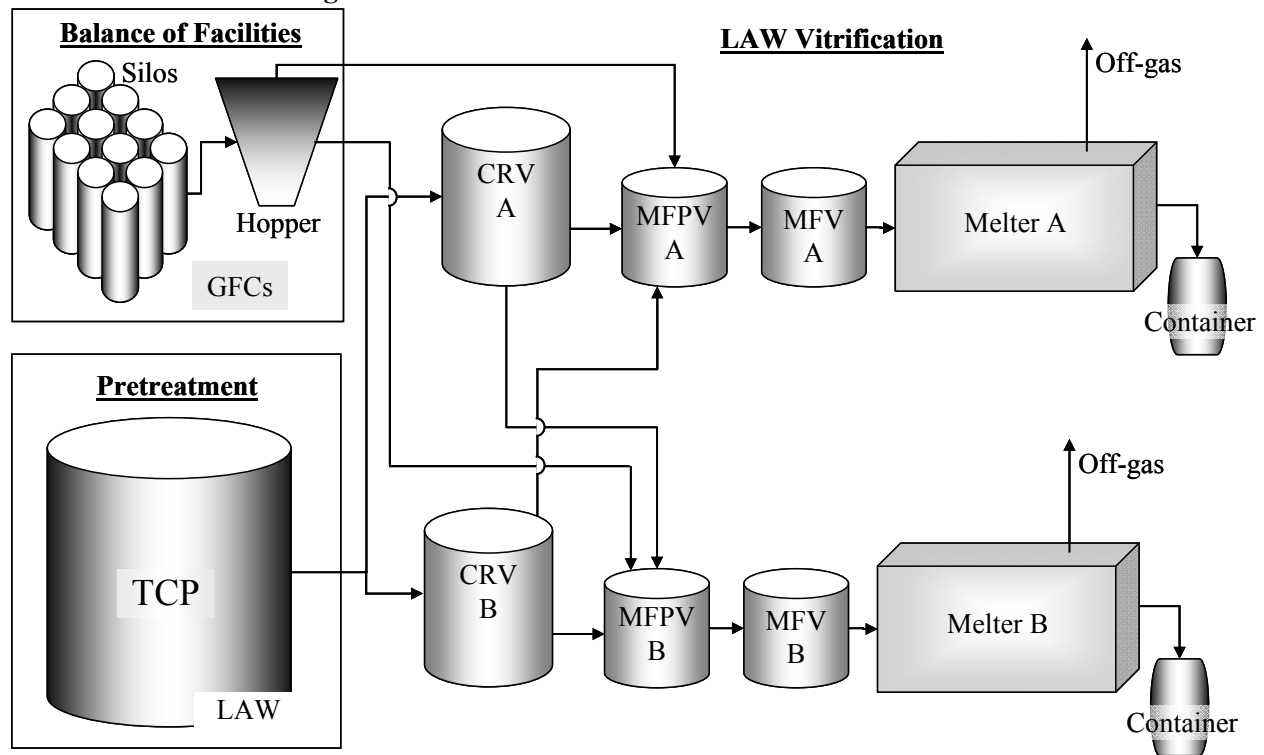


Table 1. LAW Process Vessel Sizes (L)

Description	CRV	MFPV	MFV
Batch volume (L)	34,504	12,870	12,870
Heel volume (L)	14,157	6,556	3,698
Working (=Batch+Heel) volume (L)	48,661	19,426	16,568
Volume up to overflow (L)	56,315	28,348	21,833
Vessel ID	LCP-VSL-00001/2	LFP-VSL-00001/3	LFP-VSL-00002/4
Reference	24590-LAW-M6C-LCP-00001, Rev 1	24590-LAW-M6C-LFP-00001, Rev 1	24590-LAW-M6C-LFP-00002, Rev 1

CRV: concentrate receipt vessel
 MFPV: melter feed preparation vessel
 MFV: melter feed vessel

The key process vessel volumes are summarized in Table 1. Each ILAW container contains roughly 5,911 kg of glass (assuming 94% fill height, an effective density of 2,627 kg/m³, and a total fill volume of 2.394 m³) (Andre 2004). The mass yield of LAW melter feed ranges from 800 to 960 g of glass per L of feed with a nominal average value of 880 g/L (CCN 116150).⁽¹⁾ With a nominal MFPV batch size of 12,870 L, it is expected that roughly 1.88 containers will be generated by each MFPV batch (assuming nominal values). A CRV batch is roughly 34,500 L, which is transferred to MFPV batches at roughly 8,700 L per batch (24590-LAW-M4C-20-00002) producing roughly four MFPV batches on average (may range from 2,300 L to 10,000 L, producing from 3.5 to 15 MFPV batches, depending on sodium molarity and waste loading). Therefore, a CRV batch will generate roughly 7.5 containers of glass (assuming nominal values are achieved, but may range from 6 to 28 containers, depending on sodium molarity and waste loading). The mass of glass in the LAW melter is estimated to be 17,240 kg of glass (24590-LAW-MOD-LMP-00002), which translates to three containers.

The ILAW must meet a series of constraints to be acceptable for disposal in the Hanford Site integrated disposal facility. The waste-acceptance-related constraints are in Specification 2 of the contract (DOE 2000). Additionally, key processing-related constraints will be used to ensure successful processing of the LAW into glass at the design capacity rate. The combined constraint set is summarized in Table 2. Although not listed in Table 2, ILAW must also meet the Dangerous Waste Limitations as specified in the Contract Specification paragraph 2.2.2.20 (DOE 2000). The approach to meeting the Dangerous Waste Limitations is described in detail in the petition for variance to land disposal restrictions (LDR) (24590-WTP-RPT-ENV-03-003). The petition was submitted to DOE. After thorough review, DOE will submit the petition to Environmental Protection Agency (EPA) and Washington State Department of Ecology. If successful, the LDR variance will be technology based so the only restrictions would include processing the waste by vitrification as described in the petition. This compliance strategy is specified in the ILAW PCP (24590-WTP-PL-RT-03-001), "... *During production, the WTP project will control the vitrification process to adequately treat the waste in accordance with any conditions established as part of the treatability variance.*" This specification is not listed in Table 2 because there is no calculation required to be performed by the ILAW algorithm under the current compliance strategy.

Along with the constraints listed in Table 2, there are potential issues that are not defined by numeric values, such as corrosion rates of glass contact materials (bubblers, electrodes, refractories, etc.), redox ratio, and salt accumulation. They are the issues that require attention for efficient and safe plant operations but are not currently modeled.

⁽¹⁾ These mass yield values are valid for LAWs with Na molarity close to the current target values of 10 M Na for envelopes A and C and of 5 M Na for envelope B. The target values for Na molarity are not finalized and may change.

Table 2. Summary of LAW Glass and Melt Constraints Used in ILAW Algorithm^(a)

Constraint Description	Constraint	Source
Product consistency test (PCT) normalized releases of Na, B, and Si	< 2 (g/m ²) (for Na, B, and Si)	DOE 2000 (Spec. 2.2.2.17.2)
Vapor hydration test (VHT) 200°C alteration rate	< 50 (g/m ² /d)	DOE 2000 (Spec. 2.2.2.17.3)
Viscosity at 1100°C	≤ 150 (P) ^(b)	24590-LAW-3PS-AE00-T00001, Rev. 4
Viscosity at 1150°C	≥ 20 (P)	24590-HLW-RPT-RT-05-001, Rev. 0 ^(c)
Viscosity at 1150°C	≤ 80 (P)	24590-HLW-RPT-RT-05-001, Rev. 0 ^(c)
Electrical conductivity at 1100°C	≥ 0.1 (S/cm)	24590-LAW-3PS-AE00-T00001, Rev. 4
Electrical conductivity at 1200°C	≤ 0.7 (S/cm)	24590-LAW-3PS-AE00-T00001, Rev. 4
Waste loading (wt% waste Na ₂ O in glass)	> 14, 3, and 10 (wt%) for envelopes A, B, and C LAW, respectively	DOE 2000 (Spec. 2.2.2.2)
Waste classification	< Class C limits as defined in 10CFR61.55	DOE 2000 (Spec. 2.2.2.8)
⁹⁰ Sr activity per unit volume of glass	< 20 (Ci/m ³)	DOE 2000 (Spec. 2.2.2.8)
¹³⁷ Cs activity per unit volume of glass (waste form compliance)	< 3 (Ci/m ³)	DOE 2000 (Spec. 2.2.2.8)
¹³⁷ Cs activity per unit volume of glass (system maintenance)	< 0.3 (Ci/m ³)	DOE 2000 [Section C.7 (d).(1).(iii)]
Canister surface dose rate	≤ 500 mrem/h	DOE 2000 (Spec. 2.2.2.9)

(a) ILAW must also meet the Dangerous Waste Limitations (Contract Specification paragraph 2.2.2.20, DOE 2000) although this specification is not listed in this table because there is no calculation required to be performed by the ILAW algorithm (see text above this table).

(b) Note that the lower limit of 10 P on viscosity at 1100°C, specified in 24590-LAW-3PS-AE00-T00001, Rev. 4, is unnecessary given the lower limit of 20 P on viscosity at 1150°C. This is because viscosity decreases with increasing temperature.

(c) The bases for glass viscosity constraint at 1150°C discussed for IHLW algorithm (Appendix G in 24590-HLW-RPT-RT-05-001, Rev. 0) also applies to the ILAW algorithm.

The Vitreous State Laboratory (VSL) at the Catholic University of America formulated ILAW glasses for vitrification testing and demonstrations in the Duratek pilot-scale melter (DM-3300). Each formulation was developed to meet all of the constraints listed above. The formulations were then demonstrated to meet all the processing and product-quality constraints at scales up to pilot-scale. These compositions span the range of waste compositions expected during the initial phase of WTP operation, and form the basis of the glass-composition portion of the ILAW formulation algorithm. Following the results of 24590-LAW-M4C-LFP-00002 and 24590-WTP-MRQ-PO-03-033, Muller et al. (2004) fit functions of glass-component concentrations to the ratio of Na₂O to SO₃ in the LAW.⁽²⁾ The purpose of these

⁽²⁾ The notation used in this report to identify glass composition is to assume single electropositive element oxides that are represented in their most prevalent oxidation state (e.g., Fe₂O₃, Na₂O, SO₃). Halogens are represented as single element concentrations (e.g., Cl, F). This notation is used not to imply structure or local bonding of elements in the glass/melt, but rather, to give a simple, standardized method to uniquely identify composition.

functions is to interpolate new acceptable glass compositions between glass compositions successfully demonstrated in pilot-scale melter tests.

To implement the glass-batching equations during the LAW vitrification plant operation, several steps are envisioned, including:

- LAW transfer from the TCP in the PT facility to the LAW CRV
- Sampling and chemical analyses of the LAW CRV batch
- Determination of initial ILAW composition
- Estimation of ILAW properties using glass property-composition models
- Comparison of predicted glass properties with limits or constraints
- Calculation of LAW and GFC masses for transfer to the LAW MFPV
- Transfer of LAW and GFCs to the LAW MFPV
- Transfer of the blended LAW melter feed to the LAW MFV
- Determination of final ILAW composition
- Generation of glass-composition-related portions of the ILAW Production Records.

These steps of the formulation algorithm, including the preliminary set of mass-balance equations used for feed batching and compliance with contract specifications, are described in this document. Information relevant to the calculations is included in Appendix A (Inputs Used in Calculations) and Appendix B (Results of Example Calculations). A summary of data requirements for this algorithm to be complete is included in Appendix C. Approaches used to estimate the uncertainties for waste transfer volume and GFC mass measurements are in Appendices D and E. Calculation of GFC and sucrose volume contribution to the MFPV batch volume is described in Appendix F. A discussion on the use PERT distributions for GFC composition and retention factors is in Appendix G.

This document will be updated as needed, as new data are available, or changes to approaches/constraints are made.

2 Symbols and Notation

Due to the large number of variables used in the ILAW formulation algorithm, it was necessary to develop a consistent notation to track the numerous variables. The notation uses base symbols that represent the type of value, with superscripts representing the location or vessel, and subscripts representing an index (e.g., component index, batch index). Table 3 lists the notation components that are incorporated in the symbols used in this report. Table 3 is not a complete list of all subscripts and superscripts used in this report, and includes only those that help to clarify the meaning of specific notations. A list of units is also included in Table 3. The list of specific notations and their definitions are given in Table 4. Vectors and matrices are in bold font. Note that there are changes in notation in Table 4 compared to that in Piepel et al. (2005).

Table 3. Summary of Notations used in this Report

Notation	Description
Base Symbols	
<i>a</i>	activity of radionuclides
<i>A</i>	specific activity, i.e., activity per mass of radionuclide
<i>B</i>	confidence interval in transformed predicted property (see Key Definitions section for the definition of “transformed” properties)
<i>c</i>	concentration of individual component, e.g., c_i^{CRV} is the concentration of <i>i</i> th elemental component in CRV
<i>C</i>	concentration of total components, e.g., C^{CRV} is the concentration of all glass oxide components in CRV
<i>d</i>	normalized alkali oxides (Na ₂ O and K ₂ O) mass fraction
<i>f</i>	oxide conversion factor, i.e., glass oxide mass per mass of analyte
<i>F</i>	F-distribution
<i>g</i>	mass fraction of component in glass, GFC, or feed. The mass fraction for all glass components sums to 1, i.e., $\sum_{i=1}^n g_i = 1$.
<i>G</i>	mass fraction of feed constituent, such as waste, heel, and various GFCs, in the MFPV batch, also referred to as “loading”, as in “waste loading” and “heel loading”
<i>I</i>	radionuclide inventory, activity per canister
<i>L</i>	limit
<i>m</i>	mass fraction of component in GFC. Used for GFC only, which sometimes includes volatiles that are not retained in glass (such as CO ₂ , H ₂ O), i.e., $\sum_{i=1}^n m_i \neq 1$ for some GFCs where <i>i</i> represents glass component.
<i>M</i>	mass

Notation	Description
MW	molecular weight
n	number, for example number of samples, number of variables, number of model coefficients
p	property model coefficient
P	predicted value of a transformed property (see Key Definitions section for the meaning of “transformed”)
Q	percentile
r	PCT normalized elemental release
R	activity per volume
s	standard deviation
SF	sum of fractions
t	t-distribution, target sodium molarity
\mathbf{t}	target MFPV batch composition vector
U	uncertainty
V	volume
w	weighting factor
x	mass fraction of model component. The x is different from g in that x is for model components that includes “Others” as one model component whereas g is for all components being tracked. (See Equations (3) and (4) for more information.)
ε	electrical conductivity
η	viscosity
\mathbf{H}	GFC composition matrix
λ	dilution factor
v	retention factor
ρ	density
Σ	variance-covariance matrix
ω	fraction of waste sodium
<i>Subscripts and Superscripts</i>	
$2s$	two standard deviations
can	within a canister
$comp$	composition, components
d	CRV batch index
e	canister index
ec	electrical conductivity

Notation	Description
<i>flush</i>	flush or filter wash water
<i>GFC</i>	glass forming chemical
<i>h</i>	Model term index
<i>CRV</i>	Low-activity waste concentrate receipt vessel
<i>i</i>	chemical or radionuclide component (e.g., Al, B, Ca...) index
<i>j</i>	MFPV batch index
<i>k</i>	GFC (e.g., silica, borax, ...) index
<i>l</i>	sample index, analyses index, or lower in case of limits
<i>lcci</i>	lower combined confidence interval
<i>m</i>	waste loading limit index
<i>MFPV</i>	MFPV batch
<i>MFPV_w</i>	working MFPV content, i.e., MFPV batch plus heel from the previous working MFPV
<i>pctB</i>	Product Consistency Test normalized boron response
<i>pctNa</i>	Product Consistency Test normalized sodium response
<i>pred</i>	prediction
<i>prop</i>	property
<i>rad</i>	radionuclide
<i>samp</i>	samples of a particular material
<i>suci</i>	simultaneous upper confidence interval
<i>T</i>	Temperature for viscosity or electrical conductivity
<i>u</i>	upper
<i>ucci</i>	upper combined confidence interval
<i>vis</i>	viscosity
Accent marks	
–	used to represent average (above the symbol as in \bar{g}_i)
'	used to indicate that $i \neq i'$ in model coefficients for the quadratic model terms ($P_{ii'}^{prop}$)
~	used to indicate composition after applying component retention factors (above the symbol as in \tilde{g}_i)
^	used to represent the activity of radionuclide and its standard deviation per unit volume of glass instead of unit mass of glass (above the symbol as in \hat{a}_{ie}^{can} and \hat{s}_{ie}^{can})

Notation	Description
...	used to represent the mass of GFC per g of glass (above the symbol as in $\ddot{M}_{kj}^{GFC in MFPV, target}$)
..	used to represent the mass of sucrose per liter of waste (above the symbol as in $\ddot{M}_j^{sucrose in MFPV, target}$)
Units^(a)	
°C	degree centigrade
Ci	curie
g	gram
h	hour
K	Kelvin
L	liter
ln	natural logarithm
m	meter
P	poise
S	siemens
wt%	weight percent

(a) Non-italic fonts are used to distinguish units from base symbols, subscripts, and superscripts.

Table 4. List of Symbols

Symbol	Description	Equation(s)
$a_{ie}^{rad in can}$	specific activity of the i^{th} radionuclide in the e^{th} canister (mCi/g glass)	(125) (127) (128) (130)
$\hat{a}_{ie}^{rad in can}$	activity of the i^{th} radionuclide per unit volume of glass in the e^{th} canister (Ci/m ³ glass)	(128) (130) (131)
$a_{idm}^{rad in CRV}$	specific activity of the i^{th} radionuclide in the m^{th} transfer waste transferred from the d^{th} CRV to MFPV (mCi/g oxides)	(24) (53) (100) (106)
$a_{ij}^{rad in MFPV, Step1}$ $a_{ij}^{rad in MFPV, Step3}$	specific activity of the i^{th} radionuclide in the j^{th} MFPV batch from algorithm calculation Step 1 or Step 3 before applying component retention factors (mCi/g oxides)	(53) (54) (69) (70) (100) (101) (106) (107)
$\tilde{a}_{ij}^{rad in MFPV, Step1}$ $\tilde{a}_{ij}^{rad in MFPV, Step3}$	specific activity of the i^{th} radionuclide in the j^{th} MFPV batch from algorithm calculation Step 1 or Step 3 after applying the component retention factors (mCi/g oxides)	(54) (70) (71) (75) (101) (108) (110) (125)
$\hat{\tilde{a}}_{ij}^{rad in MFPV, Step1}$ $\hat{\tilde{a}}_{ij}^{rad in MFPV, Step3}$	activity of the i^{th} radionuclide per unit volume of glass in the j^{th} MFPV batch from algorithm calculation Step 1 or Step 3 after applying retention factors (Ci/m ³ glass)	(71) (73) (74) (75) (76) (83) (108) (110) (111)
A_i	specific activity of the i^{th} radionuclide (Ci/g)	(23)

Symbol	Description	Equation(s)
B_{lcci}^{prop}	CL% lower combined confidence interval for “ <i>prop</i> ” (applicable only to “ <i>vis</i> ” and “ <i>ec</i> ”)	(16)
$B_{lcci,j}^{prop,Step1}$ $B_{ucci,j}^{prop,Step3}$	CL% lower combined confidence interval for “ <i>prop</i> ” for the j^{th} MFPV batch from algorithm calculation Step 1 or Step 3 (applicable only to “ <i>vis</i> ” and “ <i>ec</i> ”)	(67) (104)
B_{ucci}^{prop}	CL% upper combined confidence interval for “ <i>prop</i> ”	(16)
$B_{ucci,e}^{pct}$, $B_{ucci,e}^{vht}$	CL% upper combined confidence interval for “ <i>pct</i> ” ($\ln[r_B, g/L]$, $\ln[r_{Na}, g/L]$) and “ <i>vht</i> ” ($\ln[D, \mu m]$) for the e^{th} canister	(134) (135)
$B_{ucci,j}^{prop,Step1}$ $B_{lcci,j}^{prop,Step3}$	CL% upper combined confidence interval for “ <i>prop</i> ” for the j^{th} MFPV batch from algorithm calculation Step 1	(67) (83) (87) (104)
C_{id}^{CRV} (element in)	concentration of the i^{th} element in the d^{th} CRV batch associated with the j^{th} MFPV batch (mg/L)	(12) (14)
\bar{C}_{id}^{CRV} (element in)	concentration of the i^{th} component in the waste of the d^{th} CRV batch averaged over n_d^{CRV} samples analyzed (mg/L waste)	(18)
C_{idm}^{CRV} (element in)	concentration of the i^{th} component in the m^{th} transfer waste transferred from the d^{th} CRV to MFPV (mg/L waste)	(18) (21) (22) (23) (65) (69) (102) (106)
$C_{Na,dm}^{CRV}$ (element in)	concentration of Na in the m^{th} transfer waste transferred from the d^{th} CRV to MFPV (mg/L waste)	(62) (92)
$C_{NO_2,dm}^{CRV}$, $C_{NO_3,dm}^{CRV}$, and $C_{TOC,dm}^{CRV}$ (element in)	concentration of nitrite, nitrate, and total organic carbon in the m^{th} transfer waste transferred from the d^{th} CRV to MFPV (mg/L LAW)	(59)
C_{ij}^{MFPVw} (element in)	concentration of the i^{th} element in the j^{th} working MFPV (mg/L)	(120)
C_{dm}^{CRV} (oxides in)	concentration of total glass oxides in the m^{th} transfer waste transferred from the d^{th} CRV to MFPV (g oxides per L waste)	(22) (24) (53) (56) (58) (63) (96) (100) (118) (122)
C_j^{MFPV} (oxides in)	concentration of total glass oxides in the j^{th} MFPV batch (g oxides per L)	(118) (119)
C_j^{MFPVw} (oxides in)	concentration of total glass oxides in the j^{th} working MFPV (g oxides per L)	(119) (120)
C_{j-1}^{MFPVw} (oxides in)	concentration of total glass oxides in the $j-1^{th}$ (previous) working MFPV (g oxides per L)	(119)
d	Na ₂ O mass fraction plus 0.66 times K ₂ O mass fraction	(40) (41) (42) (43)
D	VHT alteration depth (μm)	General

Symbol	Description	Equation(s)
f_i	oxide conversion factor, i.e., mass of the i^{th} glass oxide per mass of the i^{th} element	(12) (21) (22) (65) (69) (102) (106) (120)
$F_{1-\alpha, (n_{pct}^{model}, n_{pct}^{data} - n_{pct}^{model})}$	100(1- α) percentile (=CL%) of an F-distribution with n_{pct}^{model} numerator degrees of freedom and $n_{pct}^{data} - n_{pct}^{model}$ denominator degrees of freedom	(8)
$F_{1-\alpha, (n_{vht}^{model}, n_{vht}^{data} - n_{vht}^{model})}$	100(1- α) percentile (=CL%) of an F-distribution with n_{vht}^{model} numerator degrees of freedom and $n_{vht}^{data} - n_{vht}^{model}$ denominator degrees of freedom	(9)
g_i	mass fraction of the i^{th} glass oxide component in glass	(3) (4)
$g_{idm}^{oxide\ in\ CRV}$	mass fraction of the i^{th} glass oxide in the m^{th} transfer waste transferred from the d^{th} CRV to MFPV (g oxide per g CRV oxides)	(25) through (30) (32) (33) (40) (44) (21) (47) (50) (51) (68) (98) (105)
$g_{Na_2O(w),e}^{oxide\ in\ can}$	mass fraction of waste Na ₂ O (waste Na ₂ O loading) in the e^{th} canister (g per g glass)	(121)
$g_{ij}^{oxide\ in\ MFPV}$	mass fraction of the i^{th} glass oxide in the j^{th} MFPV batch before applying component retention factors (g oxide per g MFPV oxides)	(12) (13)
$g_{ij}^{oxide\ in\ MFPV, initial}$	initial mass fraction of the i^{th} glass oxide in the j^{th} MFPV batch (g oxide per g MFPV oxides)	(33) through (45) (46) (84) (84)
$g_{ij}^{oxide\ in\ MFPV, initial, adj}$	adjusted initial mass fraction of the i^{th} glass oxide in the j^{th} MFPV batch (g oxide per g MFPV oxides)	(82)
$g_{ij}^{oxide\ in\ MFPV, target}$	target mass fraction of the i^{th} glass oxide in the j^{th} MFPV batch (g oxide per g MFPV oxides)	(46) (47) (82) (84)
$g_{ij}^{oxide\ in\ MFPV, adj}$	manual adjustment made to satisfy all the constraints for the target mass fraction of the i^{th} glass oxide in the j^{th} MFPV batch (g oxide per g MFPV oxides)	(81) (84)
$g_{ij}^{oxide\ in\ MFPV, target-gfc}$	target mass fraction of the i^{th} glass oxide in glass from GFC for the j^{th} MFPV batch (g oxide per g MFPV oxides)	(47) (48)
$g_{Na_2O, j}^{oxide\ in\ MFPV, pre}$	preliminary minimum Na ₂ O mass fraction in the j^{th} MFPV batch (g per g MFPV oxide)	(25) through (32) (39) (81)
$g_{Na_2O, j}^{oxide\ in\ MFPV, initial}$	initial mass fraction of Na ₂ O in the j^{th} MFPV batch (g oxide per g MFPV oxides)	(33)
$g_{Na_2O, j}^{oxide\ in\ MFPV, target}$	target mass fraction of Na ₂ O in the j^{th} MFPV batch (g oxide per g MFPV oxides)	(61)
$g_{Na_2O, j}^{oxide\ in\ MFPV, adj}$	manual adjustment of Na ₂ O concentration in the j^{th} MFPV batch required to satisfy all the constraints (g per g MFPV oxide)	(81)

Symbol	Description	Equation(s)
$\tilde{g}_{Na_2O,j}^{oxide\ in\ MFPV,\ pre-adj}$	adjusted preliminary target Na ₂ O concentration in the <i>j</i> th MFPV batch (g per g MFPV oxide)	(81)
$\tilde{g}_{ij}^{oxide\ in\ MFPV,\ Step1}$ $\tilde{g}_{ij}^{oxide\ in\ MFPV,\ Step3}$	mass fraction of the <i>i</i> th glass oxide in the <i>j</i> th MFPV batch from algorithm calculation Step 1 or Step 3 before applying component retention factors (g oxide per g MFPV oxides)	(50) (52) (54) (65) (66) (70) (98) (99) (101) (102) (103) (107) (114) (122)
$\tilde{g}_{ij}^{oxide\ in\ MFPV,\ Step1}$ $\tilde{g}_{ij}^{oxide\ in\ MFPV,\ Step3}$	mass fraction of the <i>i</i> th glass oxide in the <i>j</i> th MFPV batch from algorithm calculation Step 1 or Step 3 after applying the component retention factors (g oxide per g glass), i.e., mass of <i>i</i> th glass oxide that will remain in glass divided by the total mass of all glass oxides that will remain in glass	(13) (52) (66) (83) (85) (86) (99) (103) (123)
$\tilde{g}_{Na_2O(w),j}^{oxide\ in\ MFPV,\ Step1}$ $\tilde{g}_{Na_2O(w),j}^{oxide\ in\ MFPV,\ Step3}$	mass fraction of waste Na ₂ O (waste Na ₂ O loading) in the <i>j</i> th MFPV batch from algorithm calculation Step 1 or Step 3 (g per g glass)	(68) (105) (121)
$\tilde{g}_{ij}^{oxide\ in\ MFPVw}$	mass fraction of the <i>i</i> th glass oxide in the <i>j</i> th working MFPV (g oxide per g glass)	(114) (120)
$\tilde{g}_{i,j-1}^{oxide\ in\ MFPVw}$	mass fraction of the <i>i</i> th glass oxide in the <i>j-1</i> th (previous) working MFPV (g oxide per g glass)	(114)
$\tilde{g}_{ie}^{oxide\ in\ can}$	mass fraction of the <i>i</i> th glass oxide in the <i>e</i> th canister (g per g glass)	(123)
$G_j^{waste\ in\ MFPV,\ initial}$	initial mass fraction of glass oxides originated from waste in the <i>j</i> th MFPV batch, i.e. initial waste loading (g per g MFPV oxides)	(32) (33) (40) (44)
$G_j^{waste\ in\ MFPV,\ target}$	target mass fraction of glass oxides originated from waste in the <i>j</i> th MFPV batch, i.e. target waste loading (g per g MFPV oxides)	(47) (50) (51) (56) (58) (63) (68)
$G_j^{waste\ in\ MFPV,\ Step1}$ $G_j^{waste\ in\ MFPV,\ Step3}$	mass fraction of glass oxides originated from waste in the <i>j</i> th MFPV batch from algorithm calculation Step 1 or Step 3, i.e. waste loading (g per g MFPV oxides)	(51) (53) (96) (97) (98) (100) (105) (118)
$I_{ie}^{rad\ in\ can}$	inventory of the <i>i</i> th radionuclide in the <i>e</i> th canister (Ci)	(127)
k^{rad}	expansion factor for radionuclide concentration specification	(73) (74) (79) (80) (83)
L_u^{prop} and L_l^{prop}	upper and lower property limit for predicted “ <i>prop</i> ” transformed property value	General
L_u^a	upper limit for specific activity of the <i>i</i> th radionuclide (nCi/g glass)	(75) (77) (110) (112) (130) (132)

Symbol	Description	Equation(s)
$\hat{L}_u^{\tilde{a}_i}$	upper limit for the activity of the i^{th} radionuclide per unit glass volume (Ci/m ³ glass)	(75) (76) (77) (78) (110) (111) (112) (113) (130) (131) (132) (133)
$m_{ik}^{\text{oxide in GFC}}$	mass fraction of the i^{th} glass oxide in the k^{th} GFC (g oxide per g GFC including volatiles)	(12) (48) (50) (51) (65) (68) (69) (96) (97) (98) (102) (105) (106) (122)
\mathbf{m}_j	vector of $\ddot{M}_{kj}^{\text{GFC in MFPV,pre}}$ for $n_j^{\text{GFCs in MFPV}}$ GFCs in the j^{th} MFPV batch (g oxide per g MFPV oxides)	(48)
$M_{kj}^{\text{GFC in MFPV}}$	mass of the k^{th} GFC to add to the j^{th} MFPV batch (g)	(12)
$M_{kj}^{\text{GFC in MFPV,target,Step1}}$ $M_{kj}^{\text{GFC in MFPV,target,Step2}}$	target mass of k^{th} GFC to add to the j^{th} MFPV batch resulted from algorithm calculation Step 1 or Step 2 (g)	(57) (63) (65) (69) (89)
$M_j^{\text{sucrose in MFPV,target,Step1}}$ $M_j^{\text{sucrose in MFPV,target,Step2}}$	target mass of sucrose to add to the j^{th} MFPV batch resulted from algorithm calculation Step 1 or Step 2 (g)	(64) (90)
$M_{kj}^{\text{GFC in MFPV,measured}}$	measured mass of k^{th} GFC added to the j^{th} MFPV batch (g)	(96) (97) (102) (106) (116) (122)
$M_j^{\text{sucrose in MFPV,measured}}$	measured mass of sucrose added to the j^{th} MFPV batch (g)	(117)
$\ddot{M}_{kj}^{\text{GFC in MFPV,pre}}$	preliminary target mass of the k^{th} GFC per g of glass to add to the j^{th} MFPV batch (g per g MFPV oxides)	(48) (49)
$\ddot{M}_{kj}^{\text{GFC in MFPV,target}}$	target mass of the k^{th} GFC per g of glass to add to the j^{th} MFPV batch (g per g MFPV oxides)	(49) (50) (51) (56) (58) (63) (68)
$\ddot{M}_j^{\text{sucrose in MFPV,target}}$	target mass of sucrose required per L of waste (g/L)	(59) (60) (64)
$\ddot{M}_{kj}^{\text{GFC in MFPV,Step3}}$	mass of the k^{th} GFC per g of glass in the j^{th} MFPV batch from algorithm calculation Step 3 (g per g MFPV oxides)	(97) (98) (105)
$\tilde{M}_j^{\text{oxide in MFPV,Step3}}$	mass of total glass oxides in the j^{th} MFPV batch after applying the component retention factors from algorithm calculation Step 3 (g)	(121) (122) (123) (124) (125) (126)

Symbol	Description	Equation(s)
$M_e^{glass\ in\ can}$	mass of glass in the e^{th} canister (kg)	(127)
$MW_{C_{12}H_{22}O_{11}}$	molecular mass of sucrose (g/mole)	(59)
MW_{Na}	atomic mass of sodium (g/mole)	(62) (92)
MW_{NO_2} , MW_{NO_3} , and MW_C	molecular masses of nitrite, nitrate, and carbon (g/mole)	(59)
$n_{ec}^{comps\ in\ model}$	number of model components in the “ <i>ec</i> ” model	(7) (11)
$n_{pct}^{comps\ in\ model}$	number of model components in the “ <i>pct</i> ” model	(2) (8)
$n_{vht}^{comps\ in\ model}$	number of model components in the “ <i>vht</i> ” model	(5) (9)
$n_{vis}^{comps\ in\ model}$	number of model components in the “ <i>vis</i> ” model	(6) (10)
$n_{ec}^{data\ in\ model}$	number of data points used to fit the “ <i>ec</i> ” model	(11)
$n_{pct}^{data\ in\ model}$	number of data points used to fit the “ <i>pct</i> ” model	(8)
$n_{vht}^{data\ in\ model}$	number of data points used to fit the “ <i>vht</i> ” model	(9)
$n_{vis}^{data\ in\ model}$	number of data points used to fit the “ <i>vis</i> ” model	(10)
$n_{prop}^{terms\ in\ model}$	number of model terms in the “ <i>prop</i> ” model	(1)
$n_{ec}^{terms\ in\ model}$	number of model terms in the “ <i>ec</i> ” model	(7) (11)
$n_{pct}^{terms\ in\ model}$	number of model terms in the “ <i>pct</i> ” model	(2) (8)
$n_{vht}^{terms\ in\ model}$	number of model terms in the “ <i>vht</i> ” model	(5) (9)
$n_{vis}^{terms\ in\ model}$	number of model terms in the “ <i>vis</i> ” model	(6) (10)
$n_d^{oxides\ in\ CRV}$	number of glass oxides tracked in the d^{th} CRV batch	(12) (21) (22) (65) (102)
$n_d^{samps\ in\ CRV}$	number of samples analyzed in the d^{th} CRV batch	(14) (69) (106)
$n_k^{oxides\ in\ GFC}$	number of glass oxides in the k^{th} GFC	(96) (97) (122)

Symbol	Description	Equation(s)
$n_j^{GFCs\ in\ MFPV}$	number of GFCs used in the j^{th} MFPV batch	(12) (50) (51) (56) (58) (65) (68) (69) (96) (97) (98) (102) (105) (106) (122)
$n_j^{oxides\ in\ MFPV}$	number of glass oxides tracked in the mass balance calculations for the j^{th} MFPV batch	(45) (12) (13) (50) (51) (52) (54) (65) (66) (68) (70) (96) (99) (101) (102) (103) (105) (106) (107) (122)
$n_e^{MFPVs\ in\ can}$	number of MFPV batches that are assumed to be in the e^{th} canister	(121) (123) (124) (125) (126)
p_h^{prop}	coefficient of the h^{th} model term for the “prop” model	(1)
p_h^{ec}	coefficient of the h^{th} model term for the “ec” model (S/cm). p_h^{ec} represents all forms of the model term, i.e., p_i^{ec} , $p_{ii'}^{ec}$ (selected), and $p_i^{ec,T}$	(7)
p_h^{pct}	coefficient of the h^{th} model term for the “pct” model (ln[g/L]). p_h^{pct} represents all forms of the model term, i.e., p_i^{pct} , $p_{ii'}^{pct}$ (selected), and $p_{ii''}^{pct}$ (selected)	(2)
p_h^{vht}	coefficient of the h^{th} model term for the “vht” model (ln[g/L]). p_h^{vht} represents all forms of the model term, i.e., p_i^{vht} , $p_{ii'}^{vht}$ (selected), and $p_{ii''}^{vht}$ (selected)	(5)
p_h^{vis}	coefficient of the h^{th} model term for the “vis” model (P). p_h^{vis} represents all forms of the model term, i.e., p_i^{vis} , $p_{ii'}^{vis}$ (selected), $p_{ii''}^{vis}$ (selected), and $p_i^{vis,T}$ (selected)	(6)
p_i^{ec}	coefficient of the i^{th} model component in the “ec” model (represents Al ₂ O ₃ through Others terms in Table 8)	(7)
$p_{ii'}^{ec}$ (selected)	coefficients for the selected quadratic model terms in the “ec” model. “Selected” means that only some of the terms in curly brackets are included in the model. (represent CaO×Li ₂ O, CaO×Na ₂ O, and Li ₂ O×Na ₂ O terms in Table 8)	(7)

Symbol	Description	Equation(s)
$P_i^{ec,T}$	coefficient of the i^{th} model component for the model terms involving temperature in the “ <i>ec</i> ” model. (represents $Al_2O_3/(T/1000)$ through Others/(T/1000) terms in Table 8)	(7)
P_i^{pct}	coefficient of the i^{th} model component for the “ <i>pct</i> ” model (ln[g/L]) (represents Al_2O_3 through Others terms in Table 5)	(2)
P_{ii}^{pct} (selected) $P_{ii'}^{pct}$ (selected)	coefficients for the selected quadratic model terms. “Selected” means that only some of the terms in curly brackets are included in the model (ln[g/L]) (represent $CaO \times Li_2O$ through $(K_2O)^2$ terms in Table 5)	(2)
P_i^{vht}	coefficient of the i^{th} model component for the “ <i>vht</i> ” model (ln[g/L]) (represents Al_2O_3 through Others terms in Table 6)	(5)
P_{iii}^{vht} (selected) $P_{iii'}^{vht}$ (selected) $P_{iii''}^{vht}$ (selected)	coefficients for the selected cubic model terms. “Selected” means that only some of the terms in curly brackets are included in the model (ln[g/L]) (represent $(K_2O)^2 \times Na_2O$ through $B_2O_3 \times CaO \times Na_2O$ terms in Table 6)	(5)
P_i^{vis}	coefficient of the i^{th} model component in the “ <i>vis</i> ” model (represents Al_2O_3 through Others terms in Table 7)	(6)
P_{ii}^{vis} (selected) $P_{ii'}^{vis}$ (selected)	coefficients for the selected quadratic model terms in the “ <i>vis</i> ” model. “Selected” means that only some of the terms in curly brackets are included in the model. (represent $Al_2O_3 \times SiO_2$ through $(Li_2O)^2$ terms in Table 7)	(6)
$P_i^{vis,T}$ (selected)	coefficient of the selected i^{th} model component for the model terms involving temperature in the “ <i>vis</i> ” model. “Selected” means that only some of the terms in curly brackets are included in the model. (represents $Al_2O_3/(T/1000)^2$ through Others/(T/1000) ² terms in Table 7)	(6)
P^{pct}	transformed normalized release (= $\ln[r_B, g/L]$ and $\ln[r_{Na}, g/L]$) for <i>pct</i> = <i>pctB</i> and <i>pctNa</i> respectively	(2)
P^{vht}	transformed VHT alteration depth (ln[D, μm])	(5)
P^{prop}	transformed property “ <i>prop</i> ”, which includes $\ln(r_B, g/L)$, $\ln(r_{Na}, g/L)$, $\ln(D, \mu m)$, $\ln(\eta_T, P)$, and $\ln(\epsilon_T, S/cm)$	(1) (16)
P_e^{pct}, P_e^{vht}	predicted transformed property for “ <i>pct</i> ” ($\ln[r_B, g/L]$, $\ln[r_{Na}, g/L]$) and “ <i>vht</i> ” (ln[D, μm]) for the e^{th} canister	(134) (135)
$P_j^{prop, Step1}$ $P_j^{prop, Step3}$	predicted transformed property “ <i>prop</i> ” for the j^{th} MFPV batch from algorithm calculation Step 1 or Step 3, which includes $\ln(r_B, g/L)$, $\ln(r_{Na}, g/L)$, $\ln(D, \mu m)$, $\ln(\eta_T, P)$, and $\ln(\epsilon_T, S/cm)$	(67) (104)
\mathbf{P}^{prop}	vectors of P_h^{prop} values for the set of $n_{prop}^{terms in model}$ terms	(1)
$Q_{CL\%}^{prop}$	CL% [=100(1-α)] percentile of the distribution of $n_{simulation}^{runs of}$ property values	(15)
$Q_{50\%}^{prop}$	median predicted property value or CL% = 50% percentile of the distribution of $n_{simulation}^{runs of}$ property values	(15)
r_B	PCT normalized boron release (g/L)	General
r_{Na}	PCT normalized sodium release (g/L)	General
r_{Si}	PCT normalized silicon release (g/L)	General
$r_e^{dose in can, max, measured}$	measured maximum surface dose rate from e^{th} canister (mrem/h)	General

Symbol	Description	Equation(s)
$\bar{R}_{id}^{rad\ in\ CRV}$	activity (per unit volume) of the i^{th} radionuclide in the waste of the d^{th} CRV averaged over $n_d^{samps\ in\ CRV}$ samples analyzed (mCi/L)	(23) (24) (53) (69) (100)
$RSD_{anal,i}^{element\ in\ CRV}$	relative standard deviation (RSD) in the concentration of the i^{th} element for chemical analysis in CRV batch	(14)
$RSD_{mix\&\;samp,i}^{element\ in\ CRV}$	RSD in the concentration of the i^{th} element for mixing and sampling in CRV batch	(14)
$RSD_{biascorr,i}^{element\ in\ CRV}$	RSD in the concentration of the i^{th} element for correction of mixing and sampling biases in CRV batch	(14)
$S_{id}^{element\ in\ CRV}$	standard deviation in the concentration of the i^{th} element in the d^{th} CRV batch (mg/L)	(14)
$\tilde{S}_{ij}^{oxide\ in\ MFPV,\ Step3}$	SD for the mass fraction of the i^{th} glass oxide in the j^{th} MFPV batch after applying the component retention factors from algorithm calculation Step 3 (g per g glass)	(124) (126)
$S_{ie}^{oxide\ in\ can}$	SD for the mass fraction of the i^{th} glass oxide in the e^{th} canister (g per g glass)	(124)
$\tilde{S}_{ij}^{rad\ in\ MFPV,\ Step1}$ $\tilde{S}_{ij}^{rad\ in\ MFPV,\ Step3}$	SD for the specific activity of the i^{th} radionuclide in the j^{th} MFPV batch from algorithm calculation Step 1 or Step 3 after applying retention factors (mCi/g glass)	(72) (77) (109) (112) (126)
$\hat{S}_{ij}^{rad\ in\ MFPV,\ Step1}$ $\hat{S}_{ij}^{rad\ in\ MFPV,\ Step3}$	SD for the activity of the i^{th} radionuclide per unit volume of glass in the j^{th} MFPV batch from algorithm calculation Step 1 or Step 3 after applying retention factors (Ci/m ³ glass)	(72) (73) (74) (78) (83) (109) (112)
$S_{ie}^{rad\ in\ can}$	SD for the specific activity of the i^{th} radionuclide in the e^{th} canister (mCi/g glass)	(126) (129) (132)
$\hat{S}_{ie}^{rad\ in\ can}$	SD for the activity of the i^{th} radionuclide per unit volume of glass in the e^{th} canister (Ci/m ³ glass)	(129) (132) (133)
$S_{LL,j}^{radSF\ in\ MFPV,\ Step1}$ $S_{LL,j}^{radSF\ in\ MFPV,\ Step3}$	SD for the sum of fractions of activity to the limit of each radionuclide for long-lived radionuclides for Class C limit determination in the j^{th} MFPV batch from algorithm calculation Step 1 or Step 3	(77) (79) (83) (112)
$S_{SL,j}^{radSF\ in\ MFPV,\ Step1}$ $S_{SL,j}^{radSF\ in\ MFPV,\ Step3}$	SD for the sum of fractions of activity to the limit of each radionuclide for short-lived radionuclides for Class C limit determination in the j^{th} MFPV batch from algorithm calculation Step 1 or Step 3	(78) (80) (83) (113)
$S_{LL,e}^{radSF\ in\ can}$	SD for the sum of fractions of activity to the limit of each radionuclide for long-lived radionuclides for Class C limit determination in the e^{th} canister	(132)
$S_{SL,e}^{radSF\ in\ can}$	SD for the sum of fractions of activity to the limit of each radionuclide for short-lived radionuclides for Class C limit determination in the e^{th} canister	(133)
$SF_{LL,j}^{rad\ in\ MFPV,\ Step1}$ $SF_{LL,j}^{rad\ in\ MFPV,\ Step3}$	sum of fractions of activity to the limit of each radionuclide for long-lived radionuclides for Class C limit determination in the j^{th} MFPV batch from algorithm calculation Step 1 or Step 3	(75) (79) (83) (110)

Symbol	Description	Equation(s)
$SF_{SL,j}^{rad\ in\ MFPV,\ Step1}$ $SF_{SL,j}^{rad\ in\ MFPV,\ Step3}$	sum of fractions of activity to the limit of each radionuclide for short-lived radionuclides for Class C limit determination in the j^{th} MFPV batch from algorithm calculation Step 1	(76) (80) (83) (111)
$SF_{LL,e}^{rad\ in\ can}$	sum of fractions of activity to the limit of each radionuclide for long-lived radionuclides for Class C limit determination in the e^{th} canister	(130)
$SF_{SL,e}^{rad\ in\ can}$	sum of fractions of activity to the limit of each radionuclide for short-lived radionuclides for Class C limit determination in the e^{th} canister	(131)
$t_{[Na],j}$	target sodium molarity of the melter feed (M)	(61) (62) (92)
\mathbf{t}_j	vector of $g_{ij}^{oxide\ in\ MFPV,\ target-gfc}$ for $n_j^{oxides\ in\ MFPV}$ components in the j^{th} MFPV batch (g oxide per g MFPV oxides)	(48)
$t_{2(1-\alpha),n_{ec}^{data\ in\ model} - n_{ec}^{terms\ in\ model}}$	100(1- α) percentile (=CL%) of a two-sided t-distribution with $n_{ec}^{data\ in\ model} - n_{ec}^{terms\ in\ model}$ degrees of freedom	(11)
$t_{2(1-\alpha),n_{vis}^{data\ in\ model} - n_{vis}^{terms\ in\ model}}$	100(1- α) percentile (=CL%) of a two-sided t-distribution with $n_{vis}^{data\ in\ model} - n_{vis}^{terms\ in\ model}$ degrees of freedom	(10)
T	absolute temperature in Kelvin (K)	(6) (7)
U_{comp}^{prop}	composition uncertainty for “prop”, i.e., uncertainty in predicted “prop” due to glass composition uncertainty (in property model units)	(15) (16)
$U_{comp,j}^{prop,\ Step1}$ $U_{comp,j}^{prop,\ Step3}$	composition uncertainty for “prop” for the j^{th} MFPV batch from algorithm calculation Step 1 or Step 3 (in property model units)	(67) (104)
$U_{comp,e}^{pct}$ $U_{comp,e}^{vht}$	composition uncertainty for “pct” ($\ln[r_B, g/L]$, $\ln[r_{Na}, g/L]$) and “vht” ($\ln[D, \mu m]$) for the e^{th} canister	(134) (135)
U_{pred}^{prop}	model prediction uncertainty for “prop” (calculated per Section 4.2.1) (in property model units)	(16)
U_{pred}^{ec}	prediction uncertainty for electrical conductivity (in $\ln[S/cm]$) model, which is given as a model uncertainty half width for a CL% two-sided CI	(11)
U_{pred}^{pct}	prediction uncertainty for PCT response (PCT-B or Na normalized release, in $\ln[g/L]$) model, which is given as a model uncertainty half width for a CL% SUCI	(8)
U_{pred}^{vht}	prediction uncertainty for VHT alteration depth (in $\ln[\mu m]$) model, which is given as a model uncertainty half width for a CL% SUCI	(9)
U_{pred}^{vis}	prediction uncertainty for viscosity (in $\ln[P]$) model, which is given as a model uncertainty half width for a CL% two-sided CI	(10)
$U_{pred,j}^{prop,\ Step1}$ $U_{pred,j}^{prop,\ Step3}$	model prediction uncertainty for “prop” for the j^{th} MFPV batch from algorithm calculation Step 1 or Step 3 (in property model units)	(67) (104)
$U_{pred,e}^{pct}, U_{pred,e}^{vht}$	model prediction uncertainty for “pct” ($\ln[r_B, g/L]$, $\ln[r_{Na}, g/L]$) and “vht” ($\ln[D, \mu m]$) for the e^{th} canister	(134) (135)

Symbol	Description	Equation(s)
$V_d^{heel,CRV}$	volume of the d^{th} CRV heel required for normal operation (L). The nominal value of $V_d^{heel,CRV}$ is 15,581 L (Table 1).	(20)
$V_d^{working,CRV}$	working volume of the d^{th} CRV measured before the sampling line flush water is added to the CRV (L). The nominal value of $V_d^{working,CRV}$ is 50,085 L (Table 1). The CRV working volume for each CRV batch includes the CRV heel volume ($V_d^{heel,CRV}$) required for normal operation plus the CRV batch volume ($V_d^{batch,CRV}$) transferred from TCP.	(19)
$V_d^{smpflush,CRV}$	volume of the sampling line flush water used for the d^{th} CRV batch (L)	(19)
$V_{d,m-1}^{current,CRV}$	current volume of the d^{th} CRV measured after the $m-1^{th}$ (previous) waste transfer to MFPV (L).	(19) (20)
$V_{d,m-1}^{transflush,CRV}$	volume of the CRV-MFPV transfer line flush water used for the d^{th} CRV after the $m-1^{th}$ (previous) waste transfer to MFPV (L).	(19)
$V_{d,m-1}^{transwaste,CRV}$	volume of the $m-1^{th}$ (previous) transfer waste transferred from the d^{th} CRV to MFPV (L).	(20)
$V_{dm}^{transwaste,CRV}$	volume of the m^{th} transfer waste to be transferred from the d^{th} CRV to MFPV (L).	(55) (56) (58) (60) (62) (63) (64) (65) (69) (89) (90) (91) (93) (94)
$V_j^{working,MFPV}$	working volume for the j^{th} MFPV batch (L). The MFPV working volume includes the MFPV heel volume ($V_j^{heel,MFPV}$) required for normal operation plus the MFPV batch volume ($V_j^{batch,MFPV}$) prepared. $V_j^{working,MFPV,nominal} = 12,444$ L	(55)
$V_j^{batch,MFPV}$	volume of the j^{th} MFPV batch (L)	(114) (115) (118) (119)
$V_j^{GFC,MFPV,Step1}$ $V_j^{GFC,MFPV,Step2}$ $V_j^{GFC,MFPV,Step3}$	total volume of GFCs to be added to or in the j^{th} MFPV batch in algorithm calculation Step 1, Step 2, or Step 3, i.e., $\sum_{k=1}^{n_j^{GFCs\ in\ MFPV}} V_{kj}^{GFC,MFPV,Step1}$, $\sum_{k=1}^{n_j^{GFCs\ in\ MFPV}} V_{kj}^{GFC,MFPV,Step2}$, or $\sum_{k=1}^{n_j^{GFCs\ in\ MFPV}} V_{kj}^{GFC,MFPV,Step3}$ (L) where $V_{kj}^{GFC,MFPV,Step1}$, $V_{kj}^{GFC,MFPV,Step2}$, or $V_{kj}^{GFC,MFPV,Step3}$ is the volume of k^{th} GFC to be added to or in the j^{th} MFPV batch (L) in algorithm calculation Step 1, Step 2, or Step 3. $n_j^{GFCs\ in\ MFPV}$ is the number of GFCs used in the j^{th} MFPV batch.	(55) (56) (93) (95) (115) (116)

Symbol	Description	Equation(s)
$V_j^{dust, MFPV, Step1}$ $V_j^{dust, MFPV, Step2}$	volume of water added to control GFC dusting in the j^{th} MFPV batch in algorithm calculation Step 1 or Step 2 (L)	(55) (57) (58) (62) (91) (92) (95)
$V_j^{dust, MFPV, measured}$	measured volume of water added to control GFC dusting in the j^{th} MFPV batch	(115)
$V_j^{sucrose, MFPV, Step1}$ $V_j^{sucrose, MFPV, Step2}$ $V_j^{sucrose, MFPV, Step3}$	volume of sucrose addition to the j^{th} MFPV batch (L) in algorithm calculation Step 1, Step 2, or Step 3 (L)	(55) (60) (94) (95) (115) (117)
$V_j^{heel, MFPV}$	volume of heel in the j^{th} MFPV batch measured prior to waste transfer (L)	(55) (95) (114) (119)
$V_j^{transflush, MFPV}$	volume of water used to flush the CRV-MFPV transfer line in the j^{th} MFPV batch (L)	(55) (62)
$V_j^{transflush, MFPV, measured}$	measured volume of water used to flush the CRV-MFPV transfer line in the j^{th} MFPV batch (L)	(92) (95) (115)
$V_j^{sampflush, MFPV}$	volume of water used to flush the MFPV sampling line in the j^{th} MFPV batch (L)	(55) (62) (92) (95)
$V_j^{sampflush, MFPV, measured}$	measured volume of water used to flush the MFPV sampling line in the j^{th} MFPV batch (L)	(115)
$V_j^{dilute, MFPV, Step1}$ $V_j^{dilute, MFPV, Step2}$	volume of dilution water required to maintain satisfactory melter-feed rheological properties in the j^{th} MFPV batch in algorithm calculation Step 1 or Step 2 (L)	(55) (62) (92) (95)
$V_j^{dilute, MFPV, measured}$	measured volume of dilution water added to maintain satisfactory melter-feed rheological properties in the j^{th} MFPV batch	(115)
$V_j^{waste, MFPV}$	volume of waste transferred from CRV to the j^{th} MFPV (L)	(12) (89) (90) (91) (92) (93) (94) (95) (96) (102) (106) (115) (118) (122)
$W_j^{initial}$	initial waste loading for the j^{th} MFPV batch determined from the Na ₂ O-SO ₃ -K ₂ O and Cl-F-SO ₃ rules ($g_{Na_2O, j}^{oxide in MFPV, pre-1}$ and $g_{Na_2O, j}^{oxide in MFPV, pre-2}$) by Equations (25) and (26)	(27) (28)
$W_j^{min, K}$	minimum waste loading for the j^{th} MFPV batch when 0.54 wt% of K ₂ O limit is assumed	(27) (29)
$W_j^{min, Cr}$	minimum waste loading for the j^{th} MFPV batch when 0.08 wt% of Cr ₂ O ₃ limit is assumed	(27) (30)

Symbol	Description	Equation(s)
x_h^{ec}	component mass fraction in glass or transformed value of component mass fractions to the appropriate basis for the h^{th} model term in the “ <i>ec</i> ” model	(7)
x_h^{pct}	component mass fraction in glass or transformed value of component mass fractions to the appropriate basis for the h^{th} model term in the “ <i>pct</i> ” model	(2)
x_h^{prop}	component mass fraction in glass or transformed value of component mass fractions to the appropriate basis for the h^{th} model term in the “ <i>prop</i> ” model	(1)
x_h^{vht}	component mass fraction in glass or transformed value of component mass fractions to the appropriate basis for the h^{th} model term in the “ <i>vht</i> ” model	(5)
x_h^{vis}	component mass fraction in glass or transformed value of component mass fractions to the appropriate basis for the h^{th} model term in the “ <i>vis</i> ” model	(6)
x_i^{ec}	mass fraction of the i^{th} model component in glass for the “ <i>ec</i> ” model, $\sum_{i=1}^{n_{ec}^{model}} x_i^{ec} = 1$	(7)
x_i^{pct}	mass fraction of the i^{th} model component in glass for the “ <i>pct</i> ” model, $\sum_{i=1}^{n_{pct}^{model}} x_i^{pct} = 1$	(2)
x_i^{prop}	mass fraction of the i^{th} model component in glass for the “ <i>prop</i> ” model	(3)
x_{Others}^{prop}	mass fraction of the “Others” model component in glass for the “ <i>prop</i> ” model	(4)
x_i^{vht}	mass fraction of the i^{th} model component in glass for the “ <i>vht</i> ” model, $\sum_{i=1}^{n_{vht}^{model}} x_i^{vht} = 1$	(5)
x_h^{vis}	mass fraction of the i^{th} model component in glass for the “ <i>vis</i> ” model, $\sum_{i=1}^{n_{vis}^{model}} x_i^{vis} = 1$	(6)
\mathbf{x}^{ec}	vector of x_h^{ec} values for the set of n_{ec}^{model} terms, where x_h^{ec} is component mass fraction in glass or transformed value of component mass fractions to the appropriate basis for the h^{th} model term in the “ <i>ec</i> ” model (note that \mathbf{x}^{ec} is temperature dependent)	(11)
\mathbf{x}^{pct}	vector of x_h^{pct} values for the set of n_{pct}^{model} terms, where x_h^{pct} is component mass fraction in glass or transformed value of component mass fractions to the appropriate basis for the h^{th} model term in the “ <i>pct</i> ” model	(8)
\mathbf{x}^{prop}	vectors of x_h^{prop} values for the set of n_{prop}^{model} terms	(1)

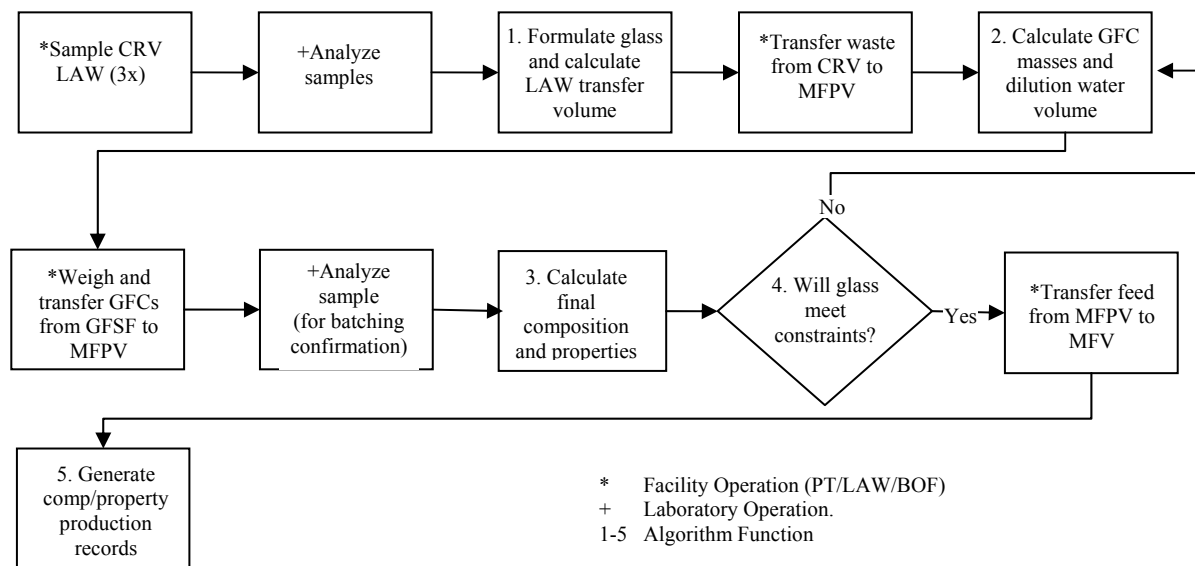
Symbol	Description	Equation(s)
\mathbf{x}^{vht}	vector of x_h^{vht} values for the set of n_{vht}^{model} terms, where x_h^{vht} is component mass fraction in glass or transformed value of component mass fractions to the appropriate basis for the h^{th} model term in the “vht” model	(9)
\mathbf{x}^{vis}	vector of x_h^{vis} values for the set of n_{vis}^{model} terms, where x_h^{vis} is component mass fraction in glass or transformed value of component mass fractions to the appropriate basis for the h^{th} model term in the “vis” model (note that \mathbf{x}^{vis} is temperature dependent)	(10)
α	a small fraction typically less than or equal to 0.1 used to represent the probability that a “100(1 – α) confidence interval” does not contain the true value	General
δ	a unitless constant larger than zero and typically smaller than 0.01 introduced to accommodate the variations resulting from Monte Carlo calculation of composition uncertainties	(83) (85) (86) (87)
ϵ_{1100}	melt electrical conductivity at 1100°C (S/cm)	General
ϵ_{1200}	melt electrical conductivity at 1200°C (S/cm)	General
η_{1100}	melt viscosity at 1100°C (P)	General
η_{1150}	melt viscosity at 1150°C (P)	General
ϵ_T	electrical conductivity (S/cm) at temperature T (K)	(7)
η_T	viscosity (P) at temperature T (K)	(6)
\mathbf{H}	11×11 matrix of $m_{ik}^{oxide\ in\ GFC}$ for GFC composition (for $i = \text{Al}_2\text{O}_3, \text{B}_2\text{O}_3, \text{CaO}, \text{Fe}_2\text{O}_3, \text{Li}_2\text{O}, \text{MgO}, \text{Na}_2\text{O}, \text{SiO}_2, \text{TiO}_2, \text{ZnO}, \text{and ZrO}_2$, with a corresponding GFC per each glass oxide component, g per g GFC including volatiles)	(48)
λ_{dm}	dilution factor caused by the addition of flush waters for the m^{th} transfer waste transferred from the d^{th} CRV to MFPV	(18) (23) (24) (53) (69) (100)
$\lambda_{d,m-1}$	dilution factor caused by the addition of flush waters for the $m-1^{th}$ (previous) transfer waste transferred from the d^{th} CRV batch to MFPV (dilution factor for the waste transferred previously)	(19)
v_i	retention factor for the i^{th} component (fraction)	(13) (52) (54) (66) (68) (70) (99) (101) (103) (105) (107) (122)
$\rho_e^{glass\ in\ can}$	density of glass in the e^{th} canister (g/L)	(128) (129)
$\rho_j^{glass\ in\ MFPV}$	density of glass in the j^{th} MFPV batch (g/L glass)	(71) (72) (108)
ρ_k	particle density of the k^{th} GFC (g/L)	(56) (116)
$\rho_{sucrose}$	particle density of sucrose (g/L)	(60) (117)
Σ^{ec}	variance-covariance matrix for the “ec” model	(11)

Symbol	Description	Equation(s)
Σ^{pct}	variance-covariance matrix for the “ <i>pct</i> ” model	(8)
Σ^{vht}	variance-covariance matrix for the “ <i>vht</i> ” model	(9)
Σ^{vis}	variance-covariance matrix for the “ <i>vis</i> ” model	(10)
ω_d	fraction of the sodium in the d^{th} CRV batch that is classified as waste sodium (unitless)	(68) (105)

3 Description of Process Steps

Figure 2 is a preliminary process flow diagram for the ILAW product compliance process.

Figure 2. Preliminary ILAW Product Qualification Process Flow Diagram



The ILAW formulation algorithm steps (those numbered activities in Figure 2) are highlighted below.

1. In the first step of the ILAW product compliance process, analytical data from the LAW CRV samples will be screened and evaluated prior to calculating glass formulation. The data screening should include, at a minimum, outlier identification, and trending evaluation. The analytical data given in concentration of chemical elements and activity of radionuclides will be converted to the forms used in glass formulation.

Glass formulation will be performed based on the composition of CRV waste and the composition of GFCs. Glass formulation does not include the content of the heel from a previous MFPV batch. The target glass composition will be calculated following the glass formulation rules described in Section 5.1.3. The glass properties with uncertainties will be calculated from the target glass formulation and compared with the constraints. The formulation will also be checked to make sure that it meets all the constraints described in Section 4.3. The resulting glass formulation will be used to calculate volume of waste transfer and the mass of GFCs including sucrose. The volume relation will be solved to calculate the waste transfer volume. The output of Step 1 calculation is the waste transfer volume.

2. In the second step, after waste transfer to the MFPV, the actual measured waste transfer volume will be used to calculate the masses of GFCs based on glass formulation completed in Step 1 (i.e., glass formulation is not performed in this step, instead the Step 1 formulation results are used to calculate the GFC masses.) The volume of dilution water will also be recalculated after accounting for changes in other process water volumes.
3. The final glass-composition estimate associated with a completed MFPV batch will be made in Step 3. The actual measured volume of waste transfer, actual measured volumes of various process waters, and

the actual measured masses of GFCs are used to calculate the final composition and predict the properties of the glass with uncertainties using glass composition-property models.

The MFPV contents including heel and newly added MFPV batch will be sampled and analyzed for major glass components to confirm proper GFC addition, but this is not a process hold point. Trending analyses will be performed on the differences between the analytical results and calculated values to detect potential errors in the MFPV batch preparation.

4. In Step 4, the projected LAW glass composition and predicted properties (corresponding to the MFPV batch) will be statistically compared (i.e., accounting for uncertainties) to composition and property constraints summarized in Section 4.3. If the constraints are met, then the MFPV batch will be transferred to the MFV for processing. If any constraint is not met then an operator will be alerted for intervention. If a product quality constraint is not met then the process may return to Step 2.
5. In Step 5, the appropriate waste form compliance quantities will be recorded for inclusion in the Production Records for ILAW containers within the current lot.

The calculation logic and equations required to implement Steps 1 through 5 are presented in detail in Section 5 and illustrated in Section 6.

4 Description of Property Predictions, Uncertainties, and Constraints

The objective of glass formulation for a given waste is to calculate the acceptable glass composition that meets various processing and product-quality related constraints. For LAW, the initial glass composition is estimated using the glass formulation rules developed by Muller et al. (2004) and supplemented by CCN 150795, described in Section 5.1.3. Several of the processing and product-quality related constraints are based on LAW glass properties implemented by property-composition models. The following subsections present the property predictions, associated uncertainty calculations, and constraints used to meet the key ILAW formulation algorithm steps, as described in Section 3.

The mass balance equations and statistical methods and formulas used in several steps of the formulation algorithm are based on compliance strategy development work in Piepel et al. (2005) and estimates of variation and uncertainty in Piepel et al. (2006). Citations are given to specific sections of those documents in subsequent sections of this report for those who want additional details contained in those documents.

4.1 Property Predictions

The melter feed should be both processable and yield an adequate product, i.e., the resultant glass should have properties within acceptable ranges. Therefore, the properties of the target glass are predicted using glass-composition property models.

The property-composition models were developed for processing and product-quality properties of LAW glasses and melts, including (Piepel et al. 2007):

- Normalized B and Na releases by PCT (r_B and r_{Na})
- Alteration depth by VHT at 200°C (D)
- Viscosity as a function of temperature (η_T)
- Electrical conductivity as a function of temperature (ϵ_T)

A general form of all the property-composition models above is given as:

$$P^{prop} = \sum_{h=1}^{n_{prop}^{model}} p_h^{prop} x_h^{prop} = (\mathbf{p}^{prop})^T \mathbf{x}^{prop} \quad (1)$$

where p^{prop} = transformed property “prop”, which includes $\ln(r_B, \text{g/L})$, $\ln(r_{Na}, \text{g/L})$, $\ln(D, \mu\text{m})$, $\ln(\eta_T, \text{P})$, and $\ln(\epsilon_T, \text{S/cm})$

n_{prop}^{model} = number of model terms in the “prop” model

p_h^{prop} = coefficient of the h^{th} model term for the “prop” model

x_h^{prop} = component mass fraction in glass or transformed value of component mass fractions to the appropriate basis for the h^{th} model term in the “prop” model

\mathbf{p}^{prop} and \mathbf{x}^{prop} = vectors of p_h^{prop} and x_h^{prop} values for the set of $n_{prop}^{terms\ in\ model}$ terms

The property models are valid only over the region of component mass fractions where experimental data were available to develop them. Thus, extrapolation beyond currently tested compositional bounds will not be done and the model validity ranges become constraints for formulating acceptable glass composition discussed in Section 4.3. Refer to Piepel et al. (2007) for detailed information on the data and methods used to develop the models and the limitations that need to be considered when using these models.

4.1.1 Product Consistency Test

The model for PCT normalized releases as a function of LAW glass composition is [Piepel et al. 2007, see Equation (5.2)]:

$$\ln(r_B, r_{Na}) = \sum_{h=1}^{n_{pct}^{terms\ in\ model}} p_h^{pct} x_h^{pct} = P^{pct}$$

$$= \sum_{i=1}^{n_{pct}^{comps\ in\ model}} p_i^{pct} x_i^{pct} + \text{Selected} \left\{ \sum_{i=1}^{n_{pct}^{comps\ in\ model}} p_{ii}^{pct} (x_i^{pct})^2 + \sum_{i < i'}^{n_{pct}^{comps\ in\ model} - 1} p_{ii'}^{pct} x_i^{pct} x_{i'}^{pct} \right\} \quad (2)$$

where

r_B, r_{Na} = normalized release for B or Na (g/L)

P^{pct} = transformed normalized release (= $\ln[r_B, \text{g/L}]$ and $\ln[r_{Na}, \text{g/L}]$) for $pct = \text{pctB}$ and pctNa respectively

$n_{pct}^{terms\ in\ model}$ = number of model terms in the “ pct ” model

p_h^{pct} = coefficient of the h^{th} model term for the “ pct ” model ($\ln[\text{g/L}]$). p_h^{pct} represents all forms of the model term, i.e., p_i^{pct} , p_{ii}^{pct} (selected), and $p_{ii'}^{pct}$ (selected)

x_h^{pct} = component mass fraction in glass or transformed value of component mass fractions to the appropriate basis for the h^{th} model term in the “ pct ” model

$n_{pct}^{comps\ in\ model}$ = number of model components in the “ pct ” model

p_i^{pct} = coefficient of the i^{th} model component for the “ pct ” model ($\ln[\text{g/L}]$) (represents Al_2O_3 through Others terms in Table 5)

p_{ii}^{pct} (selected) = coefficients for the selected quadratic model terms. “Selected” means that only some of the terms in curly brackets are included in the model ($\ln[\text{g/L}]$)

$p_{ii'}^{pct}$ (selected) = (represent $\text{CaO} \times \text{Li}_2\text{O}$ through $(\text{K}_2\text{O})^2$ terms in Table 5)

mass fraction of the i^{th} model component in glass for the “ pct ” model,

$$x_i^{pct} = \sum_{i=1}^{n_{pct}^{comps\ in\ model}} x_i^{pct} = 1$$

Existing data has shown that the r_{Si} values are always below the r_B and r_{Na} values due to Si solubility limits in the leaching solution (Piepel et al. 2007). Therefore, r_{Si} is predicted to be less than the minimum of r_B and r_{Na} and the models for the r_{Si} values are not needed.

The PCT model coefficients (p_h^{pct}) are listed in Table 5 (from Table 5.9 and Table 5.14 in Piepel et al.

2007). Table 5 also lists the model statistics including R^2 statistics, $S_{pct}^{rmse\ of\ model}$ (root mean squared error

[RMSE] for the model), and $n_{pct}^{data\ in\ model}$ (number of data points used to fit the model).

For all “prop” models, the mass fraction of the i^{th} model component is given as the mass fraction of the i^{th} glass oxide component in glass (g oxide per g glass) for all model components except for “Others” component, i.e.,

$$x_i^{prop} = g_i \quad (i \neq \text{Others}) \tag{3}$$

where x_i^{prop} is the mass fraction of the i^{th} model component in glass for the “prop” model and g_i is the mass fraction of the i^{th} glass oxide component in glass. The mass fraction of “Others” component is a sum of mass fractions of remaining components not included in the model components and is calculated as:

$$x_{Others}^{prop} = 1 - \sum_{i=1}^{n_{prop}^{comps\ in\ model} - 1} g_i \tag{4}$$

where x_{Others}^{prop} is the mass fraction of the “Others” model component in glass for the “prop” model.

Table 5. PCT Release-Composition Model Coefficients and Selected Statistical Parameters

Model Term	Model Coefficients	
	$\ln(r_B, \text{g/L})$	$\ln(r_{Na}, \text{g/L})$
Al ₂ O ₃	-31.3612	-20.7142
B ₂ O ₃	11.8101	-6.5489
CaO	-13.8404	0.0151
Fe ₂ O ₃	-16.5948	-8.4617
K ₂ O	7.9687	-0.8724
Li ₂ O	83.3036	44.7604
MgO	-21.2343	-13.8667
Na ₂ O	46.1599	9.9942
P ₂ O ₅	-19.254	-14.5324
SiO ₂	-1.6161	-4.8834
ZrO ₂	-6.6289	-0.62
Others	-5.169	3.345
CaO×Li ₂ O	-251.2654	-232.1695
CaO×Fe ₂ O ₃	212.0947	182.6191
B ₂ O ₃ ×MgO	488.8612	437.4267
B ₂ O ₃ ×Li ₂ O	-374.9533	N/A
Na ₂ O×SiO ₂	-74.3462	N/A
B ₂ O ₃ ×Na ₂ O	N/A	87.6716
(K ₂ O) ²	N/A	315.6867

Statistic	Value	Value
R ²	0.866	0.870
R ² Adjusted	0.857	0.861
R ² Predicted	0.835	0.840
R ² Validation ^(a)	0.769	0.804
$rmse\ of\ S_{pct}^{model}, \ln(g/L)$	0.291	0.255
$n_{pct}^{comps\ in\ model}$	12	12
$n_{pct}^{terms\ in\ model}$	17	17
$n_{pct}^{data\ in\ model}$	244	244

N/A: not applicable

(a) Based on data splitting method (see Table 5.9 and Table 5.14 in Piepel et al. 2007).

4.1.2 Vapor Hydration Test

The model for VHT alteration depth as a function of LAW glass composition is [Piepel et al. 2007, Equation (6.4) without the partial quadratic model terms]:

$$\begin{aligned}
 \ln(D) &= \sum_{h=1}^{n_{vht}^{terms\ in\ model}} p_h^{vht} x_h^{vht} = P^{vht} \\
 &= \sum_{i=1}^{comps\ in\ model} p_i^{vht} x_i^{vht} + \text{Selected} \left\{ \begin{aligned} &\sum_{i=1}^{comps\ in\ model} p_{iii}^{vht} (x_i^{vht})^3 + \sum_{i < i'}^{comps\ in\ model} \sum_{i''}^{comps\ in\ model} p_{iii'}^{vht} (x_i^{vht})^2 x_{i'}^{vht} \\ &+ \sum_{i < i' < i''}^{comps\ in\ model} \sum_{i'''}^{comps\ in\ model} p_{ii'i''}^{vht} x_i^{vht} x_{i'}^{vht} x_{i''}^{vht} \end{aligned} \right\} \quad (5)
 \end{aligned}$$

where

- D = VHT alteration depth (μm)
- P^{vht} = transformed VHT alteration depth (ln[D, μm])
- $n_{vht}^{terms\ in\ model}$ = number of model terms in the “vht” model coefficient of the h^{th} model term for the “vht” model (ln[g/L]) p_h^{vht} represents all forms of the model
- p_h^{vht} = term, i.e., p_i^{vht} , p_{iii}^{vht} (selected), $p_{iii'}^{vht}$ (selected), and $p_{ii'i''}^{vht}$ (selected)
- x_h^{vht} = component mass fraction in glass or transformed value of component mass fractions to the appropriate basis for the h^{th} model term in the “vht” model
- $n_{vht}^{comps\ in\ model}$ = number of model components in the “vht” model
- p_i^{vht} = coefficient of the i^{th} model component for the “vht” model (ln[g/L]) (represents Al₂O₃ through Others terms in Table 6)

p_{iii}^{vht} (selected) coefficients for the selected cubic model terms. “Selected” means that only
 $p_{iii'}^{vht}$ (selected) = some of the terms in curly brackets are included in the model (ln[g/L])
 $p_{ii'it''}^{vht}$ (selected) (represent $(K_2O)^2 \times Na_2O$ through $B_2O_3 \times CaO \times Na_2O$ terms in Table 6)

mass fraction of the i^{th} model component in glass for the “vht” model,

$$x_i^{vht} = \sum_{i=1}^{comps\ in\ model} x_i^{vht} = 1$$

The VHT model coefficients (p_h^{vht}) are listed in Table 6 (from Table 6.11 in Piepel et al. 2007). Table 6 also lists the model statistics including R^2 statistics, s_{vht}^{model} (root mean squared error [RMSE] for the model), and $n_{vht}^{data\ in\ model}$ (number of data points used to fit the model).

Table 6. VHT Alteration Depth-Composition Model Coefficients and Selected Statistical Parameters

Model Term	Coefficient, ln(D, μm)
Al ₂ O ₃	19.5685
B ₂ O ₃	18.5336
CaO	38.2412
Fe ₂ O ₃	-8.4126
K ₂ O	-39.3124
Li ₂ O	-17.8250
MgO	-8.3068
Na ₂ O	-20.6518
SiO ₂	-0.5137
ZrO ₂	-62.8457
Others	-0.4293
$(K_2O)^2 \times Na_2O$	10138.2817
$(Na_2O)^3$	872.6563
$Li_2O \times Na_2O \times SiO_2$	2139.8048
$B_2O_3 \times CaO \times Na_2O$	-1943.0687
Statistic	Value
R^2	0.744
R^2 Adjusted	0.720
R^2 Predicted	0.696
R^2 Validation ^(a)	0.677
s_{pct}^{model} , ln(g/L)	0.848
$n_{pct}^{comps\ in\ model}$	11
$n_{pct}^{terms\ in\ model}$	15
$n_{pct}^{data\ in\ model}$	165

(a) Based on data splitting method (see Table 6.11 in Piepel et al. 2007).

4.1.3 Melt Viscosity

The model for viscosity as a function of melt temperature and LAW melt composition can be expressed as [Piepel et al. 2007, see Equation (8.2)]:

$$\begin{aligned} \ln(\eta_T) &= \sum_{h=1}^{n_{vis}^{model}} p_h^{vis} x_h^{vis} = P^{vis} \\ &= \sum_{i=1}^{n_{vis}^{model}} p_i^{vis} x_i^{vis} + \text{Selected} \left\{ \sum_{i=1}^{n_{vis}^{model}} p_{ii}^{vis} (x_i^{vis})^2 + \sum_{i < i'}^{n_{vis}^{model}-1} p_{ii'}^{vis} x_i^{vis} x_{i'}^{vis} \right\} \\ &\quad + \text{Selected} \left\{ \sum_{i=1}^{n_{vis}^{model}} p_i^{vis,T} \frac{x_i^{vis}}{(T/1000)^2} \right\} \end{aligned} \quad (6)$$

where

η_T = viscosity (P) at temperature T (K)

P^{vis} = transformed viscosity at temperature T (K) ($\ln[P]$)

n_{vis}^{model} = number of model terms in the “vis” model

coefficient of the h^{th} model term for the “vis” model ($\ln[P]$). p_h^{vis} represents

p_h^{vis} = all forms of the model term, i.e., p_i^{vis} , p_{ii}^{vis} (selected), $p_{ii'}^{vis}$ (selected), and $p_i^{vis,T}$ (selected)

x_h^{vis} = component mass fraction in glass or transformed value of component mass fractions to the appropriate basis for the h^{th} model term in the “vis” model

n_{vis}^{comps} = number of model components in the “vis” model

p_i^{vis} = coefficient of the i^{th} model component in the “vis” model (represents Al_2O_3 through “Others” terms in Table 7)

p_{ii}^{vis} (selected) = coefficients for the selected quadratic model terms in the “vis” model.

$p_{ii'}^{vis}$ (selected) = “Selected” means that only some of the terms in curly brackets are included in the model. (represent $Al_2O_3 \times SiO_2$ through $(Li_2O)^2$ terms in Table 7)

$p_i^{vis,T}$ (selected) = coefficient of the selected i^{th} model component for the model terms involving temperature in the “vis” model. “Selected” means that only some of the terms in curly brackets are included in the model. (represents $Al_2O_3/(T/1000)^2$ through $Others/(T/1000)^2$ terms in Table 7)

mass fraction of the i^{th} model component in glass for the “vis” model,

$$x_i^{vis} = \sum_{i=1}^{n_{vis}^{comps}} x_i^{vis} = 1$$

T = absolute temperature in Kelvin (K)

The viscosity model coefficients (p_h^{vis}) are listed in Table 7 (from Table 8.8 in Piepel et al. 2007). Note that some of the model terms (x_h^{vis}) are temperature dependent so that the viscosity is estimated as a function of temperature. Table 7 also lists the model statistics including R^2 statistics, s_{vis}^{model} (RMSE for the model), and $n_{vis}^{data in model}$ (number of data points used to fit the model).

Table 7. Viscosity-Composition Model Coefficients and Selected Statistical Parameters

Model Term	Coefficient, $\ln(\eta_T, P)$	Statistic	Value
Al ₂ O ₃	5.5124	R ²	0.988
B ₂ O ₃	-42.3772	R ² Validation ^(a)	0.983
CaO	-10.6445	s_{vis}^{model} , $\ln(P)$	0.147
Fe ₂ O ₃	-4.6220	$n_{vis}^{comps in model}$	12
K ₂ O	-0.8689	$n_{vis}^{terms in model}$	26
Li ₂ O	10.9390	$n_{vis}^{data in model}$	171
MgO	-5.6188		
Na ₂ O	0.9073		
P ₂ O ₅	-0.8081		
SiO ₂	1.5575		
ZrO ₂	-12.0741		
Others	-9.3903		
(B ₂ O ₃) ²	198.7360		
(Li ₂ O) ²	133.6906		
Al ₂ O ₃ ×Li ₂ O	-136.5095		
(MgO) ²	-179.8249		
Al ₂ O ₃ /(T/1000) ²	24.6423		
CaO/(T/1000) ²	13.7793		
Fe ₂ O ₃ /(T/1000) ²	15.2036		
Li ₂ O/(T/1000) ²	-82.4815		
MgO/(T/1000) ²	22.7608		
Na ₂ O/(T/1000) ²	-14.5621		
P ₂ O ₅ /(T/1000) ²	24.0339		
SiO ₂ /(T/1000) ²	24.4077		
ZrO ₂ /(T/1000) ²	48.2286		
Others/(T/1000) ²	17.3800		

(b) Based on data splitting method (see Table 8.8 in Piepel et al. 2007).

4.1.4 Melt Electrical Conductivity

The model for glass melt electrical conductivity as a function of melt temperature and glass composition can be expressed as [Piepel et al. 2007, see Equation (7.2)]:

$$\begin{aligned} \ln(\varepsilon_T) &= \sum_{h=1}^{n_{ec}^{model}} p_h^{ec} x_h^{ec} = P^{ec} \\ &= \sum_{i=1}^{n_{ec}^{model}} p_i^{ec} x_i^{ec} + \text{Selected} \left\{ \sum_{i < i'}^{n_{ec}^{model}-1} p_{ii'}^{ec} x_i^{ec} x_{i'}^{ec} \right\} + \sum_{i=1}^{n_{ec}^{model}} p_i^{ec,T} \frac{x_i^{ec}}{(T/1000)} \end{aligned} \quad (7)$$

where

ε_T = electrical conductivity (S/cm) at temperature T (K)

P^{ec} = transformed electrical conductivity at temperature T (K) (ln[S/cm])

n_{ec}^{model} = number of model terms in the “ec” model

p_h^{ec} = coefficient of the h^{th} model term for the “ec” model (S/cm). p_h^{ec} represents all forms of the model term, i.e., p_i^{ec} , $p_{ii'}^{ec}$ (selected), and $p_i^{ec,T}$

x_h^{ec} = component mass fraction in glass or transformed value of component mass fractions to the appropriate basis for the h^{th} model term in the “ec” model

$n_{ec}^{comps in model}$ = number of model components in the “ec” model

p_i^{ec} = coefficient of the i^{th} model component in the “ec” model (represents Al_2O_3 through Others terms in Table 8)

$p_{ii'}^{ec}$ (selected) = coefficients for the selected quadratic model terms in the “ec” model. “Selected” means that only some of the terms in curly brackets are included in the model. (represent $CaO \times Li_2O$, $CaO \times Na_2O$, and $Li_2O \times Na_2O$ terms in Table 8)

$p_i^{ec,T}$ = coefficient of the i^{th} model component for the model terms involving temperature in the “ec” model. (represents $A_2O_3/(T/1000)$ through Others/(T/1000) terms in Table 8)

x_i^{ec} = mass fraction of the i^{th} model component in glass for the “ec” model,

$$\sum_{i=1}^{n_{ec}^{comps in model}} x_i^{ec} = 1$$

T = absolute temperature in Kelvin (K)

The electrical conductivity model coefficients (p_h^{ec}) are listed in Table 8 (from Table 7.10 in Piepel et al. 2007). Note that some of the model terms (x_h^{ec}) are temperature dependent so that the electrical

conductivity is estimated as a function of temperature. Table 8 also lists the model statistics including R² statistics, s_{ec}^{model} (RMSE for the “ec” model), and n_{ec}^{data} (number of data points used to fit the “ec” model).

Table 8. Electrical Conductivity-Composition Model Coefficients and Selected Statistical Parameters

Model Term	Coefficient, ln(ϵ_T , S/cm)	Statistic	Value
Al ₂ O ₃	2.3854	R ²	0.951
B ₂ O ₃	7.9750	R ² Validation ^(a)	0.936
CaO	5.2093	s_{vis}^{model} , ln(P)	0.151
Fe ₂ O ₃	4.3935	$n_{vis}^{comps\ in\ model}$	11
K ₂ O	7.6774	$n_{vis}^{terms\ in\ model}$	25
Li ₂ O	4.2464	$n_{vis}^{data\ in\ model}$	171
MgO	15.1675		
Na ₂ O	-2.0291		
SiO ₂	3.6811		
ZrO ₂	7.8740		
Others	11.2069		
CaO×Li ₂ O	144.9519		
CaO×Na ₂ O	79.0190		
Li ₂ O×Na ₂ O	-130.1441		
Al ₂ O ₃ /(T/1000)	-9.0593		
B ₂ O ₃ /(T/1000)	-11.0983		
CaO/(T/1000)	-30.6535		
Fe ₂ O ₃ /(T/1000)	-9.2407		
K ₂ O/(T/1000)	-11.5299		
Li ₂ O/(T/1000)	30.4827		
MgO/(T/1000)	-25.0634		
Na ₂ O/(T/1000)	12.3822		
SiO ₂ /(T/1000)	-10.1563		
ZrO ₂ /(T/1000)	-16.5390		
Others/(T/1000)	-17.7117		

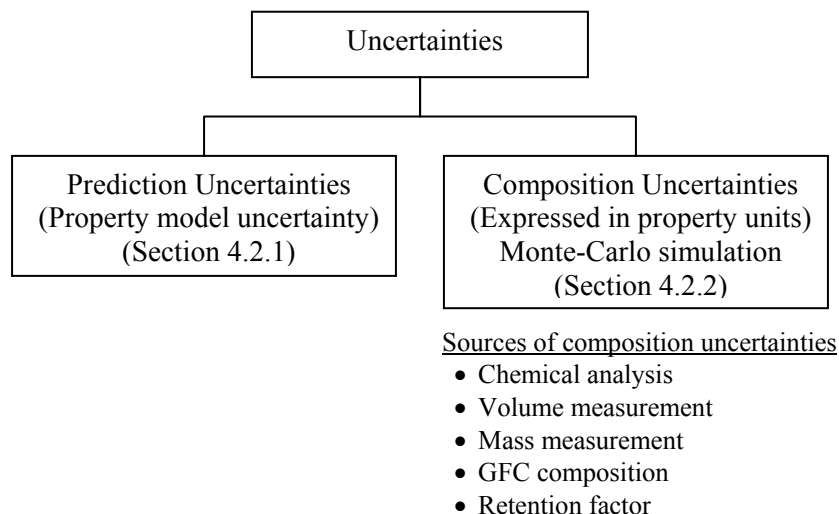
(a) Based on data splitting method (see Table 7.10 in Piepel et al. 2007).

4.2 Uncertainties for Predicted Properties

The use of the property-composition models introduces model prediction uncertainties (U_{pred}^{prop}) and composition uncertainties (U_{comp}^{prop}) that must be accounted for in comparing the predicted properties to their limits (L^{prop}). The following subsections present the equations used to calculate prediction uncertainties of property-composition models and composition uncertainties, expressed in property units, resulting from uncertain values used to estimate the glass composition. The total uncertainty combining model prediction uncertainty and composition uncertainty is also presented. A block diagram in Figure 3 summarizes the

prediction and composition uncertainties and the sources of composition uncertainties discussed in the following subsections.

Figure 3. Block Diagram Showing the Sources of Uncertainties Applied To Glass Formulation



4.2.1 Prediction Uncertainties for Predicted Properties

A confidence level percent (CL%) simultaneous confidence interval (SUCI) is used to account for prediction uncertainties for PCT and VHT as discussed in Piepel et al. (2005). A CL% two-sided confidence interval (CI) is used for viscosity and electrical conductivity that have both upper and lower limits. In summary, two types of confidence interval methods are used:

- Model uncertainty half width for a CL% simultaneous upper confidence interval (CL% SUCI) for PCT and VHT (Piepel et al. 2005, Section 5.4.3.2)
- Model uncertainty half width for a CL% two-sided confidence interval (CL% two-sided CI) for viscosity and electrical conductivity

The prediction uncertainty for PCT is calculated:

$$U_{pred}^{pct} = \sqrt{n_{pct}^{model} F_{1-\alpha, (n_{pct}^{model}, n_{pct}^{data} - n_{pct}^{model})} \left(\mathbf{x}^{pct} \right)^T \Sigma^{pct} \mathbf{x}^{pct}} \tag{8}$$

where U_{pred}^{pct} = prediction uncertainty for PCT response (PCT-B or Na normalized release, in ln[g/L]) model, which is given as a model uncertainty half width for a CL% SUCI

n_{pct}^{model} = number of model terms in the “pct” model

n_{pct}^{data} = number of data points used to fit the “pct” model

$F_{1-\alpha, (n_{pct}^{model}, n_{pct}^{data} - n_{pct}^{model})}$ = 100(1- α) percentile (=CL%) of an F-distribution with n_{pct}^{model}

numerator degrees of freedom and $n_{pct}^{data\ in\ model} - n_{pct}^{terms\ in\ model}$ denominator degrees of freedom

α = a small fraction typically less than or equal to 0.1 used to represent the probability that a “100(1- α) confidence interval” does not contain the true value

\mathbf{x}^{pct} = vector of x_h^{pct} values for the set of $n_{pct}^{terms\ in\ model}$ terms, where x_h^{pct} is component mass fraction in glass or transformed value of component mass fractions to the appropriate basis for the h^{th} model term in the “pct” model

Σ^{pct} = variance-covariance matrix for the “pct” model

A variance-covariance matrix, Σ^{prop} , is calculated for the estimated coefficients of a model fitted by regression according to, $\Sigma^{prop} = \left(s_{prop}^{rmse\ of\ model} \right)^2 \left[(\mathbf{X}^{prop})^T \mathbf{X}^{prop} \right]^{-1}$ where $s_{prop}^{rmse\ of\ model}$ is the RMSE for the “prop” model, and \mathbf{X}^{prop} is the matrix of glass composition vectors for all the data points (glasses) used to fit the “prop” model (Piepel et al. 2008). The variance-covariance matrices for PCT models (Σ^{pctB} , Σ^{pctNa}) are listed in Tables A-7 and A-8 of Appendix A.

The prediction uncertainty for VHT is calculated:

$$U_{pred}^{vht} = \sqrt{ n_{vht}^{terms\ in\ model} F_{1-\alpha, (n_{vht}^{terms\ in\ model}, n_{vht}^{data\ in\ model} - n_{vht}^{terms\ in\ model})} \left(\mathbf{x}^{vht} \right)^T \Sigma^{vht} \mathbf{x}^{vht} } \tag{9}$$

where

U_{pred}^{vht} = prediction uncertainty for VHT alteration depth (in ln[μ m]) model, which is given as a model uncertainty half width for a CL% SUCI

$n_{vht}^{terms\ in\ model}$ = number of model terms in the “vht” model

$n_{vht}^{data\ in\ model}$ = number of data points used to fit the “vht” model

$F_{1-\alpha, (n_{vht}^{terms\ in\ model}, n_{vht}^{data\ in\ model} - n_{vht}^{terms\ in\ model})}$ = 100(1- α) percentile (=CL%) of an F-distribution with $n_{vht}^{terms\ in\ model}$ numerator degrees of freedom and $n_{vht}^{data\ in\ model} - n_{vht}^{terms\ in\ model}$ denominator degrees of freedom

α = a small fraction typically less than or equal to 0.1 used to represent the probability that a “100(1- α) confidence interval” does not contain the true value

\mathbf{x}^{vht} = vector of x_h^{vht} values for the set of $n_{vht}^{terms\ in\ model}$ terms, where x_h^{vht} is component mass fraction in glass or transformed value of component mass fractions to the appropriate basis for the h^{th} model term in the

“vht” model

Σ^{vht} = variance-covariance matrix for the “vht” model

The variance-covariance matrix for VHT model (Σ^{vht}) is listed in Table A-9.

The prediction uncertainty for viscosity as a function of temperature is calculated:

$$U_{pred}^{vis} = t_{2(1-\alpha), n_{vis}^{model} - n_{vis}^{terms}} \sqrt{(\mathbf{x}^{vis})^T \Sigma^{vis} \mathbf{x}^{vis}} \quad (10)$$

- where
- U_{pred}^{vis} = prediction uncertainty for viscosity (in ln[P]) model, which is given as a model uncertainty half width for a CL% two-sided CI
 - n_{vis}^{data} = number of data points used to fit the “vis” model
 - n_{vis}^{terms} = number of model terms in the “vis” model
 - $t_{2(1-\alpha), n_{vis}^{data} - n_{vis}^{terms}}$ = 100(1- α) percentile (=CL%) of a two-sided t-distribution with $n_{vis}^{data} - n_{vis}^{terms}$ degrees of freedom
 - \mathbf{x}^{vis} = vector of x_h^{vis} values for the set of n_{vis}^{terms} terms, where x_h^{vis} is component mass fraction in glass or transformed value of component mass fractions to the appropriate basis for the h^{th} model term in the “vis” model (note that \mathbf{x}^{vis} is temperature dependent)
 - Σ^{vis} = variance-covariance matrix for the “vis” model

The variance-covariance matrix for viscosity model (Σ^{vis}) is given in Table A-10.

The prediction uncertainty for electrical conductivity as a function of temperature is calculated:

$$U_{pred}^{ec} = t_{2(1-\alpha), n_{ec}^{model} - n_{ec}^{terms}} \sqrt{(\mathbf{x}^{ec})^T \Sigma^{ec} \mathbf{x}^{ec}} \quad (11)$$

- where
- U_{pred}^{ec} = prediction uncertainty for electrical conductivity (in ln[S/cm]) model, which is given as a model uncertainty half width for a CL% two-sided CI
 - n_{ec}^{data} = number of data points used to fit the “ec” model
 - n_{ec}^{terms} = number of model terms in the “ec” model
 - $t_{2(1-\alpha), n_{ec}^{data} - n_{ec}^{terms}}$ = 100(1- α) percentile (=CL%) of a two-sided t-distribution with $n_{ec}^{data} - n_{ec}^{terms}$ degrees of freedom
 - \mathbf{x}^{ec} = vector of x_h^{ec} values for the set of n_{ec}^{terms} terms, where x_h^{ec} is component mass fraction in glass or transformed value of component mass fractions to the appropriate basis for the h^{th} model term in the “ec” model (note that \mathbf{x}^{ec} is temperature dependent)

Σ^{ec} = variance-covariance matrix for the “ec” model

The variance-covariance matrix for electrical conductivity model (Σ^{ec}) is given in Table A-11.

4.2.2 Composition Uncertainties for Predicted Properties

Glass properties are calculated from glass composition(s) based on estimated feed composition in two different steps of algorithm process steps described in Section 3: (1) Step 1 – Formulate glass and calculate LAW transfer and dilution water volumes (more specifically, sub-steps 1b, 1c, 1e, and 1f in Figure 4) and (2) Step 3 – Calculate final glass composition and properties from waste transfer and GFC masses (sub-steps 3a and 3b in Figure 4). A mass balance equation is used in Steps 1 and 3 of the algorithm to calculate the glass composition from the volume and composition of waste and mass and composition of GFCs. The composition uncertainty results from uncertain values used in the mass balance equation and is calculated using Monte Carlo simulation. The glass property models are applied to determine the impacts of the uncertain composition on property estimates.

The mass balance equations for glass formulation for the j^{th} MFPV batch are given by:

$$g_{ij}^{\text{oxide in MFPV}} = \frac{\frac{c_{id}^{\text{element in CRV}} f_i V_j^{\text{waste MFPV}}}{1000(\text{mg/g})} + \sum_{k=1}^{n_j^{\text{GFCs in MFPV}}} m_{ik}^{\text{oxide in GFC}} M_{kj}^{\text{GFC in MFPV}}}{\sum_{i=1}^{n_d^{\text{oxides in CRV}}} \frac{c_{id}^{\text{element in CRV}} f_i V_j^{\text{waste MFPV}}}{1000(\text{mg/g})} + \sum_{i=1}^{n_j^{\text{oxides in MFPV}}} \sum_{k=1}^{n_j^{\text{GFCs in MFPV}}} m_{ik}^{\text{oxide in GFC}} M_{kj}^{\text{GFC in MFPV}}} \quad (12)$$

$$\tilde{g}_{ij}^{\text{oxide in MFPV}} = \frac{g_{ij}^{\text{oxide in MFPV}} v_i}{\sum_{i=1}^{n_j^{\text{oxides in MFPV}}} g_{ij}^{\text{oxide in MFPV}} v_i} \quad (13)$$

- where
- $g_{ij}^{\text{oxide in MFPV}}$ = mass fraction of the i^{th} glass oxide in the j^{th} MFPV batch before applying the component retention factors (g oxide per g glass)
 - $\tilde{g}_{ij}^{\text{oxide in MFPV}}$ = mass fraction of the i^{th} glass oxide in the j^{th} MFPV batch after applying the component retention factors (g oxide per g glass), i.e., mass of i^{th} glass oxide that will remain in glass divided by the total mass of all glass oxides that will remain in glass
 - $c_{id}^{\text{element in CRV}}$ = concentration of the i^{th} element in the d^{th} CRV batch associated with the j^{th} MFPV batch (mg/L)
 - f_i = oxide conversion factor, i.e., mass of the i^{th} glass oxide per mass of the i^{th} element
 - $V_j^{\text{waste MFPV}}$ = volume of waste transferred from CRV to the j^{th} MFPV (L)
 - $n_j^{\text{GFCs in MFPV}}$ = number of GFCs used in the j^{th} MFPV batch

$m_{ik}^{oxides\ in\ GFC}$ = mass fraction of the i^{th} glass oxide in the k^{th} GFC (g oxide per g GFC including volatiles)

$M_{kj}^{GFC\ in\ MFPV}$ = mass of the k^{th} GFC to add to the j^{th} MFPV batch (g)

V_i = retention factor for the i^{th} component (fraction) (listed in Table A-3)

$n_d^{oxides\ in\ CRV}$ = number of glass oxides tracked in the d^{th} CRV batch (currently up to 64, listed in Table A-1)

$n_j^{oxides\ in\ MFPV}$ = number of glass oxides tracked in the mass balance calculations for the GFCs used in the j^{th} MFPV batch

As many of the parameters of this mass balance [Equations (12) and (13)] are uncertain, the resulting composition is uncertain. The various sources of uncertainty are briefly described in Table 9. The complexity of the mass balance precludes an analytical solution to the uncertainties (see Piepel et al. 2005 for more discussion). Therefore, Monte Carlo analyses of uncertainties will be used after the work of Piepel et al. (2005). Monte Carlo methods are a class of computational methods that rely on repeated random sampling to compute their results. The Monte Carlo method is often used when simulating physical and mathematical systems; it is used here to estimate the distribution of possible solutions (see Section 3.4.2 of Piepel et al. (2005) for more details on Monte Carlo analyses).

Table 9. Summary of Uncertain Input Values that Are Generated for Mass Balance Equations

Input Values	Sources of Uncertainty	Uncertainty Distribution	Uncertainty Values Location
$c_{id}^{element\ in\ CRV}$	chemical analyses, mixing and sampling of the CRV waste, and bias correction for mixing and sampling biases	Normal	Table A-2
V_j^{waste}	vessel volume estimates (from calibrated level measurements)	Normal	Appendix D
$m_k^{oxides\ in\ GFC}$	GFC composition certificates from vendors	PERT	Table A-4
$M_{kj}^{GFC\ in\ MFPV}$	GFC mass measurement and transfer	Normal	Appendix E
V_i	amount of material lost from the melter from R&T testing and production melter mass balance testing	PERT	Table A-3

For each of the uncertain input values listed in Table 9 a series of, $n^{runs\ of\ simulation}$, random numbers in normal or PERT distributions around the “estimated” (measured) values are generated with the standard deviations for the uncertainties. A discussion on the use of PERT distributions for GFC composition and retention factors is in Appendix G. The uncertainties for $c_{id}^{element\ in\ CRV}$ include the impacts of analytical uncertainties, mixing/sampling uncertainties, and uncertainties in correction for potential mixing/sampling biases, as an example for $c_{id}^{element\ in\ CRV}$:

$$s_{id}^{element\ in\ CRV} = \sqrt{\frac{\left(c_{id}^{element\ in\ CRV}\right)^2}{n_d^{samps\ in\ CRV}} \left[\left(RSD_{anal,i}^{element\ in\ CRV}\right)^2 + \left(RSD_{mix/samp,i}^{element\ in\ CRV}\right)^2 + \left(RSD_{bias\ corr,i}^{element\ in\ CRV}\right)^2 \right]} \quad (14)$$

where

- $s_{id}^{element\ in\ CRV}$ = standard deviation in the concentration of the i^{th} element in the d^{th} CRV batch (mg/L)
- $c_{id}^{element\ in\ CRV}$ = concentration of the i^{th} element in the d^{th} CRV batch (mg/L)
- $RSD_{anal,i}^{element\ in\ CRV}$ = relative standard deviation (RSD) in the concentration of the i^{th} element for chemical analysis in CRV batch
- $RSD_{mix\ \&\ samp,i}^{element\ in\ CRV}$ = RSD in the concentration of the i^{th} element for mixing and sampling in CRV batch
- $RSD_{bias\ corr,i}^{element\ in\ CRV}$ = RSD in the concentration of the i^{th} element for correction of biases in $c_{id}^{element\ in\ CRV}$
- $n_d^{samps\ in\ CRV}$ = number of samples analyzed in the d^{th} CRV batch

The RSDs for analytical and mixing/sampling uncertainties ($RSD_{anal,i}^{element\ in\ CRV}$ and $RSD_{mix\ \&\ samp,i}^{element\ in\ CRV}$ for CRV batch) are given Table A-2. However, it was assumed that there are no biases on the analytical results used for example calculations in this report. Each of the $n^{runs\ of\ simulation}$ sets of values are used to calculate a glass composition with Equations (12) and (13). The resulting $n^{runs\ of\ simulation}$ glass compositions are then used to calculate the standard deviation in each component mass fraction in the glass.

The $n^{runs\ of\ simulation}$ glass compositions are also used to predict the properties of the glasses using the property models described in Section 4.1, yielding $n^{runs\ of\ simulation}$ predicted property values. These property values are then used to quantify the composition uncertainty half widths in property units. As long as $n^{runs\ of\ simulation}$ is sufficient, and the random number distributions are close to the targeted distributions, excellent representations of the true composition uncertainties (in property units) are obtained (Piepel et al. 2005). Example calculations using RiskAMP® (as part of this work) and S-Plus® (Piepel et al. 2005) showed that $n^{runs\ of\ simulation} \geq 5000$ were adequate for implementing this method. The composition uncertainty is given by:

$$U_{comp}^{prop} = Q_{CL\%}^{prop} - Q_{50\%}^{prop} \text{ or } Q_{50\%}^{prop} - Q_{100-CL\%}^{prop} \quad (15)$$

where U_{comp}^{prop} = composition uncertainty for “prop”, i.e., uncertainty in predicted “prop” due to glass composition uncertainty (in property model units)

$$Q_{CL\%}^{prop} = CL\% [=100(1-\alpha)] \text{ percentile of the distribution of } n^{\text{runs of simulation}} \text{ property values}$$

$$Q_{50\%}^{prop} = \text{median predicted property value or } CL\% = 50\% \text{ percentile of the distribution of } n^{\text{runs of simulation}} \text{ property values}$$

4.2.3 CL% Combined Confidence Interval for Predicted Properties

Ultimately, model prediction uncertainty and composition uncertainty must be combined to obtain the total uncertainty associated with estimates of property values for LAW glass corresponding to a single MFPV batch. The method used to do this is a CL% combined confidence interval, discussed in Sections 5.4.3.2 of Piepel et al. (2005). The formula for a CL% upper combined confidence interval (UCCI) and lower combined confidence interval (LCCI) are given by:

$$B_{ucci}^{prop} = P^{prop} + U_{pred}^{prop} + U_{comp}^{prop} \text{ and } B_{lcci}^{prop} = P^{prop} - U_{pred}^{prop} - U_{comp}^{prop} \quad (16)$$

- where
- B_{ucci}^{prop} = CL% upper combined confidence interval for “prop”
 - B_{lcci}^{prop} = CL% lower combined confidence interval for “prop” (applicable only to “vis” and “ec”)
 - P^{prop} = transformed property “prop”, which includes $\ln(r_B, \text{g/L})$, $\ln(r_{Na}, \text{g/L})$, $\ln(D, \mu\text{m})$, $\ln(\eta_T, \text{P})$, and $\ln(\epsilon_T, \text{S/cm})$ (calculated per Section 4.1)
 - U_{pred}^{prop} = model prediction uncertainty for “prop” (calculated per Section 4.2.1)
 - U_{comp}^{prop} = composition uncertainty for “prop” (calculated per Section 4.2.2)

Note that CL% UCCIs (B_{ucci}^{prop}) and LCCIs (B_{lcci}^{prop}) as well as model prediction uncertainty (U_{pred}^{prop}) and composition uncertainty (U_{comp}^{prop}) are expressed in the units of the model used to predict a property ($\ln[\text{g/L}]$ for PCT responses, $\ln[\mu\text{m}]$ for VHT response, $\ln[\text{P}]$ for melt viscosity, and $\ln[\text{S/cm}]$ for melt electrical conductivity). Hence, they can be used to assess whether property constraints (as discussed in Section 4.3) are met.

4.2.4 Assumed Levels of Uncertainties for Predicted Properties

There are currently no mandatory requirements that direct the required confidence levels for the ILAW product or processing properties. The acceptable levels of uncertainties assumed for example calculations in this preliminary algorithm are 90% CL (i.e. $\alpha = 0.1$, see Section 4.2.1) for all properties, i.e., PCT, VHT, viscosity, and electrical conductivity. This 90% CL used in this report is preliminary and may be revised as directed by DOE.

a small fraction typically less than or equal to 0.1 used to represent the probability that a “100(1- α) confidence interval” does not contain the true value.

4.3 Constraints

A glass formulation is calculated to meet a set of requirements previously summarized in Table 2 in Section 1. Table 10 summarizes the glass and melt constraints for LAW, which is the same as Table 2, but with constraints expressed using symbols and units converted to those used in this report from those used in the source documents.

All the quantities for the constraints listed in Table 10 will be calculated for each MFPV batch during glass formulation (Section 5.1) to ensure that the MFPV batch meets all the waste-acceptance-related and key processing-related constraints before the batch is transferred to MFV. The calculation for each MFPV also includes the model validities described in Section 4.3.1 to ensure that all predicted properties and estimated uncertainties are valid. For canistered glass waste form, only the quantities for the waste-acceptance-related constraints (i.e., excluding viscosity and electrical conductivity from Table 10) are calculated to complete the production records (Section 5.5). The model validities are not calculated for the canistered glass waste form because they are already met for all MFPV batches that constitute the canistered glass.

Table 10. LAW Glass and Melt Constraints Used in ILAW Algorithm^(a)

Constraint Description	Constraint ^(b)	Source
PCT normalized B release	$B_{ucci}^{pctB} < \ln[4 \text{ (g/L)}]$	DOE 2000 (Spec. 2.2.2.17.2)
PCT normalized Na release	$B_{ucci}^{pctNa} < \ln[4 \text{ (g/L)}]$	DOE 2000 (Spec. 2.2.2.17.2)
VHT alteration depth	$B_{ucci}^{vht} < \ln[453 \text{ (}\mu\text{m)}]$	DOE 2000 (Spec. 2.2.2.17.3)
Viscosity at 1100°C	$B_{ucci}^{vis1100} \leq \ln[150 \text{ (P)}]$	24590-LAW-3PS- AE00-T00001, Rev. 4
Viscosity at 1150°C	$B_{lcci}^{vis1150} \geq \ln[20 \text{ (P)}]$	24590-HLW-RPT-RT- 05-001, Rev. 0
Viscosity at 1150°C	$B_{ucci}^{vis1150} \leq \ln[80 \text{ (P)}]$	24590-HLW-RPT-RT- 05-001, Rev. 0
Electrical conductivity at 1100°C	$B_{lcci}^{ec1100} \geq \ln[0.1 \text{ (S/cm)}]$	24590-LAW-3PS- AE00-T00001, Rev. 4
Electrical conductivity at 1200°C	$B_{ucci}^{ec1200} \leq \ln[0.7 \text{ (S/cm)}]$	24590-LAW-3PS- AE00-T00001, Rev. 4
Waste Na ₂ O loading	$g_{Na_2O(w)}^{oxide\ in\ MFPV} > 14, 3, \text{ and } 10 \text{ (wt\%)} \text{ for envelopes A, B, and C LAW, respectively}$	DOE 2000 (Spec. 2.2.2.2)
Waste classification	$SF_L + k^{rad} S^{SF_L} < 1$ $SF_S + k^{rad} S^{SF_S} < 1$ < Class C limits as defined in 10CFR61.55	DOE 2000 (Spec. 2.2.2.8)
⁹⁰ Sr activity in glass	$\hat{a}_{90Sr}^{rad\ in\ can} + k^{rad} \hat{s}_{90Sr}^{rad\ in\ can} < 20 \text{ (Ci/m}^3\text{)}$	DOE 2000 (Spec. 2.2.2.8)
¹³⁷ Cs activity in glass (waste form compliance)	$\hat{a}_{137Cs}^{rad\ in\ can} + k^{rad} \hat{s}_{137Cs}^{rad\ in\ can} < 3 \text{ (Ci/m}^3\text{)}$	DOE 2000 (Spec. 2.2.2.8)
¹³⁷ Cs activity in glass (system maintenance)	$\hat{a}_{137Cs}^{rad\ in\ can} + k^{rad} \hat{s}_{137Cs}^{rad\ in\ can} < 0.3 \text{ (Ci/m}^3\text{)}$	DOE 2000 [Section C.7 (d).(1).(iii)]
Canister surface dose rate	$r_{can,max,measured}^{dose\ in} \leq 500 \text{ (mrem/h)}$	DOE 2000 (Spec. 2.2.2.9)

- (a) ILAW must also meet the Dangerous Waste Limitations (Contract Specification paragraph 2.2.2.20, DOE 2000) although this specification is not listed in this table because there is no calculation required to be performed by the ILAW algorithm (See Section 1).
- (b) See Section 4.1.1 for justification to exclude the PCT Si release from the constraints.

4.3.1 Constraints Related to Glass Properties and Model Validities

For PCT, the contract (DOE 2000) Specification 2.2.2.17 requires normalized releases of Na, B, and Si to be below 2 g/m², which is equivalent to 4 g/L. The conversion from g/m² to g/L is described in ASTM (2002). The values calculated by the model are in ln(g/L). See Section 4.1.1 for justification to exclude the PCT Si release from the constraints. For VHT, the contract (DOE 2000) Specification 2.2.2.17 requires that the 200°C alteration rate be below 50 g/m²/d. The values calculated by the model are the natural logarithm of the alteration layer thickness (*D*) in ln(μm). The alteration rate limit is converted to the alteration layer thickness according to:

$$50 \left[\frac{\text{g(glass)}}{\text{m}^2(\text{glass}) \times \text{day}} \right] \cdot 24(\text{day}) \cdot \frac{1}{2.65} \left[\frac{\text{cm}^3(\text{glass})}{\text{g(glass)}} \right] \cdot \left(\frac{\mu\text{m} \cdot \text{m}^2}{\text{cm}^3} \right) = 453 \mu\text{m} \quad (17)$$

because the model data were based on 24-day VHT with glasses showing a mean density of roughly 2.65 g/cm³.

Although not required by the contract, key processing-related constraints on viscosity and electrical conductivity of glass melt are used to ensure successful processing of the LAW into glass at the design capacity rate. The viscosity constraint at 1100°C and the electrical conductivity constraints at 1100 and 1200°C are specified in *Engineering Specification for Low Activity Waste Melters*, 24590-LAW-3PS-AE00-T00001, Rev. 4. The bases for glass viscosity constraint at 1150°C discussed for IHLW algorithm (Appendix G in 24590-HLW-RPT-RT-05-001, Rev. 0) also applies to the ILAW algorithm. The viscosity constraint is in the form of two ranges with upper and lower limits (20 P ≤ η₁₁₅₀ ≤ 80 P and 10 P ≤ η₁₁₀₀ ≤ 150 P). Since viscosity increases with decreasing temperature, a glass meeting the lower viscosity limit at 1150°C of 20 P cannot fail the lower viscosity limit at 1100°C of 10 P. Therefore, only three of the four constraints need to be calculated. The electrical conductivity constraint is in the form of a range with an upper and lower limit over a range of temperatures (0.1 S/cm ≤ ε₁₁₀₀ ≤ 0.7 S/cm and 0.1 S/cm ≤ ε₁₂₀₀ ≤ 0.7 S/cm). Only the two extremes: 0.1 S/cm ≤ ε₁₁₀₀ and ε₁₂₀₀ ≤ 0.7 S/cm are considered because conductivity increases with temperature.

The constraints related to glass properties (PCT, VHT, viscosity, and electrical conductivity) are expressed based on UCCI or LCCI, B_{ucci}^{prop} or B_{ucci}^{prop} , discussed in Section 4.2.3. The equations for property predictions and uncertainties needed to calculate the UCCI or LCCI were given in Sections 4.1 and 4.2.

The UCCI or LCCI for glass properties in Table 10 are calculated using the glass property-composition models, which are subject to the model validity constraints. Three types of model validity constraints were developed by Piepel et al. (2007): single component, glass property, and multiple components.

Table 11 summarizes the model validity range for glass composition in the MFPV batch ($\tilde{g}_{ij}^{oxide in MFPV}$), expressed as single component concentrations after applying retention factors (v_i).

Table 11 also includes a column for constraints already imposed by formulating glasses following the glass formulation rules discussed in Section 5.1.3. For many components the glass formulation rules limit the target concentration to a fixed value or range of values, which is within the model validity range, and therefore the model validity constraint is not applicable. The last column in specifies applicability of the

model validity constraint depending on the model validity range and constraints predetermined by glass formulation rules.

In addition to the lower and upper bounds on the LAW glass components in Table 11, the multiple component and glass and melt property constraints restrict the composition region of validity for LAW glass property models. The glass and melt property model validity constraints given in Table 12 indirectly constrain the valid LAW glass composition region. Note that the glass and melt property model validity constraints are expressed without considering uncertainties, i.e., in terms of property values (P^{prop}) not UCCI or LCCI (B_{ucci}^{prop} or B_{ucci}^{prop}). The multiple component model validity constraints given in Table 13 specify the allowable combinations of glass components in the composition region of validity for LAW glass property models. Some of these property and multiple component model validity constraints in Table 12 and Table 13 do not restrict the composition region (last columns) beyond that defined by the constraints in .

Table 11. Model Validity Range for $\tilde{g}_{ij}^{oxide\ in\ MFPV}$ (Single Component Constraints in Mass Fraction)

Component	Model validity		Constraint by glass formulation rules	Model validity constraint applicable?
	Min	Max		
Al ₂ O ₃	0.035	0.090	Min at 0.061	Yes
B ₂ O ₃	0.060	0.131	Fixed at 0.100	No
CaO	0	0.105	Max at 0.070	No
Cl	0	0.0091	Max at 0.015	Yes
Cr ₂ O ₃	0	0.0059	Max at 0.0063	Yes
F	0	0.0035	Max at 0.049	Yes
Fe ₂ O ₃	0	0.080	Fixed at 0.055	No
K ₂ O	0	0.054	Max at 0.050	No
Li ₂ O	0	0.058	Max at 0.043	No
MgO	0	0.050	Max at 0.029	No
Na ₂ O	0.025	0.230	Min at 0.054 Max at 0.210	No
P ₂ O ₅	0	0.030	N/A	Yes
SiO ₂	0.384	0.521	N/A	Yes
SO ₃	0	0.010	Max at 0.0077	No
TiO ₂	0	0.030	Fixed at 0.014	No
ZnO	0.010	0.054	Fixed at 0.035	No
ZrO ₂	0	0.050	Fixed at 0.030	No
Sum of Minors ^(a)	0	0.0028	N/A	Yes

N/A: not applicable

(a) Sum of all components not listed individually in this table

Table 12. Model Validity Constraints for Glass and Melt Properties

Property	Constraint	Model validity constraint applicable?
PCT-B	$P^{pctB} \leq \ln[2.7 \text{ (g/L)}]$	Yes
PCT-Na	$P^{pctNa} \leq \ln[2.7 \text{ (g/L)}]$	Yes
VHT	$P^{vht} \leq \ln[1100 \text{ (}\mu\text{m)}]$	No
Viscosity at T (°C)	$-5.65 + \frac{9259.90}{T} \leq P^{vis,T} \leq -7.75 + \frac{14705.60}{T} (\ln[P])$	No
Electrical at T (°C)	$3.75 - \frac{7311.55}{T} \leq P^{ec,T} \leq 4.10 - \frac{4869.65}{T} (\ln[S/cm])$	No

Table 13. Model Validity Multiple Component Constraints (in Mass Fraction)

Composition Components	Constraint	Model validity constraint applicable?
Li ₂ O and Na ₂ O	$0.0466 - 0.5237 \tilde{g}_{Na_2O,j}^{oxide\ in\ MFPV} \leq \tilde{g}_{Li_2O,j}^{oxide\ in\ MFPV} \leq 0.0827 - 0.2839 \tilde{g}_{Na_2O,j}^{oxide\ in\ MFPV}$	Yes
Cr ₂ O ₃ and P ₂ O ₅	$-0.0018 + 0.2102 \tilde{g}_{P_2O_5,j}^{oxide\ in\ MFPV} \leq \tilde{g}_{Cr_2O_3,j}^{oxide\ in\ MFPV} \leq 0.0017 + 0.3226 \tilde{g}_{P_2O_5,j}^{oxide\ in\ MFPV}$	Yes
Na ₂ O and CaO	$0.1261 - 1.5048 \tilde{g}_{CaO,j}^{oxide\ in\ MFPV} \leq \tilde{g}_{Na_2O,j}^{oxide\ in\ MFPV} \leq 0.3191 - 1.5048 \tilde{g}_{CaO,j}^{oxide\ in\ MFPV}$	Yes
Li ₂ O and CaO	$\tilde{g}_{Li_2O,j}^{oxide\ in\ MFPV} \leq 0.0282 + 0.4565 \tilde{g}_{CaO,j}^{oxide\ in\ MFPV}$	Yes
Na ₂ O and SO ₃	$0.0947 - 18.8088 \tilde{g}_{SO_3,j}^{oxide\ in\ MFPV} \leq \tilde{g}_{Na_2O,j}^{oxide\ in\ MFPV} \leq 0.3161 - 18.8088 \tilde{g}_{SO_3,j}^{oxide\ in\ MFPV}$	Yes
Li ₂ O and SO ₃	$-0.0410 + 6.5263 \tilde{g}_{SO_3,j}^{oxide\ in\ MFPV} \leq \tilde{g}_{Li_2O,j}^{oxide\ in\ MFPV} \leq 0.0306 + 6.5263 \tilde{g}_{SO_3,j}^{oxide\ in\ MFPV}$	Yes
Na ₂ O and SiO ₂	$0.6024 - 1.3287 \tilde{g}_{SiO_2,j}^{oxide\ in\ MFPV} \leq \tilde{g}_{Na_2O,j}^{oxide\ in\ MFPV} \leq 0.8050 - 1.3287 \tilde{g}_{SiO_2,j}^{oxide\ in\ MFPV}$	Yes

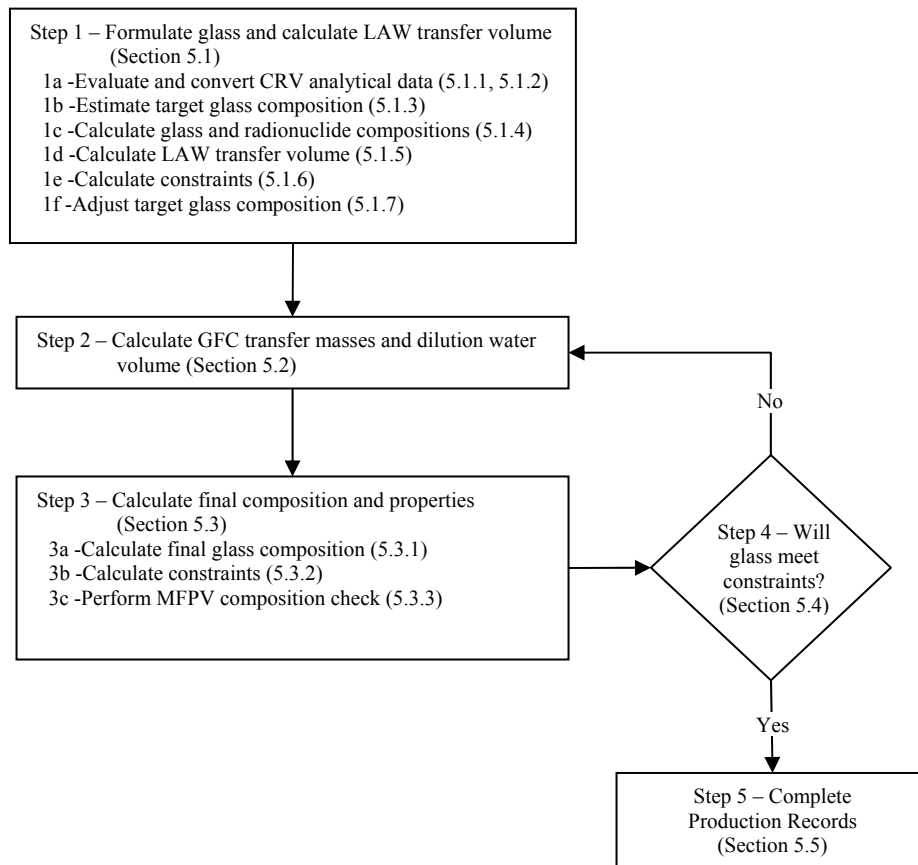
4.3.2 Constraints Not Related to Glass Properties

Additional constraints not related to glass properties include waste Na₂O loading (Specification 2.2.2.2), radionuclide concentration [waste classification and activities of ⁹⁰Sr and ¹³⁷Cs in glass; Specification 2.2.2.8 and contract Section C.7 (d).(1).(iii)], and canister surface dose rate (Specification 2.2.2.9). The equations for these constraints will be derived later in Section 5.1.6 after introducing all the equations needed. The details of the relevant contract Specifications will also be discussed in Section 5.1.6.

5 Calculation Steps

The following subsections present the detailed calculation steps discussed in Section 3. Figure 4 shows the detailed process flow diagram for algorithm Steps 1 through 5 discussed in this section.

Figure 4. Process Flow Diagram for Algorithm Steps 1 through 5



The solution of the equations described in this Section and their application to processing and product quality determination are illustrated in Section 6 for example waste compositions.

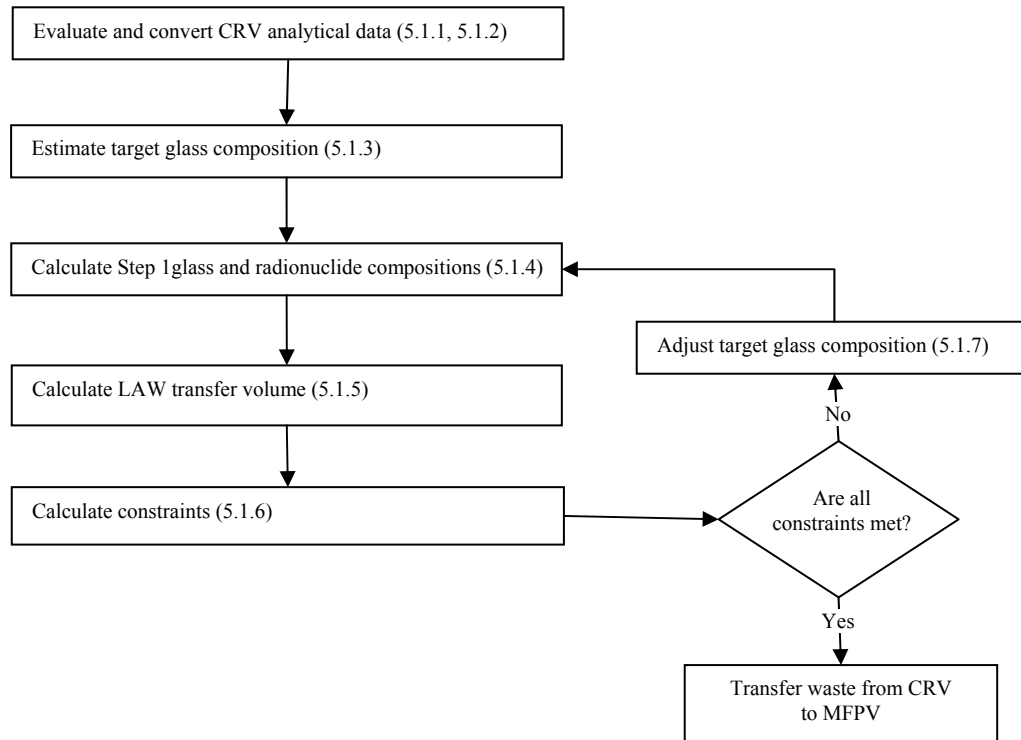
5.1 Step 1 – Glass Formulation and Calculation of LAW Transfer Volume

Step 1 uses the composition of CRV waste, volume of heel from the previous MFPV batch, and composition of GFCs to calculate the volume of waste to transfer from the CRV to the MFPV.

Figure 5 shows the detailed process flow diagram for algorithm Step 1 calculations. The target glass composition is formulated (5.1.3) from the waste composition data (Sections 5.1.1 and 5.1.2). The resulting target glass composition is used to further calculate Step 1 glass and radionuclide compositions (Section 5.1.4) and LAW transfer volume (Section 5.1.5). The Step 1 glass and radionuclide compositions and LAW transfer volume are then used to calculate all constraint quantities discussed in Section 4.3 (Section 5.1.6). If all constraints are met, the calculated LAW transfer volume based on the corresponding target glass

composition is provided to the operators of the LAW Vitrification facility so that the waste from the CRV can be transferred to the MFPV. If any of the constraints is not met, the target composition is adjusted (Section 5.1.7) and calculations described in Sections 5.1.4 through 5.1.6 are performed again to formulate the glass that meets all constraints so that the waste transfer from CRV to MFPV can be initiated.

Figure 5. Process Flow Diagram for Algorithm Step 1 Calculations



5.1.1 CRV Analytical Data Screening and Evaluation

The LAW is transferred from the TCP in the pretreatment facility to one of two CRVs in the LAW vitrification facility. The CRV is then sampled, and samples are analyzed at the analytical laboratory. The analytical data from the LAW CRV samples are screened and evaluated prior to calculating glass formulation. The evaluation of results from blanks and standards will be performed at the analytical laboratory according to their procedures (not yet developed) (*Integrated Sampling and Analysis Requirements Document (ISARD)*, Dodd and Arakali 2008, 24590-WTP-PL-PR-04-0001). The analytical data will then be screened before they are averaged and entered to the LAW formulation algorithm. The data screening will include, at a minimum,

- **Outlier Identification**— According to current plans (*System Description for LAW Concentrate Receipt Process (LCP)*, Taki and Hirzel 2004, 24590-LAW-3YD-LCP-00001, Rev 1) three samples will be taken from each CRV batch and analyzed for each analyte. Standard statistical tests for outlying data will be used.
- **Trending Evaluation**—The trending analyses are not calculated in this report. It is assumed that prepackaged statistical process control (SPC) software will be used during production.

An operator will be alerted for intervention if there are any potential concerns.

The LAW in CRV is analyzed in two steps (Dodd and Arakali 2008): LAW 1a sample is first analyzed for major components/radionuclides and then LAW 1b sample is analyzed later for minor components. The LAW 1b analytical results are not required for glass formulation, but will be used if available. In the event that the LAW 1b analyses are not available, the glass formulation will be performed based on LAW 1a analyses, but the production records will be completed using both LAW 1a and 1b samples.

5.1.2 CRV Analytical Data Conversion

The analytical data from the CRV samples will be obtained from the laboratory information management system in the form of chemical analyte concentrations and radionuclide activities per unit volume. The mass of component i per unit volume of the d^{th} CRV batch is given by $c_{id}^{\text{element in CRV}}$ (in $\mu\text{g/mL} \equiv \text{mg/L}$). The activity of radionuclide analyte i per unit volume of the d^{th} CRV batch is given by $R_{id}^{\text{rad in CRV}}$ (in $\mu\text{Ci/mL} \equiv \text{mCi/L}$).

Concentrations of some LAW components will be measured both chemically and radiochemically (then, $c_{id}^{\text{element in CRV}}$ is a sum of concentrations of all isotopes). The data for such components will be compared to the method detection limits (MDL) and minimum quantification limits (MQL) for the individual analytes. If the mass of an element, i , (e.g., $i = \text{uranium}$) from chemical analyses is greater than its MQL mass, then the chemical analyses results will be used in the mass balance for that element regardless of the accuracy of the radiochemical analyses results. Further, for consistency that concentration will be used to rescale the concentrations of each isotope of that element measured by radiochemistry (e.g., $i = {}^{232}\text{U}, {}^{233}\text{U}, {}^{234}\text{U}, {}^{235}\text{U} \dots$) using the ratio of each isotope. If the chemical analysis result is below the MDL and the radiochemical analyses results are above the MDL, then the chemical component's concentration will be set to the sum of the concentrations of the isotopes (converted to mass units). Finally, if the chemical analysis result is between the MDL and the MQL and the radiochemical analyses results are above the MDL, then the values with the lowest associated uncertainties will be used.⁽³⁾ For analytes with concentrations reported as *less than the MDL*, a concentration of zero will be used in the mass balance equations. All components with concentrations reported below the MQL but above the MDL will use analytical results with the appropriate flags assigned to them.

Multiple samples (currently three samples) are collected and analyzed for each CRV batch. The algorithm uses the average concentrations from multiple samples analyzed⁽⁴⁾. As discussed in Section 1, each CRV batch will generate roughly from 3.5 to 15 MFPV batches depending on sodium molarity of waste and waste loading in glass. The CRV waste becomes diluted by the addition of two types of flush water added to the CRV. The sample line flush water is added after samples are taken from CRV, which is performed once per each CRV batch. The CRV-MFPV line flush is performed after each waste transfer. Then, the composition of CRV batch after accounting for the flush water additions is given as:

$$c_{idm}^{\text{element in CRV}} = \bar{c}_{id}^{\text{element in CRV}} \lambda_{dm} \tag{18}$$

where $c_{idm}^{\text{element in CRV}}$ = concentration of the i^{th} component in the m^{th} transfer waste transferred from the d^{th} CRV to MFPV (mg/L waste)

⁽³⁾ This analytical data “sorting” is done outside of the ILAW formulation algorithm, i.e., the chemical and radiochemical data are “sorted” before they are entered into the algorithm.

⁽⁴⁾ The averaging of analytical data is performed outside of the ILAW formulation algorithm and the average values are entered into the algorithm.

$\frac{\text{element in}}{C_{id}^{CRV}}$ = concentration of the i^{th} component in the waste of the d^{th} CRV batch averaged over n_d^{CRV} samples analyzed (mg/L waste)

λ_{dm} = dilution factor caused by the addition of flush waters for the m^{th} transfer waste transferred from the d^{th} CRV to MFPV

The dilution factor is calculated from:

$$\lambda_{dm} = \frac{V_d^{CRV \text{ working}}}{V_d^{CRV \text{ working}} + V_d^{CRV \text{ sampflush}}} \quad \text{for } m = 1$$

$$\lambda_{dm} = \lambda_{d,m-1} \frac{V_{d,m-1}^{CRV \text{ current}}}{V_{d,m-1}^{CRV \text{ current}} + V_{d,m-1}^{CRV \text{ transflush}}} \quad \text{for } m \geq 2$$

(19)

where $V_d^{CRV \text{ working}}$ = working volume of the d^{th} CRV measured before the sampling line flush water is added to the CRV (L). The nominal value of $V_d^{CRV \text{ working}}$ is 50,085 L (Table 1). The CRV working volume for each CRV batch includes the CRV heel volume ($V_d^{CRV \text{ heel}}$) required for normal operation plus the CRV batch volume ($V_d^{CRV \text{ batch}}$) transferred from TCP.

$V_d^{CRV \text{ sampflush}}$ = volume of the sampling line flush water used for the d^{th} CRV batch (L)

$\lambda_{d,m-1}$ = dilution factor caused by the addition of flush waters for the $m-1^{\text{th}}$ transfer waste transferred from the d^{th} CRV batch to MFPV (dilution factor for the waste transferred previously)

$V_{d,m-1}^{CRV \text{ current}}$ = current volume of the d^{th} CRV measured after the $m-1^{\text{th}}$ waste transfer to MFPV (L)

$V_{d,m-1}^{CRV \text{ transflush}}$ = volume of the CRV-MFPV transfer line flush water used for the d^{th} CRV after the $m-1^{\text{th}}$ waste transfer to MFPV (L)

The waste transfer from the CRV will continue until the volume of remaining current CRV waste ($V_{d,m-1}^{CRV \text{ current}}$) is less than the volume required for next transfer (assuming the same volume used in the previous transfer) plus nominal CRV heel volume (15581 L, see Table 1). The waste from the other CRV will be used if

$$V_{d,m-1}^{CRV \text{ current}} < V_{d,m-1}^{CRV \text{ transwaste}} + V_{d,m-1}^{CRV \text{ heel}}$$

(20)

where $V_{d,m-1}^{CRV \text{ current}}$ = current volume of the d^{th} CRV measured after the $m-1^{\text{th}}$ waste transfer to MFPV (L)

$V_{d,m-1}^{transwaste\ CRV}$ = volume of the $m-1^{th}$ transfer waste transferred from the d^{th} CRV to MFPV (L)
 $V^{heel\ CRV}$ = volume of the d^{th} CRV heel required for normal operation (L). The nominal value of $V^{heel\ CRV}$ is 15,581 L (Table 1).

The ILAW formulation algorithm uses waste compositions in the form of mass fractions of glass oxides. The analytical data are converted from mg/L to the mass fraction of a glass oxide by:

$$g_{idm}^{oxide\ in\ CRV} = \frac{c_{idm}^{element\ in\ CRV} f_i}{\sum_{i=1}^{n_d^{oxides\ in\ CRV}} c_{idm}^{element\ in\ CRV} f_i} \quad (21)$$

where $g_{idm}^{oxide\ in\ CRV}$ = mass fraction of the i^{th} glass oxide in the m^{th} transfer waste transferred from the d^{th} CRV to MFPV (g oxide per g CRV oxides)
 f_i = oxide conversion factor, i.e., mass to the i^{th} glass oxide per mass of the i^{th} element, listed in Table A-1 (unitless)
 $c_{idm}^{element\ in\ CRV}$ = concentration of the i^{th} component in the m^{th} transfer waste transferred from the d^{th} CRV to MFPV (mg/L waste)
 $n_d^{oxides\ in\ CRV}$ = number of glass oxides tracked in the d^{th} CRV batch

The concentration of total glass oxides in the waste is given by:

$$C_{dm}^{oxides\ in\ CRV} = \frac{\sum_{i=1}^{n_d^{oxides\ in\ CRV}} c_{idm}^{element\ in\ CRV} f_i}{1000(mg/g)} \quad (22)$$

where $C_{dm}^{oxides\ in\ CRV}$ is the concentration of total glass oxides in the m^{th} transfer waste transferred from the d^{th} CRV to MFPV (g oxides per L waste) and the remaining notations are as defined in Equation (21).

A chemical component will be carried through the mass balance equations for each of the elements present in the radiochemical analyses. The concentration of each individual isotope, however, will be calculated on an activity per mass of glass basis.

For radionuclides, specific activities (A_i) are used to convert radionuclide activities to masses for inclusion in the mass balance:

$$c_{idm}^{element\ in\ CRV} = \frac{\overline{R}_{id}^{rad\ in\ CRV} \lambda_{dm}}{A_i} \quad (23)$$

where $c_{idm}^{element\ in\ CRV}$ = concentration of the i^{th} radionuclide in the m^{th} transfer waste transferred from the d^{th} CRV to MFPV (mg/L)

$\bar{R}_{id}^{rad\ in\ CRV}$ = activity (per unit volume) of the i^{th} radionuclide in the waste of the d^{th} CRV averaged over $n_d^{samps\ in\ CRV}$ samples analyzed (mCi/L)

λ_{dm} = dilution factor for the m^{th} transfer waste transferred from the d^{th} CRV to MFPV.

A_i = specific activity of the i^{th} radionuclide, listed in Table A-1 (Ci/g)

The resulting $c_{idm}^{element\ in\ CRV}$ values are converted to mass fractions of glass oxides by Equation (21). The mass fractions of glass oxides in waste are then used for subsequent calculations. The radionuclides that have nonradioactive elements analyzed chemically are already included in the chemical components.

For all radionuclides, the average activity per unit volume of the CRV batch ($\bar{R}_{id}^{rad\ in\ CRV}$ in mCi/L) is converted to the activity per unit mass of glass oxides in waste by

$$a_{idm}^{rad\ in\ CRV} = \frac{\bar{R}_{id}^{rad\ in\ CRV} \lambda_{dm}}{C_{dm}^{oxides\ in\ CRV}} \quad (24)$$

where $a_{idm}^{rad\ in\ CRV}$ is the specific activity of the i^{th} radionuclide in the m^{th} transfer waste transferred from the d^{th} CRV to MFPV (mCi/g oxides) and the remaining notations are as previously defined.

5.1.3 Estimation of Target Glass Composition

The initial glass composition ($g_{ij}^{oxide\ in\ MFPV, initial}$) is estimated from the waste composition data obtained in Sections 5.1.1 and 5.1.2 using the methods defined by Muller et al. (2004) and supplemented by CCN 150795. The glass formulation rules generate a unique glass composition based on waste composition, which calculates the maximum Na₂O concentration from waste in LAW glass that satisfies all the rules. The basis of the method by Muller et al. (2004) is interpolation using previous successful glass compositions. Fifteen glass compositions that were formulated by Vitreous State Laboratory for the immobilization of a full range of Hanford LAW streams are the basis for interpolation. Each of these glasses met all glass quality and processability constraints and was successfully processed at increasing scales, up to the Duratek pilot melter. These glasses not only met the numerical constraints (Table 2), but were also successfully processed at pilot scale; thereby demonstrating that non-constrained variables were appropriate for large-scale, continuous, production. The key parameters for this method include the mass fractions of Na₂O, SO₃, and K₂O in the CRV waste transferred to MFPV. These glass formulation rules were supplemented by two sets of additional rules described in CCN 150795, with one set based on the mass fractions of Cl, F, and SO₃ and the other based on the mass fractions of Cr₂O₃, K₂O, and P₂O₅ in the CRV waste transferred to MFPV.

The first step in this method (Muller et al. 2004) determines the acceptable concentration of Na₂O in the final glass ($g_{Na_2O,j}^{oxide\ in\ MFPV}$) by the following rules (Figure 6 through Figure 8) (concentration in target⁽⁵⁾ wt% in glass):

Na₂O-SO₃-K₂O rules (Muller et al. 2004) (concentration in target wt% in glass)

1. Na₂O must be at or below 21 wt% in glass.
2. Na₂O must be at or below the value of 35.875 wt% minus 42.5 times SO₃ wt% in glass.
3. SO₃ must be at or below 0.77 wt% in glass.
4. Na₂O plus 0.66 times K₂O must be at or below 21.5 wt% in glass.⁽⁶⁾

Cl-F-SO₃ rules (CCN 150795) (concentration in target wt% in glass)

5. Cl plus 0.3 times F must be at or below the value 1.4656 wt% minus 2.1111 times SO₃ wt% in glass if SO₃ in glass is at or below 0.59 wt%.
6. Cl plus 0.3 times F must be at or below 0.22 wt% in glass if SO₃ in glass is above 0.59 wt%.

Cr₂O₃-K₂O-P₂O₅ rules (CCN 150795) (concentration in target wt% in glass)

7. Cr₂O₃ in glass must be at or below 0.63 wt% and K₂O in glass must be at or below and 5 wt%.
8. If P₂O₅ in glass is below 2.79 wt%, and K₂O in glass is at or below 0.54 wt%, Cr₂O₃ in glass must be at or below 0.63 wt%.
9. If P₂O₅ in glass is below 2.79 wt% and K₂O in glass is between 0.54 wt% and 5 wt%, Cr₂O₃ in glass must be at or below 0.08 wt%.

The preliminary minimum Na₂O mass fractions in glass from the Na₂O-SO₃-K₂O rules ($g_{Na_2O,j}^{oxide\ in\ MFPV,pre-1}$) and from the Cl-F-SO₃ rules ($g_{Na_2O,j}^{oxide\ in\ MFPV,pre-2}$) for the j^{th} MFPV batch can be expressed as a function of the component mass fractions in the CRV waste:

$$g_{Na_2O,j}^{oxide\ in\ MFPV,pre-1} = \min \left\{ 0.21, \frac{0.35875}{1 + 42.5 \frac{g_{SO_3,dm}^{oxide\ in\ CRV}}{g_{Na_2O,dm}^{oxide\ in\ CRV}}}, 0.0077 \frac{g_{Na_2O,dm}^{oxide\ in\ CRV}}{g_{SO_3,dm}^{oxide\ in\ CRV}}, \frac{0.215}{1 + 0.66 \frac{g_{K_2O,dm}^{oxide\ in\ CRV}}{g_{Na_2O,dm}^{oxide\ in\ CRV}}} \right\} \quad (25)$$

⁽⁵⁾ The term “target” was used to note that the concentrations are based on assumed 100% retention in glass.

⁽⁶⁾ The 0.66 scale factor is meant to adjust for differences in molecular masses of Na₂O and K₂O.

$$g_{Na_2O,j}^{oxide\ in\ MFPV,pre-2} = \max \left\{ \frac{0.014656 \left(\frac{g_{Cl,dm}^{oxide\ in\ CRV} + 0.3 g_{F,dm}^{oxide\ in\ CRV}}{g_{Na_2O,dm}^{oxide\ in\ CRV}} \right) + 2.1111 \frac{g_{SO_3,dm}^{oxide\ in\ CRV}}{g_{Na_2O,dm}^{oxide\ in\ CRV}}}{0.0022 \left(\frac{g_{Cl,dm}^{oxide\ in\ CRV} + 0.3 g_{F,dm}^{oxide\ in\ CRV}}{g_{Na_2O,dm}^{oxide\ in\ CRV}} \right)} \right\} \quad (26)$$

where $g_{idm}^{oxide\ in\ CRV}$ is the mass fraction of the i^{th} glass oxide in the m^{th} transfer waste transferred from the d^{th} CRV to MFPV (g oxide per g CRV oxides), which supplies waste to the j^{th} MFPV batch. The preliminary minimum Na₂O mass fraction in glass from the Cr₂O₃-K₂O-P₂O₅ rules ($g_{Na_2O,j}^{oxide\ in\ MFPV,pre-3}$) is expressed as a function of component mass fractions following the logics defined by the rules 7 through 9:

$$g_{Na_2O,j}^{oxide\ in\ MFPV,pre-3} = \min \left\{ \begin{array}{l} \text{if} \left[\begin{array}{l} g_{P_2O_5,dm}^{oxide\ in\ CRV} W_j^{initial} < 0.0279, \\ \text{if} \left(\frac{g_{Cr_2O_3,dm}^{oxide\ in\ CRV} W_j^{min,K} > 0.0008, \frac{0.0054}{g_{K_2O,dm}^{oxide\ in\ CRV}}, \frac{0.05}{g_{K_2O,dm}^{oxide\ in\ CRV}}, \frac{0.05}{g_{K_2O,dm}^{oxide\ in\ CRV}} \right), \\ \frac{oxide\ in\ CRV}{g_{Na_2O,dm}^{oxide\ in\ CRV}}, \frac{oxide\ in\ CRV}{g_{Na_2O,dm}^{oxide\ in\ CRV}}, \frac{oxide\ in\ CRV}{g_{Na_2O,dm}^{oxide\ in\ CRV}} \end{array} \right], \\ \text{if} \left[\begin{array}{l} g_{P_2O_5,dm}^{oxide\ in\ CRV} W_j^{initial} < 0.0279, \\ \text{if} \left(\frac{g_{K_2O,dm}^{oxide\ in\ CRV} W_j^{min,Cr} > 0.0054, \frac{0.0008}{g_{Cr_2O_3,dm}^{oxide\ in\ CRV}}, \frac{0.0063}{g_{Cr_2O_3,dm}^{oxide\ in\ CRV}}, \frac{0.0063}{g_{Cr_2O_3,dm}^{oxide\ in\ CRV}} \right), \\ \frac{oxide\ in\ CRV}{g_{Na_2O,dm}^{oxide\ in\ CRV}}, \frac{oxide\ in\ CRV}{g_{Na_2O,dm}^{oxide\ in\ CRV}}, \frac{oxide\ in\ CRV}{g_{Na_2O,dm}^{oxide\ in\ CRV}} \end{array} \right] \end{array} \right\} \quad (7) \quad (27)$$

where $W_j^{initial}$ is the initial waste loading for the j^{th} MFPV batch determined from the Na₂O-SO₃-K₂O and Cl-F-SO₃ rules ($g_{Na_2O,j}^{oxide\ in\ MFPV,pre-1}$ and $g_{Na_2O,j}^{oxide\ in\ MFPV,pre-2}$) by Equations (25) and (26), $W_j^{min,K}$ is the minimum waste

⁽⁷⁾ The output of if(A, B, C) function is given as: if(A, B, C) equals B if the logical test A is true and if(A, B, C) equals C if the logical test A is false.

loading for the j^{th} MFPV batch when 0.54 wt% of K_2O limit is assumed, and $W_j^{\text{min,Cr}}$ is the minimum waste loading for the j^{th} MFPV batch when 0.08 wt% of Cr_2O_3 limit is assumed, which are calculated as:

$$W_j^{\text{initial}} = \frac{\min \left\{ g_{\text{Na}_2\text{O},j}^{\text{oxide in MFPV,pre-1}}, g_{\text{Na}_2\text{O},j}^{\text{oxide in MFPV,pre-2}} \right\}}{g_{\text{Na}_2\text{O},dm}^{\text{oxide in CRV}}} \quad (28)$$

$$W_j^{\text{min,K}} = \frac{\min \left\{ g_{\text{Na}_2\text{O},j}^{\text{oxide in MFPV,pre-1}}, g_{\text{Na}_2\text{O},j}^{\text{oxide in MFPV,pre-2}}, \frac{0.0054}{\frac{g_{\text{K}_2\text{O},dm}^{\text{oxide in CRV}}}{g_{\text{Na}_2\text{O},dm}^{\text{oxide in CRV}}}} \right\}}{g_{\text{Na}_2\text{O},dm}^{\text{oxide in CRV}}} \quad (29)$$

$$W_j^{\text{min,Cr}} = \frac{\min \left\{ g_{\text{Na}_2\text{O},j}^{\text{oxide in MFPV,pre-1}}, g_{\text{Na}_2\text{O},j}^{\text{oxide in MFPV,pre-2}}, \frac{0.0008}{\frac{g_{\text{Cr}_2\text{O}_3,dm}^{\text{oxide in CRV}}}{g_{\text{Na}_2\text{O},dm}^{\text{oxide in CRV}}}} \right\}}{g_{\text{Na}_2\text{O},dm}^{\text{oxide in CRV}}} \quad (30)$$

Then, the preliminary minimum Na_2O mass fraction in glass determined from all the formulation rules is given as:

$$g_{\text{Na}_2\text{O},j}^{\text{oxide in MFPV,pre}} = \min \left\{ g_{\text{Na}_2\text{O},j}^{\text{oxide in MFPV,pre-1}}, g_{\text{Na}_2\text{O},j}^{\text{oxide in MFPV,pre-2}}, g_{\text{Na}_2\text{O},j}^{\text{oxide in MFPV,pre-3}} \right\} \quad (31)$$

The waste loading is defined as the mass fraction of glass that originated from the material in the CRV. The initial waste loading ($G_j^{\text{waste in MFPV,initial}}$) is calculated according to:

$$G_j^{\text{waste in MFPV,initial}} = \frac{g_{\text{Na}_2\text{O},j}^{\text{oxide in MFPV,pre}}}{g_{\text{Na}_2\text{O},dm}^{\text{oxide in CRV}}} \quad (32)$$

The initial glass composition ($g_{ij}^{\text{oxide in MFPV,initial}}$) for the j^{th} MFPV batch is calculated by the following equations (Muller et al. 2004):

$$g_{Al_2O_3,j}^{oxide\ in\ MFPV,\ initial} = \max \left\{ 0.061, G_j^{waste\ in\ MFPV,\ initial} g_{Al_2O_3,dm}^{oxide\ in\ CRV} \right\} \quad (33)$$

$$g_{B_2O_3,j}^{oxide\ in\ MFPV,\ initial} = 0.100 \quad (34)$$

$$g_{Fe_2O_3,j}^{oxide\ in\ MFPV,\ initial} = 0.055 \quad (35)$$

$$g_{TiO_2,j}^{oxide\ in\ MFPV,\ initial} = 0.014 \quad (36)$$

$$g_{ZnO,j}^{oxide\ in\ MFPV,\ initial} = 0.035 \quad (37)$$

$$g_{ZrO_2,j}^{oxide\ in\ MFPV,\ initial} = 0.030 \quad (38)$$

$$g_{Na_2O,j}^{oxide\ in\ MFPV,\ initial} = \max \left\{ g_{Na_2O,j}^{oxide\ in\ MFPV,\ pre}, 0.054 \right\} \quad (39)$$

$$d = g_{Na_2O,j}^{oxide\ in\ MFPV,\ initial} + 0.66 G_j^{waste\ in\ MFPV,\ initial} g_{K_2O,dm}^{oxide\ in\ CRV} \quad (40)$$

$$g_{CaO,j}^{oxide\ in\ MFPV,\ initial} = 0.015 + \frac{0.055}{1 + \exp\left(\frac{d - 0.17}{0.02}\right)} \quad (41)$$

$$g_{Li_2O,j}^{oxide\ in\ MFPV,\ initial} = \max \left\{ \text{if} \left\{ \frac{(100d - 5.4)^2}{12.75^2} < 1, 0.043 \left[1 - \frac{(100d - 5.4)^2}{12.75^2} \right]^{0.7}, 0 \right\}, G_j^{waste\ in\ MFPV,\ initial} g_{Li_2O,dm}^{oxide\ in\ CRV} \right\} \quad (42)$$

$$g_{MgO,j}^{oxide\ in\ MFPV,\ initial} = 0.0148 + \frac{0.0149}{1 + \exp(100d - 9)} \quad (43)$$

$$g_{ij}^{oxide\ in\ MFPV,\ initial} = G_j^{waste\ in\ MFPV,\ initial} g_{idm}^{oxide\ in\ CRV} \quad (44)$$

$\{i \neq Al_2O_3, B_2O_3, CaO, Fe_2O_3, Li_2O, MgO, Na_2O, SiO_2, TiO_2, ZnO, ZrO_2\}$

$$g_{SiO_2,j}^{oxide\ in\ MFPV,\ initial} = 1 - \sum_{i=1, i \neq SiO_2}^{n_j^{oxide\ in\ MFPV}} g_{ij}^{oxide\ in\ MFPV,\ initial} \quad (45)$$

where $n_j^{oxides\ in\ MFPV}$ is the number of glass oxides tracked in the mass balance calculations for the j^{th} MFPV batch.

It is assumed that the radionuclide constraints will be met through the WTP process control strategy (24590-WTP-3YD-50-00002). The algorithm will confirm this assumption for each MFPV batch by calculating the constraint quantities from analyzed activities of radionuclides in the CRV and comparing them with the limits.

Figure 6. Schematic of Na₂O-SO₃-K₂O Rules for $g_{Na_2O,j}^{oxide\ in\ MFPV,pre-1}$

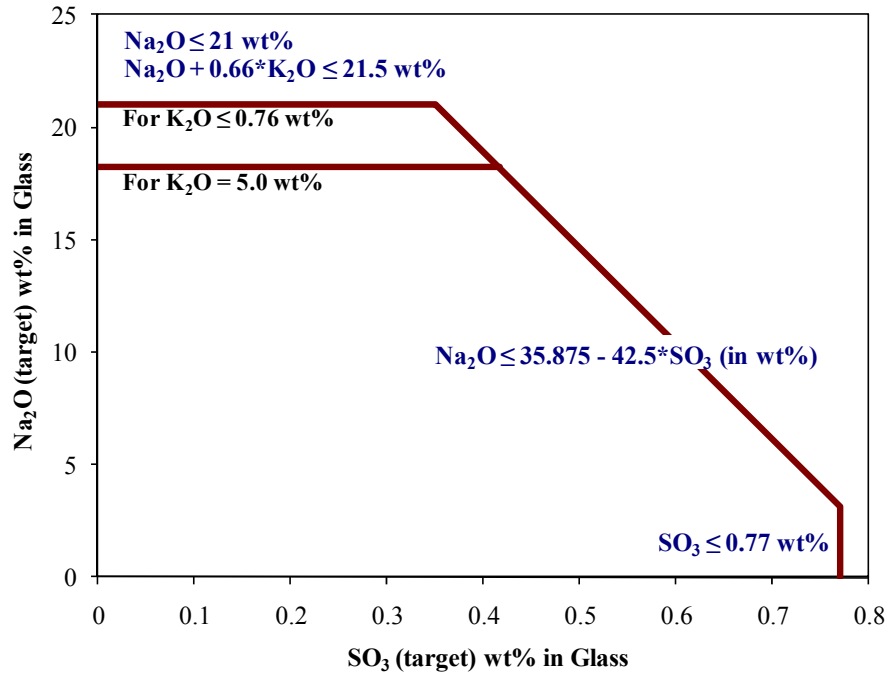


Figure 7. Schematic of Cl-F-SO₃ Rules for $\xi_{Na_2O,j}^{oxide\ in\ MFPV,pre-2}$ [H (wt%) = Cl (wt%) + 0.3*F (wt%)]

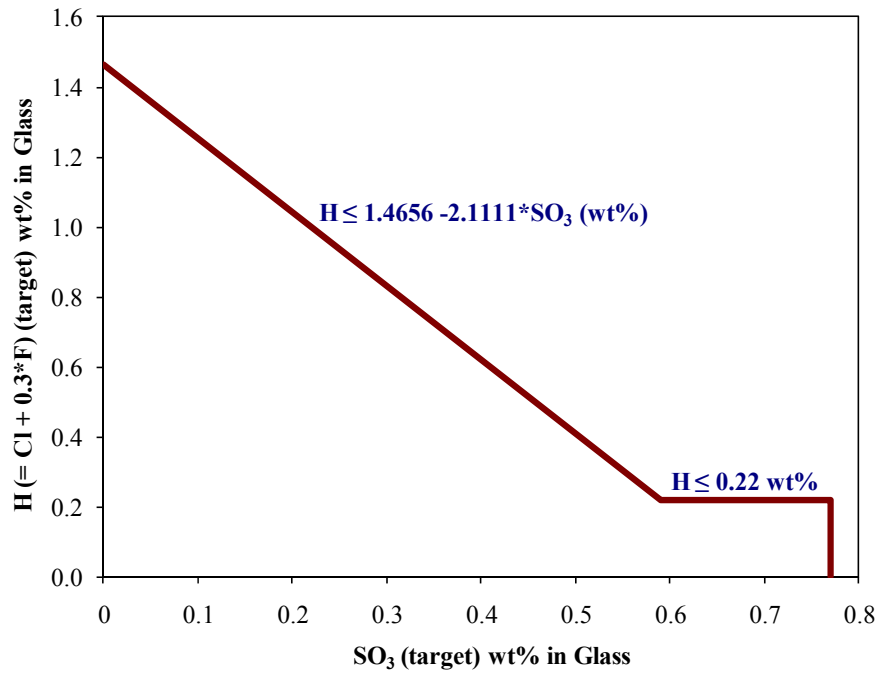
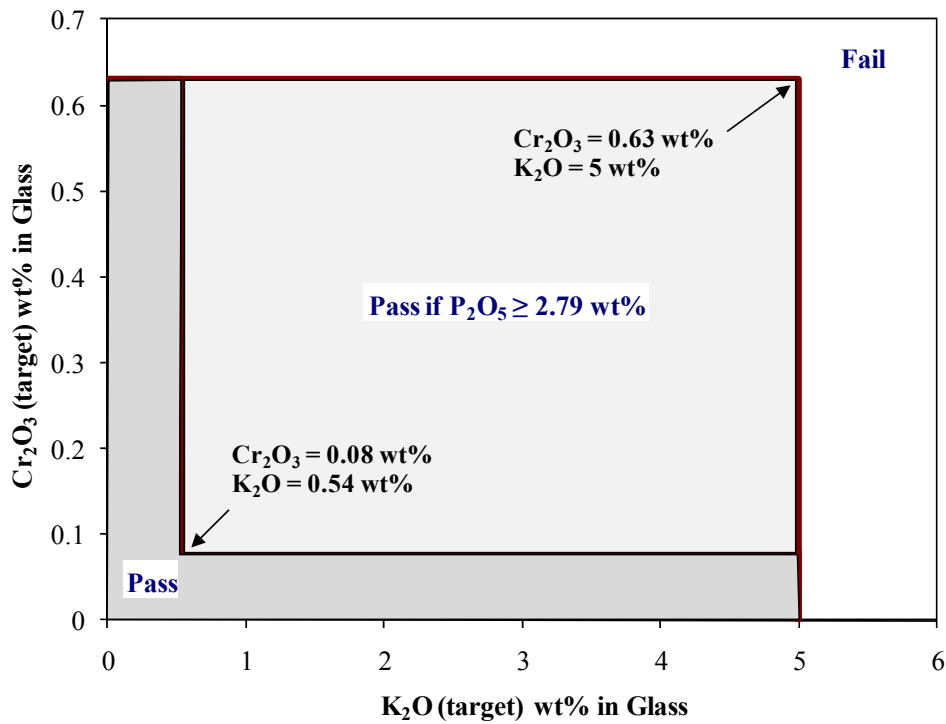


Figure 8. Schematic of Cr₂O₃-K₂O-P₂O₅ Rules for $\xi_{Na_2O,j}^{oxide\ in\ MFPV,pre-3}$



The resulting initial composition is set to target composition ($g_{ij}^{oxide\ in\ MFPV,\ target}$) for all components, i.e.

$$g_{ij}^{oxide\ in\ MFPV,\ target} = g_{ij}^{oxide\ in\ MFPV,\ initial} \quad (46)$$

and used to calculate the Step 1 glass and radionuclide compositions (Section 5.1.4) and waste transfer volume (Section 5.1.5). The resulting GFC masses and waste transfer volume are used to calculate the constraint quantities and compare them with the limits (Section 5.1.6).

5.1.4 Calculation of Step 1 Glass and Radionuclide Compositions

The target mass fractions for 11 GFC components are used to calculate the mass of each GFC required. First, the contribution from waste to the concentration of GFC components is subtracted from the target concentration in glass to obtain the target mass fractions to be supplied from GFCs according to

$$g_{ij}^{oxide\ in\ MFPV,\ target-gfc} = g_{ij}^{oxide\ in\ MFPV,\ target} - G_j^{waste\ in\ MFPV,\ target} g_{idm}^{oxide\ in\ CRV} \quad (47)$$

$\{i = Al_2O_3, B_2O_3, CaO, Fe_2O_3, Li_2O, MgO, Na_2O, SiO_2, TiO_2, ZnO, ZrO_2\}$

where $g_{ij}^{oxide\ in\ MFPV,\ target-gfc}$ is the target mass fraction of the i^{th} glass oxide in glass from GFC for the j^{th} MFPV batch (g per g MFPV oxides).

Define the GFC composition vector $\mathbf{t}_j = g_{ij}^{oxide\ in\ MFPV,\ target-gfc}$ (g per g MFPV oxides), the 11×11 matrix of GFC composition $\mathbf{H} = m_{ik}^{GFC}$ (for $i = Al_2O_3, B_2O_3, CaO, Fe_2O_3, Li_2O, MgO, Na_2O, SiO_2, TiO_2, ZnO,$ and $ZrO_2,$ g per g GFC including volatiles), and the preliminary GFC mass vector $\mathbf{m}_j = \ddot{M}_{kj}^{GFC\ in\ MFPV,\ pre}$ (g GFC per g MFPV oxides) is calculated as.

$$\mathbf{m}_j = (\mathbf{H}^T \mathbf{H})^{-1} \mathbf{H}^T \mathbf{t}_j \quad (48)$$

where

- \mathbf{m}_j = vector of $\ddot{M}_{kj}^{GFC\ in\ MFPV,\ pre}$ for $n_j^{GFCs\ in\ MFPV}$ GFCs in the j^{th} MFPV batch (g oxide per g MFPV oxides)
- $\ddot{M}_{kj}^{GFC\ in\ MFPV,\ pre}$ = preliminary target mass of the k^{th} GFC per g of glass to add to the j^{th} MFPV batch (g per g MFPV oxides)
- \mathbf{H} = 11×11 matrix of $m_{ik}^{oxide\ in\ GFC}$ for GFC composition (for $i = Al_2O_3, B_2O_3, CaO, Fe_2O_3, Li_2O, MgO, Na_2O, SiO_2, TiO_2, ZnO,$ and $ZrO_2,$ $k =$ corresponding GFC per each glass oxide component, g per g GFC including volatiles)
- $m_{ik}^{oxides\ in\ GFC}$ = mass fraction of the i^{th} glass oxide in the k^{th} GFC (g oxide per g GFC including volatiles)

\mathbf{t}_j = vector of $g_{ij}^{oxide\ in\ MFPV,\ target\ -gfc}$ for $n_j^{oxides\ in\ MFPV}$ components in the j^{th} MFPV batch (g oxide per g MFPV oxides)

$g_{ij}^{oxide\ in\ MFPV,\ target\ -gfc}$ = target mass fraction of the i^{th} glass oxide in glass from GFC for the j^{th} MFPV batch (g oxide per g MFPV oxides)

Then, the target mass of GFC per g glass is given as⁽⁸⁾

$$\ddot{M}_{kj}^{GFC\ in\ MFPV,\ target} = \max \left\{ \ddot{M}_{kj}^{GFC\ in\ MFPV,\ pre}, 0 \right\} \quad (49)$$

Because of Na₂O and Li₂O (not required from glass formulation rules) and some non-GFC components added as impurities from other GFCs, calculation of glass composition for all components requires normalization. The glass composition before applying the component retention factors is given by:

$$g_{ij}^{oxide\ in\ MFPV,\ Step1} = \frac{G_j^{waste\ in\ MFPV,\ target} g_{idm}^{oxide\ in\ CRV} + \sum_{k=1}^{n_j^{GFCs\ in\ MFPV}} m_{ik}^{oxide\ in\ GFC} \ddot{M}_{kj}^{GFC\ in\ MFPV,\ target}}{\sum_{i=1}^{n_j^{oxide\ in\ MFPV}} \left(G_j^{waste\ in\ MFPV,\ target} g_{idm}^{oxide\ in\ CRV} + \sum_{k=1}^{n_j^{GFCs\ in\ MFPV}} m_{ik}^{oxide\ in\ GFC} \ddot{M}_{kj}^{GFC\ in\ MFPV,\ target} \right)} \quad (50)$$

where $g_{ij}^{oxide\ in\ MFPV,\ Step1}$ = mass fraction of the i^{th} glass oxide in the j^{th} MFPV batch from algorithm calculation Step 1 before applying component retention factors (g oxide per g MFPV oxides)

$G_j^{waste\ in\ MFPV,\ target}$ = target mass fraction of glass oxides originated from waste in the j^{th} MFPV batch (g oxides per g glass)

$g_{idm}^{oxide\ in\ CRV}$ = mass fraction of the i^{th} glass oxide in the m^{th} transfer waste transferred from the d^{th} CRV to MFPV (g oxide per g CRV oxides)

$n_j^{GFCs\ in\ MFPV}$ = number of GFCs in the j^{th} MFPV batch

$\ddot{M}_{kj}^{GFC\ in\ MFPV,\ target}$ = target mass of k^{th} GFC per g of glass to add to the j^{th} MFPV batch (g GFC per g glass)

$m_{ik}^{oxide\ in\ GFC}$ = mass fraction of the i^{th} glass oxide in the k^{th} GFC (g oxide per g GFC including volatiles). Here, unlike \mathbf{H} in Equation (48), $m_{ik}^{oxide\ in\ GFC}$ includes all tracked

⁽⁸⁾ For some formulations, the mass fraction of GFC from Equation (48) becomes negative if the target mass fraction in glass is zero (applicable to Na₂O and Li₂O only-target mass fraction is greater than zero for all other GFC components) when there are GFCs that contain these as impurities. For simplicity, an after-linear-regression constraint of $\ddot{M}_{kj}^{GFC\ in\ MFPV,\ target} \geq 0$ was used in this case rather than a “constrained least squares” method. A comparison of the two methods showed little impact for the current GFC matrix, which has relatively small Na₂O and zero Li₂O impurities. However, if GFCs were to include more significant impurities of these components then this evaluation needs to be repeated or the “constrained least squares” methods may need to be adopted.

components beyond the 11 GFC components.

$n_j^{oxides\ in\ MFPV}$ = number of glass oxides tracked in the mass balance calculations for the j^{th} MFPV batch

From Equation (50), the final waste loading in glass for the j^{th} MFPV batch from algorithm calculation Step 1 after including the impurities from GFC is given as:

$$G_j^{waste\ in\ MFPV,\ Step1} = \frac{\sum_{i=1}^{n_j^{oxide\ in\ MFPV}} \left(G_j^{MFPV,\ target} g_{CRV}^{oxide\ in} \right)}{\sum_{i=1}^{n_j^{oxide\ in\ MFPV}} \left(G_j^{MFPV,\ target} g_{CRV}^{oxide\ in} + \sum_{k=1}^{GFCs\ in\ MFPV} m_{ik}^{GFC} \ddot{M}_{kj}^{oxide\ in\ MFPV,\ target} \right)} \quad (51)$$

where $G_j^{waste\ in\ MFPV,\ Step1}$ is the mass fraction of glass oxides originated from waste in the j^{th} MFPV batch from algorithm calculation Step 1, i.e., waste loading (g per g MFPV oxides).

Since many radionuclides and chemical components are partially lost to the offgas during melting, their concentration in glass would be overestimated if it were assumed that the melt retained 100% of their mass in the melter feed. A portion of the fraction emitted from the melter is captured in the offgas system and recycled back to pretreatment. This recycling process will increase the concentration of such species in the incoming feed, further exaggerating their estimated concentrations in glass. To help improve the estimate of glass composition, a retention factor (v_i), equal to the fraction retained in the melt, is applied. The glass composition after applying the component retention factors is:

$$\tilde{g}_{ij}^{oxide\ in\ MFPV,\ Step1} = \frac{g_{ij}^{oxide\ in\ MFPV,\ Step1} v_i}{\sum_{i=1}^{n_j^{oxides\ in\ MFPV}} g_{ij}^{oxide\ in\ MFPV,\ Step1} v_i} \quad (52)$$

where $\tilde{g}_{ij}^{oxide\ in\ MFPV,\ Step1}$ = mass fraction of the i^{th} glass oxide in the j^{th} MFPV batch from algorithm calculation Step 1 **after** applying component retention factors (g oxide per g glass)

$g_{ij}^{oxide\ in\ MFPV,\ Step1}$ = mass fraction of the i^{th} glass oxide in the j^{th} MFPV batch from algorithm calculation Step 1 **before** applying component retention factors (g oxide per g glass)

$n_j^{oxides\ in\ MFPV}$ = number of glass oxides tracked in the mass balance calculations for the j^{th} MFPV batch

v_i = retention factor for the i^{th} component (fraction) (listed in Table A-3)

The activity of radionuclides per unit mass of glass oxides in the j^{th} MFPV batch before applying component retention factors is given as:

$$\begin{aligned}
 a_{ij}^{rad\ in\ MFPV,\ Step1} &= a_{idm}^{rad\ in\ CRV} G_j^{waste\ in\ MFPV,\ Step1} \\
 &= \frac{\bar{R}_{id}^{rad\ in\ CRV} \lambda_{dm} G_j^{waste\ in\ MFPV,\ Step1}}{C_{dm}^{oxides\ in\ CRV}}
 \end{aligned} \tag{53}$$

- where $a_{ij}^{rad\ in\ MFPV,\ Step1}$ = specific activity of the i^{th} radionuclide in the j^{th} MFPV batch from algorithm calculation Step 1 before applying component retention factors (mCi/g oxides)
- $a_{idm}^{rad\ in\ CRV}$ = specific activity of the i^{th} radionuclide in the m^{th} transfer waste transferred from the d^{th} CRV to MFPV (mCi/g oxides)
- $G_j^{waste\ in\ MFPV,\ Step1}$ = (final) mass fraction of glass oxides originated from waste in the j^{th} MFPV batch from algorithm calculation Step 1, i.e. (final) waste loading (g per g MFPV oxides)
- $\bar{R}_{id}^{rad\ in\ CRV}$ = activity (per unit volume) of the i^{th} radionuclide in the waste of the d^{th} CRV averaged over $n_d^{samps\ in\ CRV}$ samples analyzed (mCi/L)
- λ_{dm} = dilution factor for the m^{th} transfer waste transferred from the d^{th} CRV to MFPV
- $C_{dm}^{oxides\ in\ CRV}$ = concentration of total glass oxides in the m^{th} transfer waste transferred from the d^{th} CRV to MFPV (g oxides per L waste)

The specific activity after applying retention factors is given as:

$$\tilde{a}_{ij}^{rad\ in\ MFPV,\ Step1} = \frac{a_{ij}^{rad\ in\ MFPV,\ Step1} v_i}{\sum_{i=1}^{n_j^{oxides\ in\ MFPV}} g_{ij}^{oxide\ in\ MFPV,\ Step1} v_i} \tag{54}$$

where $\tilde{a}_{ij}^{rad\ in\ MFPV,\ Step1}$ is the specific activity of the i^{th} radionuclide in the j^{th} MFPV batch from algorithm calculation Step 1 after applying component retention factors (mCi/g oxides) and v_i is the retention factor for the i^{th} radionuclide (fraction).

5.1.5 Calculation of LAW Transfer Volume

The two key variables considered in material transfer to the MFPV for each batch are glass composition and vessel volume. The concentrated LAW is transferred from the TCP (in PT) to one of two CRVs in the LAW vitrification facility. Each CRV has a working volume of 13,231 gal (50,085 L) and a nominal batch size of 9,115 gal (34,504 L). LAW is transferred from the CRVs into each of two MFPVs in roughly four 2,300 gal (8,700 L) batches (24590-LAW-3YD-LCP-00001, 24590-LAW-M4C-20-00002). Each MFPV has a nominal working volume of 5,132 gal (19,426 L), which is a sum of the nominal batch of 3,400 gal (12,870 L) and nominal heel of 1,732 gal (6,556 L). The target LAW transfer volume ($V_{dm}^{transwaste\ CRV}$) from the CRV to the MFPV is determined by comparing the anticipated melter feed volume with the remaining operating

capacity of the vessel. The determination of waste transfer volume ($V_{dm}^{CRV, transwaste}$) from CRV to MFPV needs to account for the volumes of:

- MFPV heel ($V_j^{MFPV, heel}$),
- CRV-MFPV transfer line flush water ($V_j^{MFPV, transflush}$),
- MFPV sampling line flush water ($V_j^{MFPV, sampflush}$),
- GFCs ($V_j^{MFPV, GFC}$),
- GFC dust control water ($V_j^{MFPV, dust}$),
- Sucrose ($V_j^{MFPV, sucrose}$),
- Dilution water ($V_j^{MFPV, dilute}$),

so that the combined volumes equal to the MFPV working volume ($V_j^{MFPV, working}$).

The volume contributions to the MFPV batch can be subdivided into three categories 1) the volumes independent of $V_{dm}^{CRV, transwaste}$ such as $V_j^{MFPV, heel}$, $V_j^{MFPV, transflush}$ and $V_j^{MFPV, sampflush}$, 2) the volumes dependent on $V_{dm}^{CRV, transwaste}$ such as $V_j^{MFPV, Step1, GFC}$, $V_j^{MFPV, Step1, dust}$, and $V_j^{MFPV, Step1, sucrose}$, and 3) the volume dependent on $V_{dm}^{CRV, transwaste}$ as well as on $V_j^{MFPV, transflush}$, $V_j^{MFPV, sampflush}$, and $V_j^{MFPV, dust}$, which is $V_j^{MFPV, Step1, dilute}$. The equation for volume calculation in Step 1 of ILAW algorithm is given as:

$$V_j^{MFPV, working} = V_{dm}^{CRV, transwaste} + V_j^{MFPV, Step1, GFC} + V_j^{MFPV, Step1, dust} + V_j^{MFPV, Step1, sucrose} + V_j^{MFPV, heel} + V_j^{MFPV, transflush} + V_j^{MFPV, sampflush} + V_j^{MFPV, Step1, dilute} \quad (55)$$

where $V_j^{MFPV, working}$ = working volume for the j^{th} MFPV batch (L). The MFPV working volume includes the MFPV heel volume ($V_j^{MFPV, heel}$) required for normal operation plus the MFPV batch volume ($V_j^{MFPV, batch}$) prepared. $V_j^{MFPV, working, nominal} = 12,444$ L

$V_{dm}^{CRV, transwaste}$ = volume of the m^{th} transfer waste to be transferred from the d^{th} CRV to MFPV (L).

$V_j^{MFPV, Step1, GFC}$ = total volume of GFCs to be added to the j^{th} MFPV batch in Step 1, i.e., $\sum_{k=1}^{n_j^{GFCs, in MFPV}} V_{kj}^{MFPV, Step1, GFC}$ (L) where $V_{kj}^{MFPV, Step1, GFC}$ is the volume of k^{th} GFC to be added to the j^{th} MFPV batch (L) in Step 1 and $n_j^{GFCs, in MFPV}$ is the number of GFCs used in the j^{th} MFPV batch.

$V_j^{dust, MFPV, Step1}$ = volume of water added to control GFC dusting in the j^{th} MFPV batch in Step 1 (L)

$V_j^{sucrose, MFPV, Step1}$ = volume of sucrose addition to the j^{th} MFPV batch in Step 1 (L)

$V_j^{heel, MFPV}$ = volume of heel in the j^{th} MFPV batch measured prior to waste transfer (L)

$V_j^{transflush, MFPV}$ = volume of water used to flush the CRV-MFPV transfer line in the j^{th} MFPV batch (L)

$V_j^{sampflush, MFPV}$ = volume of water used to flush the MFPV sampling line in the j^{th} MFPV batch (L)

$V_j^{dilute, MFPV, Step1}$ = volume of dilution water required to maintain satisfactory melter-feed rheological properties in the j^{th} MFPV batch in Step 1 (L)

Equation (55) assumes ideal mixing between slurry (waste and heel) and water (flush, dust control, and dilution), i.e., the discrepancy by nonideal mixing of a small volume of water added to the large volume of slurry is negligible.

Solving Equation (55) requires estimates of the various volumes. The $V_j^{working, MFPV}$ is given by

24590-LAW-M6C-LFP-00001, Rev 1 as 19,426 L. The heel volume $V_j^{heel, MFPV}$ will be measured before each

transfer but has a nominal value of 6,556 L (24590-LAW-M6C-LFP-00001, Rev 1). The nominal $V_j^{transflush, MFPV}$

and $V_j^{sampflush, MFPV}$ values depend on the MFPV and CRV vessels used and are summarized in Table 14 (24590-LAW-M4C-20-00002, Rev. 0). These nominal flush volumes are used for example calculations in this report but the measured values will be used in the algorithm for plant operation. MFPV to MFV and MFV to melter line flushes are not counted because they do not contribute to the MFPV volume.

Table 14. CRV-MFPV Line and Sampling Line Flush Nominal Volumes (L)

MFPV AND CRV VESSELS	$V_j^{transflush, MFPV}$	$V_j^{sampflush, MFPV}$
For LFP-VSL-00001 from LCP-VSL-00001	37.5	175.3
For LFP-VSL-00001 from LCP-VSL-00002	28.4	175.3
For LFP-VSL-00003 from LCP-VSL-00001	66.2	247.2
For LFP-VSL-00003 from LCP-VSL-00002	40.5	247.2

The remaining volumes in Equation (55), $V_j^{GFC, MFPV, Step1}$, $V_j^{dust, MFPV, Step1}$, $V_j^{sucrose, MFPV, Step1}$, and $V_j^{dilute, MFPV, Step1}$ are estimated

as a function of $V_{dm}^{transwaste, CRV}$ as described below.

Section 5.1.3 describes the general method of determining the target mass fraction of glass oxides originated from waste in glass ($G_j^{wastein, MFPV, target}$ or waste loading) and mass of each GFC per g glass ($\ddot{M}_{kj}^{GFCin, MFPV, target}$) in an MFPV batch required to calculate the $V_j^{GFC, MFPV, Step1}$ value:

$$V_j^{GFC, MFPV, Step1} = V_{dm}^{transwaste, CRV} \sum_{k=1}^{n_j^{GFCs in, MFPV}} \frac{C_{dm}^{oxide in, CRV} \ddot{M}_{kj}^{GFCin, MFPV, target}}{G_j^{wastein, MFPV, target} \rho_k} \quad (56)$$

where $C_{dm}^{oxide in, CRV}$ = concentration of total glass oxides in the m^{th} transfer waste transferred from the d^{th} CRV to MFPV, calculated by Equation (22) (g oxide per L LAW)

$\ddot{M}_{kj}^{GFCin, MFPV, target}$ = target mass of k^{th} GFC per g glass to add to the j^{th} MFPV batch (g per g glass)

$G_j^{wastein, MFPV, target}$ = target mass fraction of glass oxides originated from waste from CRV in glass for the j^{th} MFPV batch (g oxides per g glass)

ρ_k = particle density of the k^{th} GFC (g/L)

$n_j^{GFCs in, MFPV}$ = the number of GFCs in the j^{th} MFPV batch

Equation (56) assumes that the volume of GFC in the MFPV slurry is equal to the specific volume ($1/\rho_k$) of each GFC particle multiplied by its mass (see Appendix F for details).

Water is added to control dusting of the GFCs at a constant ratio (4 wt%) to total GFC mass (24590-LAW-M4C-20-00002, Rev 0). Since the dust control water volume depends on the mass of GFCs, it is also dependent on the volume of HLW transfer to the MFPV, as shown in the following equations.

$$V_j^{dust, MFPV, Step1} = \frac{0.04 M_j^{GFCs in, MFPV, target, Step1}}{1000(g/L)} \quad (57)$$

$$V_j^{dust, MFPV, Step1} = V_{dm}^{transwaste, CRV} \frac{0.04}{1000(g/L)} \sum_{k=1}^{n_j^{GFCs in, MFPV}} \frac{C_{dm}^{oxides in, CRV} \ddot{M}_{kj}^{GFCin, MFPV, target}}{G_j^{wastein, MFPV, target}} \quad (58)$$

where $M_j^{GFCs in, MFPV, target, Step1}$ is the total target mass of GFCs in the j^{th} MFPV batch from algorithm calculation Step 1 (g) and the remaining symbols are as previously defined.

Sucrose is used to control redox chemistry and ensure proper processing conditions in the melter. The amount of sucrose is determined by setting the target ratio of carbon moles (from sucrose and total organic carbon in the waste) to nitrogen moles (from nitrate and nitrite) equal to 0.75 ($C/NO_x = 0.75$). The target mass of sucrose is calculated according to Matlack et al. (2005):

$$\dot{M}_j^{sucrose\ in\ MFPV,\ target} = \max \left\{ \left[0.75 \left(\frac{c_{NO_2, dm}^{element\ in\ CRV}}{MW_{NO_2}} + \frac{c_{NO_3, dm}^{element\ in\ CRV}}{MW_{NO_3}} \right) - \frac{c_{TOC, dm}^{element\ in\ CRV}}{MW_C} \right] \frac{MW_{C_{12}H_{22}O_{11}}}{12(\text{moles of C/sucrose})}, 0 \right\} \quad (59)$$

where $\dot{M}_j^{sucrose\ in\ MFPV,\ target}$ = target mass of sucrose required per L of waste (g/L)

$c_{NO_2, dm}^{element\ in\ CRV}$, $c_{NO_3, dm}^{element\ in\ CRV}$, and $c_{TOC, dm}^{element\ in\ CRV}$ = concentration of nitrite, nitrate, and total organic carbon in the m^{th} transfer waste transferred from the d^{th} CRV to MFPV (g/L LAW)

MW_{NO_2} , MW_{NO_3} , and MW_C = molecular masses of nitrite, nitrate, and carbon (g/mole)

$MW_{C_{12}H_{22}O_{11}}$ = molecular mass of sucrose (g/mole)

$$V_j^{sucrose\ MFPV,\ Step1} = \frac{V_{dm}^{transwaste\ CRV} \dot{M}_j^{sucrose\ in\ MFPV,\ target}}{\rho_{sucrose}} \quad (60)$$

where $\rho_{sucrose}$ is the particle density of sucrose (g/L) and the remaining symbols are as previously defined. The particle densities of sucrose ($\rho_{sucrose}$) and GFCs (ρ_k) are listed in Table A-12.

Dilution water may be required to lower the risk of cementation of the blended melter feed in the MFPV and/or MFV. At low waste loading and high sodium molarities, the LAW melter feed was found to harden and not be mixable or pumpable (Poloski et al. 2004, CCN 116150). To avoid this failure of the melter feed preparation system, the WTP (CCN 116150) developed an empirical correlation between waste loading, represented by waste Na₂O mass fraction in glass, and sodium molarity ([Na]) in melter feed. Satisfactory melter-feed rheological properties were found in feeds that followed the trend in Figure 9. This trend line is used as a preliminary estimate of dilution water required to maintain the sodium molarity at the target ($t_{[Na]}$) or below in melter feed:

$$t_{[Na],j} = \frac{g_{Na_2O,j}^{oxide\ in\ MFPV,\ target} + 0.0047}{0.0249} \quad (61)$$

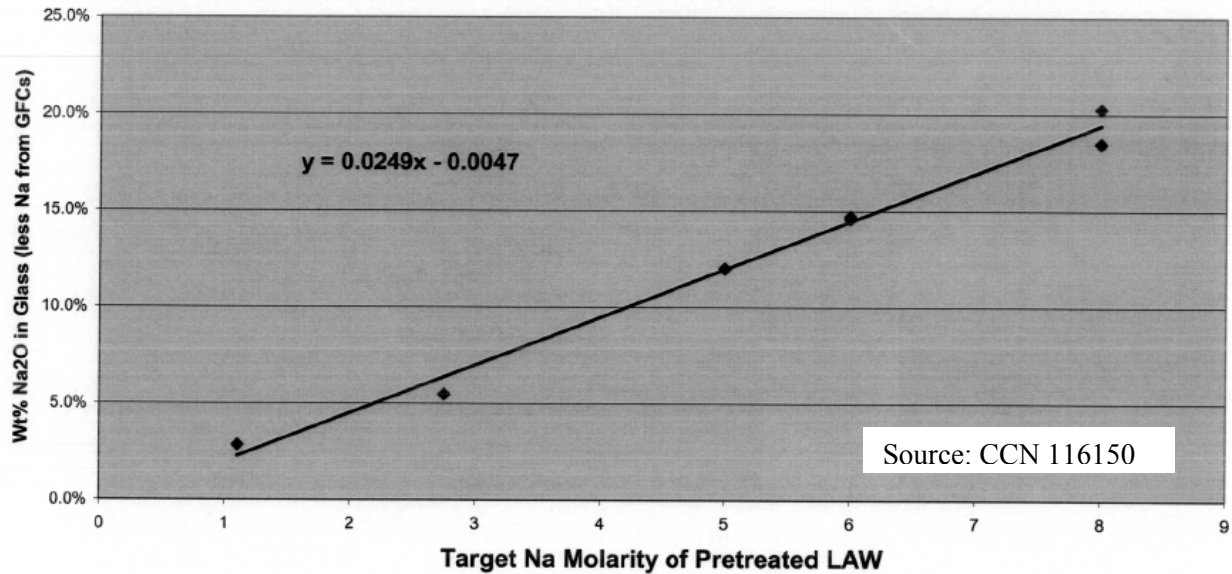
where $g_{Na_2O,j}^{oxide\ in\ MFPV,\ target}$ is the target Na₂O mass fraction in the j^{th} MFPV batch, given by Equation (46).

The target Na₂O loading and total volume of water in a given MFPV vessel is then used to estimate the required volume of dilution water ($V_j^{dilute\ MFPV,\ pre}$).

$$V_j^{dilute\ MFPV,\ Step1} = \max \left\{ \frac{c_{Na, dm}^{element\ in\ CRV} V_{dm}^{transwaste\ CRV}}{1000 MW_{Na} t_{[Na],j}} - \left(V_{dm}^{transwaste\ CRV} + V_j^{transflush\ MFPV} + V_j^{samplerflush\ MFPV} + V_j^{dust\ MFPV,\ Step1} \right), 0 \right\} \quad (62)$$

where $c_{Na, dm}^{element\ in\ CRV}$ is the sodium concentration in the m^{th} transfer waste transferred from the d^{th} CRV to MFPV (mg/L waste), MW_{Na} is the molecular mass of sodium (=22.98977 g/mole), and the remaining notations are as previously defined in Equation (55) and (61). This preliminary empirical correlation should be updated, and is meant to reduce risk of an agitated MFPV system exceeding allowable rheological properties. Other controls would be required to reduce the risk of MFPV system failure if agitation were not supplied.

Figure 9. Relationship between Sodium Molarity and Waste Loading for Successful Melter Feed



The waste transfer volume ($V_{dm}^{transwaste}$) is obtained by solving Equations (55) through (62) iteratively.

From the waste transfer volume, the target masses of GFCs and sucrose are calculated

$$M_{kj}^{GFC\ in\ MFPV, target, Step1} = \frac{C_{dm}^{oxides\ in\ CRV} \cdot \ddot{M}_{kj}^{GFC\ in\ MFPV, target} \cdot V_{dm}^{transwaste}}{G_j^{waste\ in\ MFPV, target}} \quad (63)$$

$$M_j^{sucrose\ in\ MFPV, target, Step1} = \ddot{M}_j^{sucrose\ in\ MFPV, target} \cdot V_{dm}^{transwaste} \quad (64)$$

where $M_{kj}^{GFC\ in\ MFPV, target, Step1}$ = target mass of k^{th} GFC to add to the j^{th} MFPV batch resulted from algorithm calculation Step 1 (g)

$C_{dm}^{oxides\ in\ CRV}$ = concentration of total glass oxides in the m^{th} transfer waste transferred from the d^{th} CRV to MFPV, calculated by Equation (22) (g oxide per L LAW)

$\ddot{M}_{kj}^{GFC\ in\ MFPV, target}$ = target mass of k^{th} GFC per g glass to add to the j^{th} MFPV batch (g per g glass)

$$\begin{aligned}
 V_{dm}^{transwaste\ CRV} &= \text{volume of the } m^{\text{th}} \text{ transfer waste to be transferred from the } d^{\text{th}} \text{ CRV to MFPV (L). Result of algorithm calculation Step 1.} \\
 G_j^{waste\ in\ MFPV,\ target} &= \text{target mass fraction of glass oxides originated from waste from CRV in glass for the } j^{\text{th}} \text{ MFPV batch (g oxides per g glass)} \\
 M_j^{sucrose\ in\ MFPV,\ target,\ Step1} &= \text{target mass of sucrose to add to the } j^{\text{th}} \text{ MFPV batch resulted from algorithm calculation Step 1 (g)} \\
 \dot{M}_j^{sucrose\ in\ MFPV,\ target} &= \text{target mass of sucrose required per L of waste (g/L)}
 \end{aligned}$$

These target masses of GFCs and sucrose are used to calculate the GFCs and sucrose masses in algorithm Step 2 using the measured waste transfer volume.

5.1.6 Calculation of Constraints for Algorithm Step 1

The equations to calculate the quantities for all constraints listed in Table 10 through Table 13 for algorithm Step 1 are described in this section.

5.1.6.1 Glass Property and Model Validity Constraints

The constraints related to glass properties and model validities were discussed in Section 4.3.1. For property predictions and calculations of prediction uncertainties, the g_i for x_i^{prop} and x_{Others}^{prop} in Equations (3) and (4)

is given by $\tilde{g}_{ij}^{oxide\ in\ MFPV,\ Step1}$ from Equation (52). The model validity constraints are also calculated based on

$\tilde{g}_{ij}^{oxide\ in\ MFPV,\ Step1}$. Then, these x_i^{prop} values are used in Equations (2), (5), (6), and (7) to calculate P^{prop} and Equations (8) through (11) to calculate U_{pred}^{prop} . Composition uncertainty (U_{comp}^{prop}) is calculated following the methods described in Section 4.2.2. For U_{comp}^{prop} calculation the mass balance equations given by Equation (12) and (13) are rewritten based on the values for Step 1 calculation:

$$g_{ij}^{oxide\ in\ MFPV,\ Step1} = \frac{\frac{c_{idm}^{element\ in\ CRV} f_i^{transwaste\ CRV}}{1000(\text{mg/g})} + \sum_{k=1}^{n_j^{GFCs\ in\ MFPV}} m_{ik}^{oxide\ in\ GFC} M_{kj}^{GFC\ in\ MFPV,\ target,\ Step1}}{\sum_{i=1}^{n_d^{oxides\ in\ CRV}} \frac{c_{idm}^{element\ in\ CRV} f_i^{transwaste\ CRV}}{1000(\text{mg/g})} + \sum_{i=1}^{n_j^{oxides\ in\ MFPV}} \sum_{k=1}^{n_j^{GFCs\ in\ MFPV}} m_{ik}^{oxide\ in\ GFC} M_{kj}^{GFC\ in\ MFPV,\ target,\ Step1}} \quad (65)$$

$$\tilde{g}_{ij}^{oxide\ in\ MFPV,\ Step1} = \frac{g_{ij}^{oxide\ in\ MFPV,\ Step1} v_i}{\sum_{i=1}^{n_j^{oxides\ in\ MFPV}} g_{ij}^{oxide\ in\ MFPV,\ Step1} v_i} \quad (66)$$

- where
- $g_{ij}^{oxide\ in\ MFPV, Step1}$ = mass fraction of the i^{th} glass oxide in the j^{th} MFPV batch from algorithm calculation Step 1 after applying component retention factors (g oxide per g glass)
 - $\tilde{g}_{ij}^{oxide\ in\ MFPV, Step1}$ = mass fraction of the i^{th} glass oxide in the j^{th} MFPV batch from algorithm calculation Step 1 after applying component retention factors (g oxide per g glass)
 - $C_{idm}^{element\ in\ CRV}$ = concentration of the i^{th} component in the m^{th} transfer waste transferred from the d^{th} CRV to MFPV (mg/L waste)
 - f_i = oxide conversion factor, i.e., mass of the i^{th} glass oxide per mass of the i^{th} element
 - $V_{dm}^{transwaste\ CRV}$ = volume of the m^{th} transfer waste to be transferred from the d^{th} CRV to MFPV (L)
 - $n_j^{GFCs\ in\ MFPV}$ = number of GFCs used in the j^{th} MFPV batch
 - $m_{ik}^{oxide\ in\ GFC}$ = mass fraction of the i^{th} glass oxide in the k^{th} GFC (g oxide per g GFC including volatiles). Here, unlike **H** in Equation (48), $m_{ik}^{oxide\ in\ GFC}$ includes all tracked components beyond the 11 GFC components.
 - $M_{kj}^{GFC\ in\ MFPV, target, Step1}$ = target mass of k^{th} GFC to add to the j^{th} MFPV batch resulted from algorithm calculation Step 1 (g)
 - V_i = retention factor for the i^{th} component (fraction)
 - $n_d^{oxides\ in\ CRV}$ = number of glass oxides tracked in the mass balance calculations for the d^{th} CRV batch
 - $n_j^{oxides\ in\ MFPV}$ = number of glass oxides tracked in the mass balance calculations for the j^{th} MFPV batch

The results of P^{prop} , U_{pred}^{prop} , and U_{comp}^{prop} are used to calculate CL% UCCI or LCCI (B_{ucci}^{prop} or B_{lcci}^{prop}) for glass properties (PCT, VHT, viscosity, and electrical conductivity) according to Equation (16) discussed in Section 4.2.3.

$$B_{ucci,j}^{prop, Step1} = P_j^{prop, Step1} + U_{pred,j}^{prop, Step1} + U_{comp,j}^{prop, Step1} \quad \text{and} \quad B_{lcci,j}^{prop, Step1} = P_j^{prop, Step1} - U_{pred,j}^{prop, Step1} - U_{comp,j}^{prop, Step1} \quad (67)$$

- where
- $B_{ucci,j}^{prop, Step1}$ = CL% upper combined confidence interval for predicted “prop” s for the j^{th} MFPV batch from algorithm calculation Step 1 (in property model units)
 - $B_{lcci,j}^{prop, Step1}$ = CL% lower combined confidence interval for “prop” for the j^{th} MFPV batch from algorithm calculation Step 1 (applicable only to “vis” and “ec”) (in property model units)
 - $P_j^{prop, Step1}$ = predicted “prop” transformed property values for the j^{th} MFPV batch from algorithm calculation Step 1, which includes $\ln(r_B, \text{g/L})$, $\ln(r_{Na}, \text{g/L})$, $\ln(D, \mu\text{m})$, $\ln(\eta_T, \text{P})$, and $\ln(\epsilon_T, \text{S/cm})$

$U_{pred,j}^{prop,Step1}$ = model prediction uncertainty for “prop” for the j^{th} MFPV batch from algorithm calculation Step 1 (in property model units)

$U_{comp,j}^{prop,Step1}$ = composition uncertainty for “prop” for the j^{th} MFPV batch from algorithm calculation Step 1 (in property model units)

Note that CL% UCCIs and LCCIs are expressed in the units of the model used to predict a property (e.g., ln[g/L] for PCT responses). Hence, they can be used to assess whether property constraints (as discussed in Section 4.3) are met.

In addition, the SD values for glass component mass fractions ($\tilde{s}_{ij}^{oxide\ in\ MFPV,Step1}$) for algorithm calculation Step 1 after applying retention factors are obtained by Monte Carlo simulations of Equation (66).

5.1.6.2 Waste Na₂O Loading Constraint

The Contract (DOE 2000) Specification 2.2.2.2 requires that the Na₂O mass fraction in glass that came from waste Na₂O be above 14, 3, and 10 wt%, for Envelopes A, B, and C waste products, respectively. The waste

Na₂O loading in the j^{th} MFPV batch from algorithm calculation Step 1, $g_{Na_2O(w),j}^{oxide\ in\ MFPV,Step1}$, is calculated as:

$$g_{Na_2O(w),j}^{oxide\ in\ MFPV,Step1} = \frac{g_{Na_2O,dm}^{oxide\ in\ CRV} G_j^{waste\ in\ MFPV,target} \omega_d v_i}{\sum_{i=1}^{n_j^{oxides\ in\ MFPV}} \left[g_{idm}^{oxide\ in\ CRV} G_j^{waste\ in\ MFPV,target} v_i + \left(\sum_{k=1}^{n_j^{GFCs\ in\ MFPV}} m_{ik}^{oxide\ in\ GFC} \ddot{M}_{kj}^{GFC\ in\ MFPV,target} \right) v_i \right]} \quad (68)$$

where $g_{Na_2O(w),j}^{oxide\ in\ MFPV,Step1}$ = mass fraction of waste Na₂O (waste Na₂O loading) in the j^{th} MFPV batch from algorithm calculation Step 1 (g per g glass)

$g_{Na_2O,dm}^{oxide\ in\ CRV}$ = mass fraction of Na₂O in the m^{th} transfer waste transferred from the d^{th} CRV to MFPV (g oxide per g CRV oxides)

$G_j^{waste\ in\ MFPV,target}$ = target mass fraction of glass oxides originated from waste in the j^{th} MFPV batch (g oxides per g glass)

ω_d = fraction of the sodium in the d^{th} CRV batch that is classified as waste sodium (unitless)

v_i = retention factor for the i^{th} component (fraction)

$n_j^{oxides\ in\ MFPV}$ = number of glass oxides tracked in the mass balance calculations for the j^{th} MFPV batch

$g_{idm}^{oxide\ in\ CRV}$ = mass fraction of the i^{th} glass oxide in the m^{th} transfer waste transferred from the d^{th} CRV to MFPV (g oxide per g CRV oxides)

$n_j^{GFCs\ in\ MFPV}$ = number of GFCs in the j^{th} MFPV batch

$\ddot{M}_{kj}^{GFC\ in\ MFPV,target}$ = target mass of k^{th} GFC per g of glass to add to the j^{th} MFPV batch (g GFC per g glass)

mass fraction of the i^{th} glass oxide in the k^{th} GFC (g oxide per g GFC including volatiles). Here, unlike \mathbf{H} in Equation (48), $m_{ik}^{\text{oxide in GFC}}$ includes all tracked components beyond the 11 GFC components.

The fraction of waste Na_2O includes that originating from receipt of waste from the tank farm operator and that used to wash and leach the HLW fraction of the waste in the PT facility. All other sources of chemically added sodium (including that from GFCs) are non-waste Na_2O . The operator must enter both ω_d and the waste envelope from which the glass is produced to calculate $g_{\text{Na}_2\text{O}(w),j}^{\text{oxide in MFPV}}$ and compare it to the lower limit of waste Na_2O , $L_j^{\text{Na}_2\text{O}}$.

5.1.6.3 Radionuclide Concentration Constraints

The Contract (DOE 2000) Specification 2.2.2.8 requires that the radionuclide concentrations in glass do not exceed Class C limits as defined in 10CFR61.55 and the average glass concentrations of ^{137}Cs and ^{90}Sr be lower than 3 and 20 Ci/m^3 , respectively. The Contract (DOE 2000) Section C.7 (d).(1).(iii) further requires that the pretreatment unit operation remove ^{137}Cs from the filtered supernatant to achieve 0.3 Ci/m^3 to facilitate the maintenance concept established for the ILAW melter system.

The constraints related to radionuclide concentration limitations also need to consider uncertainties originated from uncertain values used in mass balance equations. The specific activity of radionuclide in glass is calculated by

$$a_{ij}^{\text{rad in MFPV,Step1}} = \frac{\overline{R}_{id}^{\text{rad in CRV}} \lambda_{dm} V_{dm}^{\text{transwaste CRV}}}{\sum_{i=1}^{n_d^{\text{oxides in CRV}}} c_{idm}^{\text{element in CRV}} f_i V_{dm}^{\text{transwaste CRV}} + \sum_{i=1}^{n_j^{\text{oxides in MFPV}}} \sum_{k=1}^{n_j^{\text{GFCs in MFPV}}} m_{ik}^{\text{oxide in GFC}} M_{kj}^{\text{GFC in MFPV,target,Step1}}} \cdot 1000(\text{mg/g}) \quad (69)$$

$$\tilde{a}_{ij}^{\text{rad in MFPV,Step1}} = \frac{a_{ij}^{\text{rad in MFPV,Step1}} V_i}{\sum_{i=1}^{n_j^{\text{oxides in MFPV}}} g_{ij}^{\text{oxide in MFPV,Step1}} V_i} \quad (70)$$

where $a_{ij}^{\text{rad in MFPV,Step1}}$ = specific activity of the i^{th} radionuclide in the j^{th} MFPV batch from algorithm calculation Step 1 before applying retention factors (mCi/g glass)

$\overline{R}_{id}^{\text{rad in CRV}}$ = activity (per unit volume) of the i^{th} radionuclide in the waste of the d^{th} CRV averaged over $n_d^{\text{samps in CRV}}$ samples analyzed (mCi/L)

λ_{dm} = dilution factor for the m^{th} transfer waste transferred from the d^{th} CRV to MFPV

$V_{dm}^{\text{transwaste CRV}}$ = volume of the m^{th} transfer waste to be transferred from the d^{th} CRV to MFPV (L)

- $n_d^{oxides\ in\ CRV}$ = number of glass oxides tracked in the mass balance calculations for the d^{th} CRV batch
- $c_{idm}^{element\ in\ CRV}$ = concentration of the i^{th} component in the m^{th} transfer waste transferred from the d^{th} CRV to MFPV (mg/L waste)
- f_i = oxide conversion factor, i.e., mass of the i^{th} glass oxide per mass of the i^{th} element
- $n_j^{oxides\ in\ MFPV}$ = number of glass oxides tracked in the mass balance calculations for the j^{th} MFPV batch
- $n_j^{GFCs\ in\ MFPV}$ = number of GFCs used in the j^{th} MFPV batch
- $m_{ik}^{oxide\ in\ GFC}$ = mass fraction of the i^{th} glass oxide in the k^{th} GFC (g oxide per g GFC including volatiles).
- $M_{kj}^{GFC\ in\ MFPV, target, Step1}$ = target mass of k^{th} GFC to add to the j^{th} MFPV batch resulted from algorithm calculation Step 1 (g)
- $\tilde{a}_{ij}^{rad\ in\ MFPV, Step1}$ = specific activity of the i^{th} radionuclide in the j^{th} MFPV batch from algorithm calculation Step 1 after applying retention factors (mCi/g glass)
- v_i = retention factor for the i^{th} component (fraction)
- $g_{ij}^{oxide\ in\ MFPV, Step1}$ = mass fraction of the i^{th} glass oxide in the j^{th} MFPV batch from algorithm calculation Step 1 after applying component retention factors (g oxide per g glass)

Here, Equation (69) is used instead of Equation (53) so that the SD of specific activity of radionuclide in glass can be calculated based on uncertain input values summarized in Table 9. The SD values for specific activity of radionuclide ($\tilde{s}_{ij}^{rad\ in\ MFPV, Step1}$) for algorithm calculation Step 1 after applying retention factors are obtained by Monte Carlo simulations of Equation (70).

The radionuclide concentration limits are based on the activity of each radionuclide either per unit glass mass or per unit glass volume. The specific activity of radionuclides from Equation (54) and its SD are converted to per unit glass volume using:

$$\hat{a}_{ij}^{rad\ in\ MFPV, Step1} = \tilde{a}_{ij}^{rad\ in\ MFPV, Step1} \rho_j^{glass\ in\ MFPV} \tag{71}$$

$$\hat{s}_{ij}^{rad\ in\ MFPV, Step1} = \tilde{s}_{ij}^{rad\ in\ MFPV, Step1} \rho_j^{glass\ in\ MFPV} \tag{72}$$

- where
- $\hat{a}_{ij}^{rad\ in\ MFPV, Step1}$ = activity of the i^{th} radionuclide per unit volume of glass in the j^{th} MFPV batch from algorithm calculation Step 1 after applying retention factors (Ci/m³ glass)
 - $\tilde{a}_{ij}^{rad\ in\ MFPV, Step1}$ = specific activity of the i^{th} radionuclide in the j^{th} MFPV batch from algorithm calculation Step 1 after applying retention factors (mCi/g glass)
 - $\rho_j^{glass\ in\ MFPV}$ = density of glass in the j^{th} MFPV batch (g/L)

$\hat{S}_{ij}^{rad\ in\ MFPV, Step1}$ = SD for the activity of the i^{th} radionuclide per unit volume of glass in the j^{th} MFPV batch from algorithm calculation Step 1 after applying retention factors (Ci/m³ glass)

$\tilde{S}_{ij}^{rad\ in\ MFPV, Step1}$ = SD for the specific activity of the i^{th} radionuclide in the j^{th} MFPV batch from algorithm calculation Step 1 after applying retention factors (mCi/g glass)

The relation between uncertainty and standard deviation is in general given as $U = ks$ where U is the uncertainty, s is the standard deviation, and k is the expansion factor. The expansion factor for various specifications (“spec”), k^{spec} is a function of the confidence level (CL), i.e., the k value is 1 for 68.27% CL, 1.645 for 90% CL, 1.960 for 95% CL, 2 for 95.45% CL, 2.576 for 99% CL, 3 for 99.73% CL, etc.⁽⁹⁾ The requirements for ¹³⁷Cs and ⁹⁰Sr are satisfied if the following conditions are satisfied:

$$\hat{a}_{137Cs,j}^{rad\ in\ MFPV, Step1} + k^{rad} \hat{S}_{137Cs,j}^{rad\ in\ MFPV, Step1} < 0.3\ Ci/m^3 \tag{73}$$

$$\hat{a}_{90Sr,j}^{rad\ in\ MFPV, Step1} + k^{rad} \tilde{S}_{90Sr,j}^{rad\ in\ MFPV, Step1} < 20\ Ci/m^3 \tag{74}$$

where k^{rad} is the expansion factor for radionuclide concentration specification.

To demonstrate that the waste meets the classification of Class C waste or below, limiting values for $\hat{a}_{ij}^{rad\ in\ MFPV}$ and $\tilde{a}_{ij}^{rad\ in\ MFPV}$; listed in Table 15 and Table 16, are used.

Table 15. Long Lived Radionuclides Class C Limits

Radionuclide (i)	$L_u^{\hat{a}_i}$, Ci/m ³	$L_u^{a_i}$, nCi/g
⁹⁹ Tc	3	
¹²⁹ I	0.08	
TRU ^(a)		100
²⁴¹ Pu		3,500
²⁴² Cm		20,000
(a) Alpha emitting transuranic nuclides with half-life greater than 5 years for Hanford LAW (24590-WTP-PL-RT-03-001) = ²³⁷ Np, ²³⁸ Pu, ²³⁹ Pu, ²⁴⁰ Pu, ²⁴¹ Am, ²⁴² Pu, ²⁴³ Am, ²⁴³ Cm, and ²⁴⁴ Cm. The total alpha counting measured in LAW 1a sample will be used instead of TRU activity calculated as sum of activities of these nuclides measured in LAW 1b sample.		

⁽⁹⁾ The Contract Specification 2.2.2.8 and Section C.7 (d).(1).(iii) do not specify the required confidence level.

⁽¹⁰⁾ The lower of two requirements, 3 Ci/m³ for Contract (DOE 2000) Specification 2.2.2.8 and 0.3 Ci/m³ for Contract (DOE 2000) Section C.7 (d).(1).(iii), is applied.

Table 16. Short Lived Radionuclides Class C Limits

Radionuclide (j)	$L_u^{\hat{a}_i}$, Ci/m ³
⁶³ Ni	700
⁹⁰ Sr	7,000
¹³⁷ Cs	4,600

According to 10 CFR 61.55:

- (3)(iv) For wastes containing mixtures of radionuclides listed in [Table 15], the total concentration shall be determined by the sum of fractions rule described in paragraph (a)(7) of [10CFR61.55].
- (4) Classification determined by short lived radionuclides. If radioactive waste does not contain any of the radionuclides listed in [Table 15], classification shall be determined based on the concentrations shown in [Table 16]...
- (5) Classification determined by both long- and short-lived radionuclides. If radioactive waste contains a mixture of radionuclides, some of which are listed in [Table 15], and some of which are listed in [Table 16], classification shall be determined as follows: (i) If the concentration of a nuclide listed in [Table 15] does not exceed 0.1 times the value listed in [Table 15], the class shall be determined by the concentration of nuclides listed in [Table 16]. (ii) If the concentration of a nuclide listed in [Table 15] exceeds 0.1 times the value listed in [Table 15] the waste shall be Class C, provided the concentration does not exceed the value shown in... [Table 16].

The first step to classification is then to determine if there are any radionuclides with measurable

concentrations ($\hat{a}_{ij}^{rad in, MFPV, Step1}$ for ⁹⁹Tc, ¹²⁹I, ⁶³Ni, ⁹⁰Sr, and ¹³⁷Cs, or $\tilde{a}_{ij}^{rad in, MFPV, Step1}$ for TRU, ²⁴¹Pu, and ²⁴²Cm). If non-zero values are present for radionuclides only in Table 15 or only in Table 16, then only those tables are used for classification. If there are non-zero values for both tables, then Table 15 is used for classification if any one radionuclide from Table 15 is greater than 10% of its associated limit. If no Table 15 radionuclide has a concentration greater than or equal to its associated limit, then Table 16 is used for classification. The sum of fractions rule is used for classification:

$$SF_{LL,j}^{rad in, MFPV, Step1} = \sum_i^2 \frac{\hat{a}_{ij}^{rad in, MFPV, Step1}}{L_u^{\hat{a}_i}} \text{ (for } i = \text{ } ^{99}\text{Tc and } ^{129}\text{I)} + \sum_i^3 \frac{\tilde{a}_{ij}^{rad in, MFPV, Step1} \times 10^6 \text{ (nCi/mCi)}}{L_u^{\hat{a}_i}} \text{ (for } i = \text{ TRU, } ^{241}\text{Pu, and } ^{242}\text{Cm)}$$
(75)

$$SF_{SL,j}^{rad in, MFPV, Step1} = \sum_i^3 \frac{\hat{a}_{ij}^{rad in, MFPV, Step1}}{L_u^{\hat{a}_i}} \text{ (for } i = \text{ } ^{63}\text{Ni, } ^{90}\text{Sr, and } ^{137}\text{Cs)}$$
(76)

where $SF_{LL,j}^{rad in, MFPV, Step1}$ = sum of fractions of activity to the limit of each radionuclide for long-lived radionuclides for Class C limit determination in the j^{th} MFPV batch from algorithm calculation Step 1

$SF_{SL,j}^{rad in, MFPV, Step1}$ = sum of fractions of activity to the limit of each radionuclide for short-lived radionuclides for Class C limit determination in the j^{th} MFPV batch from algorithm calculation Step 1

$\hat{a}_{ij}^{rad in, MFPV, Step1}$ = activity of the i^{th} radionuclide per unit volume of glass in the j^{th} MFPV batch from algorithm calculation Step 1 after applying retention factors (Ci/m³ glass)

$\tilde{a}_{ij}^{rad in, MFPV, Step1}$ = specific activity of the i^{th} radionuclide in the j^{th} MFPV batch from algorithm calculation Step 1 after applying retention factors (mCi/g glass)

$L_u^{\hat{a}_i}$ = upper limit for the activity of the i^{th} radionuclide per unit glass volume (Ci/m³ glass)

$L_u^{a_i}$ = upper limit for specific activity of the i^{th} radionuclide (nCi/g glass)

The standard deviations for $S_{LL,j}^{rad in, MFPV, Step1}$ and $S_{SL,j}^{rad in, MFPV, Step1}$ are given as:

$$S_{LL,j}^{rad SF in, MFPV, Step1} = \sqrt{\sum_i^2 \left(\frac{\hat{S}_{ij}^{rad in, MFPV, Step1}}{L_u^{\hat{a}_i}} \right)^2 \text{ (for } i = {}^{99}\text{Tc and } {}^{129}\text{I)} + \sum_i^3 \left(\frac{\tilde{S}_{ij}^{rad in, MFPV, Step1} \times 10^6 \text{ (nCi/mCi)}}{L_u^{a_i}} \right)^2 \text{ (for } i = \text{TRU, } {}^{241}\text{Pu, and } {}^{242}\text{Cm)}} \quad (77)$$

$$S_{SL,j}^{rad SF in, MFPV, Step1} = \sqrt{\sum_i^3 \left(\frac{\hat{S}_{ij}^{rad in, MFPV, Step1}}{L_u^{\hat{a}_i}} \right)^2 \text{ (for } i = {}^{63}\text{Ni, } {}^{90}\text{Sr, and } {}^{137}\text{Cs)}} \quad (78)$$

where $S_{LL,j}^{rad SF in, MFPV, Step1}$ = SD for the sum of fractions of activity to the limit of each radionuclide for long-lived radionuclides for Class C limit determination from algorithm calculation Step 1

$S_{SL,j}^{rad SF in, MFPV, Step1}$ = SD for the sum of fractions of activity to the limit of each radionuclide for short-lived radionuclides for Class C limit determination from algorithm calculation Step 1

$\hat{S}_{ij}^{rad in, MFPV, Step1}$ = SD for the activity of the i^{th} radionuclide per unit volume of glass in the j^{th} MFPV batch from algorithm calculation Step 1 after applying retention factors (Ci/m³ glass)

$\tilde{S}_{ij}^{rad in, MFPV, Step1}$ = SD for the specific activity of the i^{th} radionuclide in the j^{th} MFPV batch from algorithm calculation Step 1 after applying retention factors (mCi/g glass)

$L_u^{\hat{a}_i}$ = upper limit for the activity of the i^{th} radionuclide per unit glass volume (Ci/m³ glass)

$L_u^{a_i}$ = upper limit for specific activity of the i^{th} radionuclide (nCi/g glass)

The Class C limit is satisfied as long as the following two conditions are satisfied:

$$SF_{LL,j}^{rad\ in\ MFPV,\ Step1} + k^{rad} S_{LL,j}^{radSF\ in\ MFPV,\ Step1} < 1 \quad (79)$$

$$SF_{SL,j}^{rad\ in\ MFPV,\ Step1} + k^{rad} S_{SL,j}^{radSF\ in\ MFPV,\ Step1} < 1 \quad (80)$$

5.1.6.4 Surface Dose Rate Constraint

The Contract (DOE 2000) Specification 2.2.2.9 requires that the surface dose rate of the canister be at or lower than 500 mrem/h. The ILAW PCP (24590-WTP-PL-RT-03-001) specifies that the compliance for this constraint will be confirmed by monitoring the surface dose rate of each ILAW container using handheld instrumentation or automated monitoring equipment prior to transfer for disposal. The surface dose rate calculation will not be performed by ILAW formulation algorithm.

5.1.7 Adjustment of Target Glass Composition

If all constraints (with uncertainties factored in) calculated from the initial glass formulation in Section 5.1.3 are met, the result of waste transfer volume calculation in Section 5.1.5 becomes the final output of Step 1 calculation.

The original glass formulation rules developed by Muller et al. (2004), Equations (25) and (32) through (45), were designed so that all the glasses formulated within these rules would pass all property requirements. It was recently discovered that some glasses formulated by applying both the Muller et al. (2004) rules and new rules (CCN 150795) fail the property and model validity constraints when applied to the present algorithm (Piepel et al. 2007). There are three changes that are likely to contribute to this: (1) new models with new model validity ranges (Piepel et al. 2007) have been implemented compared to the preliminary models and model validity ranges used to formulate the Muller et al. (2004) rules, (2) new glass formulation rules (CCN 150795) have been added, and (3) there have been changes in the projected composition of wastes from those used as a basis for the development of the Muller et al. (2004) rules.

A glass formulation study was performed to identify the constraints that fail when formulated following the steps described in Section 5.1.3 and then to develop the approach to adjust the target glass composition (i.e., deviate from the Muller et al. (2004) rules) using one set of the projected waste compositions. The same waste compositions as used for example calculations in Section 6 were used (see Section 6 for detailed description of the projected waste compositions). The results of this study are described below.

If the formulation fails one of the constraints, target Na₂O loading or target glass composition needs to be adjusted depending on which constraint is failed. The constraints that failed and the required adjustment for each failed constraint are:

1. Single component model validity constraint for F (decrease Na₂O loading)
2. Radionuclide concentration limits for ⁹⁰Sr and ¹³⁷Cs and Class C limit for long lived radionuclides caused by TRU concentration (decrease Na₂O loading)
3. Multi-component model validity constraint for Na₂O-SiO₂ (decrease Na₂O loading)
4. Multi-component model validity constraint for P₂O₅-Cr₂O₃ (decrease Na₂O loading)
5. Multi-component model validity constraint for Li₂O-SO₃ (decrease Li₂O target concentration)
6. Multi-component model validity constraint for Na₂O- SO₃ (increase Na₂O target concentration from GFC)
7. Upper limit for electrical conductivity at 1200°C (decrease Na₂O loading)
8. Upper limit for viscosity at 1150°C (increase Li₂O target concentration)

There are waste compositions that fail additional constraints after the first adjustment of target Na₂O loading or glass composition to meet the initial constraint that failed. After each adjustment of target Na₂O loading or glass composition, the calculation of waste transfer volume and predicted properties with uncertainties and all constraint quantities are calculated for adjusted formulation before next adjustment is calculated.

The adjustment of target Na₂O loading or glass composition described above, which may not work for different set of waste compositions, should be regarded as an intermediate solution. It is desirable to revise the glass formulation rules or expand the model validity range so that compliant glasses can be formulated without adjustment for all expected waste compositions, especially for those wastes that require significant decrease of Na₂O loading (i.e., waste loading). The decrease of waste loading increases the overall waste treatment cost and for some wastes a large decrease of waste loading may lead to a failure of a contract waste loading requirement. The equations used to adjust the target Na₂O loading or glass composition are described below.

If the initial formulation fails the constraints other than above listed or the adjustment described below does not lead to a compliant formulation an interruption by qualified staff is required.

5.1.7.1 Adjustment of Target Na₂O Loading

For the case of decreasing the target Na₂O loading (#1, 2, 3, 4, and 7), the adjusted preliminary target Na₂O concentration in glass ($g_{Na_2O,j}^{oxide\ in\ MFPV,pre-adj}$) is given as:

$$g_{Na_2O,j}^{oxide\ in\ MFPV,pre-adj} = g_{Na_2O,j}^{oxide\ in\ MFPV,pre} - g_{Na_2O,j}^{oxide\ in\ MFPV,adj} \quad (81)$$

where $g_{Na_2O,j}^{oxide\ in\ MFPV,pre}$ is the preliminary target Na₂O concentration in Equation (31) and $g_{Na_2O,j}^{oxide\ in\ MFPV,adj}$ (≥ 0) is the adjustment of Na₂O concentration. Then, the adjusted initial composition ($g_{ij}^{oxide\ in\ MFPV,initial,adj}$) for the j^{th} MFPV batch is obtained by applying Equations (32) through (45) in Section 5.1.3 after replacing $g_{Na_2O,j}^{oxide\ in\ MFPV,pre}$ with $g_{Na_2O,j}^{oxide\ in\ MFPV,pre-adj}$ and the superscript “*initial*” is replaced by “*initial,adj*”. The adjusted initial glass composition ($g_{ij}^{oxide\ in\ MFPV,initial,adj}$) is then set to target composition ($g_{ij}^{oxide\ in\ MFPV,target}$) for all components, i.e.

$$g_{ij}^{oxide\ in\ MFPV,target} = g_{ij}^{oxide\ in\ MFPV,initial,adj} \quad (82)$$

and used to calculate the Step 1 glass and radionuclide compositions (Section 5.1.4) and waste transfer volume (Section 5.1.5). The glass and radionuclide compositions and waste transfer volume are used to calculate the constraint quantities and compare them with the limits (Section 5.1.6).

Equation (83) computes the ratios of loading and predicted properties (with their uncertainties) to their corresponding limits (constraints) and ensures this ratio (after applying δ) is less than one. The method of

target Na₂O loading adjustment is to find the $g_{Na_2O,j}^{oxide\ in\ MFPV,adj}$ value that satisfies the following equation through iterative calculations:

$$\begin{aligned}
 & \left(\frac{\tilde{g}_{ij}^{oxide\ in\ MFPV,\ Step1}}{L_u^{\tilde{g}_i^{MFPV}}} \cdot 1 - \frac{\tilde{g}_{SiO_2,j}^{oxide\ in\ MFPV,\ Step1} - 0.384}{0.521 - 0.384} \cdot 1 - \frac{0.521 - \tilde{g}_{SiO_2,j}^{oxide\ in\ MFPV,\ Step1}}{0.521 - 0.384} \right), \\
 & \frac{\hat{a}_{90Sr,j}^{rad\ in\ MFPV,\ Step1} + k^{rad} \hat{a}_{90Sr,j}^{rad\ in\ MFPV,\ Step1}}{20}, \frac{\hat{a}_{137Cs,j}^{rad\ in\ MFPV,\ Step1} + k^{rad} \hat{a}_{137Cs,j}^{rad\ in\ MFPV,\ Step1}}{0.3}, \\
 & SF_{LL,j}^{rad\ in\ MFPV,\ Step1} + k^{rad} S_{LL,j}^{radSF\ in\ MFPV,\ Step1}, SF_{SL,j}^{rad\ in\ MFPV,\ Step1} + k^{rad} S_{SL,j}^{radSF\ in\ MFPV,\ Step1}, \\
 & 1 - \frac{\tilde{g}_{Na_2O,j}^{oxide\ in\ MFPV,\ Step1} - \left(0.6024 - 1.3287 \tilde{g}_{SiO_2,j}^{oxide\ in\ MFPV,\ Step1} \right)}{\left(0.8050 - 1.3287 \tilde{g}_{SiO_2,j}^{oxide\ in\ MFPV,\ Step1} \right) - \left(0.6024 - 1.3287 \tilde{g}_{SiO_2,j}^{oxide\ in\ MFPV,\ Step1} \right)}, \\
 \max & \left(\frac{\left(0.8050 - 1.3287 \tilde{g}_{SiO_2,j}^{oxide\ in\ MFPV,\ Step1} \right) - \tilde{g}_{Na_2O,j}^{oxide\ in\ MFPV,\ Step1}}{\left(0.8050 - 1.3287 \tilde{g}_{SiO_2,j}^{oxide\ in\ MFPV,\ Step1} \right) - \left(0.6024 - 1.3287 \tilde{g}_{SiO_2,j}^{oxide\ in\ MFPV,\ Step1} \right)} \right) + \delta = 1 \\
 & 1 - \frac{\left(0.8050 - 1.3287 \tilde{g}_{SiO_2,j}^{oxide\ in\ MFPV,\ Step1} \right) - \left(0.6024 - 1.3287 \tilde{g}_{SiO_2,j}^{oxide\ in\ MFPV,\ Step1} \right)}{\left(0.8050 - 1.3287 \tilde{g}_{SiO_2,j}^{oxide\ in\ MFPV,\ Step1} \right) - \left(0.6024 - 1.3287 \tilde{g}_{SiO_2,j}^{oxide\ in\ MFPV,\ Step1} \right)}, \\
 & 1 - \frac{\tilde{g}_{Cr_2O_3,j}^{oxide\ in\ MFPV,\ Step1} - \left(0.2102 \tilde{g}_{P_2O_5,j}^{oxide\ in\ MFPV,\ Step1} - 0.0018 \right)}{\left(0.3226 \tilde{g}_{P_2O_5,j}^{oxide\ in\ MFPV,\ Step1} + 0.0017 \right) - \left(0.2102 \tilde{g}_{P_2O_5,j}^{oxide\ in\ MFPV,\ Step1} - 0.0018 \right)}, \\
 & \left(\frac{\left(0.3226 \tilde{g}_{P_2O_5,j}^{oxide\ in\ MFPV,\ Step1} + 0.0017 \right) - \tilde{g}_{Cr_2O_3,j}^{oxide\ in\ MFPV,\ Step1}}{\left(0.3226 \tilde{g}_{P_2O_5,j}^{oxide\ in\ MFPV,\ Step1} + 0.0017 \right) - \left(0.2102 \tilde{g}_{P_2O_5,j}^{oxide\ in\ MFPV,\ Step1} - 0.0018 \right)} \right) \\
 & 1 - \frac{\left(0.3226 \tilde{g}_{P_2O_5,j}^{oxide\ in\ MFPV,\ Step1} + 0.0017 \right) - \left(0.2102 \tilde{g}_{P_2O_5,j}^{oxide\ in\ MFPV,\ Step1} - 0.0018 \right)}{\left(0.3226 \tilde{g}_{P_2O_5,j}^{oxide\ in\ MFPV,\ Step1} + 0.0017 \right) - \left(0.2102 \tilde{g}_{P_2O_5,j}^{oxide\ in\ MFPV,\ Step1} - 0.0018 \right)}, \\
 & \frac{B_{ucci,j}^{ec1200,\ Step1}}{\ln(0.7)},
 \end{aligned}
 \tag{83}$$

where $\tilde{g}_{ij}^{oxide\ in\ MFPV,\ Step1}$ = mass fraction of the i^{th} glass oxide in the j^{th} MFPV batch from algorithm calculation Step 1 after applying component retention factors (g oxide per g glass)

$L_u^{\tilde{g}_i^{MFPV}}$ = model validity upper limit for the mass fraction of the i^{th} glass oxide after applying component retention factors (g oxide per g glass) for $i = Al_2O_3, Cl, Cr_2O_3, F, P_2O_5,$ and Sum of Minors as given in Table 11

$\tilde{g}_{SiO_2,j}^{oxide\ in\ MFPV,\ Step1}$ = mass fraction of SiO_2 in the j^{th} MFPV batch from algorithm calculation Step 1 after applying component retention factors (g oxide per g glass)

k^{rad} = expansion factor for radionuclide concentration specification

- $\hat{a}_{ij}^{rad\ in\ MFPV, Step1}$ = activity of the i^{th} radionuclide ($i = {}^{90}\text{Sr}$ or ${}^{137}\text{Cs}$) per unit volume of glass in the j^{th} MFPV batch from algorithm calculation Step 1 after applying retention factors (Ci/m^3 glass)
- $\hat{S}_{90\text{Sr},j}^{rad\ in\ MFPV, Step1}$ = SD for the activity of the i^{th} radionuclide ($i = {}^{90}\text{Sr}$ or ${}^{137}\text{Cs}$) per unit volume of glass in the j^{th} MFPV batch from algorithm calculation Step 1 after applying retention factors (Ci/m^3 glass)
- $S_{LL,j}^{rad\ in\ MFPV, Step1}$ = sum of fractions of activity to the limit of each radionuclide for long-lived radionuclides for Class C limit determination in the j^{th} MFPV batch from algorithm calculation Step 1
- $S_{LL,j}^{radSF\ in\ MFPV, Step1}$ = SD for the sum of fractions of activity to the limit of each radionuclide for long-lived radionuclides for Class C limit determination from algorithm calculation Step 1
- $S_{SL,j}^{rad\ in\ MFPV, Step1}$ = sum of fractions of activity to the limit of each radionuclide for short-lived radionuclides for Class C limit determination in the j^{th} MFPV batch from algorithm calculation Step 1
- $S_{SL,j}^{radSF\ in\ MFPV, Step1}$ = SD for the sum of fractions of activity to the limit of each radionuclide for short-lived radionuclides for Class C limit determination from algorithm calculation Step 1
- $B_{ucci,j}^{ec1200, Step1}$ = CL% upper combined confidence interval for predicted “*ec1200*” for the j^{th} MFPV batch from algorithm calculation Step 1 (in property model units)
- δ = a unitless constant larger than zero and typically smaller than 0.01¹¹ introduced to accommodate the variations resulting from Monte Carlo calculation of composition uncertainties

If all constraints calculated from the adjusted target composition described above are met, the result of waste transfer volume calculation in Section 5.1.5 becomes the final output of Step 1 calculation.

5.1.7.2 Adjustment of Target Li_2O or Na_2O Concentration

For the case of adjusting target concentration of Li_2O or Na_2O (#5, 6, and 8), the Equation (46) for Li_2O or Na_2O is replaced by:

$$g_{ij}^{oxide\ in\ MFPV, target} = g_{ij}^{oxide\ in\ MFPV, initial} + g_{ij}^{oxide\ in\ MFPV, adj} \{i = \text{Li}_2\text{O}, \text{Na}_2\text{O}\} \quad (84)$$

- where
- $g_{ij}^{oxide\ in\ MFPV, target}$ = target mass fraction of the i^{th} glass oxide in the j^{th} MFPV batch (g oxide per g MFPV oxides)
 - $g_{ij}^{oxide\ in\ MFPV, initial}$ = initial mass fraction of the i^{th} glass oxide in the j^{th} MFPV batch (g oxide per g MFPV oxides)
 - $g_{ij}^{oxide\ in\ MFPV, adj}$ = adjustment made to the target mass fraction of the i^{th} glass oxide in the j^{th} MFPV batch to satisfy the constraint that failed (g oxide per g MFPV oxides). For Na_2O ($g_{\text{Na}_2\text{O},j}^{oxide\ in\ MFPV, adj} \geq 0$) the increase of Na_2O is supplied from GFC not from waste.

¹¹ The required value of δ depends on the number of simulations used in Monte Carlo calculation of composition uncertainties. The value of 0.01 was sufficiently large for 5000 simulations.

The method of target Li₂O concentration adjustment to meet the multi-component model validity constraint for Li₂O-SO₃ is to find the $\tilde{g}_{Li_2O,j}^{oxide\ in\ MFPV,adj}$ value that satisfies the following equation through iterative calculations:

$$\max \left(\begin{array}{l} 1 - \frac{\tilde{g}_{Li_2O,j}^{oxide\ in\ MFPV,Step1} - \left(6.5263 \tilde{g}_{SO_3,j}^{oxide\ in\ MFPV,Step1} - 0.0410 \right)}{\left(6.5263 \tilde{g}_{SO_3,j}^{oxide\ in\ MFPV,Step1} + 0.0306 \right) - \left(6.5263 \tilde{g}_{SO_3,j}^{oxide\ in\ MFPV,Step1} - 0.0410 \right)}, \\ \left(6.5263 \tilde{g}_{SO_3,j}^{oxide\ in\ MFPV,Step1} + 0.0306 \right) - \tilde{g}_{Li_2O,j}^{oxide\ in\ MFPV,Step1} \\ 1 - \frac{\left(6.5263 \tilde{g}_{SO_3,j}^{oxide\ in\ MFPV,Step1} + 0.0306 \right) - \tilde{g}_{Li_2O,j}^{oxide\ in\ MFPV,Step1}}{\left(6.5263 \tilde{g}_{SO_3,j}^{oxide\ in\ MFPV,Step1} + 0.0306 \right) - \left(6.5263 \tilde{g}_{SO_3,j}^{oxide\ in\ MFPV,Step1} - 0.0410 \right)} \end{array} \right) + \delta = 1 \quad (85)$$

where $\tilde{g}_{ij}^{oxide\ in\ MFPV,Step1}$ is the mass fraction of the *i*th glass oxide in the *j*th MFPV batch from algorithm calculation Step 1 after applying component retention factors (g oxide per g glass) and δ is a unitless constant larger than zero and typically smaller than 0.01 introduced to accommodate the variations resulting from Monte Carlo calculation of composition uncertainties.

The method of target Na₂O concentration adjustment to meet the multi-component model validity constraint for Na₂O-SO₃ is to find the $\tilde{g}_{Na_2O,j}^{oxide\ in\ MFPV,adj}$ value that satisfies the following equation through iterative calculations:

$$\max \left(\begin{array}{l} 1 - \frac{\tilde{g}_{Na_2O,j}^{oxide\ in\ MFPV,Step1} - \left(0.0947 - 18.8088 \tilde{g}_{SO_3,j}^{oxide\ in\ MFPV,Step1} \right)}{\left(0.3161 - 18.8088 \tilde{g}_{SO_3,j}^{oxide\ in\ MFPV,Step1} \right) - \left(0.0947 - 18.8088 \tilde{g}_{SO_3,j}^{oxide\ in\ MFPV,Step1} \right)}, \\ \left(0.3161 - 18.8088 \tilde{g}_{SO_3,j}^{oxide\ in\ MFPV,Step1} \right) - \tilde{g}_{Na_2O,j}^{oxide\ in\ MFPV,Step1} \\ 1 - \frac{\left(0.3161 - 18.8088 \tilde{g}_{SO_3,j}^{oxide\ in\ MFPV,Step1} \right) - \tilde{g}_{Na_2O,j}^{oxide\ in\ MFPV,Step1}}{\left(0.3161 - 18.8088 \tilde{g}_{SO_3,j}^{oxide\ in\ MFPV,Step1} \right) - \left(0.0947 - 18.8088 \tilde{g}_{SO_3,j}^{oxide\ in\ MFPV,Step1} \right)} \end{array} \right) + \delta = 1 \quad (86)$$

The method of target Li₂O concentration adjustment to meet the upper limit for viscosity at 1150°C is to find the $\tilde{g}_{Li_2O,j}^{oxide\ in\ MFPV,adj}$ value that satisfies the following equation through iterative calculations:

$$\frac{\exp\left(B_{ucci,j}^{vis1150,Step1}\right)}{80} + \delta = 1 \quad (87)$$

where $B_{uccl,j}^{vis1150,Step1}$ is the CL% upper combined confidence interval for predicted “vis1150” for the j^{th} MFPV batch from algorithm calculation Step 1 (in property model units).

There are no changes in the waste loading and in target concentrations for all components other than that being adjusted (Li_2O or Na_2O) and SiO_2 . The change in the target concentration of the component being adjusted is given by Equation (84), which results in the change of SiO_2 target concentration as:

$$g_{SiO_2,j}^{oxide\ in\ MFPV,\ target} = g_{SiO_2,j}^{oxide\ in\ MFPV,\ initial} - g_{ij}^{oxide\ in\ MFPV,\ adj} \quad \{i = Li_2O, Na_2O\} \quad (88)$$

where $g_{SiO_2,j}^{oxide\ in\ MFPV,\ target}$ = target mass fraction of SiO_2 in the j^{th} MFPV batch (g oxide per g MFPV oxides)
 $g_{SiO_2,j}^{oxide\ in\ MFPV,\ initial}$ = initial mass fraction of SiO_2 in the j^{th} MFPV batch (g oxide per g MFPV oxides)
 $g_{ij}^{oxide\ in\ MFPV,\ adj}$ = adjustment made to the target mass fraction of the i^{th} glass oxide in the j^{th} MFPV batch to satisfy the constraint that failed (g oxide per g MFPV oxides). For Na_2O ($g_{Na_2O,j}^{oxide\ in\ MFPV,\ adj} \geq 0$) the increase of Na_2O is supplied from GFC not from waste.

If all constraints calculated from Section 5.1.6 based on the adjusted target composition described above are met, the result of waste transfer volume calculation in Section 5.1.5 becomes the final output of Step 1 calculation.

5.2 Step 2 – Calculation of GFC Masses and Dilution Water Volume

The actual waste volume ($V_j^{waste\ MFPV}$) added to the MFPV is obtained based on the volume change in the MFPV as described in Appendix D. In Step 2, the measured waste transfer volume is used to calculate the masses of GFCs and sucrose to add to the MFPV:

$$M_{kj}^{GFC\ in\ MFPV,\ target,\ Step2} = M_{kj}^{GFC\ in\ MFPV,\ target,\ Step1} \frac{V_j^{waste\ MFPV}}{V_{dm}^{CRV}} \quad (89)$$

$$M_j^{sucrose\ in\ MFPV,\ target,\ Step2} = M_j^{sucrose\ in\ MFPV,\ target,\ Step1} \frac{V_j^{waste\ MFPV}}{V_{dm}^{CRV}} \quad (90)$$

where $M_{kj}^{GFC\ in\ MFPV,\ target,\ Step2}$ = target mass of k^{th} GFC to add to the j^{th} MFPV batch in algorithm calculation Step 2 (g)
 $M_{kj}^{GFC\ in\ MFPV,\ target,\ Step1}$ = target mass of k^{th} GFC to add to the j^{th} MFPV batch resulted from algorithm calculation Step 1 (g)
 $V_{dm}^{transwaste}$ = volume of the m^{th} transfer waste to be transferred from the d^{th} CRV to MFPV (L). Result of algorithm calculation Step 1.

$$V_j^{waste\ MFPV} = \text{measured volume of waste transferred from CRV to the } j^{\text{th}} \text{ MFPV (L)}$$

$$M_j^{sucrose\ in\ MFPV, target, Step2} = \text{target mass of sucrose to add to the } j^{\text{th}} \text{ MFPV batch in algorithm calculation Step 2 (g)}$$

$$M_j^{sucrose\ in\ MFPV, target, Step1} = \text{target mass of sucrose to add to the } j^{\text{th}} \text{ MFPV batch resulted from algorithm calculation Step 1 (g)}$$

If the volume of waste transferred is different from that calculated in Step 1, the volume of dilution water also needs to be recalculated after accounting for changes in other process water volumes, including the CRV-MFPV line flush water and dust control water (no change for MFPV sampling line flush water). After waste is transferred from CRV to MFPV the CRV-MFPV line is flushed and the flush water is added to MFPV. The actual amount of CRV-MFPV line flush water ($V_j^{transflush\ MFPV, measured}$), which can be different from the nominal values given in Table 14, is recorded and used for dilution water calculation. The volume of dust control water is calculated from the result of Step 1:

$$V_j^{dust\ MFPV, Step2} = V_j^{dust\ MFPV, Step1} \frac{V_j^{waste\ MFPV}}{V_{dm}^{CRV\ transwaste}} \quad (91)$$

where

$$V_j^{dust\ MFPV, Step2} = \text{volume of water added to control GFC dusting in the } j^{\text{th}} \text{ MFPV batch in algorithm calculation Step 2 (L)}$$

$$V_j^{dust\ MFPV, Step1} = \text{volume of water added to control GFC dusting in the } j^{\text{th}} \text{ MFPV batch in algorithm calculation Step 1 (L)}$$

$$V_{dm}^{transwaste\ CRV} = \text{volume of the } m^{\text{th}} \text{ transfer waste to be transferred from the } d^{\text{th}} \text{ CRV to MFPV (L). Result of algorithm calculation Step 1.}$$

$$V_j^{waste\ MFPV} = \text{measured volume of waste transferred from CRV to the } j^{\text{th}} \text{ MFPV (L)}$$

The volume of dilution water is calculated following Equation (62) using the actual waste volume ($V_j^{waste\ MFPV}$), actual flush water volume used ($V_j^{transflush\ MFPV, measured}$), and newly calculated dust control water volume ($V_j^{dust\ MFPV, Step2}$):

$$V_j^{dilute\ MFPV, Step2} = \max \left\{ \frac{c_{Na, dm}^{element\ in\ waste\ CRV} V_j^{waste\ MFPV}}{1000 MW_{Na} t_{[Na], j}} - \left(V_j^{waste\ MFPV} + V_j^{transflush\ MFPV, measured} + V_j^{sampler\ flush\ MFPV} + V_j^{dust\ MFPV, Step2} \right), 0 \right\} \quad (92)$$

where

$$V_j^{dilute\ MFPV, Step2} = \text{volume of dilution water required to maintain satisfactory melter-feed rheological properties in the } j^{\text{th}} \text{ MFPV batch in algorithm calculation}$$

Step 2 (L)

$c_{Na, dm}^{element\ in\ CRV}$ = concentration of Na in the m^{th} transfer waste transferred from the d^{th} CRV to MFPV (mg/L waste)

$V_j^{waste\ MFPV}$ = measured volume of waste transferred from CRV to the j^{th} MFPV (L)

MW_{Na} = molecular mass of sodium (g/mole)

$t_{[Na]}$ = target sodium molarity of the melter feed (M)

$V_j^{transflush\ MFPV, measured}$ = measured volume of water used to flush the CRV-MFPV transfer line in the j^{th} MFPV batch (L)

$V_j^{sampflush\ MFPV}$ = volume of water used to flush the MFPV sampling line in the j^{th} MFPV batch (L)

$V_j^{dust\ MFPV, Step2}$ = volume of water added to control GFC dusting in the j^{th} MFPV batch in algorithm calculation Step 2 (L)

The volume contributions of GFCs and sucrose are calculated from the ratio of target and actual waste transfer volumes:

$$V_j^{GFC\ MFPV, Step2} = V_j^{GFC\ MFPV, Step1} \frac{V_j^{waste\ MFPV}}{V_{dm}^{CRV}} \tag{93}$$

$$V_j^{sucrose\ MFPV, Step2} = V_j^{sucrose\ MFPV, Step1} \frac{V_j^{waste\ MFPV}}{V_{dm}^{CRV}} \tag{94}$$

The nominal working volume of MFPV is 19,426 L which includes nominal heel volume (6,556 L) and nominal batch volume (12,870 L). If $V_j^{waste\ MFPV} > V_{dm}^{CRV}$, the total volume of MFPV contents will increase and need to make sure that the total volume is within the allowable volume increase. It is assumed that the maximum allowable volume increase is the “High Operator Response” defined in 24590-LAW-M6C-LFP-00001, Rev 1, which is 3,331 L (dV₁₁ = 880 gal).⁽¹²⁾ For the purpose of the preliminary algorithm, the allowable increase of the MFPV volume over the nominal working volume caused by the accidentally increased waste transfer volume is assumed to be a half of this 3,331 L or 1,666 L.⁽¹³⁾ Then, the total increase of volume originated from increased waste transfer volume is expressed as:

⁽¹²⁾ This does not include the “Instrument Uncertainty” volume, dV₁₀ of 156 gal (591 L) in 24590-LAW-M6C-LFP-00001, Rev 1.

⁽¹³⁾ This is a preliminary assumption. The uncertainty in the volume transfer is not established yet. The current design is to control the volume transfer based on the level measurements in CRV and MFPV. However, WTP is evaluating the use of flow meter (to be installed primarily to check the flow to protect the pump) to control the waste transfer volume. Once the control method is established, the waste transfer volume uncertainty can be accurately estimated and it is likely that the waste volume transfer will be maintained within the nominal value.

$$\begin{aligned}
 &V_j^{waste\ MFPV} + V_j^{GFC\ MFPV, Step2} + V_j^{dust\ MFPV, Step2} + V_j^{sucrose\ MFPV, Step2} + V_j^{heel\ MFPV} \\
 &+ V_j^{transflush\ MFPV, measured} + V_j^{sampflush\ MFPV} + V_j^{dilute\ MFPV, Step2} - 19,426 < 1,666 \text{ (L)}
 \end{aligned}
 \tag{95}$$

If the actual waste transfer volume was large enough to cause the total MFPV volume increase over the allowable 1,666 L then the operator will be alerted for intervention.⁽¹⁴⁾

Half of this 3,331 L of “High Operator Response” volume is reserved for the volume uncertainty that originates from estimating volume contributions from GFCs and sucrose. The volume contribution of GFC materials and sucrose, different from that calculated based on particle density of materials, will depend on the solubility in water, adhered or embedded air, and non-ideality of mixing soluble species. Appendix F compiles and evaluates the volume contribution for the test slurry feeds found in the literature. Based on the results of this evaluation it is likely that the half of the “High Operator Response” volume of 3,331 L, 1,666 L, is sufficiently conservative to make sure that the MFPV working volume does not increase over the “High Operator Response”. If Step 3 (below) indicates a GFC adjustment is necessary, the remaining half of the “High Operator Response” volume (1,666 L) may be used for this purpose.

5.3 Step 3 – Calculation of Final Glass Composition and Properties with Uncertainties

The actual measured volume of waste transfer, actual measured volumes of flush, batch control, and dilution water, and the actual measured masses of GFCs are used to calculate the final composition and properties.

5.3.1 Final Glass Composition to Calculate the Final Glass Composition, the Final Waste

Loading ($G_j^{waste\ in\ MFPV, Step3}$) and GFC Mass per g Glass ($\ddot{M}_{kj}^{GFC\ in\ MFPV, Step3}$) are First Calculated:

$$G_j^{waste\ in\ MFPV, Step3} = \frac{C_{dm}^{oxide\ in\ waste\ CRV} V_j^{waste\ MFPV}}{C_{dm}^{oxide\ in\ waste\ CRV} V_j^{waste\ MFPV} + \sum_{k=1}^{n_j^{GFCs\ in\ MFPV}} \left(M_{kj}^{GFC\ in\ MFPV, measured} \sum_{i=1}^{n_k^{oxides\ in\ GFC}} m_{ik}^{oxide\ in\ GFC} \right)}
 \tag{96}$$

$$\ddot{M}_{kj}^{GFC\ in\ MFPV, Step3} = \frac{M_{kj}^{GFC\ in\ MFPV, measured} \left(1 - G_j^{waste\ in\ MFPV, Step3} \right)}{\sum_{k=1}^{n_j^{GFCs\ in\ MFPV}} \left(M_{kj}^{GFC\ in\ MFPV, measured} \sum_{i=1}^{n_k^{oxides\ in\ GFC}} m_{ik}^{oxide\ in\ GFC} \right)}
 \tag{97}$$

where $G_j^{waste\ in\ MFPV, Step3}$ = mass fraction of glass oxides originated from waste in the j^{th} MFPV batch from algorithm calculation Step 3, i.e. waste loading (g per g MFPV oxides)

⁽¹⁴⁾ It is unlikely that the MFPV volume increase by actual waste transfer volume increase would reach the allowable 1,666 L during normal operation.

- $C_{dm}^{oxides\ in\ CRV}$ = concentration of total glass oxides in the m^{th} transfer waste transferred from the d^{th} CRV to MFPV (g oxides per L waste)
- V_j^{waste} = volume of waste transferred from CRV to the j^{th} MFPV (L)
- $n_j^{GFCs\ in\ MFPV}$ = number of GFCs used in the j^{th} MFPV batch
- $M_{kj}^{GFC\ in\ MFPV, measured}$ = measured mass of k^{th} GFC added to the j^{th} MFPV batch (g)
- $m_{ik}^{oxides\ in\ GFC}$ = mass fraction of the i^{th} glass oxide in the k^{th} GFC (g oxide per g GFC including volatiles)
- $n_k^{oxides\ in\ GFC}$ = number of glass oxides in the k^{th} GFC
- $\ddot{M}_{kj}^{GFC\ in\ MFPV, Step3}$ = mass of the k^{th} GFC per g of glass in the j^{th} MFPV batch from algorithm calculation Step 3 (g per g MFPV oxides)

Then, the glass composition is given as:

$$g_{ij}^{oxide\ in\ MFPV, Step3} = G_j^{waste\ in\ MFPV, Step3} g_{idm}^{oxide\ in\ CRV} + \sum_{k=1}^{n_j^{GFCs\ in\ MFPV}} m_{ik}^{oxide\ in\ GFC} \ddot{M}_{kj}^{GFC\ in\ MFPV, Step3} \quad (98)$$

where $g_{ij}^{oxide\ in\ MFPV, Step3}$ is the mass fraction of the i^{th} glass oxide in the j^{th} MFPV batch from algorithm calculation Step 3 before applying component retention factors (g oxide per g MFPV oxides) and the remaining notations are as previously defined in Equations (96) and (97).

The glass composition after applying retention factors ($\tilde{g}_{ij}^{oxide\ in\ MFPV, Step3}$) is given as:

$$\tilde{g}_{ij}^{oxide\ in\ MFPV, Step3} = \frac{g_{ij}^{oxide\ in\ MFPV, Step3} v_i}{\sum_{i=1}^{n_j^{oxides\ in\ MFPV}} g_{ij}^{oxide\ in\ MFPV, Step3} v_i} \quad (99)$$

The activity of radionuclides per unit mass of glass oxides in the MFPV batch ($a_{ij}^{rad\ in\ MFPV, Step3}$) is given as:

$$a_{ij}^{rad\ in\ MFPV, Step3} = a_{idm}^{rad\ in\ CRV} G_j^{waste\ in\ MFPV, Step3} = \frac{\bar{R}_{id}^{rad\ in\ CRV} \lambda_{dm}^{waste\ in\ MFPV, Step3}}{C_{dm}^{oxides\ in\ CRV}} \quad (100)$$

where

- $a_{ij}^{rad\ in\ MFPV,\ Step3}$ = specific activity of the i^{th} radionuclide in the j^{th} MFPV batch for algorithm calculation Step 3 (mCi/g oxides)
- $a_{idm}^{rad\ in\ CRV}$ = specific activity of the i^{th} radionuclide in the m^{th} transfer waste transferred from the d^{th} CRV to MFPV (mCi/g oxides)
- $G_j^{waste\ in\ MFPV,\ Step3}$ = mass fraction of glass oxides originated from waste in the j^{th} MFPV batch from algorithm calculation Step 3, i.e. waste loading (g per g MFPV oxides)
- $\bar{R}_{id}^{rad\ in\ CRV}$ = activity (per unit volume) of the i^{th} radionuclide in the waste of the d^{th} CRV averaged over $n_d^{samps\ in\ CRV}$ samples analyzed (mCi/L)
- λ_{dm} = dilution factor for the m^{th} transfer waste transferred from the d^{th} CRV to MFPV
- $C_{dm}^{oxides\ in\ CRV}$ = concentration of total glass oxides in the m^{th} transfer waste transferred from the d^{th} CRV to MFPV (g oxides per L waste)

The specific activity after applying retention factors ($\tilde{a}_{ij}^{oxide\ in\ MFPV,\ Step3}$) is given as:

$$\tilde{a}_{ij}^{rad\ in\ MFPV,\ Step3} = \frac{a_{ij}^{rad\ in\ MFPV,\ Step3} V_i}{\sum_{i=1}^{oxides\ in\ MFPV} g_{ij}^{oxide\ in\ MFPV,\ Step3} V_i} \quad (101)$$

5.3.2 Constraints for Algorithm Step 3

The equations to calculate the quantities for all constraints listed in Table 10 through Table 13 for algorithm Step 3 are described in this section. The same equations derived in Section 5.1.6 for algorithm Step 1 are also employed using the symbols corresponding to algorithm Step 3.

5.3.2.1 Glass Property and Model Validity Constraints

For property predictions and calculations of prediction uncertainties, the g_i for x_i^{prop} and x_{Others}^{prop} in Equations (3) and (4) is given by $\tilde{g}_{ij}^{oxide\ in\ MFPV,\ Step3}$ from Equation (99). The model validity constraints are also calculated based on $\tilde{g}_{ij}^{oxide\ in\ MFPV,\ Step3}$. Then, these x_i^{prop} values are used in Equations (2), (5), (6), and (7) to calculate P^{prop} and Equations (8) through (11) to calculate U_{pred}^{prop} . Composition uncertainty (U_{comp}^{prop}) is calculated following the methods described in Section 4.2.2. For U_{comp}^{prop} calculation the mass balance equations given by Equation (12) and (13) are rewritten based on the values for Step 3 calculation:

$$g_{ij}^{oxide\ in\ MFPV,\ Step3} = \frac{\frac{element\ in\ waste}{c_{idm}^{CRV} f_i V_j^{MFPV}} + \sum_{k=1}^{GFCs\ in\ MFPV} m_{ik}^{oxide\ in\ GFC} M_{kj}^{GFC\ in\ MFPV,\ measured}}{1000(mg/g)} + \frac{\sum_{i=1}^{oxides\ in\ CRV} c_{idm}^{CRV} f_i V_j^{MFPV}}{1000(mg/g)} + \sum_{i=1}^{oxides\ in\ MFPV} \sum_{k=1}^{GFCs\ in\ MFPV} m_{ik}^{oxide\ in\ GFC} M_{kj}^{GFC\ in\ MFPV,\ measured}} \quad (102)$$

$$\tilde{g}_{ij}^{oxide\ in\ MFPV,\ Step3} = \frac{g_{ij}^{oxide\ in\ MFPV,\ Step3} V_i}{\sum_{i=1}^{oxides\ in\ MFPV} g_{ij}^{oxide\ in\ MFPV,\ Step3} V_i} \quad (103)$$

- where
- $g_{ij}^{oxide\ in\ MFPV,\ Step3}$ = mass fraction of the i^{th} glass oxide in the j^{th} MFPV batch from algorithm calculation Step 3 after applying component retention factors (g oxide per g glass)
 - $\tilde{g}_{ij}^{oxide\ in\ MFPV,\ Step3}$ = mass fraction of the i^{th} glass oxide in the j^{th} MFPV batch from algorithm calculation Step 3 after applying component retention factors (g oxide per g glass)
 - $c_{idm}^{element\ in\ CRV}$ = concentration of the i^{th} component in the m^{th} transfer waste transferred from the d^{th} CRV to MFPV (mg/L waste)
 - f_i = oxide conversion factor, i.e., mass of the i^{th} glass oxide per mass of the i^{th} element
 - V_j^{waste} = volume of waste transferred from CRV to the j^{th} MFPV (L)
 - $n_j^{GFCs\ in\ MFPV}$ = number of GFCs used in the j^{th} MFPV batch
 - $m_{ik}^{oxide\ in\ GFC}$ = mass fraction of the i^{th} glass oxide in the k^{th} GFC (g oxide per g GFC including volatiles). Here, unlike **H** in Equation (48), $m_{ik}^{oxide\ in\ GFC}$ includes all tracked components beyond the 11 GFC components.
 - $M_{kj}^{GFC\ in\ MFPV,\ measured}$ = measured mass of k^{th} GFC added to the j^{th} MFPV batch (g)
 - V_i = retention factor for the i^{th} component (fraction)
 - $n_d^{oxides\ in\ CRV}$ = number of glass oxides tracked in the d^{th} CRV batch
 - $n_j^{oxides\ in\ MFPV}$ = number of glass oxides tracked in the mass balance calculations for the j^{th} MFPV batch

The results of P^{prop} , U_{pred}^{prop} , and U_{comp}^{prop} are used to calculate CL% UCCI or LCCI (B_{ucci}^{prop} or B_{lcci}^{prop}) for glass properties (PCT, VHT, viscosity, and electrical conductivity) according to Equation (16) discussed in Section 4.2.3.

$$B_{ucci,j}^{prop,Step3} = P_j^{prop,Step3} + U_{pred,j}^{prop,Step3} + U_{comp,j}^{prop,Step3} \quad \text{and} \quad B_{lcci,j}^{prop,Step3} = P_j^{prop,Step3} - U_{pred,j}^{prop,Step3} - U_{comp,j}^{prop,Step3} \quad (104)$$

where $B_{ucci,j}^{prop,Step3}$ = CL% upper combined confidence interval for predicted “prop” s for the j^{th} MFPV batch from algorithm calculation Step 3

$B_{lcci,j}^{prop,Step3}$ = CL% lower combined confidence interval for “prop” for the j^{th} MFPV batch from algorithm calculation Step 3 (applicable only to “vis” and “ec”)

$P_j^{prop,Step3}$ = predicted “prop” transformed property values for the j^{th} MFPV batch from algorithm calculation Step 3, which includes $\ln(r_B, g/L)$, $\ln(r_{Na}, g/L)$, $\ln(D, \mu m)$, $\ln(\eta_T, P)$, and $\ln(\epsilon_T, S/cm)$

$U_{pred,j}^{prop,Step3}$ = model prediction uncertainty for “prop” for the j^{th} MFPV batch from algorithm calculation Step 3

$U_{comp,j}^{prop,Step3}$ = composition uncertainty for “prop” for the j^{th} MFPV batch from algorithm calculation Step 3

The CL% UCCIs and LCCIs, expressed in the units of the model used to predict a property (e.g., $\ln[g/L]$ for PCT responses), are used to assess whether property constraints (as discussed in Section 4.3) are met.

5.3.2.2 Waste Na₂O Loading Constraint

The waste Na₂O loading in the j^{th} MFPV batch from algorithm calculation Step 3 is calculated as:

$$g_{Na_2O(w),j}^{oxide\ in\ MFPV,Step3} = \frac{g_{Na_2O,dm}^{oxide\ in\ CRV} G_j^{waste\ in\ MFPV,Step3} \omega_d v_i}{\sum_{i=1}^{n_j^{oxides\ in\ MFPV}} \left[g_{idm}^{oxide\ in\ CRV} G_j^{waste\ in\ MFPV,Step3} v_i + \left(\sum_{k=1}^{n_j^{GFCs\ in\ MFPV}} m_{ik}^{oxide\ in\ GFC} \dot{M}_{kj}^{GFC\ in\ MFPV,Step3} \right) v_i \right]} \quad (105)$$

where $g_{Na_2O(w),j}^{oxide\ in\ MFPV,Step3}$ = mass fraction of waste Na₂O (waste Na₂O loading) in the j^{th} MFPV batch from algorithm calculation Step 3 (g per g glass)

$g_{Na_2O,dm}^{oxide\ in\ CRV}$ = mass fraction of Na₂O in the m^{th} transfer waste transferred from the d^{th} CRV to MFPV (g oxide per g CRV oxides)

$G_j^{waste\ in\ MFPV,Step3}$ = mass fraction of glass oxides originated from waste in the j^{th} MFPV batch from algorithm calculation Step 3, i.e. waste loading (g per g MFPV oxides)

ω_d = fraction of the sodium in the d^{th} CRV batch that is classified as waste sodium (unitless)

v_i = retention factor for the i^{th} component (fraction)

$n_j^{oxides\ in\ MFPV}$ = number of glass oxides tracked in the mass balance calculations for the j^{th} MFPV batch

$g_{idm}^{oxide\ in\ CRV}$ = mass fraction of the i^{th} glass oxide in the m^{th} transfer waste transferred from the d^{th} CRV to MFPV (g oxide per g CRV oxides)

$n_j^{GFCs\ in\ MFPV}$ = number of GFCs in the j^{th} MFPV batch

$\dot{M}_{kj}^{GFC\ in\ MFPV,\ Step3}$ = mass of the k^{th} GFC per g of glass in the j^{th} MFPV batch from algorithm calculation Step 3 (g per g MFPV oxides)

$m_{ik}^{oxide\ in\ GFC}$ = mass fraction of the i^{th} glass oxide in the k^{th} GFC (g oxide per g GFC including volatiles). Here, unlike **H** in Equation (48), $m_{ik}^{oxide\ in\ GFC}$ includes all tracked components beyond the 11 GFC components.

The $g_{Na_2O(w),j}^{oxide\ in\ MFPV,\ Step3}$ value is compared to L_{Na}^{W} to confirm that each MFPV batch meets the waste Na₂O loading constraint.

5.3.2.3 Radionuclide Concentration Constraints

The specific activity of radionuclide in glass is calculated by

$$a_{ij}^{rad\ in\ MFPV,\ Step3} = \frac{a_{idm}^{rad\ in\ CRV} V_j^{waste\ MFPV}}{\sum_{i=1}^{n_d^{oxides\ in\ CRV}} \frac{c_{idm}^{element\ in\ CRV} f_i V_j^{waste\ MFPV}}{1000(mg/g)} + \sum_{i=1}^{n_j^{oxides\ in\ MFPV}} \sum_{k=1}^{n_j^{GFCs\ in\ MFPV}} m_{ik}^{oxide\ in\ GFC} M_{kj}^{GFC\ in\ MFPV,\ measured}} \quad (106)$$

$$\tilde{a}_{ij}^{rad\ in\ MFPV,\ Step3} = \frac{a_{ij}^{rad\ in\ MFPV,\ Step3} V_i}{\sum_{i=1}^{n_j^{oxides\ in\ MFPV}} g_{ij}^{oxide\ in\ MFPV,\ Step3} V_i} \quad (107)$$

where $a_{ij}^{rad\ in\ MFPV,\ Step3}$ = specific activity of the i^{th} radionuclide in the j^{th} MFPV batch from algorithm calculation Step 3 before applying retention factors (mCi/g glass)

$a_{idm}^{rad\ in\ CRV}$ = specific activity of the i^{th} radionuclide in the m^{th} transfer waste transferred from the d^{th} CRV to MFPV (mCi/g oxides)

$V_j^{waste\ MFPV}$ = volume of waste transferred from CRV to the j^{th} MFPV (L)

$n_d^{oxides\ in\ CRV}$ = number of glass oxides tracked in the mass balance calculations for the d^{th} CRV batch

$c_{idm}^{element\ in\ CRV}$ = concentration of the i^{th} component in the m^{th} transfer waste transferred from the d^{th} CRV to MFPV (mg/L waste)

f_i = oxide conversion factor, i.e., mass of the i^{th} glass oxide per mass of the i^{th} element

- $n_j^{oxides\ in\ MFPV}$ = number of glass oxides tracked in the mass balance calculations for the j^{th} MFPV batch
- $n_j^{GFCs\ in\ MFPV}$ = number of GFCs used in the j^{th} MFPV batch
- $m_{ik}^{oxide\ in\ GFC}$ = mass fraction of the i^{th} glass oxide in the k^{th} GFC (g oxide per g GFC including volatiles).
- $M_{kj}^{GFC\ in\ MFPV, measured}$ = measured mass of k^{th} GFC added to the j^{th} MFPV batch (g)
- $\tilde{a}_{ij}^{rad\ in\ MFPV, Step3}$ = specific activity of the i^{th} radionuclide in the j^{th} MFPV batch from algorithm calculation Step 3 after applying retention factors (mCi/g glass)
- v_i = retention factor for the i^{th} component (fraction)
- $g_{ij}^{oxide\ in\ MFPV, Step3}$ = mass fraction of the i^{th} glass oxide in the j^{th} MFPV batch from algorithm calculation Step 3 after applying component retention factors (g oxide per g glass)

The SD values for glass component mass fractions ($\tilde{s}_{ij}^{oxide\ in\ MFPV, Step3}$) and radionuclide concentrations ($\tilde{s}_{ij}^{rad\ in\ MFPV, Step3}$) for algorithm calculation Step 3 after applying retention factors are obtained by Monte Carlo simulations of Equations (103) and (107) respectively.

The specific activity of radionuclides from Equation (101) and its SD are converted to per unit glass volume using:

$$\hat{a}_{ij}^{rad\ in\ MFPV, Step3} = \tilde{a}_{ij}^{rad\ in\ MFPV, Step3} \rho_j^{glass\ in\ MFPV} \tag{108}$$

$$\hat{s}_{ij}^{rad\ in\ MFPV, Step3} = \tilde{s}_{ij}^{rad\ in\ MFPV, Step3} \rho_j^{glass\ in\ MFPV} \tag{109}$$

- where
- $\hat{a}_{ij}^{rad\ in\ MFPV, Step3}$ = activity of the i^{th} radionuclide per unit volume of glass in the j^{th} MFPV batch from algorithm calculation Step 3 after applying retention factors (Ci/m³ glass)
 - $\tilde{a}_{ij}^{rad\ in\ MFPV, Step3}$ = specific activity of the i^{th} radionuclide in the j^{th} MFPV batch from algorithm calculation Step 3 after applying retention factors (mCi/g glass)
 - $\rho_j^{glass\ in\ MFPV}$ = density of glass in the j^{th} MFPV batch (g/L)
 - $\hat{s}_{ij}^{rad\ in\ MFPV, Step3}$ = SD for the activity of the i^{th} radionuclide per unit volume of glass in the j^{th} MFPV batch from algorithm calculation Step 3 after applying retention factors (Ci/m³ glass)
 - $\tilde{s}_{ij}^{rad\ in\ MFPV, Step3}$ = SD for the specific activity of the i^{th} radionuclide in the j^{th} MFPV batch from algorithm calculation Step 3 after applying retention factors (mCi/g glass)

The requirements for ^{137}Cs and ^{90}Sr are satisfied if $\hat{a}_{137\text{Cs},j}^{\text{rad in MFPV,Step3}} + k^{\text{rad}} \hat{S}_{137\text{Cs},e}^{\text{rad in MFPV,Step3}} < 0.3 \text{ Ci/m}^3$ and $\hat{a}_{90\text{Sr},j}^{\text{rad in MFPV,Step3}} + k^{\text{rad}} \hat{S}_{90\text{Sr},e}^{\text{rad in MFPV,Step3}} < 20 \text{ Ci/m}^3$ where k^{rad} is the expansion factor for the radionuclide concentration specification.

To demonstrate that the waste meets the classification of Class C waste or below, limiting values for $\hat{a}_{ij}^{\text{rad in MFPV}}$ and $\hat{a}_{ij}^{\text{rad in MFPV}}$; listed in Table 15 and Table 16 given in Section 5.1.6.3, are used.

The first step to classification is then to determine if there are any radionuclides with measurable concentrations ($\hat{a}_{ij}^{\text{rad in MFPV,Step3}}$ for ^{99}Tc , ^{129}I , ^{63}Ni , ^{90}Sr , and ^{137}Cs , or $\hat{a}_{ij}^{\text{rad in MFPV,Step3}}$ for TRU, ^{241}Pu , and ^{242}Cm). If non-zero values are present for radionuclides only in Table 15 or only in Table 16, then only those tables are used for classification. If there are non-zero values for both tables, then Table 15 is used for classification if any one radionuclide from Table 15 is greater than 10% of its associated limit. If no Table 15 radionuclide has a concentration greater than or equal to its associated limit, then Table 16 is used for classification. The sum of fractions rule for algorithm calculation Step 3 is given as:

$$SF_{LL,j}^{\text{rad in MFPV,Step3}} = \sum_i^2 \frac{\hat{a}_{ij}^{\text{rad in MFPV,Step3}}}{L_u^{\hat{a}_i}} \text{ (for } i = ^{99}\text{Tc and } ^{129}\text{I)} + \sum_i^3 \frac{\hat{a}_{ij}^{\text{rad in MFPV,Step3}} \times 10^6 \text{ (nCi/mCi)}}{L_u^{a_i}} \text{ (for } i = \text{TRU, } ^{241}\text{Pu, and } ^{242}\text{Cm)}$$
(110)

$$SF_{SL,j}^{\text{rad in MFPV,Step3}} = \sum_i^3 \frac{\hat{a}_{ij}^{\text{rad in MFPV,Step3}}}{L_u^{\hat{a}_i}} \text{ (for } i = ^{63}\text{Ni, } ^{90}\text{Sr, and } ^{137}\text{Cs)}$$
(111)

where $SF_{LL,j}^{\text{rad in MFPV,Step3}}$ = sum of fractions of activity to the limit of each radionuclide for long-lived radionuclides for Class C limit determination in the j^{th} MFPV batch from algorithm calculation Step 3

$SF_{SL,j}^{\text{rad in MFPV,Step3}}$ = sum of fractions of activity to the limit of each radionuclide for short-lived radionuclides for Class C limit determination in the j^{th} MFPV batch from algorithm calculation Step 3

$\hat{a}_{ij}^{\text{rad in MFPV,Step3}}$ = activity of the i^{th} radionuclide per unit volume of glass in the j^{th} MFPV batch from algorithm calculation Step 3 after applying retention factors (Ci/m^3 glass)

$\tilde{a}_{ij}^{\text{rad in MFPV,Step3}}$ = specific activity of the i^{th} radionuclide in the j^{th} MFPV batch from algorithm calculation Step 3 after applying retention factors (mCi/g glass)

$L_u^{\hat{a}_i}$ = upper limit for the activity of the i^{th} radionuclide per unit glass volume (Ci/m^3 glass)

$L_u^{a_i}$ = upper limit for specific activity of the i^{th} radionuclide (nCi/g glass)

The standard deviations for $SF_{LL,j}^{rad in, MFPV, Step3}$ and $SF_{SL,j}^{rad in, MFPV, Step3}$ are given as:

$$S_{LL,j}^{rad SF in, MFPV, Step3} = \sqrt{\sum_i^2 \left(\frac{\hat{S}_{ij}^{rad in, MFPV, Step3}}{L_u^{\hat{a}_i}} \right)^2 \text{ (for } i = {}^{99}\text{Tc and } {}^{129}\text{I)} + \sum_i^3 \left(\frac{\tilde{S}_{ij}^{rad in, MFPV, Step3} \times 10^6 \text{ (nCi/mCi)}}{L_u^{a_i}} \right)^2 \text{ (for } i = \text{TRU, } {}^{241}\text{Pu, and } {}^{242}\text{Cm)}} \quad (112)$$

$$S_{SL,j}^{rad SF in, MFPV, Step3} = \sqrt{\sum_i^3 \left(\frac{\hat{S}_{ij}^{rad in, MFPV, Step3}}{L_u^{\hat{a}_i}} \right)^2 \text{ (for } i = {}^{63}\text{Ni, } {}^{90}\text{Sr, and } {}^{137}\text{Cs)}} \quad (113)$$

- where
- $S_{LL,j}^{rad SF in, MFPV, Step3}$ = SD for the sum of fractions of activity to the limit of each radionuclide for long-lived radionuclides for Class C limit determination in the j^{th} MFPV batch from algorithm calculation Step 3
 - $S_{SL,j}^{rad SF in, MFPV, Step3}$ = SD for the sum of fractions of activity to the limit of each radionuclide for short-lived radionuclides for Class C limit determination in the j^{th} MFPV batch from algorithm calculation Step 3
 - $\hat{S}_{ij}^{rad in, MFPV, Step3}$ = SD for the activity of the i^{th} radionuclide per unit volume of glass in the j^{th} MFPV batch from algorithm calculation Step 3 after applying retention factors (Ci/m³ glass)
 - $\tilde{S}_{ij}^{rad in, MFPV, Step3}$ = SD for the specific activity of the i^{th} radionuclide in the j^{th} MFPV batch from algorithm calculation Step 3 after applying retention factors (mCi/g glass)
 - $L_u^{\hat{a}_i}$ = upper limit for the activity of the i^{th} radionuclide per unit glass volume (Ci/m³ glass)
 - $L_u^{a_i}$ = upper limit for specific activity of the i^{th} radionuclide (nCi/g glass)

The Class C limit is satisfied if $SF_{LL,j}^{rad in, MFPV, Step3} + k^{rad} S_{LL,j}^{rad SF in, MFPV, Step3} < 1$ and $SF_{SL,j}^{rad in, MFPV, Step3} + k^{rad} S_{SL,j}^{rad SF in, MFPV, Step3} < 1$.

5.3.2.4 Surface Dose Rate Constraint

As mentioned in Section 5.1.6.4, the surface dose rate calculation will not be performed by ILAW formulation algorithm.

5.3.3 MFPV Composition Check

The MFPV contents including heel and newly added MFPV batch will be sampled and analyzed for major glass components (ISARD sample point = LAW6). The glass composition of working MFPV (batch + heel) is calculated as:

$$g_{ij}^{oxide\ in\ MFPVw} = \frac{g_{ij}^{oxide\ in\ MFPV,\ Step\ 3} V_j^{batch\ MFPV} + g_{i,j-1}^{oxide\ in\ heel\ MFPVw} V_j^{heel\ MFPV}}{V_j^{batch\ MFPV} + V_j^{heel\ MFPV}} \quad (114)$$

where $g_{ij}^{oxide\ in\ MFPVw}$ = mass fraction of the i^{th} glass oxide in the j^{th} working MFPV (g oxide per g glass)

$g_{ij}^{oxide\ in\ MFPV,\ Step\ 3}$ = mass fraction of the i^{th} glass oxide in the j^{th} MFPV batch from algorithm calculation Step 3 before applying component retention factors (g oxide per g MFPV oxides)

$V_j^{batch\ MFPV}$ = volume of the j^{th} MFPV batch (L)

$g_{i,j-1}^{oxide\ in\ MFPVw}$ = mass fraction of the i^{th} glass oxide in the $j-1^{th}$ working MFPV (g oxide per g glass)

$V_j^{heel\ MFPV}$ = volume of heel in the j^{th} MFPV batch measured prior to waste transfer (L)

The MFPV batch volume is calculated as a sum of measured waste transfer volume ($V_j^{waste\ MFPV}$), measured water volumes ($V_j^{dust\ MFPV,\ measured}$, $V_j^{transflush\ MFPV,\ measured}$, $V_j^{sampflush\ MFPV,\ measured}$, and $V_j^{dilute\ MFPV,\ measured}$), estimated volume contributions by GFC and sucrose ($V_j^{GFC\ MFPV,\ Step\ 3}$ and $V_j^{sucrose\ MFPV,\ Step\ 3}$):

$$V_j^{batch\ MFPV} = V_j^{waste\ MFPV} + V_j^{GFC\ MFPV,\ Step\ 3} + V_j^{dust\ MFPV,\ measured} + V_j^{sucrose\ MFPV,\ Step\ 3} + V_j^{transflush\ MFPV,\ measured} + V_j^{sampflush\ MFPV,\ measured} + V_j^{dilute\ MFPV,\ measured} \quad (115)$$

Volume contributions by GFC and sucrose are estimated from measured GFC and sucrose masses ($M_{kj}^{GFC\ in\ MFPV,\ measured}$ and $M_j^{sucrose\ in\ MFPV,\ measured}$):

$$V_j^{GFC\ MFPV,\ Step\ 3} = \sum_{k=1}^{n_j^{GFC\ in\ MFPV}} \frac{M_{kj}^{GFC\ in\ MFPV,\ measured}}{\rho_k} \quad (116)$$

$$V_j^{sucrose\ MFPV,\ Step\ 3} = \frac{M_j^{sucrose\ in\ MFPV,\ measured}}{\rho_{sucrose}} \quad (117)$$

where ρ_k and $\rho_{sucrose}$ are the densities of k^{th} GFC and sucrose, respectively.

The estimated glass oxides content in the MFPV (after completing batch preparation, “estimated” because the volume contributions of GFCs and sucrose are estimated) is given as:

$$C_j^{oxides\ in\ MFPV} = \frac{C_{dm}^{CRV\ waste} V_j^{MFPV}}{G_j^{MFPV,\ Step3\ batch} V_j^{MFPV}} \quad (118)$$

- where
- $C_j^{oxides\ in\ MFPV}$ = concentration of total glass oxides in the j^{th} MFPV batch (g oxides per L)
 - $C_{dm}^{CRV\ waste}$ = concentration of total glass oxides in the m^{th} transfer waste transferred from the d^{th} CRV to MFPV (g oxides per L waste)
 - $V_j^{MFPV\ waste}$ = volume of waste transferred from CRV to the j^{th} MFPV (L)
 - $G_j^{MFPV,\ Step3\ waste\ in}$ = mass fraction of glass oxides originated from waste in the j^{th} MFPV batch from algorithm calculation Step 3, i.e. waste loading (g per g MFPV oxides)
 - $V_j^{batch\ MFPV}$ = volume of the j^{th} MFPV batch (L)

Then, the estimated glass oxides content ($C_j^{oxides\ in\ MFPVw}$) and elemental composition ($C_{ij}^{element\ in\ MFPVw}$) in the working MFPV is given as:

$$C_j^{oxides\ in\ MFPVw} = \frac{C_j^{oxides\ in\ MFPV} V_j^{batch\ MFPV} + C_{j-1}^{oxides\ in\ MFPVw} V_j^{heel\ MFPV}}{V_j^{batch\ MFPV} + V_j^{heel\ MFPV}} \quad (119)$$

$$C_{ij}^{element\ in\ MFPVw} = \frac{g_{ij}^{oxide\ in\ MFPVw} C_j^{oxides\ in\ MFPVw}}{f_i} \quad (120)$$

- where
- $C_j^{oxides\ in\ MFPVw}$ = concentration of total glass oxides in the j^{th} working MFPV (g oxides per L)
 - $C_j^{oxides\ in\ MFPV}$ = concentration of total glass oxides in the j^{th} MFPV batch (g oxides per L)
 - $V_j^{batch\ MFPV}$ = volume of the j^{th} MFPV batch (L)
 - $C_{j-1}^{oxides\ in\ MFPVw}$ = concentration of total glass oxides in the $j-1^{th}$ working MFPV (g oxides per L)
 - $V_j^{heel\ MFPV}$ = volume of heel in the j^{th} MFPV batch measured prior to waste transfer (L)

$c_{ij}^{element\ in\ MFPVw}$ = concentration of the i^{th} element in the j^{th} working MFPV (mg/L)

$g_{ij}^{oxide\ in\ MFPVw}$ = mass fraction of the i^{th} glass oxide in the j^{th} working MFPV (g oxide per g glass)

f_i = oxide conversion factor, i.e., mass of the i^{th} glass oxide per mass of the i^{th} element

The resulting $c_{ij}^{element\ in\ MFPV,working}$ values are compared with the analytical results. Trending analyses will be performed on the differences between the analytical results and calculated values to detect potential errors in the MFPV batch preparation, e.g., weighing of GFCs. The trending analyses are not calculated in this report. It is assumed that prepackaged statistical process control (SPC) software will be used during production.

5.4 Step 4 – Comparison of Final Composition and Properties with Constraints

The resulting constraint quantities are compared to their limits discussed in Section 4.3. If any of the constraints is not met, an operator will be alerted for intervention. For product quality related properties (e.g., those properties required to meet Contract Specification 2) this comparison is a hold point for transfer of melter feed to the MFV. Once the comparison is successful, the hold point is lifted.

5.5 Step 5 – Completion of Production Records

The production records for ILAW will include portions related to the container, the waste form, and the containerized waste form. This section discusses the calculations required to generate those portions of the production records related to the waste form.

Production records document the composition of the waste forms and demonstrate that they meet all the related specifications from the WTP Contract (DOE 2000). The specifications and an overview of the WTP project's strategy for complying with the specifications are contained in the *ILAW Product Compliance Plan (PCP)* (24590-WTP-PL-RT-03-001). Piepel et al. (2005) developed statistical methods for implementing the compliance strategies to meet several specifications. Those equations and methods were adapted in several parts of the formulation algorithm.

ILAW product requirements are listed in Specification 2.2.2 of the contract (DOE 2000). A series of calculations are performed based on the final glass composition for each MFPV batch. Those requirements, which are not described here (2.2.2.1, 2.2.2.3 through 2.2.2.5, 2.2.2.10 through 2.2.2.16, 2.2.2.18, and 2.2.2.20 through 2.2.2.22), are not related to the glass composition and so are not addressed through these calculations (24590-WTP-PL-RT-03-001).

The requirements that will be satisfied, at least partially, by the production records are listed in Table 17. The calculations used to generate these parts of the production records are discussed in the following subsections. Each subsection starts by quoting the PCP for "during production compliance activities". All specifications related to waste form are based on the content of canistered glass.

**Table 17. Summary of Production Records Related Waste Form Specifications
 (24590-WTP-PL-RT-03-001)**

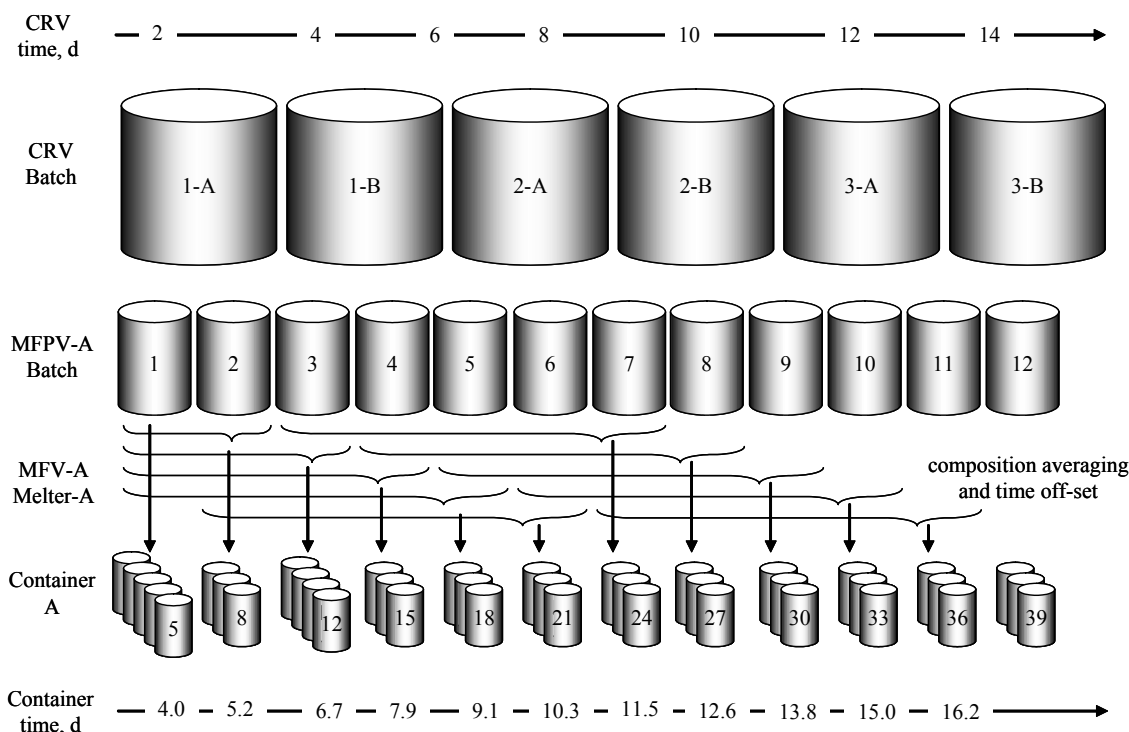
Contract Specification Number	Description	Section in This Report
2.2.2.2	Waste Loading	5.5.1
2.2.2.6	Chemical Composition Documentation	5.5.2
2.2.2.7	Radiological Composition Documentation	5.5.3
2.2.2.8	Radionuclide Concentration Limitations	5.5.4
2.2.2.9	Surface Dose Rate Limitations	5.5.5
2.2.2.17	Waste Form Testing	5.5.6
2.2.2.23	Manifesting	5.5.7

The composition of LAW glass generated from a single MFPV batch and its properties are calculated as described in Section 5.3. However, the production records are based on a canistered glass as discussed above. It should be noted that the melter feed making up each individual MFPV batch doesn't necessarily correspond to the glass in any particular canister. Rather, there is blending of batches by the material within the MFPV (with heel from previous MFPV), within the MFV (which is continually fed to the melter), and within the melter itself. This blending occurs because the vessels (MFPV, MFV, and melter) are well mixed so rather than "plug flow" of material from the MFPV to the canister, there is material blending of several MFPV batches to make up a container. Implicit to this strategy is the assumption that blending MFPV batches and heels that have been correctly formulated will yield a blended glass formulation meeting all constraints. A complication related to container composition averaging is that the compositions must be available for the Production Records at the time the container is transferred to DOE or the contractor.

Therefore, a moving average is used that does not include MFPV batches analyzed after the time of individual container production. The composition is averaged over five MFPV batches (since this is roughly equivalent to three melter volumes of glass) and is then assigned to the glasses in three consecutive canisters. There is an offset between time of the j^{th} MFPV batch and its associated containers. The time is roughly 2 days to process the amount of glass in one MFPV batch, one MFV batch, and one-half the mass of glass in the melter at the nominal operating rate of 15,000 kg of glass per day. In summary, the average composition from five MFPV batches are assigned to the glasses in three canisters with the time off-set of 2 days between the start of feed transfer from the first MFPV batch of five to the MFV and the start of pour to the first canister of three. Figure 10 illustrates the contribution and timing of various CRV and MFPV batches, which MFPV batches contribute to the composition of which containers, and the general timing of the process.

WTP contract Specification 13.2.1 (as of M153 of DOE 2000) specifies that: ... *The certification and acceptance of ILAW product shall be done on a lot basis. The lot size shall be proposed by the Contractor, and agreed to by DOE.* ... Currently, the proposed lot size is the amount of glass contained in three canisters that have the same composition calculated from five MFPV batches discussed above.

Figure 10. Schematic of Glass Composition Averaging over MFPV Batches and ILAW Containers



Through normal operation, these equations adequately address the changing composition of glass in canisters. However, at the beginning of hot commissioning operation, the residual glass in the melter from cold commissioning must be taken into account. This will be performed by assuming that the melter is perfectly mixed and MFPV batches are added to the melter after each container is cast with equal equivalent glass mass as the container just filled. The residual cold commissioning glass will be diluted away as the melter feed is added. The calculation for the initial hot commissioning glass is not included in the ILAW formulation algorithm and needs to be performed separately. There will be initial hot commissioning glass containers that do not meet the waste loading requirement identified in Specification 2.2.2.2. Current WTP contract specifies that ...DOE will accept these containers and provide credit for these containers in the Hot Commissioning Capacity Test... (Specification 13.2.2, as of M152 of DOE 2000)

5.5.1 Specification 2.2.2.2—Waste Loading

Waste Loading: The loading of waste sodium from Envelope A in the ILAW glass shall be greater than 14 weight percent based on Na₂O. The loading of waste sodium from Envelope B in the ILAW glass shall be greater than 3.0 weight percent based on Na₂O. The loading of waste sodium from Envelope C in the ILAW glass shall be greater than 10 weight percent (wt%) based on Na₂O.

According to the ILAW PCP (24590-WTP-PL-RT-03-001):

[PCP Section 4.1.2: Waste Loading]... During production operations, the WTP project expects to perform the following activities:

- Control the LAW vitrification process such that prepared LAW melter feed matches a target composition that is formulated to meet or exceed sodium loading while complying with specifications. (A, D, T)

- Determine the total Na₂O loading based on sampling and analysis of each LAW feed batch and measurements of the GFCs masses added. These determinations may be confirmed infrequently by chemical analysis of ILAW product samples. (A, T)
- Non-waste sodium additions (such as ultrafilter cleaning and ion exchange column regeneration) will be recorded and included in mass balance calculations. The LAW feed analysis will be adjusted by mass balance to account for average non-waste sodium introduced during feed processing. This adjustment will provide the waste sodium loading. (A)
- Report the waste Na₂O loading in the ILAW production documentation for all ILAW produced from a production lot. (D, A)

The ILAW production documentation will include identification of the LAW feed envelope, the metric tons of ILAW produced per metric ton of sodium feed, and the calculated waste Na₂O loading in the ILAW glass product.

According to this specification, the Na₂O mass fraction in glass that came from waste Na₂O ($g_{Na_2O(w)}^{oxide\ in\ MFPV}$) must be above the limit ($L_l^{W_{Na}}$), i.e., $L_l^{W_{Na}} < g_{Na_2O(w)}^{oxide\ in\ MFPV}$. The limit is 14 wt%, 3, and 10, for Envelopes A, B, and C waste products, respectively. The method of demonstrating that this specification is met during production is to calculate and report $g_{Na_2O(w),j}^{oxide\ in\ MFPV}$ and the waste envelope in the Production Records.

The waste Na₂O loading in each MFPV batch is calculated by Equation (105). The mass weighted average over a group of MFPV batches is given by:

$$g_{Na_2O(w),e}^{oxide\ in\ can} = \frac{\sum_{j=1}^{MFPVs\ in\ n_e^{can}} \left(g_{Na_2O(w),j}^{oxide\ in\ MFPV,Step3} \tilde{M}_j^{oxide\ in\ MFPV,Step3} \right)}{\sum_{j=1}^{MFPVs\ in\ n_e^{can}} \tilde{M}_j^{oxide\ in\ MFPV,Step3}} \quad (121)$$

- where
- $g_{Na_2O(w),e}^{oxide\ in\ can}$ = mass fraction of waste Na₂O (waste Na₂O loading) in the eth canister (g per g glass)
 - $g_{Na_2O(w),j}^{oxide\ in\ MFPV,Step3}$ = mass fraction of waste Na₂O (waste Na₂O loading) in the jth MFPV batch from algorithm calculation Step 3 (g per g glass)
 - $n_e^{MFPVs\ in\ can}$ = number of MFPV batches that are assumed to be in the eth canister
 - $\tilde{M}_j^{oxide\ in\ MFPV,Step3}$ = mass of total glass oxides in the jth MFPV batch after applying the component retention factors from algorithm calculation Step 3 (g)

The summation is performed over $n_e^{MFPVs\ in\ can}$ batches within a group, $j, j-1, j-2, \dots, j-(n_e^{MFPVs\ in\ can} - 1)$. The mass of total glass oxides in the jth MFPV batch after applying the component retention factors from algorithm calculation Step 3 (g), $\tilde{M}_j^{oxide\ in\ MFPV,Step3}$, is given as:

$$\tilde{M}_j^{\text{oxide in MFPV, Step 3}} = \left[C_{dm}^{\text{oxide in CRV}} V_j^{\text{waste MFPV}} + \sum_{k=1}^{n_j^{\text{GFCs in MFPV}}} \left(M_{kj}^{\text{GFC in MFPV, measured}} \sum_{i=1}^{n_k^{\text{oxides in GFC}}} m_{ik}^{\text{oxide in GFC}} \right) \right] \sum_{i=1}^{n_j^{\text{oxides in MFPV}}} \left(g_{ij}^{\text{oxide in MFPV, Step 3}} v_i \right) \quad (122)$$

where

- $C_{dm}^{\text{oxide in CRV}}$ = mass fraction of waste Na₂O (waste Na₂O loading) in the jth MFPV batch from algorithm calculation Step 3 (g per g glass)
- $V_j^{\text{waste MFPV}}$ = volume of waste transferred from CRV to the jth MFPV (L)
- $n_j^{\text{GFCs in MFPV}}$ = number of GFCs in the jth MFPV batch
- $M_{kj}^{\text{GFC in MFPV, measured}}$ = measured mass of kth GFC added to the jth MFPV batch (g)
- $n_k^{\text{oxides in GFC}}$ = number of glass oxides in the kth GFC
- $m_{ik}^{\text{oxide in GFC}}$ = mass fraction of the ith glass oxide in the kth GFC (g oxide per g GFC including volatiles). Here, unlike **H** in Equation (48), $m_{ik}^{\text{oxide in GFC}}$ includes all tracked components beyond the 11 GFC components.
- $n_j^{\text{oxides in MFPV}}$ = number of glass oxides tracked in the mass balance calculations for the jth MFPV batch
- $g_{ij}^{\text{oxide in MFPV, Step 3}}$ = mass fraction of the ith glass oxide in the jth MFPV batch from algorithm calculation Step 3 before applying component retention factors (g oxide per g MFPV oxides)
- v_i = retention factor for the ith component (fraction)

5.5.2 Specification 2.2.2.6 – Chemical Composition Documentation

Chemical Composition Documentation: *The chemical composition of the waste form, filler, and package shall be identified.*

2.2.2.6.2 Chemical Composition During Production: *The production documentation (Table C.5-1.1, Deliverable 6.7) shall provide the chemical composition of each waste form, optional filler, and package. The reported composition shall include elements (excluding oxygen) present in concentrations greater than 0.5 percent by weight and elements and compounds required to meet regulatory or Contract requirements.*

According to the ILAW PCP (24590-WTP-PL-RT-03-001):

[PCP Section 4.1.6.2: Chemical Composition During Production] ... During production operations, the WTP project expects to perform the following characterization and reporting activities:

- Qualified sampling, test methods, analytical techniques, and models will be used to demonstrate compliance with this requirement during production. As new methods become available, they may be evaluated for development and qualification for use in ILAW production. (A, D, T)
- The WTP project’s Quality Assurance Manual (QAM), 24590-WTP-QAM-QA-06-001, requires the GFC supplier facility to follow a WTP project approved QA program (QAP) and perform

audit and surveillance activities at the WTP vitrification facility to ensure that quality materials are used in GFC addition. GFC suppliers will be required to certify the compositions and uncertainties of GFCs (major components as well as impurities) and to provide chemical analysis data. (A, I)

- *The impurities in GFCs will be kept to a minimum by requiring the vendor to supply the material at a specific purity level and certify it with material test reports. If the glass forming chemical (for example, Fe₂O₃) contains Al₂O₃ as a major impurity, it will be accounted for in the calculation of the amount of GFC to be added to the waste batch. (A, I)*
- *ILAW chemical composition will be controlled during production operations by sampling and chemically analyzing LAW feed, and calculating required additions of GFCs necessary to yield ILAW satisfying all WTP contract and processing requirements. In addition, volume transfers of CRV batches and mass of GFCs transferred to the MFPV will be verified within measurement uncertainties. (A, D, I, T)*
- *The product control aspects of the strategy for compliance with this requirement will be implemented as part of a larger process control system for LAW vitrification. Aspects of the product control system that are part of the compliance strategy will be conducted according to NQA-1 (ASME 2000) requirements and documented in the ILAW production documentation. The process will be operated within control limits based on parameters and results from qualification activities. (A, D, T)*
- *The means and standard deviations of reportable glass components will be calculated over the chemical composition determinations of ILAW produced as a given production lot is being processed. Standard deviations will be computed to account for multiple sources of variation and uncertainty. (A, I)*

The following information will be reported in the ILAW production documentation:

- *The estimated composition of the ILAW glass. The estimated composition will be calculated using a mass balance based upon the analyses of LAW feed samples, the volume of waste transferred from the CRV to the MFPV, the composition of the GFCs as provided in the vendor certifications, and the masses of GFCs added (as measured in the glass former batching facility), as well as the estimated volume and composition of the tank heels in the MFPV. The reported compositions will span several ILAW containers corresponding to a production lot. If a shard sample is taken from an individual container and analyzed, that composition will also be reported for that container. Reportable glass components will include those at concentrations greater than 0.5 wt% in the glass plus those necessary to meet regulatory or contract requirements.*
- *The chemical composition of any optional filler material and the quantity added to each filled container, if any.*
- *The materials of construction for the ILAW container.*

The mass weighted average composition over a group of MFPV batches is given by:

$$g_{ie}^{oxide\ in\ can} = \frac{\sum_{j=1}^{MFPV\ s\ in\ n_c^{can}} \left(\tilde{g}_{ij}^{oxide\ in\ MFPV,\ Step\ 3} \tilde{M}_j^{oxide\ in\ MFPV,\ Step\ 3} \right)}{\sum_{j=1}^{MFPV\ s\ in\ n_c^{can}} \tilde{M}_j^{oxide\ in\ MFPV,\ Step\ 3}} \quad (123)$$

where $g_{ie}^{oxidein,can}$ = mass fraction of the i^{th} glass oxide in the e^{th} canister (g per g glass)

$\tilde{g}_{ij}^{oxidein,MFPV,Step3}$ = mass fraction of the i^{th} glass oxide in the j^{th} MFPV batch from algorithm calculation Step 3 after applying the component retention factors (g oxide per g glass), i.e., mass of i^{th} glass oxide that will remain in glass divided by the total mass of all glass oxides that will remain in glass

$n_e^{MFPVsin,can}$ = number of MFPV batches that are assumed to be in the e^{th} canister

$\tilde{M}_j^{oxidein,MFPV,Step3}$ = mass of total glass oxides in the j^{th} MFPV batch after applying the component retention factors from algorithm calculation Step 3 (g)

The summation is performed over $n_e^{MFPVsin,can}$ batches within a group, $j, j-1, j-2, \dots$ and $j-(n_e^{MFPVsin,can}-1)$.

The mass weighted SD of glass composition is

$$s_{ie}^{oxidein,can} = \frac{\sqrt{\sum_{j=1}^{n_e^{MFPVsin,can}} \left(\tilde{g}_{ij}^{oxidein,MFPV,Step3} \tilde{M}_j^{oxidein,MFPV,Step3} \right)^2}}{\sum_j \tilde{M}_j^{oxidein,MFPV,Step3}} \quad (124)$$

where $s_{ie}^{oxidein,can}$ = SD for the mass fraction of the i^{th} glass oxide in the e^{th} canister (g per g glass)

$\tilde{s}_{ij}^{oxidein,MFPV,Step3}$ = SD for the mass fraction of the i^{th} glass oxide in the j^{th} MFPV batch after applying the component retention factors from algorithm calculation Step 3 (g per g glass). This is obtained from Monte Carlo simulation for composition uncertainty calculation discussed in Section 4.2.2.

$n_e^{MFPVsin,can}$ = number of MFPV batches that are assumed to be in the e^{th} canister

$\tilde{M}_j^{oxidein,MFPV,Step3}$ = mass of total glass oxides in the j^{th} MFPV batch after applying the component retention factors from algorithm calculation Step 3 (g)

The waste form composition is documented during production by reporting the $g_{ie}^{oxidein,can}$ values from Equation

(123) and $s_{ie}^{oxidein,can}$ values from Equation (124) in the Production Records. Currently, it is planned to calculate

$g_{ie}^{oxidein,can}$ values for all components (i) for which analytical data are available for a particular container.

However, it may be advantageous to trim the number of components to only those with concentrations greater than 0.5 wt% plus those associated with other limits and specifications. In any case, only the appropriate subset of i will be reported in the Production Records.

The addition of optional filler material and production of the final ILAW container data package are not part of the ILAW formulation algorithm.

5.5.3 Specification 2.2.2.7—Radiological Composition Documentation

Radiological Composition Documentation: The radionuclide composition of the waste form shall be documented. Radionuclides shall be identified that are significant as defined in NUREG/BR-0204 and 49CFR172.101 (Table 2). Technetium-99 (⁹⁹Tc) shall be considered to be significant at concentrations greater than 0.003 Ci/m³ in the ILAW form. The inventories shall be indexed to December 31, 2002. The documentation shall be consistent with the radiological description format described in NUREG/BR-0204.

2.2.2.7.2 Radionuclide Composition During Production: The ILAW production documentation (Table C.5-1.1, Deliverable 6.7) shall identify the radionuclide inventory in each ILAW package produced. The actual inventory indexed at the month of product transfer and the inventory indexed to December 31, 2002, shall be reported.

According to the ILAW PCP (24590-WTP-PL-RT-03-001):

[PCP Section 4.1.7: Radiological Composition Documentation] ... During production operations, the WTP project expects to conduct the following activities to comply with this requirement:

- Collect and perform radiochemical analysis on process samples to determine the concentrations of significant radionuclides as defined in NUREG/BR-0204 (NRC 1995b) and 49 CFR 172.101, Table 2. (D, T)
- Apply the ratio method to estimate radionuclide concentrations for those radionuclides not directly measured, if necessary. (A)
- Calculate the means and standard deviations of the radionuclide inventory determinations for ILAW containers produced from a given LAW production lot for each significant radionuclide. (A)
- Calculate radionuclide inventories indexed to the month of product transfer and to 31 December 2002 using a computer code (for example, MicroShield™ [Grove 1996]) for each significant radionuclide. (A)

Inventories of reported radionuclides in Ci per container based on CRV analyses will be included in the ILAW production documentation for each significant radionuclide. The documentation will be consistent with the radiological description format described in NUREG/BR-0204 (NRC 1995b).

Indexing of radionuclide data to a specified date will be performed by the laboratory, before entering into the ILAW formulation algorithm. The mass weighted average specific activity of radionuclides over a group of MFPV batches is given by

$$a_{ie}^{rad\ in\ can} = \frac{\sum_{j=1}^{MFPVs\ in} \left(\tilde{a}_{ij}^{rad\ in\ MFPV, Step3} \tilde{M}_j^{oxide\ in\ MFPV, Step3} \right)}{\sum_{j=1}^{MFPVs\ in} \tilde{M}_j^{oxide\ in\ MFPV, Step3}} \tag{125}$$

where $a_{ie}^{rad\ in\ can}$ = specific activity of the *i*th radionuclide in the *e*th canister (mCi/g glass)

- $\tilde{a}_{ij}^{rad\ in\ MFPV,\ Step3}$ = specific activity of the i^{th} radionuclide in the j^{th} MFPV batch after applying the component retention factors for algorithm calculation Step 3 (mCi/g oxides)
- $n_e^{MFPVs\ in\ can}$ = number of MFPV batches that are assumed to be in the e^{th} canister
- $\tilde{M}_j^{oxide\ in\ MFPV,\ Step3}$ = mass of total glass oxides in the j^{th} MFPV batch after applying the component retention factors from algorithm calculation Step 3 (g)

The mass weighted SD of specific activity is

$$S_{ie}^{rad\ in\ can} = \frac{\sqrt{\sum_{j=1}^{n_e^{MFPVs\ in\ can}} \left(\tilde{S}_{ij}^{rad\ in\ MFPV,\ Step3} \tilde{M}_j^{oxide\ in\ MFPV,\ Step3} \right)^2}}{\sum_j^{n_e^{MFPVs\ in\ can}} \tilde{M}_j^{oxide\ in\ MFPV,\ Step3}} \quad (126)$$

- where
- $S_{ie}^{rad\ in\ can}$ = SD for the specific activity of the i^{th} radionuclide in the e^{th} canister (mCi/g glass)
 - $\tilde{S}_{ij}^{rad\ in\ MFPV,\ Step3}$ = SD for the specific activity of the i^{th} radionuclide in the j^{th} MFPV batch after applying the component retention factors from algorithm calculation Step 3 (g per g glass). This is obtained from Monte Carlo simulation during composition uncertainty calculations discussed in Section 4.2.2.
 - $n_e^{MFPVs\ in\ can}$ = number of MFPV batches that are assumed to be in the e^{th} canister
 - $\tilde{M}_j^{oxide\ in\ MFPV,\ Step3}$ = mass of total glass oxides in the j^{th} MFPV batch after applying the component retention factors from algorithm calculation Step 3 (g)

The inventory of each radionuclide in each canister of LAW glass (the reporting quantity) is given by:

$$I_{ie}^{rad\ in\ can} = a_{ie}^{rad\ in\ can} M_e^{glass\ in\ can} \quad (127)$$

- where
- $I_{ie}^{rad\ in\ can}$ = inventory of the i^{th} radionuclide in the e^{th} canister (Ci)
 - $a_{ie}^{rad\ in\ can}$ = specific activity of the i^{th} radionuclide in the e^{th} canister (mCi/g glass)
 - $M_e^{glass\ in\ can}$ = mass of glass in the e^{th} canister (kg)

The mass of glass in the container is assumed to be $M_e^{glass\ in\ can} = 5,911$ kg (the average value measured in the full-scale container filling experiments [Andre 2004]). During plant operation, $M_e^{glass\ in\ can}$ will be obtained from direct measurement or correlation with fill height.

The inventories and concentrations of radionuclides will be calculated for all radionuclides with measured values from the laboratory samples. For those radionuclides with “less-than” values reported by the laboratory, the detection limit will be used in calculations of concentration and an appropriate flag will be carried with the results. The Production Records will report only those values required (e.g., those radionuclides with concentrations considered significant according to the specification above).

5.5.4 Specification 2.2.2.8—Radionuclide Concentration Limitations

Radionuclide Concentration Limitations: The radionuclide concentration of the ILAW form shall not exceed Class C limits as defined in 10CFR61.55. In addition, the average glass concentrations of Cesium-137 (¹³⁷Cs), Strontium-90 (⁹⁰Sr) shall be limited as follows: ¹³⁷Cs < 3 Ci/m³ and ⁹⁰Sr < 20 Ci/m³. The method used to perform concentration averaging should be identified in the ILAW Product Compliance Plan.

According to the ILAW PCP (24590-WTP-PL-RT-03-001):

[PCP Section 4.1.8: Radiological Concentration Limitations] ... During production, the WTP project expects to perform the following activities:

- *Determine the radionuclide concentrations in the ILAW product through analysis of a combination of process samples, flowsheet calculations, or periodic confirmatory product samples. Radionuclide concentrations will be determined routinely based upon samples taken from the ILAW CRVs. (A, T)*
- *Verify that radionuclide concentrations are less than Class C limits as defined in 10 CFR 61.55 and as described in the Nuclear Regulatory Commission’s Branch Technical Position on Concentration Averaging and Encapsulation (NRC 1995a). (A, I, T)*
- *Verify that the average concentrations for the following radionuclides are below their respective concentration limits: ¹³⁷Cs < 3 Ci/m³, ⁹⁰Sr < 20 Ci/m³, and TRU < 100 nCi/g. The average concentrations will be determined by calculating the means of radionuclide concentrations, measured in process or confirmatory product samples, for all containers submitted for acceptance. (A, I, T)*
- *Calculate a running average of radionuclide concentrations by summing the actual inventories of each radionuclide in the ILAW product presented to date and dividing by the total volume of waste in these containers. (A)*

Inventories of reported radionuclides in Ci per container based on CRV analyses will be included in the ILAW production documentation for each significant radionuclide. The WTP project will also report running averages of radionuclide concentrations over all ILAW product containers presented to date for acceptance on a waste type basis in the ILAW production documentation.

The radionuclide concentration limits are based on the activity of each radionuclide either per unit glass mass or per unit glass volume. The specific activity of radionuclides and its SD from Equations (125) and (126) are converted to per unit glass volume using:

$$\hat{a}_{ie}^{can} = a_{ie}^{can} \rho_e^{glass\ in\ can} \tag{128}$$

$$\hat{s}_{ie}^{can} = s_{ie}^{can} \rho_e^{glass\ in\ can} \tag{129}$$

where $\hat{a}_{ie}^{rad\ in\ can}$ = activity of the i^{th} radionuclide per unit volume of glass in the e^{th} canister (Ci/m³ glass)

$a_{ie}^{rad\ in\ can}$ = specific activity of the i^{th} radionuclide in the e^{th} canister (mCi/g glass)

$\rho_e^{glass\ in\ can}$ = density of glass in the e^{th} canister (g/L)

$\hat{s}_{ie}^{rad\ in\ can}$ = SD for the activity of the i^{th} radionuclide per unit volume of glass in the e^{th} canister (Ci/m³ glass)

$s_{ie}^{rad\ in\ can}$ = SD for the specific activity of the i^{th} radionuclide in the e^{th} canister (mCi/g glass)

The requirements for ¹³⁷Cs and ⁹⁰Sr are satisfied if $\hat{a}_{137Cs,e}^{rad\ in\ can} + k^{rad} \hat{s}_{137Cs,e}^{rad\ in\ can} < 3\text{ Ci/m}^3$ and

$\hat{a}_{90Sr,e}^{rad\ in\ can} + k^{rad} \hat{s}_{90Sr,e}^{rad\ in\ can} < 20\text{ Ci/m}^3$ where k^{rad} is the expansion factor for radionuclide concentration specification. Note that the Contract (DOE 2000) Section C.7 (d).(1).(iii) requirement of 0.3 Ci/m³ ¹³⁷Cs is not relevant to product compliance and not required in the production records.

To demonstrate that the waste meets the classification of Class C waste or below, limiting values for $\hat{a}_{ie}^{rad\ in\ can}$ and $a_{ie}^{rad\ in\ can}$; listed in Table 15 and Table 16 given in Section 5.1.6.3, are used.

The first step to classification is then to determine if there are any radionuclides with measurable concentrations ($\hat{a}_{ie}^{rad\ in\ can}$ for ⁹⁹Tc, ¹²⁹I, ⁶³Ni, ⁹⁰Sr, and ¹³⁷Cs, or $a_{ie}^{rad\ in\ can}$ for TRU, ²⁴¹Pu, and ²⁴²Cm). If non-zero values are present for radionuclides only in Table 15 or only in Table 16, then only those tables are used for classification. If there are non-zero values for both tables, then Table 15 is used for classification if any one radionuclide from Table 15 is greater than 10% of its associated limit. If no Table 15 radionuclide has a concentration greater than or equal to its associated limit, then Table 16 is used for classification. The sum of fractions rule is given as:

$$SF_{LL,e}^{can} = \sum_i^2 \frac{\hat{a}_{ie}^{rad\ in\ can}}{L_u^{\hat{a}_i}} \text{ (for } i = {}^{99}\text{Tc and } {}^{129}\text{I)} + \sum_i^3 \frac{a_{ie}^{can} \times 10^6 \text{ (nCi/mCi)}}{L_u^{a_i}} \text{ (for } i = \text{TRU, } {}^{241}\text{Pu, and } {}^{242}\text{Cm)}$$
(130)

$$SF_{SL,e}^{can} = \sum_i^3 \frac{\hat{a}_{ie}^{can}}{L_u^{\hat{a}_i}} \text{ (for } i = {}^{63}\text{Ni, } {}^{90}\text{Sr, and } {}^{137}\text{Cs)}$$
(131)

where $SF_{LL,e}^{can}$ = sum of fractions of activity to the limit of each radionuclide for long-lived radionuclides for Class C limit determination in the e^{th} canister

- $S_{SL,e}^{rad\ in\ can}$ = sum of fractions of activity to the limit of each radionuclide for short-lived radionuclides for Class C limit determination in the e^{th} canister
- $\hat{a}_{ie}^{rad\ in\ can}$ = activity of the i^{th} radionuclide per unit volume of glass in the e^{th} canister (Ci/m³ glass)
- $a_{ie}^{rad\ in\ can}$ = specific activity of the i^{th} radionuclide in the e^{th} canister (mCi/g glass)
- $L_u^{a_i}$ = upper limit for specific activity of the i^{th} radionuclide (nCi/g glass)
- $L_u^{\hat{a}_i}$ = upper limit for the activity of the i^{th} radionuclide per unit glass volume (Ci/m³ glass)

The standard deviations for $S_{LL,e}^{rad\ in\ can}$ and $S_{SL,e}^{rad\ in\ can}$ are given as:

$$S_{LL,e}^{rad\ SF\ in\ can} = \sqrt{\sum_i^2 \left(\frac{\hat{S}_{ie}^{rad\ in\ can}}{L_u^{\hat{a}_i}} \right)^2 \text{ (for } i = {}^{99}\text{Tc and } {}^{129}\text{I)} + \sum_i^3 \left(\frac{S_{ie}^{rad\ in\ can} \times 10^6 \text{ (nCi/mCi)}}{L_u^{a_i}} \right)^2 \text{ (for } i = \text{TRU, } {}^{241}\text{Pu, and } {}^{242}\text{Cm)}} \quad (132)$$

$$s^{SF_S} = \sqrt{\sum_i^3 \left(\frac{\hat{S}_{ie}^{rad\ in\ can}}{L_u^{\hat{a}_i}} \right)^2 \text{ (for } i = {}^{63}\text{Ni, } {}^{90}\text{Sr, and } {}^{137}\text{Cs)}} \quad (133)$$

- where
- $S_{LL,e}^{rad\ SF\ in\ can}$ = SD for the sum of fractions of activity to the limit of each radionuclide for long-lived radionuclides for Class C limit determination in the e^{th} canister
 - $S_{SL,e}^{rad\ SF\ in\ can}$ = SD for the sum of fractions of activity to the limit of each radionuclide for short-lived radionuclides for Class C limit determination in the e^{th} canister
 - $\hat{S}_{ie}^{rad\ in\ can}$ = SD for the activity of the i^{th} radionuclide per unit volume of glass in the e^{th} canister (Ci/m³ glass)
 - $S_{ie}^{rad\ in\ can}$ = SD for the specific activity of the i^{th} radionuclide in the e^{th} canister (mCi/g glass)
 - $L_u^{\hat{a}_i}$ = upper limit for the activity of the i^{th} radionuclide per unit glass volume (Ci/m³ glass)
 - $L_u^{a_i}$ = upper limit for specific activity of the i^{th} radionuclide (nCi/g glass)

The Class C limit is satisfied if $S_{LL,e}^{rad\ in\ can} + k^{rad} S_{LL,e}^{rad\ SF\ in\ can} < 1$ and $S_{SL,e}^{rad\ in\ can} + k^{rad} S_{SL,e}^{rad\ SF\ in\ can} < 1$.

5.5.5 Specification 2.2.2.9—Surface Dose Rate Limitations

Surface Dose Rate Limitations: *The dose rate at any point on the external surface of the package shall not exceed 500 mrem/hr.*

According to the ILAW PCP (24590-WTP-PL-RT-03-001):

[PCP Section 4.1.9: Surface Dose Rate Limitations] ... During production, the WTP project expects to perform the following activities:

- *Check radionuclide concentrations projected for compliance with WTP contract Specification 2.2.2.7, Radiological Composition Documentation, to verify that they will be lower in the ILAW product than the maximum used to demonstrate compliance with this specification. (A)*
- *Confirm compliance with this requirement by monitoring the surface dose rate of each ILAW container using handheld instrumentation or automated monitoring equipment prior to transfer for disposal. (I)*

Surface dose rates measured for each container will be reported in the ILAW production documentation.

No calculation is needed by ILAW formulation algorithm.

5.5.6 Specification 2.2.2.17—Waste form Testing

Waste form Testing:

2.2.2.17.2 Product Consistency Test: *The normalized mass loss of sodium, silicon, and boron shall be measured using a seven day product consistency test run at 90°C as defined in ASTM C1285-98. The test shall be conducted with a glass to water ratio of 1 gram of glass (-100 +200 mesh) per 10 milliliters of water. The normalized mass loss shall be less than 2.0 grams/m². Qualification testing shall include glass samples subjected to representative waste form cooling curves. The product consistency test shall be conducted on waste form samples that are statistically representative of the production glass.*

2.2.2.17.3 Vapor Hydration Test: *The glass corrosion rate shall be measured using at least a seven day vapor hydration test run at 200°C as defined in the DOE concurred upon ILAW Product Compliance Plan. The measured glass alteration rate shall be less than 50 grams/(m²·day). Qualification testing shall include glass samples subjected to representative waste form cooling curves. The vapor hydration test shall be conducted on waste form samples that are representative of the production glass.*

According to the ILAW PCP (24590-WTP-PL-RT-03-001):

[PCP Section 4.1.17: Waste Form Testing] ... During production operations, the WTP project expects to perform the following characterization and reporting activities:

- *The chemical composition of the ILAW product will be determined and controlled as described in the response to WTP contract Specification 2.2.2.6. (A, I, T)*
- *The PCT and VHT property composition models will be applied using the ILAW glass chemical composition determinations for each MFPV batch. The outcomes will be predicted PCT and VHT values, and calculated uncertainties of the predictions for each chemical composition determination. (A)*
- *The predicted PCT and VHT values for glasses produced over a production lot will be used to calculate means, standard deviations, and statistical intervals. The calculations will account for*

variations and uncertainties in the predicted property values due to variations in glass composition, as well as uncertainties due to glass sampling, glass chemical analyses, other measurement uncertainties and the PCT and VHT property composition models. Statistical variance and error propagation methods will be used, and will be discussed in detail in the ILAW PQR after they are developed and applied. (A)

The ILAW production documentation will include the chemical composition of ILAW glass as oxides as calculated from CRV samples and masses of GFCs added and the predicted PCT and VHT calculated from PCT and VHT glass property composition models.

The glass properties will be calculated for the final estimated composition of canistered glass using the glass property models described in Section 4.1. The predicted properties for PCT normalized releases (P^{pct} , $\ln[r_B, \text{g/L}]$ and $\ln[r_{Na}, \text{g/L}]$) and VHT alteration depth (P^{vht} , $\ln[D, \mu\text{m}]$) are calculated using Equations (2) and (5) with model coefficients (p_h^{pct} and p_h^{vht}) given in Table 5 and Table 6 and glass composition (for x_h^{pct} and x_h^{vht}) given by Equation (123). The prediction uncertainties (U_{pred}^{pct} and U_{pred}^{vht}) are calculated using Equations (8) and (9) and the same composition (for \mathbf{x}^{pct} and \mathbf{x}^{vht}) given by Equation (123). The composition uncertainties (U_{comp}^{pct} and U_{comp}^{vht}) are calculated using Monte Carlo simulation method described in Section 4.2.2 based on nominal glass composition given by Equation (123) with SD given by Equation (124).

The UCCIs for PCT normalized releases and VHT alteration depths are given as:

$$B_{ucci,e}^{pct} = P_e^{pct} + U_{pred,e}^{pct} + U_{comp,e}^{pct} \quad (134)$$

$$B_{ucci,e}^{vht} = P_e^{vht} + U_{pred,e}^{vht} + U_{comp,e}^{vht} \quad (135)$$

where $B_{ucci,e}^{pct}$, $B_{ucci,e}^{vht}$ = CL% upper combined confidence interval for “pct” ($\ln[r_B, \text{g/L}]$, $\ln[r_{Na}, \text{g/L}]$)⁽¹⁵⁾ and “vht” ($\ln[D, \mu\text{m}]$) for the e^{th} canister
 P_e^{pct} , P_e^{vht} = predicted transformed property for “pct” ($\ln[r_B, \text{g/L}]$, $\ln[r_{Na}, \text{g/L}]$) and “vht” ($\ln[D, \mu\text{m}]$) for the e^{th} canister (calculated per Section 4.1)
 $U_{pred,e}^{pct}$, $U_{pred,e}^{vht}$ = model prediction uncertainty for “pct” ($\ln[r_B, \text{g/L}]$, $\ln[r_{Na}, \text{g/L}]$) and “vht” ($\ln[D, \mu\text{m}]$) for the e^{th} canister (calculated per Section 4.2.1)
 $U_{comp,e}^{pct}$, $U_{comp,e}^{vht}$ = composition uncertainty for “pct” ($\ln[r_B, \text{g/L}]$, $\ln[r_{Na}, \text{g/L}]$) and “vht” ($\ln[D, \mu\text{m}]$) for the e^{th} canister (calculated per Section 4.2.2)

5.5.7 Specification 2.2.2.23—Manifesting

***Manifesting:** A shipping manifest shall be prepared for delivery with each shipment of ILAW product. Information on the manifest shall satisfy the requirements in DOE Manual 435.1-1, Chapter IV, Section I.(2), and NUREG/BR-0204. Any package containing dangerous waste must be labeled and manifested in accordance with WAC 173-303-370 and the Dangerous Waste Portion of the Resource Conservation and Recovery Act Permit for the Treatment, Storage, and Disposal of Dangerous Wastes (Permit No. WA 7890008967).*

According to the ILAW PCP (24590-WTP-PL-RT-03-001):

⁽¹⁵⁾ See Section 4.1.1 for justification to exclude the PCT Si release from the constraints.

[PCP Section 4.1.23: Manifesting]... During production operations, the WTP project expects to perform the following activities:

- *Prepare the documentation necessary to transfer the ILAW from the WTP to the onsite ILAW disposal site. Information needed to complete the radioactive shipping records will be available from*
 - *Sampling and analysis (T)*
 - *Process knowledge (I)*
- *Maintain and make available for inspection transportation records as required by DOE, Ecology, and DOT. (I)*

During production, documentation satisfying the requirements of this specification and confirmation that the ILAW product meets radioactive shipment record requirements will be provided with each shipment of ILAW to the disposal site.

Waste composition and radionuclide concentrations/inventories will be put in the Production Records. The equations required to manifest the waste are taken from above subsections.

6 Calculation Examples

To demonstrate the calculation steps described in Section 5 and aid in understanding how they are solved, an example set of waste compositions is carried through most of the calculations. The wastes needed to have both chemical and radionuclide information available and would benefit from having waste composition variations. For this purpose, the waste compositions generated by the *WTP Dynamic Flowsheet Model* (G2) were chosen (24590-WTP-RPT-PO-07-002, Rev. 0). The G2 model run selected for example calculations (MRQ07-0003 as described in 24590-WTP-MDD-PR-01-002, Rev. 9⁽¹⁶⁾) represents one of many recent G2 runs. The G2 model output data in the form of chemical snapshots of the CRV contents were used.

The selected G2 run produced total 4998 CRV batches with 2499 batches per each CRV: LCP-VSL-00001 (designated as CRV-A in this report) and LCP-VSL-00002 (CRV-B). The order of CRV batches is $A_1, B_1, A_2, B_2, \dots, A_{2499}, B_{2499}$. The eight sequential datasets, representing the A_{10}^{th} through B_{13}^{th} CRV batches, are given in Table B.1 in Appendix B and are used for example calculations in this report. The composition is reported in the format of mass of each of 96 (non-zero) analytes and a total batch volume. The mass values per batch were converted to concentration units that would be reported by the WTP laboratory during operation (in elemental concentrations and radionuclide activities per unit volume of CRV waste).⁽¹⁷⁾ The

G2 data on CRV batch are taken as the average analytical results of three replicate CRV samples ($\bar{C}_{id}^{\text{element in CRV}}$ for chemical components and $\bar{R}_{id}^{\text{rad in CRV}}$ for radionuclides).

The G2 data on CRV batch composition includes the trace components that will not be analyzed from the CRV samples. For components that are listed for both chemical analyte and radionuclide(s), the data on chemical elements are used for oxide conversion because for G2 data the concentration of chemical element includes all isotopes. Note that this approach is solely for example calculations in this report using the G2 output. During WTP operation, the analytical data conversion procedures described in Section 5.1.2 are used.

The volume of CRV was from 53033 to 53279 L within the first 250 CRV batches, which are higher than the present design of working volume of CRV (48661 L). For example calculations, the volume for each CRV batch was randomly generated based on the uncertainty estimation (SD = 724.3 L) described in Appendix D around the nominal working volume of 48661 L. Similarly the heel volume for the calculation of each MFPV batch was also randomly generated based on the uncertainty estimation (SD = 447.2 L) described in Appendix D around the nominal working volume of 6556 L. The resulting working volume of the A_{11}^{th} CRV was 48709 L and the heel volume for the A_{101}^{th} MFPV batch was 6712 L.

6.1 Example Step 1 – Glass Formulation and Calculation of LAW Transfer Volume

The waste compositions of CRV used to perform the calculations was that of the A_{11}^{th} CRV batch as estimated by the mentioned G2 run. The laboratory will screen the data and scale the radionuclide concentrations to the appropriate date, per their procedures.

⁽¹⁶⁾ The same G2 run was used for IHLW algorithm example calculations and IHLW WQR calculations and will be used for ILAW PQR calculations.

⁽¹⁷⁾ The methods of converting the G2 composition data into laboratory units are not relevant to the scope of this report and will not be discussed here.

6.1.1 CRV Analytical Data Screening and Evaluation

The analytical data from the LAW CRV samples are screened and evaluated prior to calculating glass formulation. No examples are given in this report for data screening and evaluation, which will be performed using the dedicated SPC software during production.

6.1.2 CRV Analytical Data Conversion

This subsection illustrates the calculations for the G2 example to convert analytical data into the appropriate form for glass formulation calculations, discussed in Section 5.1.2. The formulation algorithm uses waste compositions in the form of mass fractions of glass oxides. The analytical data are converted from mg/L or mCi/L of analytes to mass fraction of glass oxide by Equations (21) and (23). With the f_i and A_i values listed in Table A-1, the analytical $\bar{c}_{i,A11}^{element\ in\ CRV}$ and $\bar{R}_{i,A11}^{rad\ in\ CRV}$ values listed in Table B-1 are converted to the correct format for glass formulation. Table B-2 lists the glass oxide mass fractions for all 64 components in the A11th CRV for the 1st waste transfer ($d = A11$ and $m = 1$). For NO₂, NO₃, and TOC (treated as elements in $\bar{c}_{id}^{element\ in\ CRV}$ format), the concentrations per waste volume are still used after converting them from mg/L to g/L. For radionuclides, the specific activities are calculated using Equation (24).

The first step is to obtain the dilution factor according to Equation (19):

$$\lambda_{A11,1} = \frac{V_{A11}^{working\ CRV}}{V_{A11}^{working\ CRV} + V_{A11}^{samplflush\ CRV}} = \frac{48,709\ (L)}{48,709\ (L) + 71.2\ (L)} = 0.99854 \quad (136)$$

Then, use the result to calculate the $c_{i,A11,1}^{element\ in\ CRV}$ values from $\bar{c}_{i,A11}^{element\ in\ CRV}$ according to Equation (18):

$$c_{i,A11,1}^{element\ in\ CRV} = \bar{c}_{i,A11}^{element\ in\ CRV} \lambda_{A11,1} \quad (137)$$

To provide examples, concentrations of Al and Cs and activities of Cs isotopes were taken from the A11th CRV composition in Table B-1 to calculate the mass fractions of the glass oxides Al₂O₃ and Cs₂O. It was assumed that the first waste transfer from the A11th CRV batch in Table B-1 represents the feed stream for the A101th MFPV batch.

Combining Equations (18), (21), and (22) for Al and Cs yields:

$$g_{Al_2O_3,A11,1}^{oxide\ in\ CRV} = \frac{\bar{c}_{Al,A11}^{element\ in\ CRV} f_{Al} \lambda_{A11,1}}{C_{A11,1}^{oxide\ in\ CRV}} = \frac{9.7247 \times 10^3\ (mg/L) \times 1.8895 \times 0.99854}{260.58\ (g/L) \times 1000\ (mg/g)} = 0.07041 \quad (138)$$

$$g_{Cs_2O,A11,1}^{oxide\ in\ CRV} = \frac{\bar{c}_{Cs,A11}^{element\ in\ CRV} f_{Cs} \lambda_{A11,1}}{C_{A11,1}^{oxide\ in\ CRV}} = \frac{3.2623 \times 10^{-3}\ (mg/L) \times 1.0602 \times 0.99854}{260.58\ (g/L) \times 1000\ (mg/g)} = 1.3254 \times 10^{-8} \quad (139)$$

For Cs isotopes, the activity data are converted to elemental concentrations following Equation (23):

$$c_{137\text{Cs},A11,1}^{CRV} = \frac{\overline{R}_{137\text{Cs},A11}^{CRV} \lambda_{A11,1}}{A_{137\text{Cs}}} = \frac{5.6786 \times 10^{-2} \text{ (mCi/L)} \times 0.99854}{86.55 \text{ (Ci/g)}} = 6.5515 \times 10^{-4} \text{ (mg/L)} \quad (140)$$

$$c_{134\text{Cs},A11,1}^{CRV} = \frac{\overline{R}_{134\text{Cs},A11}^{CRV} \lambda_{A11,1}}{A_{134\text{Cs}}} = \frac{2.6649 \times 10^{-7} \text{ (mCi/L)} \times 0.99854}{1293 \text{ (Ci/g)}} = 2.0580 \times 10^{-10} \text{ (mg/L)} \quad (141)$$

Combining Equations (21) and (22) for ¹³⁷Cs and ¹³⁴Cs yields:

$$g_{137\text{Cs}_2\text{O},A11,1}^{CRV} + g_{134\text{Cs}_2\text{O},A11,1}^{CRV} = \frac{c_{137\text{Cs},A11,1}^{CRV} f_{137\text{Cs}} + c_{134\text{Cs},A11,1}^{CRV} f_{134\text{Cs}}}{C_{A11,1}^{CRV}} \quad (142)$$

$$= \frac{6.5515 \times 10^{-4} \text{ (mg/L)} \times 1.0584 + 2.0580 \times 10^{-10} \text{ (mg/L)} \times 1.0597}{260.58 \text{ (g/L)} \times 1000 \text{ (mg/g)}} = 2.661 \times 10^{-9}$$

The combined $g_{\text{Cs}_2\text{O},A11,1}^{CRV}$ value of 2.6661×10^{-9} from ¹³⁷Cs and ¹³⁴Cs is smaller than the value obtained from the concentration of chemical Cs, 1.3254×10^{-8} , which includes all isotopes.

The specific activities of ¹³⁷Cs and ¹³⁴Cs are calculated using Equation (24):

$$a_{137\text{Cs},A11,1}^{CRV} = \frac{\overline{R}_{137\text{Cs},A11}^{CRV} \lambda_{A11,1}}{C_{A11,1}^{CRV}} = \frac{5.6786 \times 10^{-2} \text{ (mCi/L)} \times 0.99854}{260.58 \text{ (g/L)}} = 2.1760 \times 10^{-4} \text{ (mCi/g)} \quad (143)$$

$$a_{134\text{Cs},A11,1}^{CRV} = \frac{\overline{R}_{134\text{Cs},A11}^{CRV} \lambda_{A11,1}}{C_{A11,1}^{CRV}} = \frac{2.6649 \times 10^{-7} \text{ (mCi/L)} \times 0.99854}{260.58 \text{ (g/L)}} = 1.0212 \times 10^{-9} \text{ (mCi/g)} \quad (144)$$

In the examples above, the total glass oxide concentration ($C_{A11,1}^{CRV}$) of 260.58 g/L was obtained by summing over all 64 glass oxide components tracked in the calculations according to Equation (22):

$$C_{A11,1}^{CRV} = \frac{\sum_{i=1}^{64} c_{i,A11,1}^{CRV} f_i}{1000 \text{ (mg/g)}} \quad (145)$$

The composition of the 1st transfer waste transferred from the A11th CRV in the format for glass formulation is given in Table B-2.

6.1.3 Estimation of Target Glass Composition

The first step is to obtain the preliminary minimum Na₂O mass fraction that meets the glass formulation rules defined by Muller et al. (2004) and CCN 150795 from Equations (25) through (31). From Equation (25) for the Na₂O-SO₃-K₂O rules for the A101th MFPV batch to obtain $g_{Na_2O,A101}^{oxide\ in\ MFPV,\ pre-1}$:

$$\begin{aligned}
 g_{Na_2O,A101}^{oxide\ in\ MFPV,\ pre-1} &= \min \left\{ 0.21, \frac{0.35875}{1 + 42.5 \frac{g_{SO_3,A11,1}^{oxide\ in\ CRV}}{g_{Na_2O,A11,1}^{oxide\ in\ CRV}}}, 0.0077 \frac{g_{Na_2O,A11,1}^{oxide\ in\ CRV}}{g_{SO_3,A11,1}^{oxide\ in\ CRV}}, \frac{0.215}{1 + 0.66 \frac{g_{K_2O,A11,1}^{oxide\ in\ CRV}}{g_{Na_2O,A11,1}^{oxide\ in\ CRV}}} \right\} \\
 &= \min \left\{ 0.21, \frac{0.35875}{1 + 42.5 \frac{1.5515 \times 10^{-2}}{8.2030 \times 10^{-1}}}, 0.0077 \frac{8.2030 \times 10^{-1}}{1.5515 \times 10^{-2}}, \frac{0.215}{1 + 0.66 \frac{6.2008 \times 10^{-2}}{8.2030 \times 10^{-1}}} \right\} \\
 &= \min \{0.21, 0.1989, 0.4071, 0.2048\} \\
 &= 0.1989
 \end{aligned} \tag{146}$$

From Equation (26) for the Cl-F-SO₃ rules for the A101th MFPV batch to obtain $g_{Na_2O,A101}^{oxide\ in\ MFPV,\ pre-2}$:

$$\begin{aligned}
 g_{Na_2O,A101}^{oxide\ in\ MFPV,\ pre-2} &= \max \left\{ \frac{0.014656}{\left(\frac{g_{Cl,A11,1}^{oxide\ in\ CRV}}{g_{Na_2O,A11,1}^{oxide\ in\ CRV}} + 0.3 \frac{g_{F,A11,1}^{oxide\ in\ CRV}}{g_{Na_2O,A11,1}^{oxide\ in\ CRV}} \right) + 2.1111 \frac{g_{SO_3,A11,1}^{oxide\ in\ CRV}}{g_{Na_2O,A11,1}^{oxide\ in\ CRV}}}, \frac{0.0022}{\left(\frac{g_{Cl,A11,1}^{oxide\ in\ CRV}}{g_{Na_2O,A11,1}^{oxide\ in\ CRV}} + 0.3 \frac{g_{F,A11,1}^{oxide\ in\ CRV}}{g_{Na_2O,A11,1}^{oxide\ in\ CRV}} \right)} \right\} \\
 &= \max \left\{ \frac{0.014656}{\left(\frac{1.0657 \times 10^{-2} + 0.3 \times 4.4190 \times 10^{-3}}{8.2030 \times 10^{-1}} \right) + 2.1111 \frac{1.5515 \times 10^{-2}}{8.2030 \times 10^{-1}}}, \frac{0.0022}{\left(\frac{1.0657 \times 10^{-2} + 0.3 \times 4.4190 \times 10^{-3}}{8.2030 \times 10^{-1}} \right)} \right\} \\
 &= \max \{0.2687, 0.1506\} \\
 &= 0.2687
 \end{aligned} \tag{147}$$

The preliminary minimum Na₂O mass fraction in glass for the A101th MFPV batch from the Cr₂O₃-K₂O-P₂O₅ rules ($g_{Na_2O,A101}^{oxide\ in\ MFPV,pre-3}$) is obtained following the logics defined by the rules 7 through 9 in Section 5.1.3. To obtain the $g_{Na_2O,A101}^{oxide\ in\ MFPV,pre-3}$ value, the $W_{A101}^{initial}$, $W_{A101}^{min,K}$, and $W_{A101}^{min,Cr}$ values need to be first calculated from Equations (28) through (30) as below:

$$W_{A101}^{initial} = \frac{\min \left\{ g_{Na_2O,A101}^{oxide\ in\ MFPV,pre-1}, g_{Na_2O,A101}^{oxide\ in\ MFPV,pre-2} \right\}}{g_{Na_2O,A11,1}^{oxide\ in\ CRV}} = \frac{\min \{0.1989, 0.2687\}}{8.2030 \times 10^{-1}} = 0.2424 \quad (148)$$

$$W_{A101}^{min,K} = \frac{\min \left\{ g_{Na_2O,A101}^{oxide\ in\ MFPV,pre-1}, g_{Na_2O,A101}^{oxide\ in\ MFPV,pre-2}, \frac{0.0054}{g_{K_2O,A11,1}^{oxide\ in\ CRV}} \right\}}{g_{Na_2O,A11,1}^{oxide\ in\ CRV}} \quad (149)$$

$$= \frac{\min \left\{ 0.1989, 0.2687, \frac{0.0054}{6.2008 \times 10^{-2}} \right\}}{8.2030 \times 10^{-1}} = 0.0871$$

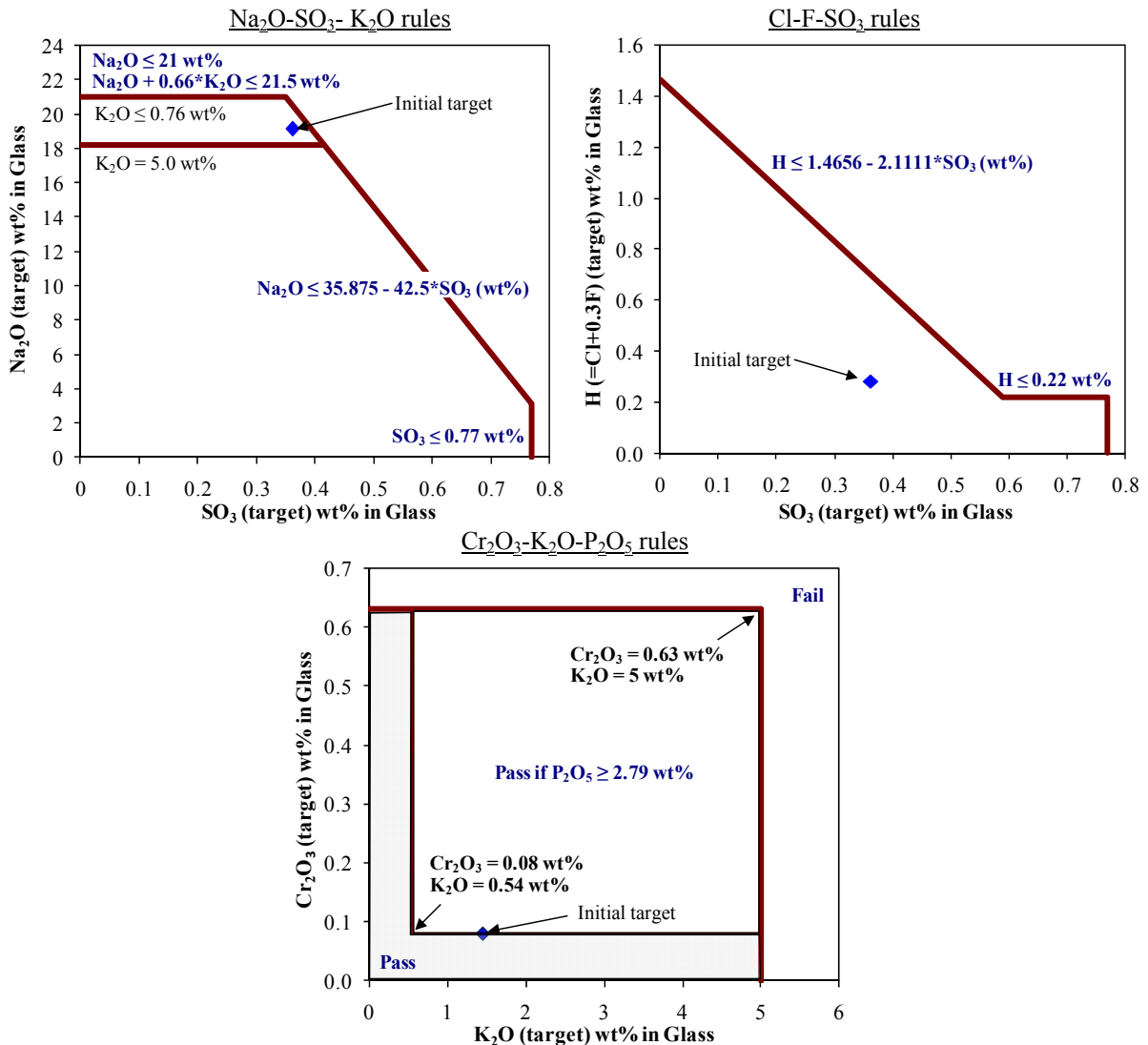
$$W_{A101}^{min,Cr} = \frac{\min \left\{ g_{Na_2O,A101}^{oxide\ in\ MFPV,pre-1}, g_{Na_2O,A101}^{oxide\ in\ MFPV,pre-2}, \frac{0.0008}{g_{Cr_2O_3,A11,1}^{oxide\ in\ CRV}} \right\}}{g_{Na_2O,A11,1}^{oxide\ in\ CRV}} \quad (150)$$

$$= \frac{\min \left\{ 0.1989, 0.2687, \frac{0.0008}{3.4310 \times 10^{-3}} \right\}}{8.2030 \times 10^{-1}} = 0.23317$$

$$\begin{aligned}
 g_{Na_2O, A101}^{oxide\ in\ MFPV, pre} &= \min \left\{ g_{Na_2O, A101}^{oxide\ in\ MFPV, pre-1}, g_{Na_2O, A101}^{oxide\ in\ MFPV, pre-2}, g_{Na_2O, A101}^{oxide\ in\ MFPV, pre-3} \right\} \\
 &= \min \{0.1989, 0.2687, 0.1913\} \\
 &= 0.1913
 \end{aligned}
 \tag{152}$$

Figure 11 shows the schematics of glass formulation rules showing the data point for the initial composition in three plots for Na₂O-SO₃-K₂O rules, Cl-F-SO₃ rules, and Cr₂O₃-K₂O-P₂O₅ rules. It can be seen from Figure 11 that the waste loading was limited by Cr₂O₃ concentration to meet the Cr₂O₃-K₂O-P₂O₅ rules.

Figure 11. Schematics of Glass Formulation Rules Showing the Initial Glass Composition for the A101th MFPV Batch [H (wt%) = Cl (wt%) + 0.3*F (wt%)]



The initial waste loading ($G_j^{wastein\ MFPV, initial}$) for the A101th MFPV batch is calculated using Equation (32):

$$G_{A101}^{wastein} = \frac{g_{Na_2O,A101}^{oxide\ in\ MFPV,\ pre}}{g_{Na_2O,A11,1}^{oxide\ in\ CRV}} = \frac{0.1913}{8.2030 \times 10^{-1}} = 0.23317 \quad (153)$$

Then the initial glass composition ($g_{i,A101}^{oxide\ in\ MFPV,\ initial}$) for the A101th MFPV batch is calculated following

Equations (33) through (45) for all 64 ($=n_j^{oxides\ in\ MFPV}$) glass oxide components. Example calculations are given below for Al₂O₃, Na₂O, CaO, Li₂O, MgO, Cr₂O₃ (an example for non-GFC component), and SiO₂:

$$g_{Al_2O_3,A101}^{oxide\ in\ MFPV,\ initial} = \max \left\{ 0.061, G_{A101}^{wastein} g_{Al_2O_3,A11,1}^{oxide\ in\ CRV} \right\} \quad (154)$$

$$= \max \left\{ 0.061, 0.23317 \times 7.0410 \times 10^{-2} \right\} = \max \{ 0.061, 0.0164 \} = 0.061$$

$$g_{Na_2O,A101}^{oxide\ in\ MFPV,\ initial} = \max \left\{ g_{Na_2O,A101}^{oxide\ in\ MFPV,\ pre}, 0.054 \right\} = \max \{ 0.1913, 0.054 \} = 0.1913 \quad (155)$$

$$d = g_{Na_2O,A101}^{oxide\ in\ MFPV,\ initial} + 0.66 G_{A101}^{wastein} g_{K_2O,A11,1}^{oxide\ in\ CRV} \quad (156)$$

$$= 0.1913 + 0.66 \times 0.23317 \times 6.2008 \times 10^{-2} = 0.2008$$

$$g_{CaO,A101}^{oxide\ in\ MFPV,\ initial} = 0.015 + \frac{0.055}{1 + \exp\left(\frac{d - 0.17}{0.02}\right)} = 0.015 + \frac{0.055}{1 + \exp\left(\frac{0.2008 - 0.17}{0.02}\right)} = 0.0247 \quad (157)$$

$$g_{Li_2O,A101}^{oxide\ in\ MFPV,\ initial} = 0.043 \left[1 - \frac{(100d - 5.4)^2}{12.75^2} \right]^{0.7} \quad (18) \quad (158)$$

$$= 0.043 \left[1 - \frac{(100 \times 0.2008 - 5.4)^2}{12.75^2} \right]^{0.7} = 0.043 [1 - 1.32566]^{0.7} = 0$$

$$g_{MgO,A101}^{oxide\ in\ MFPV,\ initial} = 0.0148 + \frac{0.0149}{1 + \exp(100d - 9)} \quad (159)$$

$$= 0.0148 + \frac{0.0149}{1 + \exp(100 \times 0.2008 - 9)} = 0.0148$$

$$g_{Cr_2O_3,A101}^{oxide\ in\ MFPV,\ initial} = G_{A101}^{wastein} g_{Cr_2O_3,A11,1}^{oxide\ in\ CRV} = 0.23317 \times 3.4310 \times 10^{-3} = 0.0008 \quad (160)$$

$\{i \neq Al_2O_3, B_2O_3, CaO, Fe_2O_3, Li_2O, MgO, Na_2O, SiO_2, TiO_2, ZnO, ZrO_2\}$

⁽¹⁸⁾ Imaginary result was set to zero.

$$g_{SiO_2,A101}^{oxide\ in\ MFPV,\ initial} = 1 - \sum_{i=1, i \neq SiO_2}^{oxide\ in\ MFPV} n_j g_{i,A101}^{oxide\ in\ MFPV,\ initial} = 1 - 0.5502 = 0.4498 \quad (161)$$

The resulting initial glass composition ($g_{i,A101}^{oxide\ in\ MFPV,\ initial}$) for all 64 glass oxide components given in the 2nd column of Table B-3 is set to the target composition following Equation (46):

$$g_{i,A101}^{oxide\ in\ MFPV,\ target} = g_{i,A101}^{oxide\ in\ MFPV,\ initial} \quad (162)$$

This target composition is used to calculate the GFC masses and Step 1 compositions (Section 6.1.4) and LAW transfer volume (Section 6.1.5). The resulting GFC masses and waste transfer volume are used to calculate the constraint quantities and compare them with the limits (Section 6.1.6).

6.1.4 Calculation of Step 1 Glass and Radionuclide Compositions

The target mass fractions for 11 GFC components are used to calculate the target mass fractions to be supplied from GFCs using Equation (47):

$$g_{i,A101}^{oxide\ in\ MFPV,\ target-gfc} = g_{i,A101}^{oxide\ in\ MFPV,\ target} - G_{A101}^{waste\ in\ MFPV,\ target} g_{i,A11,1}^{oxide\ in\ CRV} \quad (163)$$

$\{i = Al_2O_3, B_2O_3, CaO, Fe_2O_3, Li_2O, MgO, Na_2O, SiO_2, TiO_2, ZnO, ZrO_2\}$

The waste contribution ($G_{A101}^{waste\ in\ MFPV,\ target} g_{i,A11,1}^{oxide\ in\ CRV}$) values are in the 3rd column and the resulting $g_{i,A101}^{oxide\ in\ MFPV,\ target-gfc}$

values for 11 GFC components are in the 4th column of Table B-3. These $g_{i,A101}^{oxide\ in\ MFPV,\ target-gfc}$ values (t_{A101}) and

H (11×11 matrix of $m_{ik}^{oxide\ in\ GFC}$ given in Table A-6) are used to calculate the preliminary target mass of each

GFC per g glass ($\ddot{M}_{k,A101}^{GFC\ in\ MFPV,\ pre} = m_{A101}$) using Equation (48). The resulting values $\ddot{M}_{k,A101}^{GFC\ in\ MFPV,\ pre}$ are given in

Table 18. Then, the target mass of GFC per g glass is calculated using Equation (49) and also given in Table 18.

Table 18. Preliminary Target Mass ($\ddot{M}_{k,A101}^{GFC\ in\ MFPV,\ pre}$) and Target Mass ($\ddot{M}_{k,A101}^{GFC\ in\ MFPV,\ target}$) of Each GFC per g Glass for the A101th MFPV Batch

GFC (k)	$\ddot{M}_{k,A101}^{GFC\ in\ MFPV,\ pre}$	$\ddot{M}_{k,A101}^{GFC\ in\ MFPV,\ target}$
Kyanite	7.5092E-02	7.5092E-02
Boric Acid	1.7684E-01	1.7684E-01
Wollastonite	5.1734E-02	5.1734E-02
Hematite	5.3216E-02	5.3216E-02
Li carbonate	-4.3225E-18	0
Olivine	3.0508E-02	3.0508E-02
Na carbonate	-5.6791E-04	0

Silica	3.6491E-01	3.6491E-01
Rutile	1.4190E-02	1.4190E-02
Zincite	3.5051E-02	3.5051E-02
Zircon	4.5078E-02	4.5078E-02

Then the full composition of GFCs are used to calculate the glass composition from Step 1 calculation following Equation (50):

$$g_{i,A101}^{oxide\ in\ MFPV,\ Step1} = \frac{G_{A101}^{waste\ in\ MFPV,\ target} g_{i,A11,1}^{oxide\ in\ CRV} + \sum_{k=1}^{11} m_{ik}^{oxide\ in\ GFC} \ddot{M}_{k,A101}^{GFC\ in\ MFPV,\ target}}{\sum_{i=1}^{64} \left(G_{A101}^{waste\ in\ MFPV,\ target} g_{i,A11,1}^{oxide\ in\ CRV} + \sum_{k=1}^{11} m_{ik}^{oxide\ in\ GFC} \ddot{M}_{k,A101}^{GFC\ in\ MFPV,\ target} \right)} \quad (164)$$

Table B-4a shows the waste contribution ($G_{A101}^{waste\ in\ MFPV,\ target} g_{i,A11,1}^{oxide\ in\ CRV}$) (2nd column, the same as the 3rd column of Table B-3), the GFC contribution ($\sum_{k=1}^{11} m_{ik}^{oxide\ in\ GFC} \ddot{M}_{k,A101}^{GFC\ in\ MFPV,\ target}$) (3rd column), and the resulting $g_{i,A101}^{oxide\ in\ MFPV,\ Step1}$ values (4th column) for the A101th MFPV Batch. From Table B-4a the denominator of Equation (164) is given as:

$$\begin{aligned} & \sum_{i=1}^{64} \left(G_{A101}^{waste\ in\ MFPV,\ target} g_{i,A11,1}^{oxide\ in\ CRV} + \sum_{k=1}^{11} m_{ik}^{oxide\ in\ GFC} \ddot{M}_{k,A101}^{GFC\ in\ MFPV,\ target} \right) \\ &= \sum_{i=1}^{64} \left(G_{A101}^{waste\ in\ MFPV,\ target} g_{i,A11,1}^{oxide\ in\ CRV} \right) + \sum_{i=1}^{64} \left(\sum_{k=1}^{11} m_{ik}^{oxide\ in\ GFC} \ddot{M}_{k,A101}^{GFC\ in\ MFPV,\ target} \right) = 0.233165 + 0.767826 = 1.000991 \end{aligned} \quad (165)$$

Then, the resulting waste loading in glass of the A101th MFPV Batch after including the GFC impurities is calculated from Equation (51):

$$G_{A101}^{oxide\ in\ MFPV,\ Step1} = \frac{\sum_{i=1}^{64} G_{A101}^{waste\ in\ MFPV,\ target} g_{i,A11,1}^{oxide\ in\ CRV}}{\sum_{i=1}^{64} \left(G_{A101}^{waste\ in\ MFPV,\ target} g_{i,A11,1}^{oxide\ in\ CRV} + \sum_{k=1}^{11} m_{ik}^{oxide\ in\ GFC} \ddot{M}_{k,A101}^{GFC\ in\ MFPV,\ target} \right)} = \frac{0.233165}{1.000991} = 0.23293 \quad (166)$$

The final composition after applying retention factors is calculated using Equation (52):

$$\tilde{g}_{i,A101}^{oxide\ in\ MFPV,\ Step1} = \frac{g_{i,A101}^{oxide\ in\ MFPV,\ Step1} v_i}{\sum_{i=1}^{64} g_{i,A101}^{oxide\ in\ MFPV,\ Step1} v_i} \quad (167)$$

Table B-4a also includes the $g_{i,A101}^{oxide\ in\ MFPV,Step1} v_i$ values (5th column) and the $\tilde{g}_{i,A101}^{oxide\ in\ MFPV,Step1}$ results (6th column) using

$$\sum_{i=1}^{64} g_{i,A101}^{oxide\ in\ MFPV,Step1} v_i = 0.99410.$$

The specific activity (activity per unit mass of glass oxides) of radionuclides in the A101th MFPV batch before applying retention factors ($a_{i,A101}^{rad\ in\ MFPV,Step1}$) is calculated using Equation (53):

$$\begin{aligned} a_{i,A101}^{rad\ in\ MFPV,Step1} &= a_{i,A11,1}^{rad\ in\ CRV} G_{A101}^{waste\ in\ MFPV,Step1} \\ &= \frac{\bar{R}_{i,A11}^{rad\ in\ CRV} \lambda_{A11,1} G_{A101}^{waste\ in\ MFPV,Step1}}{C_{A11,1}^{oxides\ in\ CRV}} = \frac{\bar{R}_{i,A11}^{rad\ in\ CRV} (mCi/L) \times 0.99854 \times 0.23293}{260.58(g/L)} \quad (mCi/g) \end{aligned} \quad (168)$$

The specific activity after applying retention factors ($\tilde{a}_{i,A101}^{oxide\ in\ MFPV,Step1}$) is calculated using Equation (54):

$$\tilde{a}_{i,A101}^{rad\ in\ MFPV,Step1} = \frac{a_{i,A101}^{rad\ in\ MFPV,Step1} v_i}{\sum_{i=1}^{64} g_{i,A101}^{oxide\ in\ MFPV,Step1} v_i} = \frac{a_{i,A101}^{rad\ in\ MFPV,Step1} v_i}{0.99410} \quad (169)$$

The results of $a_{i,A101}^{rad\ in\ MFPV,Step1}$ (2nd column) and $\tilde{a}_{i,A101}^{oxide\ in\ MFPV,Step1}$ (3rd column) are given in Table B-5a. Table B-5a also includes the SD values for specific activities of radionuclides in glass ($\tilde{s}_{ii,A101}^{rad\ in\ MFPV,Step1}$) for algorithm calculation Step 1 after applying retention factors obtained from Monte Carlo simulations of Equation (70).

6.1.5 Calculation of LAW Transfer Volume

The volumes involved in Equation (55) for the A101th MFPV batch is given below. From Table 1 the target working volume is:

$$V_{A101}^{working\ MFPV} = 19,426\ L \quad (170)$$

As mentioned earlier, the A101th MFPV batch, the volume of heel was assumed as 6,712 L, i.e.,

$$V_{A101}^{heel\ MFPV} = 6,712\ L \quad (171)$$

From Table 14, for the LFP-VSL-00001 (MFPV-A) from LCP-VSL-00001 (CRV-A), the CRV-MFPV line flush and sampling flush volumes are given as:

$$V_{A101}^{transflush\ MFPV} = 37.5\ L \quad (172)$$

$$V_{A101}^{samplerush, MFPV} = 175.3 \text{ L} \quad (173)$$

During plant operation the actual measured volume of these flush waters will be used. For the example calculation in this report, the nominal values are used instead of random generation similar to CRV working and MFPV heel volumes for simplicity.

The rest of volumes are calculated based on the glass formulation described in Section 6.1.3. The volume occupied by GFCs is expressed as function of waste transfer volume using Equation (56):

$$\begin{aligned} V_{A101}^{GFC, MFPV, Step1} &= V_{A11,1}^{transwaste, CRV} \sum_{k=1}^{GFCs \text{ in } n_{A101}^{MFPV}} \frac{C_{A11,1}^{oxide \text{ in } CRV} \ddot{M}_{k,A101}^{GFC \text{ in } MFPV, target}}{G_{A101}^{waste \text{ in } MFPV, target} \rho_k} \\ &= V_{A11,1}^{transwaste, CRV} \sum_{k=1}^{11} \frac{260.58(\text{g/L}) \times \ddot{M}_{k,A101}^{GFC \text{ in } MFPV, target} (\text{g/g glass})}{0.23317(\text{g/g glass}) \times \rho_k (\text{g/L})} \\ &= 0.37472 V_{A11,1}^{transwaste, CRV} \end{aligned} \quad (174)$$

The $\ddot{M}_{k,A101}^{GFC \text{ in } MFPV, target}$ values are given in the third column of Table 18 and ρ_k values are in Table A-12.

The dust control water volume is calculated using Equation (58):

$$\begin{aligned} V_{A101}^{dust, MFPV, Step1} &= V_{A11,1}^{transwaste, CRV} \frac{0.04}{1000(\text{g/L})} \sum_{k=1}^{GFCs \text{ in } n_{A101}^{MFPV}} \frac{C_{A11,1}^{oxides \text{ in } CRV} \ddot{M}_{k,A101}^{GFC \text{ in } MFPV, target}}{G_{A101}^{waste \text{ in } MFPV, target}} \\ &= V_{A11,1}^{transwaste, CRV} \frac{0.04}{1000(\text{g/L})} \sum_{k=1}^{11} \frac{260.58(\text{g/L}) \times \ddot{M}_{k,A101}^{GFC \text{ in } MFPV, target} (\text{g/g glass})}{0.23317(\text{g/g glass})} \\ &= V_{A11,1}^{transwaste, CRV} \frac{0.04 \times 946.165}{1000(\text{g/L})} \\ &= 0.037847 V_{A11,1}^{transwaste, CRV} \end{aligned} \quad (175)$$

The target mass of sucrose is calculated using Equation (59):

$$\begin{aligned} \ddot{M}_{A101}^{sucrose \text{ in } MFPV, target} &= \max \left\{ \left[0.75 \left(\frac{c_{NO_2, A11,1}^{element \text{ in } CRV}}{MW_{NO_2}} + \frac{c_{NO_3, A11,1}^{element \text{ in } CRV}}{MW_{NO_3}} \right) - \frac{c_{TOC, A11,1}^{element \text{ in } CRV}}{MW_C} \right] \frac{MW_{C_{12}H_{22}O_{11}}}{12(\text{moles of C/sucrose})}, 0 \right\} \\ &= \max \left\{ \left[0.75 \left(\frac{27.981}{46.0055} + \frac{73.780}{62.0049} \right) - \frac{1.1356(\text{g/L})}{12.0110(\text{g/mole})} \right] \frac{342.3001(\text{g/mole})}{12(\text{moles of C/sucrose})}, 0 \right\} \\ &= \max \{ 35.7714, 0 \} = 35.7714 \text{ (g/L waste)} \end{aligned} \quad (176)$$

Then the volume of sucrose is calculated using Equation (60):

$$V_{A101}^{sucrose, MFPV, Step1} = \frac{V_{A11,1}^{transwaste, CRV} \cdot \dot{M}_{A101}^{sucrose, in, MFPV, target}}{\rho_{sucrose}} = V_{A11,1}^{transwaste, CRV} \frac{35.7714(\text{g/L waste})}{1549.0(\text{g/L})} = 0.023093 V_{A11,1}^{transwaste, CRV} \quad (177)$$

For the required volume of dilution water calculation, the target sodium molarity is first calculated using Equation (61):

$$t_{[Na], A101} = \frac{g_{Na_2O, A101}^{oxide, in, MFPV, target} + 0.0047}{0.0249} = \frac{0.1913 + 0.0047}{0.0249} = 7.870 \text{ M} \quad (178)$$

Then, dilution water volume is calculated from Equation (62):

$$\begin{aligned} V_{A101}^{dilute, MFPV, Step1} &= \max \left\{ \frac{c_{Na, A11,1}^{element, in, transwaste, CRV} V_{A11,1}^{CRV}}{1000 MW_{Na} t_{[Na], A101}} - \left(V_{A11,1}^{transwaste, CRV} + V_{A101}^{transflush, MFPV} + V_{A101}^{samplerush, MFPV} + V_{A101}^{dust, MFPV, Step1} \right), 0 \right\} \\ &= \max \left\{ \frac{158576.4(\text{mg/L}) \times V_{A11,1}^{transwaste, CRV}}{1000(\text{mg/g}) \times 22.9898(\text{g/mole}) \times 7.870(\text{moles/L})} - \left(V_{A11,1}^{transwaste, CRV} + 37.5 + 175.3 + \frac{0.04}{1000(\text{g/L})} \sum_{k=1}^{11} \frac{258.45(\text{g/L}) \times \dot{M}_{k, A101}^{GFC, in, MFPV, target} (\text{g/g glass})}{0.23126(\text{g/g glass})} \right), 0 \right\} \\ &= \max \left\{ 0.87644 V_{A11,1}^{transwaste, CRV} - \left(V_{A11,1}^{transwaste, CRV} + 37.5 + 175.3 + 0.037847 V_{A11,1}^{transwaste, CRV} \right), 0 \right\} \\ &= \max \left\{ -0.161404 V_{A11,1}^{transwaste, CRV} - 212.7, 0 \right\} \end{aligned} \quad (179)$$

Equations (170) through (179) provide the volume values or express them in terms of the waste transfer volume ($V_{dm}^{transwaste, CRV}$) for all the volumes involved in Equation (55) for the A101th MFPV batch. Then, Equation (55) is written as:

$$\begin{aligned}
 V_{A101}^{working\ MFPV} &= 19426 \text{ (L)} \\
 &= V_{A11,1}^{transwaste\ CRV} + V_{A101}^{GFC\ MFPV, Step1} + V_{A101}^{dust\ MFPV, Step1} + V_{A101}^{sucrose\ MFPV, Step1} + V_{A101}^{heel\ MFPV} \\
 &\quad + V_{A101}^{transflush\ MFPV} + V_{A101}^{sampflush\ MFPV} + V_{A101}^{dilute\ MFPV, Step1} \\
 &= V_{A11,1}^{transwaste\ CRV} + 0.37472V_{A11,1}^{transwaste\ CRV} + 0.037847V_{A11,1}^{transwaste\ CRV} + 0.023093V_{A11,1}^{transwaste\ CRV} + 6712.0 \\
 &\quad + 37.5 + 175.3 + \max \left\{ -0.161404V_{A11,1}^{transwaste\ CRV} - 212.7, 0 \right\}
 \end{aligned} \tag{180}$$

Equation (180) was solved iteratively to obtain the waste transfer volume ($V_{dm}^{transwaste\ CRV}$) of 8707.7 L. This result of $V_{dm}^{transwaste\ CRV}$ is used to calculate the volumes that were expressed in terms of $V_{dm}^{transwaste\ CRV}$, then Equation (180) is rewritten as:

$$19426 \text{ (L)} = 8707.7 + 3262.9 + 329.6 + 201.1 + 6712.0 + 37.5 + 175.3 + 0.0 \text{ (L)} \tag{181}$$

This $V_{dm}^{transwaste\ CRV}$ value is used for calculation of composition uncertainties required for the calculation of Step 1 constraints in Section 6.1.6.

From the waste transfer volume, the target masses of GFCs and sucrose are calculated using Equations (63) and (64):

$$\begin{aligned}
 M_{k,A101}^{GFC\ in\ MFPV, target, Step1} &= \frac{C_{A11,1}^{oxides\ in\ CRV} \cdot \ddot{M}_{k,A101}^{GFC\ in\ MFPV, target} \cdot V_{A11,1}^{transwaste\ CRV}}{G_{A101}^{waste\ in\ MFPV, target}} \\
 &= \frac{260.58(\text{g/L}) \times \ddot{M}_{k,A101}^{GFC\ in\ MFPV, target} (\text{g/g glass}) \times 8707.7(\text{L})}{0.23317}
 \end{aligned} \tag{182}$$

$$M_{A101}^{sucrose\ in\ MFPV, target, Step1} = \ddot{M}_{A101}^{sucrose\ in\ MFPV, target} V_{A11,1}^{transwaste\ CRV} = 35.77(\text{g/L waste}) \times 8707.7(\text{L}) = 311.49 \text{ (kg)} \tag{183}$$

Table 19 summarizes the resulting masses of GFCs and sucrose from Step 1 calculation for the A101th MFPV Batch.

Table 19. Masses of GFCs and Sucrose from Step 1 Calculation for the A101th MFPV Batch

GFC (k)/sucrose	$M_{k,A101}^{GFC\ in\ MFPV, target, Step1}$, kg
Kyanite	730.77
Boric Acid	1720.90
Wollastonite	503.45
Hematite	517.88

Lithium carbonate	0
Olivine	296.89
Sodium carbonate	0
Silica	3551.14
Rutile	138.09
Zincite	341.10
Zircon	438.69
Sucrose	311.49
Total	8550.39

6.1.6 Calculation of Constraints for Algorithm Step 1

Example calculations for each constraint or each group of constraints are provided in the following subsections.

6.1.6.1 Glass Property and Model Validity Constraints

The glass composition applying retention factors ($\tilde{g}_{i,A101}^{oxideinMFPV,Step1}$) calculated based on Equation (167) and given in the last column of Table B-4a is used for calculation of glass property and model validity constraints. Predicted glass properties including PCT normalized B and Na releases, VHT alteration depth, melt viscosity, and melt electrical conductivity are calculated using the composition-property models described in Section 4.1. The equations required for calculating prediction and composition uncertainties and CL% combined confidence intervals for predicted properties are given in Sections 4.2.1 through 4.2.3. Calculations for PCT normalized B release are provided below as an example. Calculations for all other properties follow the same methods.

Equation (2) and the model coefficients (p_h^{pctB}) given in Table 5 are used to calculate the predicted PCT response of the glass as demonstrated in Table 20 for PCT normalized B release.

Table 20. Example Calculation for Predicted PCT Normalized B Release, $P_{A101}^{pctB,Step1}$ in ln[g/L]

Model Term = <i>h</i>	p_h^{pctB}	$x_{h,A101}^{pctB,Step1}$	$P_h^{pctB} x_{h,A101}^{pctB,Step1}$
Al ₂ O ₃	-31.3612	6.1232E-02	-1.9203E+00
B ₂ O ₃	11.8101	9.9457E-02	1.1746E+00
CaO	-13.8404	2.4801E-02	-3.4326E-01
Fe ₂ O ₃	-16.5948	5.5187E-02	-9.1583E-01
K ₂ O	7.9687	1.4030E-02	1.1180E-01
Li ₂ O	83.3036	3.0512E-07	2.5418E-05
MgO	-21.2343	1.4871E-02	-3.1577E-01
Na ₂ O	46.1599	1.9088E-01	8.8110E+00
P ₂ O ₅	-19.254	1.9766E-03	-3.8057E-02
SiO ₂	-1.6161	4.5172E-01	-7.3002E-01
ZrO ₂	-6.6289	3.0143E-02	-1.9981E-01
Others	-5.169	5.5705E-02	-2.8794E-01
CaO×Li ₂ O	-251.2654	7.5675E-09	-1.9014E-06
B ₂ O ₃ ×MgO	488.8612	1.4790E-03	7.2303E-01
B ₂ O ₃ ×Li ₂ O	-374.9533	3.0346E-08	-1.1379E-05

Na ₂ O×SiO ₂	-74.3462	8.6223E-02	-6.4104E+00
CaO×Fe ₂ O ₃	212.0947	1.3687E-03	2.9030E-01
Sum	N/A	N/A	-0.0507

N/A: not applicable

The prediction uncertainty corresponding to a 90% SUCI for PCT normalized B release is calculated following Equation (8):

$$U_{pred,A101}^{pctB,Step1} = \sqrt{n_{pctB}^{model} F_{1-\alpha,(n_{pctB}^{model}, n_{pctB}^{data}, n_{pctB}^{model})} \left(\mathbf{x}_{A101}^{pctB,Step1} \right)^T \Sigma^{pctB} \mathbf{x}_{A101}^{pctB,Step1}} \quad (184)$$

$$= \sqrt{17 \times 1.28991 \times 0.0012984} = 0.1687 \text{ ln(g/L)}$$

As described in Section 4.2.2, composition uncertainties are estimated using Monte Carlo simulation of mass balance equations given by Equations (65) and (66) for the A101th MFPV batch:

$$g_{i,A101}^{oxide in MFPV,Step1} = \frac{\frac{element\ in\ CRV}{c_{i,A11,1}^{CRV}} \frac{tarnswaste}{f_i V_{A11,1}^{CRV}} + \sum_{k=1}^{11} \frac{oxide\ in\ GFC}{m_{ik}^{GFC}} M_{k,A101}^{MFPV,target,Step1}}{\sum_{i=1}^{64} \frac{element\ in\ CRV}{c_{i,A11,1}^{CRV}} \frac{tarnswaste}{f_i V_{A11,1}^{CRV}} + \sum_{i=1}^{64} \sum_{k=1}^{11} \frac{oxide\ in\ GFC}{m_{ik}^{GFC}} M_{k,A101}^{MFPV,target,Step1}} \cdot 1000(\text{mg/g}) \quad (185)$$

$$\tilde{g}_{i,A101}^{oxide in MFPV,Step1} = \frac{g_{i,A101}^{oxide in MFPV,Step1} v_i}{\sum_{i=1}^{64} g_{i,A101}^{oxide in MFPV,Step1} v_i} \quad (186)$$

In this method, the uncertain variables in the mass balance equations are given random values (5000 “simulations” for this example) that conform to a certain statistical distribution as summarized here:

- volume of waste to be transferred from CRV to MFPV (normal distribution based on nominal value of 8707.7 L from Section 6.1.5 and SD of 447.2 L from Appendix D)
- concentration of each element in the CRV (normal distribution based on nominal values in Table B-1 and SD values calculated by Equation (14) using RSD values given in Table A-2)
- mass of each GFC to be added to the MFPV (normal distribution based on nominal values given in Table 19 and SD values calculated following the methods described in Appendix E)
- concentration of each oxide in each GFC (PERT distribution based on minimum, most likely, and maximum values given in Table A-4)
- retention factor of each component (calculated from PERT distribution of ln(DF) based on Min, Median, and Max ln(DF) values in Table A-3)

Figure 12 shows an example distribution for 5000 random values of $V_{A11,1}^{transwaste,CRV}$ based on a nominal volume of 8707.7 L and SD of 447.2 L. Likewise four other uncertain variables listed above are given 5000 random values from associated statistical distributions. The result is 5000 glass compositions, which are used to

calculate 5000 predicted values for all properties. An example distribution of 5000 PCT normalized B release values ($P_{A101}^{pctB, Step1}$ in $\ln[g/L]$) is given in Figure 13.

Figure 12. Example Histogram of 5000 Random $V_{A11,1}^{transwaste, CRV}$ Values (L) for Monte Carlo Simulation

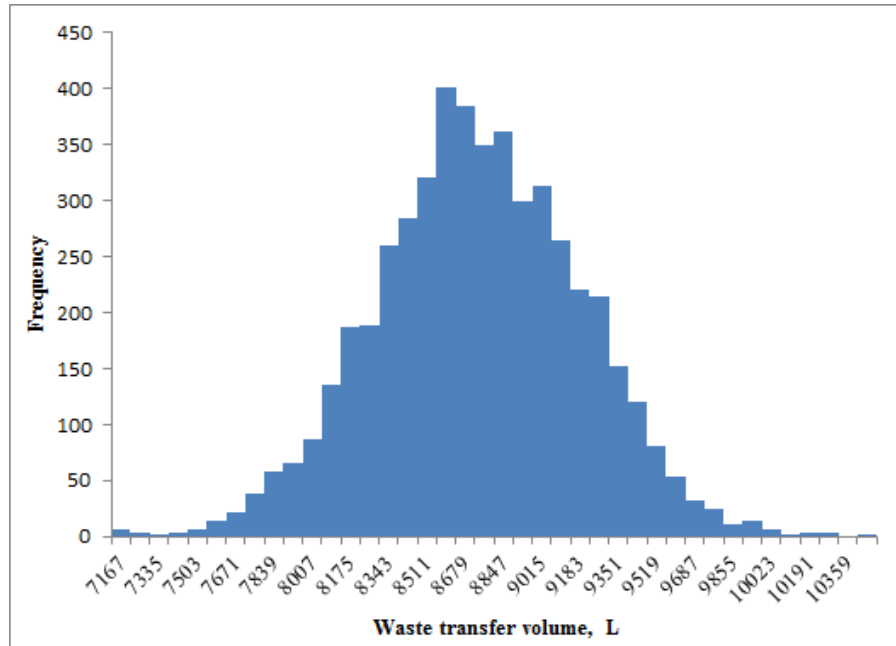
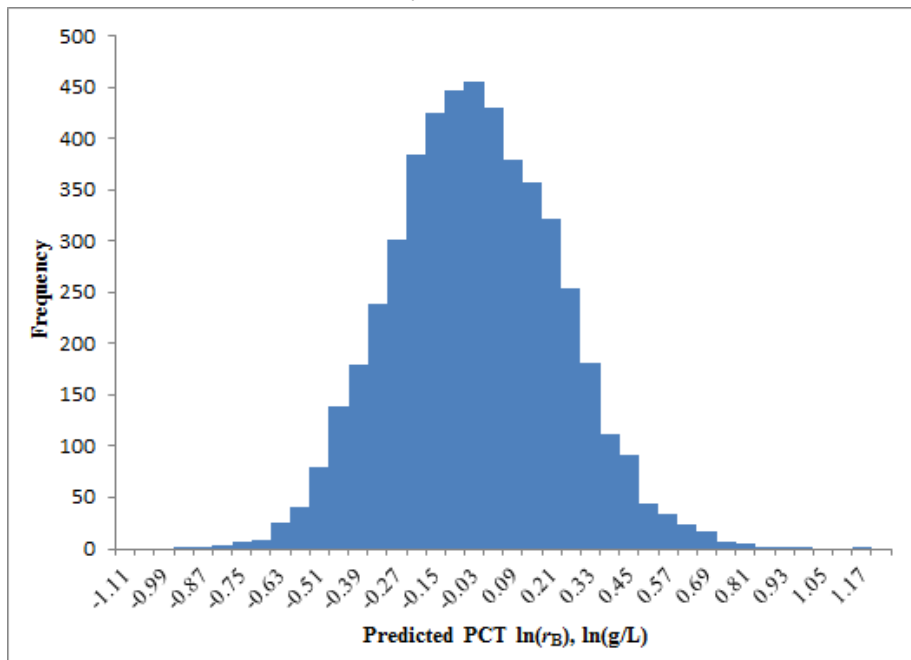


Figure 13. Histogram of 5000 Predicted $P_{A101}^{pctB, Step1}$ Values ($\ln[g/L]$) from Monte Carlo Simulation



The composition uncertainty of the PCT normalized B release for the A101th MFPV batch is calculated using Equation (15):

$$U_{comp,A101}^{pctB,Step1} = Q_{90\%,A101}^{pctB,Step1} - Q_{50\%,A101}^{pctB,Step1} = 0.2749 - (-0.0607) = 0.3356 \quad (187)$$

Then, the UCCI of the PCT normalized B release for the A101th MFPV batch is calculated using Equation (16):

$$\begin{aligned} B_{ucci,A101}^{pctB,Step1} &= P_{A101}^{pctB,Step1} + U_{pred,A101}^{pctB,Step1} + U_{comp,A101}^{pctB,Step1} \\ &= -0.0507 + 0.1687 + 0.3356 \\ &= 0.4536 \end{aligned} \quad (188)$$

Table 21 summarizes the predicted properties, uncertainties, and UCCI/LCCI values for the A101th MFPV batch compared with the corresponding limits. As shown in Table 21, all constraints were satisfied except for the upper limit for viscosity at 1150°C ($L_u^{vis1150} = 4.3820 \ln[g/L]$). The failure to meet the upper limit for viscosity at 1150°C requires that the glass formulation needs to be adjusted, which will be done in Section 6.1.7.

Table 21. Predicted Properties, Uncertainties, and UCCI/LCCI Values for the A101th MFPV Batch Compared with the Corresponding Limits

Property	Unit	$P_{A101}^{prop,Step1}$	$U_{pred,A101}^{prop,Step1}$	$U_{comp,A101}^{prop,Step1}$	$B_{ucci,A101}^{prop,Step1}$ or $B_{lcci,A101}^{prop,Step1}$	L_u^{prop} or L_l^{prop}
$\ln(r_B)$	ln[g/L]	-0.0507	0.1687	0.3356	0.4536	< 1.3863
$\ln(r_{Na})$	ln[g/L]	-0.1406	0.1759	0.2868	0.3221	< 1.3863
$\ln(D)$	ln[μm]	2.2926	0.7076	1.2235	4.2237	< 6.1159
$\ln(\eta_{1100}), u$	ln[P]	4.7126	0.0361	0.2552	5.0039	≤ 5.0106
$\ln(\eta_{1150}), l$	ln[P]	4.2092	0.0363	0.2301	3.9428	≥ 2.9957
$\ln(\eta_{1150}), u$	ln[P]	4.2092	0.0363	0.2355	4.4811	≤ 4.3820
$\ln(\epsilon_{1100}), l$	ln[S/cm]	-1.0720	0.0346	0.1822	-1.2888	≥ -2.3026
$\ln(\epsilon_{1200}), u$	ln[S/cm]	-0.7157	0.0352	0.1621	-0.5184	≤ -0.3567

Shaded row represents the property that does not meet the limit

Table 22 summarizes the model validity constraint values for the A101th MFPV batch compared with the corresponding limits. As shown in Table 22, all model validity constraints were satisfied.

Table 22. Model Validity Constraints for the A101th MFPV Batch Compared with the Corresponding Limits

Constraint	Value	Lower Limit	Upper Limit
Model validity single component constraints ($\tilde{g}_{i,A101}^{oxideinMFPV,Step1}$)			
Al ₂ O ₃	0.06123	0.035	0.0900
Cl	0.00136	0	0.0091
Cr ₂ O ₃	0.00086	0	0.0059
F	0.00076	0	0.0035
P ₂ O ₅	0.00198	0	0.030
SiO ₂	0.45172	0.384	0.521

Constraint	Value	Lower Limit	Upper Limit
Sum of Minors	0.00051	0	0.0028
Model validity PCT constraints			
$P_{A101}^{pctB, Step1}$ (ln[g/L])	-0.0507	NA	0.9933
$P_{A101}^{pctNa, Step1}$ (ln[g/L])	-0.1406	NA	0.9933
Model validity multiple component constraints (based on $\tilde{g}_{i,A101}^{oxide\ in\ MFPV, Step1}$, lower and upper limits are a function of concentration of other component)			
Li ₂ O function of Na ₂ O	0.00000	-0.05336	0.02851
Cr ₂ O ₃ function of P ₂ O ₅	0.00086	-0.00138	0.00234
Na ₂ O function of CaO	0.19088	0.08878	0.28178
Li ₂ O function of CaO	0.00000	0.00000	0.03952
Na ₂ O function of SO ₃	0.19088	0.03647	0.25787
Li ₂ O function of SO ₃	0.00000	-0.02079	0.05081
Na ₂ O function of SiO ₂	0.19088	0.00220	0.20480

NA: not applicable

6.1.6.2 Waste Na₂O Loading Constraint

The waste Na₂O loading in the A101th MFPV batch from algorithm calculation Step 1 is calculated using Equation (68):

$$\begin{aligned}
 \tilde{g}_{Na_2O(w), A101}^{oxide\ in\ MFPV, Step1} &= \frac{\tilde{g}_{Na_2O, A11, 1}^{oxide\ in\ CRV} G_{A101}^{waste\ in\ MFPV, target} \omega_{A11} v_i}{\sum_{i=1}^{64} \left[\tilde{g}_{i, A11, 1}^{oxide\ in\ CRV} G_{A101}^{waste\ in\ MFPV, target} v_i + \left(\sum_{k=1}^{11} m_{ik}^{oxide\ in\ GFC} \ddot{M}_{kj}^{GFC\ in\ MFPV, target} \right) v_i \right]} \\
 &= \frac{0.82030 \times 0.23317 \times 0.95 \times 0.99136}{\sum_{i=1}^{64} \left[\tilde{g}_{i, A11, 1}^{oxide\ in\ CRV} 0.23317 v_i \right] + \sum_{i=1}^{64} \left[\left(\sum_{k=1}^{11} m_{ik}^{oxide\ in\ GFC} \ddot{M}_{kj}^{GFC\ in\ MFPV, target} \right) v_i \right]} \\
 &= \frac{0.18013}{0.22893 + 0.76616} = 0.18102
 \end{aligned} \tag{189}$$

For this example calculation, it was assumed that the A11th CRV waste was designated as Envelope A with $\omega_{A11} = 0.95$ (where ω_{A11} is the fraction of the sodium in the A11th CRV batch that is classified as waste

sodium). The Envelope A constraint $\tilde{g}_{Na_2O(w), A101}^{oxide\ in\ MFPV, Step1} \geq L_l^{W_{Na}} = 0.14$ was met.

6.1.6.3 Radionuclide Concentration Constraints

The specific activities of radionuclides in glass after applying retention factors ($\tilde{a}_{i, A101}^{rad\ in\ MFPV, Step1}$) required to calculate the constraints pertinent to radionuclide concentrations were given in the 3rd column of Table B-5a from Section 6.1.4. The SD values for specific activities of radionuclides in glass ($\tilde{s}_{ii, A101}^{rad\ in\ MFPV, Step1}$) for algorithm

calculation Step 1 after applying retention factors were obtained by Monte Carlo simulations of Equation (70) and given in the 4th column of Table B-5a. These values are used to calculate the constraints for ¹³⁷Cs and ⁹⁰Sr according to Equations (73) and (74) as below:

$$\begin{aligned} & \hat{a}_{137Cs,A101}^{rad\ in\ MFPV,Step1} + k^{rad} \hat{S}_{137Cs,A101}^{rad\ in\ MFPV,Step1} \\ &= \tilde{a}_{137Cs,A101}^{rad\ in\ MFPV,Step1} \rho_{A101}^{glass\ in\ MFPV} + k^{rad} \tilde{S}_{137Cs,A101}^{rad\ in\ MFPV,Step1} \rho_{A101}^{glass\ in\ MFPV} \\ &= 4.48192E-05(\text{mCi/g}) \times 2730(\text{g/L}) + 2 \times 5.15875E-06(\text{mCi/g}) \times 2730(\text{g/L}) \\ &= 0.1505(\text{Ci/m}^3) < 0.3 \text{ Ci/m}^3 \end{aligned} \tag{190}$$

$$\begin{aligned} & \hat{a}_{90Sr,A101}^{rad\ in\ MFPV,Step1} + k^{rad} \hat{S}_{90Sr,A101}^{rad\ in\ MFPV,Step1} \\ &= \tilde{a}_{90Sr,A101}^{rad\ in\ MFPV,Step1} \rho_{A101}^{glass\ in\ MFPV} + k^{rad} \tilde{S}_{90Sr,A101}^{rad\ in\ MFPV,Step1} \rho_{A101}^{glass\ in\ MFPV} \\ &= 5.57167E-04(\text{mCi/g}) \times 2730(\text{g/L}) + 2 \times 2.87069E-05(\text{mCi/g}) \times 2730(\text{g/L}) \\ &= 1.6778(\text{Ci/m}^3) < 20 \text{ Ci/m}^3 \end{aligned} \tag{191}$$

where k^{rad} is the expansion factor for radionuclide concentration specification.

Table 23. Calculation of Sum of Fractions for Long Lived Radionuclides Class C Limits in the A101th MFPV batch

Radio-nuclide (i)	$L_u^{\hat{a}_i}$, Ci/m ³	$L_u^{a_i}$, nCi/g	$\hat{a}_{i,A101}^{rad\ in\ MFPV,Step1}$, Ci/m ³	$\tilde{a}_{i,A101}^{rad\ in\ MFPV,Step1}$, nCi/g	$\frac{\hat{a}_{i,A101}^{rad\ in\ MFPV,Step1}}{L_u^{\hat{a}_i}}$ or $\frac{\tilde{a}_{i,A101}^{rad\ in\ MFPV,Step1}}{L_u^{a_i}}$
⁹⁹ Tc	3		0.06123		0.02041
¹²⁹ I	0.08		1.487E-04		0.00186
TRU ^(a)		100		1.2026	0.01203
²⁴¹ Pu		3,500		1.2257	3.502E-04
²⁴² Cm		20,000		0.00271	1.354E-07
$SF_{LL,A101}^{rad\ in\ MFPV,Step1}$					0.03465

(a) Alpha emitting transuranic nuclides with half-life greater than 5 years for Hanford LAW (24590-WTP-PL-RT-03-001) = ²³⁷Np, ²³⁸Pu, ²³⁹Pu, ²⁴⁰Pu, ²⁴¹Am, ²⁴²Pu, ²⁴³Am, ²⁴³Cm, and ²⁴⁴Cm. These are quantified by total alpha measurement.

Table 24. Calculation of SD for Sum of Fractions for Long Lived Radionuclides Class C Limits in the A101th MFPV batch

Radio-nuclide (i)	$L_u^{\hat{a}_i}$, Ci/m ³	$L_u^{a_i}$, nCi/g	$\hat{S}_{i,A101}^{rad\ in\ MFPV,Step1}$, Ci/m ³	$\tilde{S}_{i,A101}^{rad\ in\ MFPV,Step1}$, nCi/g	$\frac{\hat{S}_{i,A101}^{rad\ in\ MFPV,Step1}}{L_u^{\hat{a}_i}}$ or $\frac{\tilde{S}_{i,A101}^{rad\ in\ MFPV,Step1}}{L_u^{a_i}}$
⁹⁹ Tc	3		0.02136		0.00712
¹²⁹ I	0.08		5.299E-05		0.00066
TRU ^(a)		100		0.0472	0.00047
²⁴¹ Pu		3,500		0.1157	3.356E-05

²⁴² Cm		20,000		0.000196	9.813E-09
$S_{LL,A101}^{radSF in MFPV, Step1}$					0.00717

(a) Alpha emitting transuranic nuclides with half-life greater than 5 years for Hanford LAW (24590-WTP-PL-RT-03-001) = ²³⁷Np, ²³⁸Pu, ²³⁹Pu, ²⁴⁰Pu, ²⁴¹Am, ²⁴²Pu, ²⁴³Am, ²⁴³Cm, and ²⁴⁴Cm. These are quantified by total alpha measurement.

Table 25. Calculation of Sum of Fractions for Short Lived Radionuclides Class C Limits in the A101th MFPV batch

Radionuclide (j)	$L_u^{\hat{a}_i}, \text{Ci/m}^3$	$\hat{\alpha}_{i,A101}^{rad in MFPV, Step1}, \text{Ci/m}^3$	$\frac{\hat{\alpha}_{i,A101}^{rad in MFPV, Step1}}{L_u^{\hat{a}_i}}$
⁶³ Ni	700	0.08494	1.213E-04
⁹⁰ Sr	7,000	1.52106	2.173E-04
¹³⁷ Cs	4,600	0.12236	2.660E-05
$S_{SL,A101}^{rad in MFPV, Step1}$			3.652E-04

Table 26. Calculation of SD for Sum of Fractions for Short Lived Radionuclides Class C Limits in the A101th MFPV batch

Radionuclide (j)	$L_u^{\hat{a}_i}, \text{Ci/m}^3$	$\hat{S}_{i,A101}^{rad in MFPV, Step1}, \text{Ci/m}^3$	$\frac{\hat{S}_{i,A101}^{rad in MFPV, Step1}}{L_u^{\hat{a}_i}}$
⁶³ Ni	700	0.00604	8.624E-06
⁹⁰ Sr	7,000	0.07837	1.120E-05
¹³⁷ Cs	4,600	0.01408	3.062E-06
$S_{SL,A101}^{radSF in MFPV, Step1}$			1.446E-05

The Class C limit is satisfied as long as the two conditions by Equations (79) and (80) are satisfied:

$$SF_{LL,A101}^{rad in MFPV, Step1} + k^{rad} S_{LL,A101}^{radSF in MFPV, Step1} = 0.03465 + 2 \times 0.00717 = 0.04898 < 1 \tag{192}$$

$$SF_{SL,A101}^{rad in MFPV, Step1} + k^{rad} S_{SL,A101}^{radSF in MFPV, Step1} = 3.654E-04 + 2 \times 1.446E-05 = 3.942E-04 < 1 \tag{193}$$

6.1.6.4 Surface Dose Rate Constraint

The surface dose rate calculation is not performed by ILAW formulation algorithm.

6.1.7 Adjustment of Target Glass Composition

The initial target formulation for the example A101th MFPV Batch failed the upper limit for viscosity at 1150°C as discussed in Section 6.1.6, which requires an increase of Li₂O target concentration according to

the approach described in Section 5.1.7.2. The required adjustment of Li₂O target concentration is obtained by solving Equation (87) using the δ value of 0.005:

$$\frac{\exp\left(B_{ucci,A101}^{vis1150,Step1}\right)}{80} + 0.005 = 1 \quad (194)$$

The $\frac{\exp\left(B_{ucci,j}^{vis1150,Step1}\right)}{80}$ value before adjustment was 1.104 and becomes 0.995 (this value will change

slightly after Monte-Carlo run based on new target composition) when the $g_{Li_2O,A101}^{oxide\ in\ MFPV,adj}$ is 0.0019. Then, Equation (88) is used to calculate adjusted Li₂O target concentration:

$$g_{Li_2O,A101}^{oxide\ in\ MFPV,target} = g_{Li_2O,A101}^{oxide\ in\ MFPV,initial} + g_{Li_2O,A101}^{oxide\ in\ MFPV,adj} = 0 + 0.00190 = 0.00190 \quad (195)$$

The above adjustment of target Li₂O mass fraction affects the target mass fraction of SiO₂ only i.e., there is no change for all other components and waste loading. The target SiO₂ mass fraction is calculated using Equation (88), i.e., by subtracting the adjusted Li₂O mass fraction from the initial SiO₂ as below:

$$g_{SiO_2,A101}^{oxide\ in\ MFPV,target} = g_{SiO_2,A101}^{oxide\ in\ MFPV,initial} - g_{Li_2O,A101}^{oxide\ in\ MFPV,adj} = 0.44983 - 0.00190 = 0.44793 \quad (196)$$

For all other components and waste loading,

$$g_{i,A101}^{oxide\ in\ MFPV,target} = g_{i,A101}^{oxide\ in\ MFPV,initial} \quad \{i \neq Li_2O, SiO_2\} \quad (197)$$

$$G_{A101}^{waste\ in\ MFPV,target} = G_{A101}^{waste\ in\ MFPV,initial} = 0.23317 \quad (198)$$

The Step 1 glass and radionuclide compositions (Section 5.1.4), waste transfer volume (Section 5.1.5), and Step 1 constraints (Section 5.1.6) are calculated following the same methods illustrated in Sections 6.1.4, 6.1.5, and 6.1.6. The results of these calculations are summarized below.

6.1.8 Calculation of Step 1 Glass and Radionuclide Compositions after Target Glass Composition Adjustment

There is no change in the waste contribution ($G_{A101}^{waste\ in\ MFPV,target} g_{i,A11,1}^{oxide\ in\ CRV}$) to the Step 1 glass composition given in the 6th column of Table B-3 compared to that before target glass composition adjustment given in the 3rd column. The adjusted target composition is given in the 5th column and the resulting target GFC composition ($g_{i,A101}^{oxide\ in\ MFPV,target-gfc}$) values for 11 GFC components are in the last column of Table B-3.

The preliminary target mass of GFCs per g glass ($\ddot{M}_{k,A101}^{GFC\ in\ MFPV,pre}$) and target mass of GFCs per g glass ($\ddot{M}_{k,A101}^{GFC\ in\ MFPV,target}$) are given in Table 27 (corresponding to Table 18 given before target glass composition adjustment).

Table 27. Preliminary Target and Target Masses of Each GFC per g Glass for the A101th MFPV Batch after Target Glass Composition Adjustment

GFC (<i>k</i>)	$\ddot{M}_{k,A101}^{GFC\ in\ MFPV,pre}$	$\ddot{M}_{k,A101}^{GFC\ in\ MFPV,target}$
Kyanite	7.5098E-02	7.5098E-02
Boric Acid	1.7684E-01	1.7684E-01
Wollastonite	5.1698E-02	5.1698E-02
Hematite	5.3216E-02	5.3216E-02
Li carbonate	4.7256E-03	4.7256E-03
Olivine	3.0507E-02	3.0507E-02
Na carbonate	-5.7320E-04	0.0000E+00
Silica	3.6302E-01	3.6302E-01
Rutile	1.4191E-02	1.4191E-02
Zincite	3.5051E-02	3.5051E-02
Zircon	4.5078E-02	4.5078E-02

Table B-4b shows the waste contribution ($G_{A101}^{waste\ in\ MFPV,target}$ $g_{i,A11,1}^{oxide\ in\ CRV}$) (2nd column), the GFC contribution ($\sum_{k=1}^{11} \ddot{M}_{k,A101}^{GFC\ in\ MFPV,target} m_{ik}^{oxide\ in\ GFC}$) (3rd column), and the resulting $g_{i,A101}^{oxide\ in\ MFPV,Step1}$ values (4th column) for the A101th

MFPV Batch after target composition adjustment. Table B-4b also includes the $g_{i,A101}^{oxide\ in\ MFPV,Step1} \nu_i$ values (5th column) and the $\tilde{g}_{i,A101}^{oxide\ in\ MFPV,Step1}$ results (6th column) using $\sum_{i=1}^{64} g_{i,A101}^{oxide\ in\ MFPV,Step1} \nu_i = 0.994096$. The specific activity of

radionuclides in the A101th MFPV batch before applying retention factors ($a_{i,A101}^{rad\ in\ MFPV,Step1}$) and after applying retention factors ($\tilde{a}_{i,A101}^{oxide\ in\ MFPV,Step1}$) are given in Table B-5b.

6.1.9 Calculation of LAW Transfer Volume after Target Glass Composition Adjustment

The GFC and dust water control volumes per unit volume of LAW and the volume of dilution water change after the target adjustment. Equation (180) for the A101th MFPV batch is rewritten with the volumes changed after target glass composition adjustment:

$$\begin{aligned}
 V_{A101}^{working\ MFPV} &= 19426 \text{ (L)} \\
 &= V_{A11,1}^{transwaste\ CRV} + V_{A101}^{GFC\ MFPV, Step1} + V_{A101}^{dust\ MFPV, Step1} + V_{A101}^{sucrose\ MFPV, Step1} + V_{A101}^{heel\ MFPV} \\
 &\quad + V_{A101}^{transflush\ MFPV} + V_{A101}^{sampfush\ MFPV} + V_{A101}^{dilute\ MFPV, Step1} \tag{199} \\
 &= V_{A11,1}^{transwaste\ CRV} + 0.37641V_{A11,1}^{transwaste\ CRV} + 0.037972V_{A11,1}^{transwaste\ CRV} + 0.023093V_{A11,1}^{transwaste\ CRV} + 6712.0 \\
 &\quad + 37.5 + 175.3 + \max \left\{ -0.161529V_{A11,1}^{transwaste\ CRV} - 212.7, 0 \right\}
 \end{aligned}$$

Equation (199) was solved iteratively to obtain the waste transfer volume ($V_{dm}^{transwaste\ CRV}$) of 8696.7 L compared to the result of 8707.7 L before the target composition adjustment. This result of $V_{dm}^{transwaste\ CRV}$ is used to calculate the volumes that were expressed in terms of $V_{dm}^{transwaste\ CRV}$, then Equation (199) is rewritten as:

$$19426 \text{ (L)} = 8696.7 + 3273.5 + 330.2 + 200.8 + 6712.0 + 37.5 + 175.3 + 0.0 \text{ (L)} \tag{200}$$

This $V_{dm}^{transwaste\ CRV}$ value is used for calculation of composition uncertainties required for the calculation of Step 1 constraints in Section 6.1.10.

The target masses of GFCs and sucrose are calculated from the waste transfer volume. Table 28 summarizes the resulting masses of GFCs and sucrose from Step 1 calculation for the A101th MFPV Batch after target composition adjustment.

Table 28. Masses of GFCs and Sucrose from Step 1 Calculation for the A101th MFPV Batch after Target Composition Adjustment

GFC (k)/sucrose	$M_{k,A101}^{GFC\ in\ MFPV, target, Step1}$
Kyanite	729.90
Boric Acid	1718.73
Wollastonite	502.47
Hematite	517.23
Lithium carbonate	45.93
Olivine	296.51
Sodium carbonate	0
Silica	3528.27
Rutile	137.92
Zincite	340.67
Zircon	438.13
Sucrose	311.09
Total	8566.83

6.1.10 Calculation of Constraints for Algorithm Step 1 after Target Glass Composition Adjustment

The same calculations of the constraints described in Section 6.1.6 are performed with adjusted target glass and radionuclide compositions. Table 29 summarizes the predicted properties, uncertainties, and UCCI/LCCI values for the Step 1 composition of the A101th MFPV batch after composition adjustment and applying the retention factors compared with the corresponding limits. Table 29 shows that all the property constraints are met after composition adjustments.

Table 29. Predicted Properties, Uncertainties, and UCCI/LCCI Values for the A101th MFPV Batch Compared with the Corresponding Limits (After Formulation Adjustment)

Property	Unit	$P_{A101}^{prop, Step1}$	$U_{pred, A101}^{prop, Step1}$	$U_{comp, A101}^{prop, Step1}$	$B_{ucci, A101}^{prop, Step1}$ or $B_{lcci, A101}^{prop, Step1}$	L_u^{prop} or L_l^{prop}
$\ln(r_B)$	ln[g/L]	0.0551	0.1537	0.3585	0.5674	< 1.3863
$\ln(r_{Na})$	ln[g/L]	-0.0571	0.1651	0.3016	0.4096	< 1.3863
$\ln(D)$	ln[μm]	2.6093	0.6303	1.2962	4.5358	< 6.1159
$\ln(\eta_{1100}), u$	ln[P]	4.6071	0.0326	0.2520	4.8916	≤ 5.0106
$\ln(\eta_{1150}), l$	ln[P]	4.1112	0.0328	0.2414	3.8370	≥ 2.9957
$\ln(\eta_{1150}), u$	ln[P]	4.1112	0.0328	0.2323	4.3763	≤ 4.3820
$\ln(\epsilon_{1100}), l$	ln[S/cm]	-1.0550	0.0321	0.1773	-1.2644	≥ -2.3026
$\ln(\epsilon_{1200}), u$	ln[S/cm]	-0.7025	0.0327	0.1649	-0.5049	≤ -0.3567

Table 30 summarizes the calculation results for additional constraints for the Step 1 composition of the A101th MFPV batch after composition adjustment and applying the retention factors compared with the corresponding limits. Table 30 shows that all the model validity, waste Na₂O loading, and radionuclide concentration constraints are met.

Table 30. Additional Constraints for the A101th MFPV Batch after Composition Adjustment Compared with the Corresponding Limits

Constraint	Value	Lower Limit	Upper Limit
Model validity single component constraints ($\tilde{g}_{i,A101}^{oxide\ in\ MFPV, Step1}$)			
Al ₂ O ₃	0.06123	0.035	0.090
Cl	0.00136	0	0.0091
Cr ₂ O ₃	0.00086	0	0.0059
F	0.00076	0	0.0035
P ₂ O ₅	0.00198	0	0.030
SiO ₂	0.44981	0.384	0.521
Sum of Minors	0.00051	0	0.0028
Model validity PCT constraints			
$P_{A101}^{pctB, Step1}$ (ln[g/L])	0.0551	NA	0.9933
$P_{A101}^{pctNa, Step1}$ (ln[g/L])	-0.0571	NA	0.9933
Model validity multiple component constraints (based on $\tilde{g}_{i,A101}^{oxide\ in\ MFPV, Step1}$, lower and upper limits are a function of concentration of other component)			
Li ₂ O function of Na ₂ O	0.00190	-0.05337	0.02851
Cr ₂ O ₃ function of P ₂ O ₅	0.00086	-0.00138	0.00234
Na ₂ O function of CaO	0.19088	0.08878	0.28178
Li ₂ O function of CaO	0.00190	0.00000	0.03952
Na ₂ O function of SO ₃	0.19088	0.03645	0.25785
Li ₂ O function of SO ₃	0.00190	-0.02079	0.05081
Na ₂ O function of SiO ₂	0.19088	0.00474	0.20734
Waste Na₂O loading constraint			
$\tilde{g}_{Na_2O(w), A101}^{oxide\ in\ MFPV, Step1}$ (a)	0.1810	0.14	NA
Radionuclide Concentration Constraints			
$\hat{a}_{137Cs, A101}^{rad\ in\ MFPV, Step1} + k^{rad} \hat{S}_{137Cs, A101}^{rad\ in\ MFPV, Step1}$ (Ci/m ³)	0.1503	NA	0.3
$\hat{a}_{90Sr, A101}^{rad\ in\ MFPV, Step1} + k^{rad} \hat{S}_{90Sr, A101}^{rad\ in\ MFPV, Step1}$ (Ci/m ³)	1.6796	NA	20
$SF_{LL, A101}^{rad\ in\ MFPV, Step1} + k^{rad} S_{LL, A101}^{radSF\ in\ MFPV, Step1}$	0.04869	NA	1
$SF_{SL, A101}^{rad\ in\ MFPV, Step1} + k^{rad} S_{SL, A101}^{radSF\ in\ MFPV, Step1}$	0.00039	NA	1

NA: not applicable

(a) It was assumed that the fraction of sodium in the A11th CRV that is classified as waste sodium (ω_{A11}) was 95% and waste in the A11th CRV was designated as Envelope A.

6.2 Example Step 2 – Calculation of GFC Masses and Dilution Water Volume

The waste transfer volume calculated in Section from Step 1 is provided to the operators of the LAW Vitrification and Pretreatment facilities so that they can initiate the waste transfer from the CRV to the MFPV. After transferring the waste, the actual waste volume ($V_j^{waste\ MFPV}$) added to the MFPV is obtained and used to calculate the GFC/sucrose masses and dilution water volume in Step 2 calculation. For the purpose of this example calculation, it was assumed that the actual waste volume ($V_{A101}^{waste\ MFPV}$) was 8957.6 L, 3% higher than the target of 8696.7 L. The masses of GFCs and sucrose to add to the MFPV are calculated using Equations (89) and (90):

$$M_{k,A101}^{GFC\ in\ MFPV,\ target,\ Step2} = M_{k,A101}^{GFC\ in\ MFPV,\ target,\ Step1} \frac{V_{A101}^{waste\ MFPV}}{V_{A11,1}^{transwaste\ CRV}} = M_{k,A101}^{GFC\ in\ MFPV,\ target,\ Step1} \frac{8957.6\ (L)}{8696.7\ (L)} \quad (201)$$

$$M_{A101}^{sucrose\ in\ MFPV,\ target,\ Step2} = M_{A101}^{sucrose\ in\ MFPV,\ target,\ Step1} \frac{V_{A101}^{waste\ MFPV}}{V_{A11,1}^{transwaste\ CRV}} = 311.09(kg) \frac{8957.6(L)}{8696.7(L)} = 320.43\ (kg) \quad (202)$$

The results of the Step 2 calculations are included in Table 31.

Table 31. Masses of GFCs and Sucrose from Step 2 Calculation for the A101th MFPV Batch

GFC (k)/sucrose	$M_{k,A101}^{GFC\ in\ MFPV,\ target,\ Step2}$
Kyanite	751.80
Boric Acid	1770.30
Wollastonite	517.54
Hematite	532.74
Lithium carbonate	47.31
Olivine	305.40
Sodium carbonate	0.00
Silica	3634.13
Rutile	142.06
Zincite	350.89
Zircon	451.28
Sucrose	320.43
Total	8823.88

The volumes of dust control water and dilution water for Step 2 are calculated based on actual volume of waste transferred using Equations (91) and (92):

$$V_{A101}^{dust, Step2} = V_{A101}^{dust, Step1} \frac{V_{A101}^{waste, MFPV}}{V_{A11,1}^{transwaste, CRV}} = 330.2(L) \frac{8957.6(L)}{8696.7(L)} = 340.1 (L) \quad (203)$$

$$V_{A101}^{dilute, Step2} = \max \left\{ \frac{C_{Na, A11,1}^{element\ in\ CRV} V_{A101}^{waste, MFPV}}{1000MW_{Na} t_{[Na], A101}} - \left(V_{A101}^{waste, MFPV} + V_{A101}^{transflush, MFPV, measured} + V_{A101}^{samplerush, MFPV} + V_{A101}^{dust, MFPV, Step2} \right), 0 \right\}$$

$$= \max \left\{ \frac{158576.4(mg/L) \times 8957.6}{1000(mg/g) \times 22.9898(g/mole) \times 7.870(moles/L)} - \right. \quad (204)$$

$$\left. \frac{0}{(8957.6 + 37.5 + 175.3 + 340.1), 0} \right\}$$

$$= \max \{-1659.7, 0\} = 0$$

The volume contributions of GFCs and sucrose are calculated using Equations (93) and (94):

$$V_{A101}^{GFC, Step2} = V_{A101}^{GFC, Step1} \frac{V_{A101}^{waste, MFPV}}{V_{A11,1}^{transwaste, CRV}} = 3273.5(L) \frac{8957.6(L)}{8696.7(L)} = 3371.8 (L) \quad (205)$$

$$V_{A101}^{sucrose, Step2} = V_{A101}^{sucrose, Step1} \frac{V_{A101}^{waste, MFPV}}{V_{A11,1}^{transwaste, CRV}} = 200.8(L) \frac{8957.6(L)}{8696.7(L)} = 206.9 (L) \quad (206)$$

Then, the total increase of volume originated from increased waste transfer volume is calculated using Equation (95) as:

$$V_{A101}^{waste, MFPV} + V_{A101}^{GFC, Step2} + V_{A101}^{dust, Step2} + V_{A101}^{sucrose, Step2} + V_{A101}^{heel, MFPV}$$

$$+ V_{A101}^{transflush, MFPV, measured} + V_{A101}^{samplerush, MFPV} + V_{A101}^{dilute, MFPV, Step2} - 19,426$$

$$= 8957.6 + 3371.8 + 340.1 + 206.9 + 6712 + 37.5 + 175.3 + 0 - 19,426 \quad (207)$$

$$= 19,801.1 - 19,426$$

$$= 375.1 < 1,666 (L)$$

In this example, because the actual waste transfer volume increase was small enough not to cause the total MFPV volume increase over the allowable 1,666 L, it is safe to continue normal operation.

6.3 Example Step 3 – Calculation of Final Glass Composition and Properties with Uncertainties

The actual measured volume of waste transfer, actual measured volumes of flush, batch control, and dilution water, and the actual measured masses of GFCs are used to calculate the final composition and properties. For example calculations, the actual measured masses of GFCs and sucrose were random generated based on the SD values discussed in Appendix E and given in the 2nd column of Table 32.

Table 32. Assumed Values for the Measured Masses of GFCs and Sucrose in Step 3 Calculation and Calculated GFC/Sucrose Masses per g Glass for the A101th MFPV Batch

GFC	$M_{k,A101}^{GFC\ in\ MFPV,\ measured}$ kg	$\sum_{i=1}^{64} m_{ik}^{oxide\ in\ GFC}$	$M_{k,A101}^{GFC\ in\ MFPV,\ measured} \sum_{i=1}^{64} m_{ik}^{oxide\ in\ GFC}$ kg	$\ddot{M}_{k,A101}^{GFC\ in\ MFPV,\ Step3}$ g/g glass
Kyanite	752.1	0.99665	749.6	0.07505
Boric Acid	1770.0	0.56527	1000.5	0.17663
Wollastonite	517.7	0.99135	513.2	0.05166
Hematite	532.6	1.00546	535.5	0.05315
Lithium carbonate	47.4	0.40702	19.3	0.00473
Olivine	305.3	0.98994	302.2	0.03047
Sodium carbonate	0.0	0.58420	0.0	0.00000
Silica	3634.4	0.99891	3630.5	0.36268
Rutile	142.1	0.98793	140.4	0.01418
Zincite	350.7	0.99829	350.1	0.03500
Zircon	451.2	0.98731	445.5	0.04503
Sucrose	320.3	NA	NA	NA
Total	8823.8	NA	7686.8	NA

NA: not applicable

6.3.1 Final Glass Composition

The final waste loading ($G_{A101}^{waste\ in\ MFPV,\ Step3}$) and GFC mass per g glass ($\ddot{M}_{k,A101}^{GFC\ in\ MFPV,\ Step3}$) are calculated using Equations (96) and (97):

$$\begin{aligned}
 G_{A101}^{waste\ in\ MFPV,\ Step3} &= \frac{C_{A11,1}^{CRV} V_{A101}^{waste\ MFPV}}{C_{A11,1}^{CRV} V_{A101}^{waste\ MFPV} + \sum_{k=1}^{11} \left(M_{k,A101}^{GFC\ in\ MFPV,\ measured} \sum_{i=1}^{64} m_{ik}^{oxide\ in\ GFC} \right)} \\
 &= \frac{260.58(\text{g/L}) \times 8957.6(\text{L})}{260.58(\text{g/L}) \times 8957.6(\text{L}) + \sum_{k=1}^{11} \left(M_{k,A101}^{GFC\ in\ MFPV,\ measured} \sum_{i=1}^{64} m_{ik}^{oxide\ in\ GFC} \right)} \\
 &= \frac{2334.2(\text{kg})}{2334.2(\text{kg}) + 7686.8(\text{kg})} = 0.23293
 \end{aligned} \tag{208}$$

$$\begin{aligned}
 \ddot{M}_{k,A101}^{GFC\ in\ MFPV,\ Step3} &= \frac{M_{k,A101}^{GFC\ in\ MFPV,\ measured} \left(1 - G_{A101}^{waste\ in\ MFPV,\ Step3} \right)}{\sum_{k=1}^{11} \left(M_{k,A101}^{GFC\ in\ MFPV,\ measured} \sum_{i=1}^{64} m_{ik}^{oxide\ in\ GFC} \right)} = \frac{M_{k,A101}^{GFC\ in\ MFPV,\ measured} (1 - 0.23293)}{7686.8(\text{kg})}
 \end{aligned} \tag{209}$$

Calculation of $\ddot{M}_{k,A101}^{GFC\ in\ MFPV,\ Step3}$ values using Equation (209) is illustrated in Table 32. Then, the glass composition is calculated using Equation (98):

$$\begin{aligned}
 g_{i,A101}^{oxide\ in\ MFPV,\ Step3} &= G_{A101}^{waste\ in\ MFPV,\ Step3} g_{i,A11,1}^{oxide\ in\ CRV} + \sum_{k=1}^{11} \ddot{M}_{k,A101}^{GFC\ in\ MFPV,\ Step3} m_{ik}^{oxide\ in\ GFC} \\
 &= 0.23293 \times g_{i,A11,1}^{oxide\ in\ CRV} + \sum_{k=1}^{11} \ddot{M}_{k,A101}^{GFC\ in\ MFPV,\ Step3} m_{ik}^{oxide\ in\ GFC}
 \end{aligned} \tag{210}$$

The $g_{i,A11,1}^{oxide\ in\ CRV}$ values are given in Table B-2, $\ddot{M}_{k,A101}^{GFC\ in\ MFPV,\ Step3}$ values are in Table 32, and $m_{ik}^{oxide\ in\ GFC}$ values are in

Table A-5. Table B-6 show the waste contribution ($G_{A101}^{waste\ in\ MFPV,\ Step3} g_{i,A11,1}^{oxide\ in\ CRV}$) (2nd column), the GFC contribution

($\sum_{k=1}^{11} \ddot{M}_{k,A101}^{GFC\ in\ MFPV,\ Step3} m_{ik}^{oxide\ in\ GFC}$) (3rd column), and the resulting $g_{i,A101}^{oxide\ in\ MFPV,\ Step3}$ values (4th column) for the A101th

MFPV Batch. The glass composition after applying retention factors ($\tilde{g}_{i,A101}^{oxide\ in\ MFPV,\ Step3}$) is calculated using Equation (99):

$$\tilde{g}_{i,A101}^{oxide\ in\ MFPV,Step3} = \frac{g_{i,A101}^{oxide\ in\ MFPV,Step3} v_i}{\sum_{i=1}^{64} g_{i,A101}^{oxide\ in\ MFPV,Step3} v_i} \quad (211)$$

Table B-6 also includes the $g_{i,A101}^{oxide\ in\ MFPV,Step3} v_i$ values (5th column) and the $\tilde{g}_{i,A101}^{oxide\ in\ MFPV}$ results (6th column) using

$$\sum_{i=1}^{64} g_{i,A101}^{oxide\ in\ MFPV,Step3} v_i = 0.99410.$$

The activity of radionuclides per unit mass of glass oxides in the A101th MFPV batch ($a_{i,A101}^{rad\ in\ MFPV,Step3}$) is calculated using Equation (100):

$$\begin{aligned} a_{i,A101}^{rad\ in\ MFPV,Step3} &= a_{i,A11,1}^{rad\ in\ CRV} G_{A101}^{waste\ in\ MFPV,Step3} \\ &= \frac{\bar{R}_{i,A11}^{rad\ in\ CRV} \lambda_{A11,1}^{waste\ in\ MFPV,Step3} G_{A101}^{waste\ in\ MFPV,Step3}}{C_{A11,1}^{oxides\ in\ CRV}} = \frac{\bar{R}_{i,A11}^{rad\ in\ CRV} (mCi/L) \times 0.99854 \times 0.23293}{260.58(g/L)} \quad (mC/g) \end{aligned} \quad (212)$$

The specific activity after applying retention factors ($\tilde{a}_{i,A101}^{oxide\ in\ MFPV,Step3}$) is calculated using Equation (101):

$$\tilde{a}_{i,A101}^{oxide\ in\ MFPV,Step3} = \frac{a_{i,A101}^{rad\ in\ MFPV,Step3} v_i}{\sum_{i=1}^{64} g_{i,A101}^{oxide\ in\ MFPV,Step3} v_i} = \frac{a_{i,A101}^{rad\ in\ MFPV,Step3} v_i}{0.99410} \quad (213)$$

The results of $a_{i,A101}^{rad\ in\ MFPV,Step3}$ and $\tilde{a}_{i,A101}^{oxide\ in\ MFPV,Step3}$ are in Table B-7.

6.3.2 Final Predicted Properties and Uncertainties

The glass composition given in Table B-6 is used to calculate the final predicted properties with uncertainties.

Table 33 summarizes the predicted properties, uncertainties, and UCCI/LCCI values for the Step 3 composition of the A101th MFPV batch after applying the retention factors compared with the corresponding limits. As expected, Table 33 shows that all the property constraints are met.

Table 33. Predicted Properties, Uncertainties, and UCCI/LCCI Values for Final Composition from Step 3 Calculation of the A101th MFPV Batch Compared with the Corresponding Limits

Property	Unit	P^{prop}	U_{pred}^{prop}	U_{comp}^{prop}	$B_{ucci,lcci}^{prop}$	L^{prop}
$\ln(r_B)$	ln[g/L]	0.0540	0.1537	0.3366	0.5443 <	1.3863
$\ln(r_{Na})$	ln[g/L]	-0.0579	0.1651	0.2852	0.3924 <	1.3863

$\ln(D)$	$\ln[\mu\text{m}]$	2.6105	0.6303	1.2035	4.4442	<	6.1159
$\ln(\eta_{1100}), u$	$\ln[\text{P}]$	4.6076	0.0326	0.2523	4.8925	<	5.0106
$\ln(\eta_{1150}), l$	$\ln[\text{P}]$	4.1117	0.0328	0.2254	3.8536	>	2.9957
$\ln(\eta_{1150}), u$	$\ln[\text{P}]$	4.1117	0.0328	0.2333	4.3779	<	4.3820
$\ln(\varepsilon_{1100}), l$	$\ln[\text{S/cm}]$	-1.0551	0.0321	0.1766	-1.2638	>	-2.3026
$\ln(\varepsilon_{1200}), u$	$\ln[\text{S/cm}]$	-0.7026	0.0327	0.1528	-0.5172	<	-0.3567

Table 34 summarizes the calculation results for additional constraints given in Table 10 through Table 13 for the Step 3 composition of the A101th MFPV batch compared with the corresponding limits. There are no or only minor differences between the results from Step 1 (Table 30) and Step 3 (Table 34) calculations, resulting from formulation different caused by the differences in the target and measured GFC masses.

Table 34. Additional Constraints for the Step 3 composition of the A101th MFPV Batch Compared with the Corresponding Limits

Constraint	Value	Lower Limit	Upper Limit
Model validity single component constraints ($\tilde{g}_{i,A101}^{\text{oxide in MFPV, Step3}}$)			
Al ₂ O ₃	0.06125	0.035	0.090
Cl	0.00136	0	0.0091
Cr ₂ O ₃	0.00086	0	0.0059
F	0.00076	0	0.0035
P ₂ O ₅	0.00198	0	0.030
SiO ₂	0.44984	0.384	0.521
Sum of Minors	0.00051	0	0.0028
Model validity PCT constraints			
$P_{A101}^{\text{pctB, Step3}}$ (ln[g/L])	0.0540	NA	0.9933
$P_{A101}^{\text{pctNa, Step3}}$ (ln[g/L])	-0.0579	NA	0.9933
Model validity multiple component constraints (based on $\tilde{g}_{i,A101}^{\text{oxide in MFPV, Step3}}$, lower and upper limits are a function of concentration of other component)			
Li ₂ O function of Na ₂ O	0.00191	-0.05336	0.02851
Cr ₂ O ₃ function of P ₂ O ₅	0.00086	-0.00138	0.00234
Na ₂ O function of CaO	0.19088	0.08877	0.28177
Li ₂ O function of CaO	0.00191	0.00000	0.03953
Na ₂ O function of SO ₃	0.19088	0.03645	0.25785
Li ₂ O function of SO ₃	0.00191	-0.02079	0.05081
Na ₂ O function of SiO ₂	0.19088	0.00469	0.20729
Waste Na₂O loading constraint			
$\tilde{g}_{\text{Na}_2\text{O}(w), A101}^{\text{oxide in MFPV, Step3}}$ (a)	0.1810	0.14	NA
Radionuclide Concentration Constraints			
$\tilde{a}_{137\text{Cs}, A101}^{\text{rad in MFPV, Step3}} + k \tilde{s}_{137\text{Cs}, A101}^{\text{rad in MFPV, Step3}}$ (Ci/m ³)	0.1501	NA	0.3

Constraint	Value	Lower Limit	Upper Limit
$\hat{a}_{90Sr,A101}^{rad\ in\ MFPV,Step3} + k^{rad} \hat{s}_{90Sr,A101}^{rad\ in\ MFPV,Step3}$ (Ci/m ³)	1.6777	NA	20
$SF_{LL,A101}^{rad\ in\ MFPV,Step3} + k^{rad} S_{LL,A101}^{radSF\ in\ MFPV,Step3}$	0.04843	NA	1
$SF_{SL,A101}^{rad\ in\ MFPV,Step3} + k^{rad} S_{SL,A101}^{radSF\ in\ MFPV,Step3}$	0.00039	NA	1

NA: not applicable

(a) It was assumed that the fraction of sodium in the A11th CRV that is classified as waste sodium (ω_{A11}) was 95% and waste in the A11th CRV was designated as Envelope A.

6.4 Example Step 4 – Comparison of Final Composition and Properties with Constraints

Table 33 and Table 34 already compared the predicted properties with uncertainties and additional constraint quantities to their limits and confirmed that all the constraints are met for the A101th MFPV batch.

If prediction plus composition uncertainty for any property is outside the range of acceptability, an operator will be alerted for intervention. For product quality related properties (e.g., those properties required to meet Contract Specification 1) this comparison is a hold point for transfer of melter feed to the MFV. Once the comparison is successful, the hold point is lifted.

6.5 Example Step 5 – Completion of Production Records

As discussed in Section 5.5, the productions records are calculated per glass canister basis. With the canister compositions and masses, compliance with the product requirements is demonstrated. These requirements are discussed in the same order as in Section 5.5.

The example calculations given in Section 6.1 through 6.4 through were performed for one MFPV batch (assumed as A101th MFPV) based on the 1st transfer waste transferred from the A11th CRV. Similar calculations were also performed for the next 9 MFPV batches for a total of 10, from A101th to B105th, MFPV batches. These 10 MFPV batches required three CRV batches, A11, B11, and A12. The compositions of these CRV batches are given in Table B-1 in the units that would be reported by the WTP laboratory.

During these calculations, to simulate the use of actual measured data, the following values were random generated:

- Actual CRV working volume around the nominal value of 48661 L
- Actual MFPV heel volume around the nominal value of 6556 L
- Actual waste transfer volume around the Step 1 target value
- Actual GFC masses around the Step 2 target values

The actual water volumes for flush waters, dust control water, and dilution water were assumed to be the same as nominal or target values.

The results of above calculations are in Tables B-8 through B-10. Table B-8 summarizes the input data and results of various processing parameters, Table B-9 waste and final glass compositions and SD for glass composition, and Table B-10 results on various constraint quantities including glass properties and uncertainties. Calculations of quantities for production records based on these 10 MFPV batches are given

in the following subsections. It was assumed that the A501th through A503th canisters consist of five MFPV-A batches (MFPV-A101, A102, A103, A104, and A105) and B501th through B503th canisters consist of five MFPV-B batches (MFPV-B101, B102, B103, B104, and B105).

6.5.1 Specification 2.2.2.2—Waste Loading

The mass weighted average composition over 5 MFPV batches is calculated using Equation (121):

$$g_{Na_2O(w),e}^{oxide\ in\ can} = \frac{\sum_{j=1}^5 \left(g_{Na_2O(w),j}^{oxide\ in\ MFPV} M_j^{oxide\ in\ MFPV, Step3} \right)}{\sum_{j=1}^5 M_j^{oxide\ in\ MFPV, Step3}} \tag{214}$$

The waste Na₂O loading ($g_{Na_2O(w),j}^{oxide\ in\ MFPV}$) data are given in Table B-10 and the total glass oxides mass ($M_j^{oxide\ in\ MFPV, Step3}$) data are in Table B-8. Table 35 summarizes the calculation of waste Na₂O loading for the A501th and B501th canisters.

Table 35. Calculation of Waste Na₂O loading for the A501th and B501th Canisters

MFPV batch	Waste Na ₂ O loading	Mass of glass before retention factor adjustment, kg	MFPV batch	Waste Na ₂ O loading	Mass of glass before retention factor adjustment, kg
MFPV-A101	0.181	10021.0	MFPV-B101	0.181	9888.9
MFPV-A102	0.181	9952.3	MFPV-B102	0.188	9872.2
MFPV-A103	0.188	9727.5	MFPV-B103	0.188	9537.2
MFPV-A104	0.162	10562.6	MFPV-B104	0.162	10431.4
MFPV-A105	0.162	10508.8	MFPV-B105	0.162	10510.9
Result for A501 th canister	0.174		Result for B501 th canister	0.176	

6.5.2 Specification 2.2.2.6— Chemical Composition Documentation

The composition of canister glass is calculated using Equation (123) and its SD using Equation (124):

$$g_{ie}^{oxide\ in\ can} = \frac{\sum_{j=1}^5 \left(\tilde{g}_{ij}^{oxide\ in\ MFPV, Step3} \tilde{M}_j^{oxide\ in\ MFPV, Step3} \right)}{\sum_{j=1}^5 \tilde{M}_j^{oxide\ in\ MFPV, Step3}} \tag{215}$$

$$s_{ie}^{oxidein,can} = \frac{\sqrt{\sum_{j=1}^5 \left(\tilde{s}_{ij}^{oxidein,MFPV,Step3} \tilde{M}_j^{oxidein,MFPV,Step3} \right)^2}}{\sum_j \tilde{M}_j^{oxidein,MFPV,Step3}} \tag{216}$$

The $g_{ie}^{oxidein,can}$ and $s_{ie}^{oxidein,can}$ values are given in Table B-9 and $\tilde{M}_j^{oxidein,MFPV,Step3}$ values are in Table B-8. The results of above calculations for the A501th and B501th Canisters are listed in Table 36.

Table 36. Chemical Composition of Glass in the A501th and B501th Canisters

Canister	Canister-A501		Canister-B501	
	$g_{i,A501}^{oxidein,can}$	$s_{i,A501}^{oxidein,can}$	$g_{i,B501}^{oxidein,can}$	$s_{i,B501}^{oxidein,can}$
Ac2O3	5.9378E-14	1.8996E-15	5.9962E-14	1.9402E-15
Ag2O	2.8932E-07	1.5987E-08	2.9145E-07	1.6180E-08
Al2O3	6.1237E-02	5.2295E-04	6.1228E-02	5.2893E-04
Am2O3	1.7190E-10	5.8095E-12	1.7157E-10	5.7174E-12
As2O5	1.2226E-06	1.4387E-07	1.2263E-06	1.4256E-07
B2O3	9.9444E-02	7.2539E-04	9.9453E-02	7.2445E-04
BaO	2.5847E-07	1.1210E-08	2.5919E-07	1.1157E-08
BeO	1.2236E-06	2.8384E-08	1.2356E-06	2.8349E-08
Bi2O3	4.4129E-06	1.6742E-07	4.4083E-06	1.7576E-07
CaO	2.9011E-02	3.4698E-04	2.8492E-02	3.4140E-04
CdO	4.2937E-06	5.9074E-07	4.3022E-06	5.9677E-07
Ce2O3	2.4914E-07	1.6798E-08	2.4860E-07	1.6625E-08
Cl	1.3292E-03	1.6680E-04	1.3408E-03	1.6885E-04
Cm2O3	9.6195E-14	3.9052E-15	9.6934E-14	3.8902E-15
CoO	4.4360E-07	2.9839E-08	4.4810E-07	3.0450E-08
Cr2O3	8.6126E-04	2.8340E-05	8.6122E-04	2.8233E-05
Cs2O	2.7260E-09	1.7125E-10	2.7438E-09	1.7203E-10
CuO	8.1441E-07	5.5070E-08	8.2091E-07	5.5109E-08
Eu2O3	3.1195E-11	6.7517E-13	3.1421E-11	6.7438E-13
F	7.5395E-04	6.1782E-05	7.6445E-04	6.2504E-05
Fe2O3	5.5174E-02	4.2994E-04	5.5182E-02	4.2662E-04
Gd2O3	0.0000E+00	0.0000E+00	0.0000E+00	0.0000E+00
HgO	0.0000E+00	0.0000E+00	0.0000E+00	0.0000E+00
I	3.0867E-07	4.8554E-08	3.1179E-07	4.9280E-08
K2O	1.3455E-02	3.3878E-04	1.3584E-02	3.4094E-04
La2O3	3.8107E-07	1.2274E-08	3.8314E-07	1.2332E-08
Li2O	3.2768E-03	2.7670E-05	2.8425E-03	2.7580E-05
MgO	1.4867E-02	1.3234E-04	1.4871E-02	1.3027E-04
MnO	1.4259E-04	1.5348E-05	1.4154E-04	1.5291E-05
MoO3	1.2206E-05	4.0822E-07	1.2263E-05	4.0999E-07
Na2O	1.8394E-01	5.1260E-03	1.8533E-01	5.1083E-03
Nb2O5	8.3341E-09	2.6933E-10	8.5801E-09	2.7462E-10
Nd2O3	1.1843E-06	5.1378E-08	1.1937E-06	5.1858E-08
NiO	1.4190E-04	7.7801E-06	1.4230E-04	7.8159E-06
NpO2	1.1719E-07	2.6984E-09	1.1762E-07	2.7010E-09
P2O5	1.9503E-03	5.9577E-05	1.9600E-03	5.9579E-05
Pa2O5	2.6611E-10	3.4933E-11	2.6869E-10	3.5179E-11
PbO	3.1368E-05	1.3514E-06	3.1727E-05	1.3573E-06

Canister	Canister-A501		Canister-B501	
	$\overset{\text{oxide in}}{g_{i,A501}^{can}}$	$\overset{\text{oxide in}}{S_{i,A501}^{can}}$	$\overset{\text{oxide in}}{g_{i,B501}^{can}}$	$\overset{\text{oxide in}}{S_{i,B501}^{can}}$
PdO	7.2034E-06	3.1064E-07	7.2748E-06	3.1521E-07
Pr2O3	1.0322E-08	4.4436E-10	1.0420E-08	4.5572E-10
PuO2	8.6271E-09	1.9720E-10	8.6252E-09	1.9725E-10
RaO	3.5087E-12	4.1045E-13	3.5429E-12	4.1531E-13
Rb2O	1.4284E-06	9.7181E-08	1.4422E-06	9.8079E-08
Rh2O3	3.2300E-06	7.4843E-08	3.2628E-06	7.4920E-08
RuO2	1.5279E-05	3.7936E-07	1.5453E-05	3.8069E-07
SO3	3.0764E-03	1.4671E-04	3.0794E-03	1.4718E-04
Sb2O3	2.6523E-07	3.1000E-08	2.6529E-07	3.1142E-08
SeO2	2.1375E-06	2.4905E-07	2.1492E-06	2.5179E-07
SiO2	4.5186E-01	3.1904E-03	4.5123E-01	3.1694E-03
Sm2O3	6.8520E-08	3.8034E-09	6.8750E-08	3.8067E-09
SnO2	6.0563E-08	2.6412E-09	6.0942E-08	2.6088E-09
SrO	1.3040E-07	3.0325E-09	1.3035E-07	3.0178E-09
Ta2O5	4.2542E-08	1.8486E-09	4.2965E-08	1.8618E-09
Tc2O7	2.0510E-06	3.1509E-07	2.0595E-06	3.1741E-07
TeO2	1.0220E-07	1.1941E-08	1.0324E-07	1.2142E-08
ThO2	4.0771E-06	2.7557E-07	4.0830E-06	2.7580E-07
TiO2	1.4033E-02	1.2383E-04	1.4035E-02	1.2085E-04
Tl2O	7.3309E-07	7.3726E-08	7.3046E-07	7.3822E-08
UO3	5.8464E-05	1.9327E-06	5.8712E-05	1.9627E-06
V2O5	5.9802E-05	8.7013E-06	5.9827E-05	8.7866E-06
WO3	1.2019E-05	2.7741E-07	1.2135E-05	2.7847E-07
Y2O3	6.6051E-07	4.4754E-08	6.6695E-07	4.5200E-08
ZnO	3.5079E-02	2.5230E-04	3.5091E-02	2.4900E-04
ZrO2	3.0136E-02	2.2882E-04	3.0139E-02	2.2709E-04
SUM	1.0000E+00	NA	1.0000E+00	NA

The waste form composition is documented during production by reporting the $\overset{\text{oxide in}}{g_{ie}^{can}}$ values from Equation (123) in the Production Records. Currently, it is planned to calculate $\overset{\text{oxide in}}{g_{ie}^{can}}$ values for all components (*i*) for which analytical data are available for a particular container. However, it may be advantageous to trim the number of components to only those with concentrations greater than 0.5 wt% plus those associated with other limits and specifications. In any case, only the appropriate subset of *i* will be reported in the Production Records.

The addition of optional filler material and production of the final ILAW container data package are not part of the ILAW formulation algorithm.

6.5.3 Specification 2.2.2.7—Radiological Composition Documentation

The specific activity of radionuclides in each canister is calculated using Equation (125) and its SD using Equation (126):

$$a_{ie}^{rad\ in\ can} = \frac{\sum_{j=1}^5 \left(\tilde{a}_{ij}^{rad\ in\ MFPV, Step3} \tilde{M}_j^{oxide\ in\ MFPV, Step3} \right)}{\sum_{j=1}^5 \tilde{M}_j^{oxide\ in\ MFPV, Step3}} \tag{217}$$

$$s_{ie}^{rad\ in\ can} = \frac{\sqrt{\sum_{j=1}^5 \left(\tilde{s}_{ij}^{rad\ in\ MFPV, Step3} \tilde{M}_j^{oxide\ in\ MFPV, Step3} \right)^2}}{\sum_j \tilde{M}_j^{oxide\ in\ MFPV, Step3}} \tag{218}$$

The $a_{ie}^{rad\ in\ can}$ and $s_{ie}^{rad\ in\ can}$ values are given Table B-9 and $\tilde{M}_j^{oxide\ in\ MFPV, Step3}$ values are in Table B-8. The results of above calculations for the A501th and B501th Canisters are listed in Table 37.

Table 37. Specific Activities of Radionuclides in the A501th and B501th Canisters

Canister	Canister-A501		Canister-B501	
	$a_{i,A501}^{rad\ in\ can}$	$s_{i,A501}^{rad\ in\ can}$	$a_{i,B501}^{rad\ in\ can}$	$s_{i,B501}^{rad\ in\ can}$
Unit	mCi/g glass	mCi/g glass	mCi/g glass	mCi/g glass
59Ni	3.3472E-07	1.0736E-08	3.3777E-07	1.0848E-08
60Co	5.3639E-07	1.2425E-08	5.3858E-07	1.2392E-08
63Ni	3.0508E-05	9.8276E-07	3.0785E-05	9.9130E-07
79Se	9.9416E-07	9.9396E-08	9.9679E-07	9.9626E-08
90Sr	5.4680E-04	1.2710E-05	5.5065E-04	1.2632E-05
90Y	5.2940E-04	1.2267E-05	5.3313E-04	1.2272E-05
93mNb	1.3901E-03	4.4922E-05	1.4311E-03	4.5802E-05
93Zr	8.1602E-06	2.6273E-07	8.2091E-06	2.6361E-07
99Tc	2.2407E-05	3.4423E-06	2.2500E-05	3.4676E-06
106Ru	4.7546E-10	2.1079E-11	4.7403E-10	2.0994E-11
113mCd	6.0358E-06	1.9477E-07	6.0562E-06	1.9595E-07
125Sb	1.1587E-06	1.1275E-07	1.1552E-06	1.1337E-07
126Sn	1.3712E-06	5.9796E-08	1.3797E-06	5.9064E-08
129I	5.4573E-08	8.5840E-09	5.5124E-08	8.7124E-09
134Cs	2.1221E-10	1.7332E-11	2.1315E-10	1.7270E-11
137mBa	8.7747E-02	2.0433E-03	8.8181E-02	2.0330E-03
137Cs	4.4909E-05	2.2913E-06	4.5169E-05	2.2978E-06
151Sm	1.5561E-03	8.6375E-05	1.5614E-03	8.6452E-05
152Eu	2.6729E-07	6.2017E-09	2.6774E-07	6.1346E-09
154Eu	5.4817E-06	1.2746E-07	5.5288E-06	1.2759E-07
155Eu	2.4642E-06	5.7108E-08	2.4731E-06	5.7128E-08
226Ra	3.2344E-09	3.7852E-10	3.2659E-09	3.8302E-10
227Ac	3.8837E-09	1.2425E-10	3.9219E-09	1.2690E-10
228Ra	1.2977E-09	2.1289E-10	1.2991E-09	2.1196E-10
229Th	1.8629E-10	2.4561E-11	1.8562E-10	2.4442E-11
231Pa	1.0714E-08	1.4064E-09	1.0817E-08	1.4163E-09
232Th	3.9270E-10	1.2706E-11	3.9326E-10	1.2679E-11

Canister	Canister-A501		Canister-B501	
	$a_{i,A501}^{can}$ rad in can	$S_{i,A501}^{can}$ rad in can	$a_{i,B501}^{can}$ rad in can	$S_{i,B501}^{can}$ rad in can
232U	5.2612E-10	1.2171E-11	5.2662E-10	1.2163E-11
233U	2.4604E-08	5.7071E-10	2.4719E-08	5.7249E-10
234U	1.4153E-08	3.2624E-10	1.4250E-08	3.2647E-10
235U	5.3477E-10	1.7169E-11	5.3831E-10	1.7253E-11
236U	9.8127E-10	2.2759E-11	9.8869E-10	2.2862E-11
237Np	7.2759E-08	1.6754E-09	7.3028E-08	1.6770E-09
238Pu	3.7893E-08	8.7870E-10	3.7946E-08	8.7215E-10
238U	1.0577E-08	3.4113E-10	1.0646E-08	3.4241E-10
239Pu	4.4142E-07	1.0291E-08	4.4133E-07	1.0285E-08
240Pu	1.0764E-07	3.4720E-09	1.0759E-07	3.4945E-09
241Am	5.3429E-07	1.8087E-08	5.3326E-07	1.7799E-08
241Pu	1.2268E-06	5.3282E-08	1.2250E-06	5.2798E-08
242Cm	2.7044E-09	8.6873E-11	2.7068E-09	8.6997E-11
242Pu	1.1876E-11	3.8190E-13	1.1873E-11	3.7935E-13
243Am	8.6297E-11	3.7908E-12	8.6537E-11	3.8211E-12
243Cm	3.1863E-10	1.3825E-11	3.2100E-10	1.3892E-11
244Cm	6.4958E-09	2.8185E-10	6.5463E-09	2.8067E-10
TRU	1.2009E-06	2.1183E-08	1.2001E-06	2.0939E-08

6.5.4 Specification 2.2.2.8—Radionuclide Concentration Limitations

The specific activity data given in Table 37 are used to calculate the quantities for radionuclide concentration limitations. For those radionuclides with limits expressed in Ci/m³ unit, the specific activities and their SD's are converted to the activities per unit glass volume using Equations (128) and (129). The sum of fractions of activity values are calculated using Equations (130) and (131) based on the Class C limits for each radionuclide given in Table 15 and Table 16. The k^{rad} was assumed to be 2, which represents 95.45% confidence level. The results of these calculations are summarized in Table 38.

Table 38. Results of Calculating the Quantities for Radionuclide Concentration Limitations in the A501th and B501th Canisters

Constraint	Canister-A501	Canister-B501
$\hat{a}_{137Cs,e}^{can} + k^{rad} \hat{S}_{137Cs,e}^{can}$ (Ci/m ³)	0.1351	0.1359
$\hat{a}_{90Sr,e}^{can} + k^{rad} \hat{S}_{90Sr,e}^{can}$ (Ci/m ³)	1.5621	1.5722
$SF_{LL,e}^{can} + k^{rad} S_{LL,e}^{radSF in can}$	0.04092	0.04106
$SF_{SL,e}^{can} + k^{rad} S_{SL,e}^{radSF in can}$	0.00037	0.00037

6.5.5 Specification 2.2.2.9—Surface Dose Rate Limitations

As mentioned in Section 5.5.5, the surface dose rate calculation is not performed but the measured dose rate will be included in the production records.

6.5.6 Specification 2.2.2.17—Waste form Testing

The glass composition and its SD values given in Table 36 are used to calculate the predicted PCT and VHT responses and uncertainties. The results of calculations described in Section 5.5.6 are summarized in Table 39.

Table 39. Summary of PCT and VHT Results for the ILAW in the A501th and B501th Canisters

Property	P^{prop}	U_{pred}^{prop}	U_{comp}^{prop}	$B_{ucci,lcci}^{prop}$
Canister-A501				
$\ln(r_B)$	-0.0263	0.1469	0.1289	0.2495
$\ln(r_{Na})$	-0.1087	0.1567	0.1093	0.1573
$\ln(D)$	2.3468	0.6200	0.4598	3.4266
Canister-B501				
$\ln(r_B)$	-0.0134	0.1478	0.1268	0.2630
$\ln(r_{Na})$	-0.0996	0.1583	0.1086	0.1672
$\ln(D)$	2.3706	0.6246	0.4833	3.4785

6.5.7 Specification 2.2.2.17—Manifesting

The data required for manifesting of the glass composition and radionuclide concentrations were all demonstrated above. Those required elements will be included in the waste manifest that accompanies the Production Records.

7 Summary and Recommendations

This report documents the current ILAW formulation algorithm. The algorithm is still preliminary; a number of WTP plant performance assumptions (e.g. analytical uncertainty, see Appendix C) were made because of a lack of data. These assumptions need to be updated as data become available. The equations required to meet the entire product compliance-related constraints, along with a few key processing constraints, are described in some detail. Additional detail is available in Piepel et al. (2005) for equations that were used or adapted from that document. The inputs to the equations are values measured during processing of waste at WTP and values obtained through design, research, and testing before production. Preliminary values for the constants currently available are documented in Appendix A. A detailed example is followed through most of the equations, with the results described in the text and tabulated in Appendix B. A summary of data requirements for this algorithm to be complete is included in Appendix C.

It is recommended that the approach and equations described in this document be used to calculate 1) target glass compositions, 2) LAW transfers to the MFPV, 3) GFC mass additions to the MFPV, 4) resulting glass compositions, 5) glass properties, and 6) uncertainties in glass composition and properties until it is updated with plant performance data or changes to the processing and/or qualification approach. It is further recommended that those values listed as preliminary or described as a value to be updated be tracked and updated when possible. This document will be updated as needed, as new data are available or changes to approaches/constraints are made.

This set of equations will make a suitable starting point for the development of plant control and waste form compliance software. In addition, sufficient data to perform an initial check of any to-be-developed software are included in Appendix B.

8 References

8.1 Project Documents

- 24590-BOF-3YD-GFR-00001, Rev 0. *System Description for the WTP Glass Formers Reagent System (GFR).*
- 24590-HLW-RPT-RT-05-001, Rev. 0, *Preliminary IHLW Formulation Algorithm Description.*
- 24590-LAW-3PS-AE00-T00001, Rev. 4, *Engineering Specification for Low Activity Waste Melters.*
- 24590-LAW-3YD-LCP-00001, Rev. 2, *System Description for the LAW Concentrate Receipt Process (LCP).*
- 24590-LAW-3YD-LFP-00001, Rev. 2, *System Description for the Low-Activity Waste Melter Feed Process System (LFP).*
- 24590-LAW-M0D-LMP-00002, Rev. 1, *Data Sheet Low Activity Waste Melter 2.*
- 24590-LAW-M4C-20-00002, Rev. 0, *LAW LCP and LFP Batch Volumes (LCP-VSL-00001,-00002, LFP-VSL-00001, -00002, -00003, -00004).*
- 24590-LAW-M4C-LFP-00002, Rev. B *WTP Calculation Sheet: Determining the LAW Glass Former Constituents and Amounts for G2 and ACM Models.*
- 24590-LAW-M6C-LCP-00001, Rev. 1, *Concentrate Receipt Vessels LCP-VSL-00001/00002 Sizing.*
- 24590-LAW-M6C-LFP-00001, Rev. 1, *LFP-VSL-00001 and LFP-VSL-00003 Sizing.*
- 24590-LAW-M6C-LFP-00002, Rev. 1, *LFP-VSL-00002 and LFP-VSL-00004 Sizing.*
- 24590-LAW-RPT-RT-10-001, Rev. 0, *Component Partitioning between Glass and Offgas Streams in Low-Activity Waste Melters.*
- 24590-LAW-RPT-RT-11-001, Rev. 0, *Evaluation of Mixing, Sampling, and Level Uncertainties for ILAW Glass Qualification.*
- 24590-WTP-3PS-JL10-T0002, Rev 0, *Engineering Specification for Radar Level Measurement.*
- 24590-WTP-3YD-50-00002, Rev. 0, *WTP Integrated Process Strategy Description.*
- 24590-WTP-MDD-PR-01-002, Rev. 9, *Dynamic (G2) Model Model Design Document.*
- 24590-WTP-MRQ-PO-03-033, Rev. 0, *Update RAM Data for the LMP System, Appendix A.*
- 24590-WTP-PL-PR-04-0001, Rev. 2, *Integrated Sampling and Analysis Requirements Document.*
- 24590-WTP-PL-RT-03-001, Rev. 4, *ILAW Product Compliance Plan.*
- 24590-WTP-RPT-ENV-03-003, Rev. 1, *Land Disposal Restriction Treatability Variance Petition for Hanford Tank Waste.*
- 24590-WTP-RPT-PO-07-002, Rev. 0, *Dynamic (G2) Flowsheet Assessment of the Effect of M-12 Modifications on Pretreatment Capacity.*
- CCN 111456. Memorandum, David Dodd/Bruce Kaiser to JD Vienna: *Estimated Analytical Measurement Uncertainties for Selected Analytes.*
- CCN 116150. Memorandum, JM Perez to JD Vienna: *LAW Melter Feed Property Correlations.* 16 March 2005.

CCN 132102. Memorandum, David Dodd/Bruce Kaiser to JD Vienna: *Estimated Analytical Measurements Uncertainties of Selected HLW Analytes*.

CCN 150795. Memorandum, JD Vienna to L Petkus: *Halide, Chromate, and Phosphate Impacts on LAW Glass Salt Limits*.

8.2 Codes and Standards

10 CFR 61.55, *Licensing Requirements for Land Disposal of Radioactive Waste, Waste Classification*. Code of Federal Regulations, as amended.

49 CFR 172.101, *Purpose and Use of Hazardous Materials Table*. Code of Federal Regulations, as amended.

8.3 Other Documents

Andre, L. 2004. *Prototypic LAW Container and HLW Canister Glass Fill Test Results Report*. TRR-PLT-080, Rev. 0, Duratek, Inc., Columbia, MD.

ASTM. 2002. *Standard Test Methods for Determining Chemical Durability of Nuclear, Hazardous, and Mixed Waste Glasses and Multiphase Glass Ceramics: The Product Consistency Test (PCT)*. ASTM C 1285-02, American Society for Testing and Materials, West Conshohocken, PA.

Deiner, G, M Brandys, TB Edwards, DS Dickey, KS Matlack, and IL Pegg. 2006. *Test Plan: Pretreated Waste and Melter Feed Composition Variability Testing Using HLW and LAW Simulants*, VSL-06T1000-1. River Protection Project, Waste Treatment Plant, Richland, WA. 24590-101-TSA-W000-0009-176-00001, Rev 00B.

DOE. 2000. Contract DE-AC27-01RV14136, as amended, U.S. Department of Energy, Richland, WA.

Eibling, RE, RF Schumacher, and EK Hansen. 2003. *Development of Simulants To Support Mixing Tests for High Level Waste and Low Activity Waste*, WSRC-TR-2003-00220, Rev. 0, Westinghouse Savannah River Company, Aiken, SC.

Matlack, KS, W Gong, and IL Pegg. 2003a. *DuraMelter 100 Sub-Envelope Changeover Testing Using LAW Sub-Envelopes A1 and C1 Feeds in Support of the LAW Pilot Melter*, VSL-02R62N0-6, Rev. 0, Vitreous State Laboratory, The Catholic University of America, Washington, DC. 24590-101-TSA-W000-0009-106-07, Rev. 00C.

Matlack, KS, W Gong, and IL Pegg. 2003b. *DuraMelter 100 Sub-Envelope Changeover Testing Using LAW Sub-Envelope A2 and B1 Feeds in Support of the LAW Pilot Melter*, VSL-03R3410-1, Rev. 0, Vitreous State Laboratory, The Catholic University of America, Washington, DC. 24590-101-TSA-W000-0009-144-04, Rev. 00A

Matlack, KS, W Gong, and IL Pegg. 2003c. *Compositional Variation Tests on DuraMelter 100 with LAW Sub-Envelope B2 Feed in Support of the LAW Pilot Melter*, VSL-03R3410-2, Rev. 0, Vitreous State Laboratory, The Catholic University of America, Washington, DC. 24590-101-TSA-W000-0009-135-04, Rev. 00B

Matlack, KS, W Gong, and IL Pegg. 2003d. *DuraMelter 100 Sub-Envelope Changeover Testing Using LAW Sub-Envelope A3 and C2 Feeds in Support of the LAW Pilot Melter*, VSL-03R3410-3, Rev. 0, Vitreous State Laboratory, The Catholic University of America, Washington, DC. 24590-101-TSA-W000-0009-106-17, Rev. 00B.

Matlack, KS, W Gong, T Bardakci, N D'Angelo, M Brandys, WK Kot, and IL Pegg. 2005. *Regulatory Off-Gas Emissions Testing on the DM1200 Melter System Using HLW and LAW Simulants*, VSL-05R5830-

- 1, Rev. 0, Vitreous State Laboratory, The Catholic University of America, Washington, D.C. – 24590-101-TSA-W000-0009-166-00001.
- Muller, IS, G Diener, I Joseph, and IL Pegg. 2004. *Proposed Approach for Development of LAW Glass Formulation Correlation*. VSL-04L4460-1, Rev. 0, Vitreous State Laboratory, The Catholic University of America, Washington, DC.
- Muller, IS, H Gan, AC Buechele, and IL Pegg. 2002. *Enhanced K-3 Refractory Corrosion with LAW AZ-102 Glass Formulations*, VSL-02S4600-1, Rev. 0, Vitreous State Laboratory, The Catholic University of America, Washington, DC.
- Muller, IS, H Gan, IL Pegg, SK Cooley, and GF Piepel. 2005. *Phase I ILAW PCT and VHT Model Development*. VSL-04R4480-2, Rev. 0, Vitreous State Laboratory, The Catholic University of America, Washington, DC.
- Piepel, GF, BG Amidan, A Heredia-Langner, DR Weier, and SK Cooley. 2005. *Statistical Methods and Results for WTP IHLW and ILAW Compliance*. WTP-RPT-072, Rev. 0, Battelle—Pacific Northwest Division, Richland, WA.
- Piepel GF, Cooley SK, Muller I, Gan H, Joseph I, and Pegg IL. 2007. *ILAW PCT, VHT, Viscosity and Electrical Conductivity Model Development*. VSL-07R1230-1, Rev 0, Vitreous State laboratory, Catholic University of America, Washington DC.
- Poloski, A, H Smith, G Smith, and T Calloway. 2004. *Technical Basis for LAW Vitrification Stream Physical and Rheological Property Bounding Conditions*. PNWD-3398, WTP-RPT-098, Rev. 0, Battelle—Pacific Northwest Division, Richland, WA.
- Schumacher, RF. 2003. *Characterization of HLW and LAW Glass Formers – Final Report*, WSRC-TR-2002-00282, Rev. 1 (SRT-RPP-2002-00146. Rev. 1), Westinghouse Savannah River Company, Aiken, SC.
- Schumacher, RF, EK Hansen, TM Jones, and JE Josephs. 2003. *Evaluation of Wetting Agents to Mitigate Dusting of Glass Forming Chemicals During Delivery to the Melter Feed Preparation Vessel*, WSRC-TR-2003-00209, Rev. 0, Westinghouse Savannah River Company, Aiken, SC.

Appendix A—Inputs Used in Calculations

Table A-1. Oxide Conversion Factors (f_i) for Chemical Elements and Radionuclides and Specific Activities (A_i) for Radionuclides

Element	Glass oxide	f_i	Radionuclide	Glass oxide	f_i	A_i , Ci/g
Ac	Ac2O3	NA	59Ni	59NiO	1.2714800	7.982E-02
Ag	Ag2O	1.0741618	60Co	60CoO	1.2669102	1.131E+03
Al	Al2O3	1.8894637	63Ni	63NiO	1.2542412	5.738E+01
Am	Am2O3	NA	79Se	79SeO2	1.4054638	6.969E-02
As	As2O5	1.5338715	90Sr	90SrO	1.1779550	1.388E+02
B	B2O3	3.2198779	90Y	90Y2O3	1.2669393	5.437E+05
Ba	BaO	1.1165059	93mNb	93mNb2O5	1.4305248	2.386E+02
Be	BeO	2.7753081	93Zr	93ZrO2	1.3444224	2.515E-03
Bi	Bi2O3	1.1148390	99Tc	99Tc2O7	1.5661615	1.711E-02
Ca	CaO	1.3992065	106Ru	106RuO2	1.3018755	3.349E+03
Cd	CdO	1.1423295	113mCd	113mCdO	1.1417075	2.311E+02
Ce	Ce2O3	1.1712814	125Sb	125Sb2O3	1.1919928	1.037E+03
Cl	Cl	1.0000000	126Sn	126SnO2	1.2539587	2.839E-02
Cm	Cm2O3	NA	129I	129I	1.0000000	1.768E-04
Co	CoO	1.2714836	134Cs	134Cs2O	1.0596993	1.293E+03
Cr	Cr2O3	1.4615558	137mBa	137mBaO	1.1167839	5.382E+08
Cs	Cs2O	1.0601909	137Cs	137Cs2O	1.0583920	8.655E+01
Cu	CuO	1.2517767	151Sm	151Sm2O3	1.1589344	2.632E+01
Eu	Eu2O3	NA	152Eu	152Eu2O3	1.1578888	1.740E+02
F	F	1.0000000	154Eu	154Eu2O3	1.1558383	2.703E+02
Fe	Fe2O3	1.4297294	155Eu	155Eu2O3	1.1548329	4.762E+02
Gd	Gd2O3	1.1526175	226Ra	226RaO	1.0707860	9.885E-01
Hg	HgO	1.0797617	227Ac	227Ac2O3	1.1057099	7.232E+01
I	I	NA	228Ra	228RaO	1.0701728	2.727E+02
K	K2O	1.2046048	229Th	229ThO2	1.1397132	2.127E-01
La	La2O3	1.1727729	231Pa	231Pa2O5	1.1731267	4.723E-02
Li	Li2O	2.1525285	232Th	232ThO2	1.1379033	1.097E-07
Mg	MgO	1.6582761	232U	232UO3	1.2068558	2.207E+01
Mn	MnO	1.2912262	233U	233UO3	1.2059655	9.633E-03
Mo	MoO3	1.5002939	234U	234UO3	1.2050846	6.217E-03
Na	Na2O	1.3479678	235U	235UO3	1.2042094	2.161E-06
Nb	Nb2O5	NA	236U	236UO3	1.2033426	6.468E-05
Nd	Nd2O3	1.1663831	237Np	237NpO2	1.1349887	7.047E-04
Ni	NiO	1.2725928	238Pu	238PuO2	1.1344205	1.712E+01
Np	NpO2	NA	238U	238UO3	1.2016299	3.361E-07
P	P2O5	2.2913672	239Pu	239PuO2	1.1338571	6.202E-02
Pa	Pa2O5	NA	240Pu	240PuO2	1.1332983	2.269E-01
Pb	PbO	1.0772172	241Am	241Am2O3	1.0995578	3.427E+00
Pd	PdO	1.1503420	241Pu	241PuO2	1.1327437	1.030E+02
Pr	Pr2O3	1.1703179	242Cm	242Cm2O3	1.0991457	3.311E+03
Pu	PuO2	NA	242Pu	242PuO2	1.1321942	3.954E-03
Ra	RaO	NA	243Am	243Am2O3	1.0987369	1.997E-01
Rb	Rb2O	1.0935990	243Cm	243Cm2O3	1.0987369	4.903E+01
Rh	Rh2O3	1.2332149	244Cm	244Cm2O3	1.0983316	8.093E+01

Element	Glass oxide	<i>f_i</i>
Ru	RuO2	1.3166004
S	SO3	2.4968565
Sb	Sb2O3	1.1971065
Se	SeO2	1.4052533
Si	SiO2	2.1393352
Sm	Sm2O3	NA
Sn	SnO2	NA
Sr	SrO	1.1825999
Ta	Ta2O5	1.2210498
Tc	Tc2O7	NA
Te	TeO2	1.2507743
Th	ThO2	1.1379032
Ti	TiO2	1.6683124
Tl	Tl2O	1.0391407
U	UO3	1.2016486
V	V2O5	1.7851850
W	WO3	1.2610726
Y	Y2O3	1.2699384
Zn	ZnO	1.2446766
Zr	ZrO2	1.3507717

NA: not applicable (these components have radionuclides only)

Table A-2. Minimum, CRV Analytical %RSD, and CRV Mixing and Sampling %RSD

Element	MRQ mg/L	Analytical High %RSD	Analytical Low %RSD	CRV mix/samp %RSD
Ac	NA	NA	NA	NA
Ag	0.2	20	5	1.47%
Al	18	5	5	1.47%
Am	NA	NA	NA	NA
As	2.8	25	10	1.47%
B	0.4	25	10	1.47%
Ba	0.4	15	5	1.47%
Be	0.03	25	5	1.47%
Bi	0.9	15	10	1.47%
Ca	2	15	5	1.47%
Cd	0.06	10	5	1.47%
Ce	2	25	10	1.47%
Cl	19	10	10	1.47%
Cm	NA	NA	NA	NA
Co	0.1	25	10	1.47%
Cr	0.7	5	5	1.47%
Cs	0.1	15	10	1.47%
Cu	2	25	10	1.47%
Eu	NA	NA	NA	NA
F	19	10	10	1.47%
Fe	2	5	5	1.47%
Gd ^(a)	1	15	5	1.47%
Hg	0.001	10	5	1.47%
I	NA	NA	NA	NA
K	10	5	5	1.47%
La	0.6	10	5	1.47%
Li	0.3	15	5	1.47%
Mg	9	25	10	1.47%
Mn	2	15	5	1.47%
Mo	3	10	5	1.47%
Na	200	10	10	1.47%
Nb	NA	NA	NA	NA
Nd	1	15	5	1.47%
Ni	7	10	5	1.47%
Np	NA	NA	NA	NA
P	12	15	10	1.47%
Pa	NA	NA	NA	NA
Pb	0.9	15	15	1.47%
Pd	1	15	15	1.47%
Pr	1	15	10	1.47%
Pu	NA	NA	NA	NA
Ra	NA	NA	NA	NA
Rb	10	25	15	1.47%
Rh	0.004	20	5	1.47%
Ru	0.02	25	5	1.47%
S	10	10	5	1.47%

Element	MRQ mg/L	Analytical High %RSD	Analytical Low %RSD	CRV mix/samp %RSD
Sb	0.3	25	10	1.47%
Se	4	25	10	1.47%
Si	4	15	5	1.47%
Sm	NA	NA	NA	NA
Sn	NA	NA	NA	NA
Sr	0.01	5	5	1.47%
Ta	0.2	15	5	1.47%
Tc	NA	NA	NA	NA
Te	1	25	10	1.47%
Th ^(b)	2	25	10	1.47%
Ti	0.07	25	5	1.47%
Tl	0.02	25	10	1.47%
U ^(a)	1	15	5	1.47%
V	0.07	15	5	1.47%
W	0.2	15	5	1.47%
Y	0.6	25	5	1.47%
Zn	4	25	5	1.47%
Zr	2	15	5	1.47%
Radionuclide	MRQ mCi/L	Analytical High %RSD	Analytical Low %RSD	CRV mix/samp %RSD
59Ni	7.982E-07	10	10	1.47%
60Co	1.131E-05	5	5	1.47%
63Ni	5.738E-02	10	10	1.47%
79Se	6.969E-05	15	10	1.47%
90Sr	1.388E-06	5	5	1.47%
90Y ^(d)	1.388E-06	5	5	1.47%
93mNb	2.386E-04	15	10	1.47%
93Zr	2.515E-06	10	10	1.47%
99Tc	1.711E-06	10	10	1.47%
106Ru ^(c)	2.009E-03	15	10	1.47%
113mCd	4.622E-05	25	10	1.47%
125Sb	3.111E-04	25	5	1.47%
126Sn	5.678E-06	20	15	1.47%
129I	1.768E-04	15	10	1.47%
134Cs	4.526E-06	25	10	1.47%
137mBa ^(d)	1.731E-06	15	5	1.47%
137Cs	1.731E-06	15	5	1.47%
151Sm	5.264E-01	20	10	1.47%
152Eu	1.740E-06	5	5	1.47%
154Eu	2.703E-06	5	5	1.47%
155Eu	4.762E-05	5	5	1.47%
226Ra	9.885E-07	25	10	1.47%
227Ac	7.232E-07	50	10	1.47%
228Ra	2.727E-03	50	25	1.47%
229Th	6.381E-04	50	50	1.47%
231Pa	1.417E-04	50	50	1.47%
232Th	3.291E-10	25	10	1.47%

Radionuclide	MRQ mCi/L	Analytical High %RSD	Analytical Low %RSD	CRV mix/samp %RSD
232U	6.621E-08	25	5	1.47%
233U	9.633E-07	10	5	1.47%
234U	6.217E-06	5	5	1.47%
235U	2.161E-07	10	5	1.47%
236U	6.468E-08	10	5	1.47%
237Np	7.047E-07	10	5	1.47%
238Pu	1.712E-07	5	5	1.47%
238U	6.722E-09	10	10	1.47%
239Pu	6.202E-08	5	5	1.47%
240Pu	2.269E-09	10	10	1.47%
241Am	3.427E-06	10	10	1.47%
241Pu	1.030E-07	15	15	1.47%
242Cm	3.311E-06	10	10	1.47%
242Pu	3.954E-11	10	10	1.47%
243Am	3.994E-08	15	15	1.47%
243Cm	9.806E-07	15	15	1.47%
244Cm	2.428E-06	15	15	1.47%

NA: not applicable (these components have radionuclides only)

Note Analytical High and Low %RSD are from CCN 111456. CRV mixing and sampling %RSD is from 24590-LAW-RPT-RT-11-001, Rev 0.

- (a) Data not available in CCN 111456. The value for Nd was assumed.
- (b) Data not available in CCN 111456. The value for Ce was assumed.
- (c) Data not available in CCN 111456. The value for 106Ru given for HLW in CCN 132102 was assumed.
- (d) Data for 90Y and 137mBa are not given in CCN 111456 because they are short-lived daughters of 90Sr and 137Cs. The same %RSDs as for 90Sr and 137Cs were assumed.

Table A-3. Decontamination Factor (DF) in ln(DF)^(a) and Nominal Retention Factor (ν_i)

Component	ln(DF), Min	ln(DF), Median	ln(DF), Max	Notes ^(a)	ν_i , Nominal ^(b)
Ac2O3	2.9601	6.8772	11.1239	Non-volatile	0.99721
Ag2O	1.8563	4.1940	6.4944	Semi-volatile	0.97803
Al2O3	5.0764	7.0814	8.8901	Non-volatile from data	0.99888
Am2O3	1.8563	4.1940	6.4944	Semi-volatile	0.97803
As2O5	0.0945	1.5296	4.2370	Volatile	0.77121
B2O3	3.7080	4.5886	5.8519	Semi-volatile from data	0.98968
BaO	2.9601	6.8772	11.1239	Non-volatile	0.99721
BeO	2.9601	6.8772	11.1239	Non-volatile	0.99721
Bi2O3	1.8563	4.1940	6.4944	Semi-volatile	0.97803
CaO	5.2311	7.0825	8.6034	Non-volatile from data	0.99892
CdO	2.9601	6.8772	11.1239	Non-volatile	0.99721
Ce2O3	2.9601	6.8772	11.1239	Non-volatile	0.99721
Cl	0.0979	0.7583	1.9095	Volatile from data	0.54407
Cm2O3	2.9601	6.8772	11.1239	Non-volatile	0.99721
CoO	2.9601	6.8772	11.1239	Non-volatile	0.99721
Cr2O3	1.8563	3.0681	5.3033	Semi-volatile from data	0.95261
Cs2O	0.4700	2.3609	4.2370	Volatile from data	0.87902
CuO	2.9601	6.8772	11.1239	Non-volatile	0.99721
Eu2O3	2.9601	6.8772	11.1239	Non-volatile	0.99721
F	0.1179	1.4682	2.4361	Volatile from data	0.72984
Fe2O3	4.9381	6.6712	8.8984	Non-volatile from data	0.99848
Gd2O3	2.9601	6.8772	11.1239	Non-volatile	0.99721
HgO	0.0000	0.0000	0.0000	Assumed	0
I	0.0945	0.5807	2.2660	Volatile from data	0.50961
K2O	2.0669	3.3844	5.5607	Semi-volatile from data	0.96423
La2O3	2.9601	6.8772	11.1239	Non-volatile	0.99721
Li2O	3.4689	5.9870	7.2894	Non-volatile from data	0.99601
MgO	7.2464	8.8618	11.0268	Non-volatile from data	0.99984
MnO	2.9601	6.8772	11.1239	Non-volatile	0.99721
MoO3	1.8563	4.1940	6.4944	Semi-volatile	0.97803
Na2O	3.4874	4.8633	6.4944	Semi-volatile from data	0.99136
Nb2O5	2.9601	6.8772	11.1239	Non-volatile	0.99721
Nd2O3	2.9601	6.8772	11.1239	Non-volatile	0.99721
NiO	3.9299	4.7875	6.3835	Non-volatile from data	0.99187
NpO2	2.9601	6.8772	11.1239	Non-volatile	0.99721
P2O5	2.9601	5.1381	6.7822	Non-volatile from data	0.99169
Pa2O5	2.9601	6.8772	11.1239	Non-volatile	0.99721
PbO	3.2542	4.4716	6.2971	Semi-volatile from data	0.98796
PdO	2.9601	6.8772	11.1239	Non-volatile	0.99721
Pr2O3	2.9601	6.8772	11.1239	Non-volatile	0.99721
PuO2	2.9601	6.8772	11.1239	Non-volatile	0.99721
RaO	0.0945	1.5296	4.2370	Volatile	0.77121
Rb2O	1.8563	4.1940	6.4944	Semi-volatile	0.97803
Rh2O3	2.9601	6.8772	11.1239	Non-volatile	0.99721
RuO2	1.8563	4.1940	6.4944	Semi-volatile	0.97803
SO3	0.6308	1.9694	3.2089	Volatile from data	0.84032
Sb2O3	0.0945	1.5296	4.2370	Volatile	0.77121

Component	ln(DF), Min	ln(DF), Median	ln(DF), Max	Notes ^(a)	v _i , Nominal ^(b)
SeO2	0.0945	1.5296	4.2370	Volatile	0.77121
SiO2	5.3471	7.5372	9.7527	Non-volatile from data	0.99926
Sm2O3	2.9601	6.8772	11.1239	Non-volatile	0.99721
SnO2	2.9601	6.8772	11.1239	Non-volatile	0.99721
SrO	2.9601	6.8772	11.1239	Non-volatile	0.99721
Ta2O5	2.9601	6.8772	11.1239	Non-volatile	0.99721
Tc2O7	0.0953	0.4700	1.6094	Volatile from data	0.43049
TeO2	0.0945	1.5296	4.2370	Volatile	0.77121
ThO2	2.9601	6.8772	11.1239	Non-volatile	0.99721
TiO2	4.6308	6.1247	8.0740	Non-volatile from data	0.99752
Tl2O	0.0945	1.5296	4.2370	Volatile	0.77121
UO3	2.9601	6.8772	11.1239	Non-volatile	0.99721
V2O5	1.8563	4.1940	6.4944	Semi-volatile	0.97803
WO3	2.9601	6.8772	11.1239	Non-volatile	0.99721
Y2O3	2.9601	6.8772	11.1239	Non-volatile	0.99721
ZnO	4.7353	6.2383	7.8709	Non-volatile from data	0.99773
ZrO2	7.2204	8.7143	11.1239	Non-volatile from data	0.99982

(a) 24590-LAW-RPT-RT-10-001, Rev. 0

(b) Obtained from 500,000 Monte Carlo simulations for ln(DF) and used for nominal glass composition calculation.

Table A-4. GFC Compositions: Minimum, Most Likely, and Maximum Values Used for Composition Uncertainty Calculations in Monte Carlo Method

Minimum											
Comp	Kyanite	Boric Acid	Wollastonite	Hematite	Li Carbonate	Olivine	Na Carbonate	Silica	Rutile	Zincite	Zircon
Ac2O3	0	0	0	0	0	0	0	0	0	0	0
Ag2O	0	0	0	0	0	0	0	0	0	0	0
Al2O3	0.54	0	0.0013	0.0099	0	0.0003	0	0.0004	0	0	0.001
Am2O3	0	0	0	0	0	0	0	0	0	0	0
As2O5	0	0	0	0	0	0	0	0	0	0	0
B2O3	0	0.5625	0	0	0	0	0	0	0	0	0
BaO	0	0	0	0	0	0	0	0	0	0	0
BeO	0	0	0	0	0	0	0	0	0	0	0
Bi2O3	0	0	0	0	0	0	0	0	0	0	0
CaO	0	0	0.4477	0	0	0	0	0	0	0	0
CdO	0	0	0	0	0	0	0	0	0	0	0
Ce2O3	0	0	0	0	0	0	0	0	0	0	0
Cl	0	0	0	0	0	0	0	0	0	0	0
Cm2O3	0	0	0	0	0	0	0	0	0	0	0
CoO	0	0	0	0	0	0	0	0	0	0	0
Cr2O3	0	0	0	0	0	0	0	0	0	0	0
Cs2O	0	0	0	0	0	0	0	0	0	0	0
CuO	0	0	0	0	0	0	0	0	0	0	0
Eu2O3	0	0	0	0	0	0	0	0	0	0	0
F	0	0	0	0	0	0	0	0	0	0	0
Fe2O3	0.0042	0	0.0029	0.9615	0	0.0468	0	0.0001	0	0	0.0006
Gd2O3	0	0	0	0	0	0	0	0	0	0	0
HgO	0	0	0	0	0	0	0	0	0	0	0
I	0	0	0	0	0	0	0	0	0	0	0
K2O	0	0	0	0	0	0	0	0	0	0	0
La2O3	0	0	0	0	0	0	0	0	0	0	0
Li2O	0	0	0	0	0.4	0	0	0	0	0	0
MgO	0	0	0	0.0001	0	0.4634	0	0	0	0	0
MnO	0	0	0.0009	0.0003	0	0	0	0	0	0	0
MoO3	0	0	0	0	0	0	0	0	0	0	0
Na2O	0	0	0	0	0	0	0.5831	0	0	0	0
Nb2O5	0	0	0	0	0	0	0	0	0	0	0
Nd2O3	0	0	0	0	0	0	0	0	0	0	0
NiO	0	0	0	0	0	0.0022	0	0	0	0	0
NpO2	0	0	0	0	0	0	0	0	0	0	0
P2O5	0	0	0	0.0018	0	0	0	0	0	0	0
Pa2O5	0	0	0	0	0	0	0	0	0	0	0
PbO	0	0	0	0	0	0	0	0	0	0	0
PdO	0	0	0	0	0	0	0	0	0	0	0
Pr2O3	0	0	0	0	0	0	0	0	0	0	0
PuO2	0	0	0	0	0	0	0	0	0	0	0
RaO	0	0	0	0	0	0	0	0	0	0	0
Rb2O	0	0	0	0	0	0	0	0	0	0	0
Rh2O3	0	0	0	0	0	0	0	0	0	0	0
RuO2	0	0	0	0	0	0	0	0	0	0	0

Minimum											
Comp	Kyanite	Boric Acid	Wollas-tonite	Hematite	Li Carbonate	Olivine	Na Carbonate	Silica	Rutile	Zincite	Zircon
SO3	0	0	0	0.0006	0	0	0	0	0	0	0
Sb2O3	0	0	0	0	0	0	0	0	0	0	0
SeO2	0	0	0	0	0	0	0	0	0	0	0
SiO2	0.39	0	0.48	0.0084	0	0.4085	0	0.992	0	0	0.32
Sm2O3	0	0	0	0	0	0	0	0	0	0	0
SnO2	0	0	0	0	0	0	0	0	0	0	0
SrO	0	0	0	0	0	0	0	0	0	0	0
Ta2O5	0	0	0	0	0	0	0	0	0	0	0
Tc2O7	0	0	0	0	0	0	0	0	0	0	0
TeO2	0	0	0	0	0	0	0	0	0	0	0
ThO2	0	0	0	0	0	0	0	0	0	0	0
TiO2	0.005	0	0.0001	0	0	0	0	0	0.928	0	0.0007
Tl2O	0	0	0	0	0	0	0	0	0	0	0
UO3	0	0	0	0	0	0	0	0	0	0	0.0003
V2O5	0	0	0	0	0	0	0	0	0	0	0
WO3	0	0	0	0	0	0	0	0	0	0	0
Y2O3	0	0	0	0	0	0	0	0	0	0	0
ZnO	0	0	0	0	0	0	0	0	0	0.993	0
ZrO2	0	0	0	0	0	0	0	0	0	0	0.65

Most Likely											
Comp	Kyanite	Boric Acid	Wollas-tonite	Hematite	Li Carbonate	Olivine	Na Carbonate	Silica	Rutile	Zincite	Zircon
Ac2O3	0	0	0	0	0	0	0	0	0	0	0
Ag2O	0	0	0	0	0	0	0	0	0	0	0
Al2O3	0.5703	0	0.002	0.015	0	0.0019	0	0.0014	0.005	0	0.0025
Am2O3	0	0	0	0	0	0	0	0	0	0	0
As2O5	0	0	0	0	0	0	0	0	0	0	0
B2O3	0	0.5652	0	0	0	0	0	0	0	0	0
BaO	0	0	0	0	0	0	0	0	0	0	0
BeO	0	0	0	0	0	0	0	0	0	0	0
Bi2O3	0	0	0	0	0	0	0	0	0	0	0
CaO	0.0003	0	0.475	0.0004	0	0.0002	0	0.0001	0	0	0
CdO	0	0	0	0	0	0	0	0	0	0.0001	0
Ce2O3	0	0	0	0	0	0	0	0	0	0	0
Cl	0	0	0	0	0.0001	0	0.0002	0	0	0	0
Cm2O3	0	0	0	0	0	0	0	0	0	0	0
CoO	0	0	0	0	0	0	0	0	0	0	0
Cr2O3	0	0	0	0	0.0001	0.0013	0	0	0.0016	0	0
Cs2O	0	0	0	0	0	0	0	0	0	0	0
CuO	0	0	0	0	0	0	0	0	0	0	0
Eu2O3	0	0	0	0	0	0	0	0	0	0	0
F	0	0	0	0	0	0	0	0	0	0	0
Fe2O3	0.0078	0	0.004	0.97	0	0.0768	0	0.0002	0.007	0	0.0008
Gd2O3	0	0	0	0	0	0	0	0	0	0	0
HgO	0	0	0	0	0	0	0	0	0	0	0
I	0	0	0	0	0	0	0	0	0	0	0

Most Likely											
Comp	Kyanite	Boric Acid	Wollastonite	Hematite	Li Carbonate	Olivine	Na Carbonate	Silica	Rutile	Zincite	Zircon
K2O	0	0	0	0	0	0	0	0	0	0	0
La2O3	0	0	0	0	0	0	0	0	0	0	0
Li2O	0	0	0	0	0.402	0	0	0	0	0	0
MgO	0.0001	0	0.001	0.001	0.0001	0.4801	0	0.0001	0	0	0
MnO	0	0	0.001	0.0012	0	0	0	0	0	0	0
MoO3	0	0	0	0	0	0	0	0	0	0	0
Na2O	0.0042	0	0	0	0.0008	0.0003	0.5837	0.0002	0	0	0
Nb2O5	0	0	0	0	0	0	0	0	0	0	0
Nd2O3	0	0	0	0	0	0	0	0	0	0	0
NiO	0	0	0	0	0	0.0037	0	0	0	0	0
NpO2	0	0	0	0	0	0	0	0	0	0	0
P2O5	0	0	0	0.0027	0	0	0	0	0	0	0
Pa2O5	0	0	0	0	0	0	0	0	0	0	0
PbO	0	0	0	0	0	0	0	0	0	0	0
PdO	0	0	0	0	0	0	0	0	0	0	0
Pr2O3	0	0	0	0	0	0	0	0	0	0	0
PuO2	0	0	0	0	0	0	0	0	0	0	0
RaO	0	0	0	0	0	0	0	0	0	0	0
Rb2O	0	0	0	0	0	0	0	0	0	0	0
Rh2O3	0	0	0	0	0	0	0	0	0	0	0
RuO2	0	0	0	0	0	0	0	0	0	0	0
SO3	0	0	0	0.0007	0.0003	0	0.0001	0	0	0	0
Sb2O3	0	0	0	0	0	0	0	0	0	0	0
SeO2	0	0	0	0	0	0	0	0	0	0	0
SiO2	0.4067	0	0.51	0.0135	0	0.4252	0	0.997	0.022	0	0.3225
Sm2O3	0	0	0	0	0	0	0	0	0	0	0
SnO2	0	0	0	0	0	0	0	0	0	0	0
SrO	0	0	0	0	0	0	0	0	0	0	0
Ta2O5	0	0	0	0	0	0	0	0	0	0	0
Tc2O7	0	0	0	0	0	0	0	0	0	0	0
TeO2	0	0	0	0	0	0	0	0	0	0	0
ThO2	0	0	0	0	0	0	0	0	0	0	0
TiO2	0.0079	0	0.0002	0	0	0	0	0.0001	0.932	0	0.001
Tl2O	0	0	0	0	0	0	0	0	0	0	0
UO3	0	0	0	0	0	0	0	0	0	0	0.0004
V2O5	0	0	0	0	0	0	0	0	0.0045	0	0
WO3	0	0	0	0	0	0	0	0	0	0	0
Y2O3	0	0	0	0	0	0	0	0	0	0	0
ZnO	0	0	0	0	0	0	0	0	0	0.999	0
ZrO2	0	0	0	0	0	0	0	0	0.019	0	0.66

Maximum											
Comp	Kyanite	Boric Acid	Wollastonite	Hematite	Li Carbonate	Olivine	Na Carbonate	Silica	Rutile	Zincite	Zircon
Ac2O3	0	0	0	0	0	0	0	0	0	0	0
Ag2O	0	0	0	0	0	0	0	0	0	0	0
Al2O3	0.6	0	0.0027	0.0201	0	0.0078	0	0.004	0.0075	0	0.004

Maximum											
Comp	Kyanite	Boric Acid	Wollas-tonite	Hema-tite	Li Carbonate	Olivine	Na Carbonate	Silica	Rutile	Zincite	Zircon
Am2O3	0	0	0	0	0	0	0	0	0	0	0
As2O5	0	0	0	0	0	0	0	0	0	0	0
B2O3	0	0.568	0	0	0	0	0	0	0	0	0
BaO	0	0	0	0	0	0	0	0	0	0	0
BeO	0	0	0	0	0	0	0	0	0	0	0
Bi2O3	0	0	0	0	0	0	0	0	0	0	0
CaO	0.0004	0	0.5023	0.0008	0.022	0.0003	0.0001	0.0002	0	0	0
CdO	0	0	0	0	0	0	0	0	0	0.0002	0
Ce2O3	0	0	0	0	0	0	0	0	0	0	0
Cl	0	0	0	0	0.0001	0	0.0002	0	0	0	0
Cm2O3	0	0	0	0	0	0	0	0	0	0	0
CoO	0	0	0	0	0	0	0	0	0	0	0
Cr2O3	0	0	0	0	0.0002	0.0078	0.0006	0	0.0075	0	0
Cs2O	0	0	0	0	0	0	0	0	0	0	0
CuO	0	0	0	0	0	0	0	0	0	0	0
Eu2O3	0	0	0	0	0	0	0	0	0	0	0
F	0	0	0	0	0	0	0	0	0	0	0
Fe2O3	0.01	0	0.0051	0.9785	0.0001	0.1068	0.0001	0.0004	0.025	0.0001	0.0009
Gd2O3	0	0	0	0	0	0	0	0	0	0	0
HgO	0	0	0	0	0	0	0	0	0	0	0
I	0	0	0	0	0	0	0	0	0	0	0
K2O	0.0007	0	0	0	0.0001	0	0	0.0002	0	0	0
La2O3	0	0	0	0	0	0	0	0	0	0	0
Li2O	0	0	0	0	0.4044	0	0	0	0	0	0
MgO	0.0004	0	0.001	0.0037	0.0002	0.4934	0.0001	0.0001	0	0	0
MnO	0	0	0.0011	0.0039	0	0	0	0	0	0.0001	0
MoO3	0	0	0	0	0	0	0	0	0	0	0
Na2O	0.0042	0	0	0	0.0011	0.0004	0.5848	0.0002	0	0	0
Nb2O5	0	0	0	0	0	0	0	0	0	0	0
Nd2O3	0	0	0	0	0	0	0	0	0	0	0
NiO	0	0	0	0	0	0.0052	0	0	0	0	0
NpO2	0	0	0	0	0	0	0	0	0	0	0
P2O5	0	0	0	0.0054	0	0	0	0	0.0007	0	0
Pa2O5	0	0	0	0	0	0	0	0	0	0	0
PbO	0	0	0	0	0	0	0	0	0	0.0001	0
PdO	0	0	0	0	0	0	0	0	0	0	0
Pr2O3	0	0	0	0	0	0	0	0	0	0	0
PuO2	0	0	0	0	0	0	0	0	0	0	0
RaO	0	0	0	0	0	0	0	0	0	0	0
Rb2O	0	0	0	0	0	0	0	0	0	0	0
Rh2O3	0	0	0	0	0	0	0	0	0	0	0
RuO2	0	0	0	0	0	0	0	0	0	0	0
SO3	0	0.0003	0	0.0009	0.0004	0	0.0002	0	0.0007	0	0
Sb2O3	0	0	0	0	0	0	0	0	0	0	0
SeO2	0	0	0	0	0	0	0	0	0	0	0
SiO2	0.42	0	0.53	0.0186	0	0.4385	0	0.999	0.025	0	0.325
Sm2O3	0	0	0	0	0	0	0	0	0	0	0

Maximum											
Comp	Kyanite	Boric Acid	Wollastonite	Hematite	Li Carbonate	Olivine	Na Carbonate	Silica	Rutile	Zincite	Zircon
SnO2	0	0	0	0	0	0	0	0	0	0	0
SrO	0	0	0	0	0	0	0	0	0	0	0
Ta2O5	0	0	0	0	0	0	0	0	0	0	0
Te2O7	0	0	0	0	0	0	0	0	0	0	0
TeO2	0	0	0	0	0	0	0	0	0	0	0
ThO2	0	0	0	0	0	0	0	0	0	0	0
TiO2	0.016	0	0.0003	0	0	0	0	0.0005	0.936	0	0.0014
Tl2O	0	0	0	0	0	0	0	0	0	0	0
UO3	0	0	0	0	0	0	0	0	0	0	0.0008
V2O5	0	0	0	0	0	0	0	0	0.0075	0	0
WO3	0	0	0	0	0	0	0	0	0	0	0
Y2O3	0	0	0	0	0	0	0	0	0	0	0
ZnO	0	0	0	0	0	0	0	0	0	0.9999	0
ZrO2	0	0	0	0	0	0	0	0	0.025	0	0.67

Table A-5. GFC Compositions: Nominal Composition Used for Nominal Glass Composition Calculation Obtained by 50,000 Monte Carlo Simulations

Nominal						
Comp	Kyanite	Boric Acid	Wollastonite	Hematite	Li Carbonate	Olivine
Ac2O3	0	0	0	0	0	0
Ag2O	0	0	0	0	0	0
Al2O3	5.7022E-01	0	2.0031E-03	1.5000E-02	0	2.6103E-03
Am2O3	0	0	0	0	0	0
As2O5	0	0	0	0	0	0
B2O3	0	5.6522E-01	0	0	0	0
BaO	0	0	0	0	0	0
BeO	0	0	0	0	0	0
Bi2O3	0	0	0	0	0	0
CaO	2.6660E-04	0	4.7510E-01	3.9931E-04	3.6573E-03	1.8367E-04
CdO	0	0	0	0	0	0
Ce2O3	0	0	0	0	0	0
Cl	0	0	0	0	8.3241E-05	0
Cm2O3	0	0	0	0	0	0
CoO	0	0	0	0	0	0
Cr2O3	0	0	0	0	1.0008E-04	2.1723E-03
Cs2O	0	0	0	0	0	0
CuO	0	0	0	0	0	0
Eu2O3	0	0	0	0	0	0
F	0	0	0	0	0	0
Fe2O3	7.5678E-03	0	4.0029E-03	9.7006E-01	1.6695E-05	7.6858E-02
Gd2O3	0	0	0	0	0	0
HgO	0	0	0	0	0	0
I	0	0	0	0	0	0
K2O	1.1645E-04	0	0	0	1.6577E-05	0
La2O3	0	0	0	0	0	0
Li2O	0	0	0	0	0.402061902	0
MgO	1.3317E-04	0	8.3461E-04	1.2988E-03	9.9860E-05	4.7949E-01
MnO	0	0	1.0001E-03	1.4992E-03	0	0
MoO3	0	0	0	0	0	0
Na2O	3.4953E-03	0	0	0	7.1550E-04	2.6723E-04
Nb2O5	0	0	0	0	0	0
Nd2O3	0	0	0	0	0	0
NiO	0	0	0	0	0	3.7037E-03
NpO2	0	0	0	0	0	0
P2O5	0	0	0	2.9962E-03	0	0
Pa2O5	0	0	0	0	0	0
PbO	0	0	0	0	0	0
PdO	0	0	0	0	0	0
Pr2O3	0	0	0	0	0	0
PuO2	0	0	0	0	0	0
RaO	0	0	0	0	0	0
Rb2O	0	0	0	0	0	0
Rh2O3	0	0	0	0	0	0
RuO2	0	0	0	0	0	0

Nominal						
Comp	Kyanite	Boric Acid	Wollastonite	Hematite	Li Carbonate	Olivine
SO3	0	4.9790E-05	0	7.1674E-04	2.6638E-04	0
Sb2O3	0	0	0	0	0	0
SeO2	0	0	0	0	0	0
SiO2	4.0608E-01	0	5.0821E-01	1.3493E-02	0	4.2466E-01
Sm2O3	0	0	0	0	0	0
SnO2	0	0	0	0	0	0
SrO	0	0	0	0	0	0
Ta2O5	0	0	0	0	0	0
Tc2O7	0	0	0	0	0	0
TeO2	0	0	0	0	0	0
ThO2	0	0	0	0	0	0
TiO2	8.7694E-03	0	1.9986E-04	0	0	0
Tl2O	0	0	0	0	0	0
UO3	0	0	0	0	0	0
V2O5	0	0	0	0	0	0
WO3	0	0	0	0	0	0
Y2O3	0	0	0	0	0	0
ZnO	0	0	0	0	0	0
ZrO2	0	0	0	0	0	0

Nominal (continued)					
Comp	Na Carbonate	Silica	Rutile	Zincite	Zircon
Ac2O3	0	0	0	0	0
Ag2O	0	0	0	0	0
Al2O3	0	1.6566E-03	4.5844E-03	0	2.5022E-03
Am2O3	0	0	0	0	0
As2O5	0	0	0	0	0
B2O3	0	0	0	0	0
BaO	0	0	0	0	0
BeO	0	0	0	0	0
Bi2O3	0	0	0	0	0
CaO	1.6584E-05	1.0045E-04	0	0	0
CdO	0	0	0	1.0008E-04	0
Ce2O3	0	0	0	0	0
Cl	1.6674E-04	0	0	0	0
Cm2O3	0	0	0	0	0
CoO	0	0	0	0	0
Cr2O3	1.0015E-04	0	2.3093E-03	0	0
Cs2O	0	0	0	0	0
CuO	0	0	0	0	0
Eu2O3	0	0	0	0	0
F	0	0	0	0	0
Fe2O3	1.6688E-05	2.1680E-04	8.8351E-03	1.6578E-05	7.8329E-04
Gd2O3	0	0	0	0	0
HgO	0	0	0	0	0
I	0	0	0	0	0

Nominal (continued)					
Comp	Na Carbonate	Silica	Rutile	Zincite	Zircon
K2O	0	3.3482E-05	0	0	0
La2O3	0	0	0	0	0
Li2O	0	0	0	0	0
MgO	1.6635E-05	8.3341E-05	0	0	0
MnO	0	0	0	1.6592E-05	0
MoO3	0	0	0	0	0
Na2O	5.8378E-01	1.6693E-04	0	0	0
Nb2O5	0	0	0	0	0
Nd2O3	0	0	0	0	0
NiO	0	0	0	0	0
NpO2	0	0	0	0	0
P2O5	0	0	1.1719E-04	0	0
Pa2O5	0	0	0	0	0
PbO	0	0	0	1.6637E-05	0
PdO	0	0	0	0	0
Pr2O3	0	0	0	0	0
PuO2	0	0	0	0	0
RaO	0	0	0	0	0
Rb2O	0	0	0	0	0
Rh2O3	0	0	0	0	0
RuO2	0	0	0	0	0
SO3	1.0011E-04	0	1.1701E-04	0	0
Sb2O3	0	0	0	0	0
SeO2	0	0	0	0	0
SiO2	0	9.9651E-01	1.8817E-02	0	3.2253E-01
Sm2O3	0	0	0	0	0
SnO2	0	0	0	0	0
SrO	0	0	0	0	0
Ta2O5	0	0	0	0	0
Tc2O7	0	0	0	0	0
TeO2	0	0	0	0	0
ThO2	0	0	0	0	0
TiO2	0	1.5000E-04	9.3206E-01	0	1.0169E-03
Tl2O	0	0	0	0	0
UO3	0	0	0	0	4.5003E-04
V2O5	0	0	4.2517E-03	0	0
WO3	0	0	0	0	0
Y2O3	0	0	0	0	0
ZnO	0	0	0	9.9815E-01	0
ZrO2	0	0	1.6837E-02	0	6.6004E-01

Table A-6. GFC Compositions: 11x11 Matrix of Nominal GFC Composition Used in Initial Calculation of GFC Masses from Target GFC Composition

Comp\GFC	Kyanite	Boric Acid	Wollastonite	Hematite	Li Carbonate	Olivine
Al2O3	5.7022E-01	0	2.0031E-03	1.5000E-02	0	2.6103E-03
B2O3	0	5.6522E-01	0	0	0	0
CaO	2.6660E-04	0	4.7510E-01	3.9931E-04	3.6573E-03	1.8367E-04
Fe2O3	7.5678E-03	0	4.0029E-03	9.7006E-01	1.6695E-05	7.6858E-02
Li2O	0	0	0	0	4.0206E-01	0
MgO	1.3317E-04	0	8.3461E-04	1.2988E-03	9.9860E-05	4.7949E-01
Na2O	3.4953E-03	0	0	0	7.1550E-04	2.6723E-04
SiO2	4.0608E-01	0	5.0821E-01	1.3493E-02	0	4.2466E-01
TiO2	8.7694E-03	0	1.9986E-04	0	0	0
ZnO	0	0	0	0	0	0
ZrO2	0	0	0	0	0	0

Comp\GFC	Na Carbonate	Silica	Rutile	Zincite	Zircon
Al2O3	0	1.6566E-03	4.5844E-03	0	2.5022E-03
B2O3	0	0	0	0	0
CaO	1.6584E-05	1.0045E-04	0	0	0
Fe2O3	1.6688E-05	2.1680E-04	8.8351E-03	1.6578E-05	7.8329E-04
Li2O	0	0	0	0	0
MgO	1.6635E-05	8.3341E-05	0	0	0
Na2O	5.8378E-01	1.6693E-04	0	0	0
SiO2	0	9.9651E-01	1.8817E-02	0	3.2253E-01
TiO2	0	1.5000E-04	9.3206E-01	0	1.0169E-03
ZnO	0	0	0	9.9815E-01	0
ZrO2	0	0	5.7022E-01	0	6.6004E-01

Table A-7. Variance-Covariance Matrices for PCT-B Model

Term	Al2O3	B2O3	CaO	Fe2O3	K2O	Li2O	MgO	Na2O
Al2O3	4.5411	-0.8535	-0.0978	0.0909	0.9952	-4.5759	-0.0689	-4.8201
B2O3	-0.8535	6.5050	-0.4167	-0.6563	-0.0878	10.2294	11.4075	-2.3603
CaO	-0.0978	-0.4167	9.0851	8.3041	2.1673	6.1810	1.3799	-5.4011
Fe2O3	0.0909	-0.6563	8.3041	10.3431	2.0919	3.0053	0.5102	-7.1887
K2O	0.9952	-0.0878	2.1673	2.0919	3.0456	0.4433	0.6721	-5.0192
Li2O	-4.5759	10.2294	6.1810	3.0053	0.4433	72.0621	-0.5370	2.9757
MgO	-0.0689	11.4075	1.3799	0.5102	0.6721	-0.5370	68.0494	-1.9809
Na2O	-4.8201	-2.3603	-5.4011	-7.1887	-5.0192	2.9757	-1.9809	27.1863
P2O5	0.6100	0.0070	1.5476	1.8056	1.3508	-0.8300	-0.1016	-4.0699
SiO2	-0.9005	-1.0301	-1.5567	-1.7741	-1.0531	-1.5044	-1.2803	4.9330
ZrO2	1.2709	0.5252	-0.5915	-0.6713	0.6179	-3.7898	2.2079	-6.7996
Others	0.6941	0.1474	0.7187	1.4425	0.4403	-2.8944	-1.3257	-4.6686
CaO*Li2O	3.9237	-5.0328	-82.4567	-50.8286	-6.5335	-198.0406	-87.7450	-26.7093
B2O3*MgO	5.7135	-125.6845	0.4841	10.4487	13.4220	-18.4379	-703.1255	-33.3977
B2O3*Li2O	50.1661	-109.6279	-0.4991	20.5465	17.2896	-538.7395	4.6201	-49.6081
Na2O*SiO2	11.8034	4.2468	13.4194	17.4395	12.8827	-6.2908	-2.2819	-67.5964
CaO*Fe2O3	11.6489	7.9481	-122.4661	-130.7800	-21.6787	-107.5801	-26.9959	33.8730

Term	P2O5	SiO2	ZrO2	Others	CaO*Li2O	B2O3*MgO
Al2O3	0.6100	-0.9005	1.2709	0.6941	3.9237	5.7135
B2O3	0.0070	-1.0301	0.5252	0.1474	-5.0328	-125.6845
CaO	1.5476	-1.5567	-0.5915	0.7187	-82.4567	0.4841
Fe2O3	1.8056	-1.7741	-0.6713	1.4425	-50.8286	10.4487
K2O	1.3508	-1.0531	0.6179	0.4403	-6.5335	13.4220
Li2O	-0.8300	-1.5044	-3.7898	-2.8944	-198.0406	-18.4379
MgO	-0.1016	-1.2803	2.2079	-1.3257	-87.7450	-703.1255
Na2O	-4.0699	4.9330	-6.7996	-4.6686	-26.7093	-33.3977
P2O5	7.9409	-0.9021	0.5266	0.9485	17.4291	6.7145
SiO2	-0.9021	1.2395	-1.2130	-1.0866	0.6220	0.4196
ZrO2	0.5266	-1.2130	7.7654	0.9872	22.7654	-6.3621
Others	0.9485	-1.0866	0.9872	3.4495	13.2488	18.5875
CaO*Li2O	17.4291	0.6220	22.7654	13.2488	2855.3392	1162.9848
B2O3*MgO	6.7145	0.4196	-6.3621	18.5875	1162.9848	8018.1830
B2O3*Li2O	9.8905	2.2332	20.6910	24.3367	343.3240	227.1726
Na2O*SiO2	10.5893	-12.6902	16.5233	11.6207	86.3608	175.8912
CaO*Fe2O3	-16.7213	12.3915	32.4518	-3.4768	1009.9195	225.1001

Term	B2O3*Li2O	Na2O*SiO2	CaO*Fe2O3
Al2O3	50.1661	11.8034	11.6489
B2O3	-109.6279	4.2468	7.9481
CaO	-0.4991	13.4194	-122.4661
Fe2O3	20.5465	17.4395	-130.7800
K2O	17.2896	12.8827	-21.6787
Li2O	-538.7395	-6.2908	-107.5801
MgO	4.6201	-2.2819	-26.9959

Term	B2O3*Li2O	Na2O*SiO2	CaO*Fe2O3
Na2O	-49.6081	-67.5964	33.8730
P2O5	9.8905	10.5893	-16.7213
SiO2	2.2332	-12.6902	12.3915
ZrO2	20.6910	16.5233	32.4518
Others	24.3367	11.6207	-3.4768
CaO*Li2O	343.3240	86.3608	1009.9195
B2O3*MgO	227.1726	175.8912	225.1001
B2O3*Li2O	5204.8656	138.6761	301.8835
Na2O*SiO2	138.6761	172.0205	-71.7517
CaO*Fe2O3	301.8835	-71.7517	2124.8909

Table A-8. Variance-Covariance Matrix for PCT-Na Model

Term	Al2O3	B2O3	CaO	Fe2O3	K2O	Li2O	MgO
Al2O3	2.6367	-0.2222	-0.7385	-0.9214	0.3894	0.0726	0.0444
B2O3	-0.2222	7.6234	-1.8619	-1.2119	0.0080	-2.1700	8.3156
CaO	-0.7385	-1.8619	6.5491	5.5974	-0.3900	4.5648	1.3215
Fe2O3	-0.9214	-1.2119	5.5974	6.7804	-0.7335	3.5350	0.5885
K2O	0.3894	0.0080	-0.3900	-0.7335	15.7842	0.2329	1.0913
Li2O	0.0726	-2.1700	4.5648	3.5350	0.2329	12.5785	0.1544
MgO	0.0444	8.3156	1.3215	0.5885	1.0913	0.1544	52.5669
Na2O	-0.2025	2.8308	-0.8383	-0.5800	-0.1269	0.0640	-2.6874
P2O5	-0.0847	-0.9891	0.7250	0.6211	0.6935	-0.0688	0.1514
SiO2	-0.0931	-0.8349	-0.3090	-0.3470	0.0011	-0.4073	-1.0574
ZrO2	0.0893	-0.2650	-1.4150	-1.8620	0.5222	-1.8244	1.9660
Others	-0.1842	-0.0865	-0.0130	0.2671	-0.9330	-0.6020	-0.9052
CaO*Li2O	-2.8191	2.1879	-70.6074	-48.1835	7.4888	-130.1176	-66.8946
CaO*Fe2O3	10.9332	22.0585	-93.0576	-98.1200	4.8711	-59.0421	-22.4845
B2O3*MgO	-5.5808	-105.5970	-7.7365	-4.3021	-8.5036	-0.2581	-540.0123
B2O3*Na2O	0.3251	-40.8666	9.5918	4.2261	-1.1662	9.1771	5.6624
K2O*K2O	-7.5665	-13.1053	30.6658	30.2914	-313.1547	24.6694	-8.6805

Term	Na2O	P2O5	SiO2	ZrO2	Others
Al2O3	-0.2025	-0.0847	-0.0931	0.0893	-0.1842
B2O3	2.8308	-0.9891	-0.8349	-0.2650	-0.0865
CaO	-0.8383	0.7250	-0.3090	-1.4150	-0.0130
Fe2O3	-0.5800	0.6211	-0.3470	-1.8620	0.2671
K2O	-0.1269	0.6935	0.0011	0.5222	-0.9330
Li2O	0.0640	-0.0688	-0.4073	-1.8244	-0.6020
MgO	-2.6874	0.1514	-1.0574	1.9660	-0.9052
Na2O	2.8123	-0.5161	-0.4047	-0.6056	-0.2447
P2O5	-0.5161	5.7728	-0.0060	-0.2731	0.2061
SiO2	-0.4047	-0.0060	0.2645	0.0507	-0.1846
ZrO2	-0.6056	-0.2731	0.0507	4.8825	-0.1335
Others	-0.2447	0.2061	-0.1846	-0.1335	2.0567
CaO*Li2O	7.1486	9.1275	4.6965	11.8234	4.2279
CaO*Fe2O3	9.7084	-10.6784	4.0376	30.3392	-0.8944
B2O3*MgO	22.8696	-2.1734	10.8288	-17.9346	5.6599
B2O3*Na2O	-29.0184	7.2277	4.3856	4.3044	2.0542
K2O*K2O	-2.7077	-4.3109	-1.1330	-21.3201	13.3522

Term	CaO*Li2O	CaO*Fe2O3	B2O3*MgO	B2O3*Na2O	K2O*K2O
Al2O3	-2.8191	10.9332	-5.5808	0.3251	-7.5665
B2O3	2.1879	22.0585	-105.5970	-40.8666	-13.1053
CaO	-70.6074	-93.0576	-7.7365	9.5918	30.6658
Fe2O3	-48.1835	-98.1200	-4.3021	4.2261	30.2914
K2O	7.4888	4.8711	-8.5036	-1.1662	-313.1547
Li2O	-130.1176	-59.0421	-0.2581	9.1771	24.6694
MgO	-66.8946	-22.4845	-540.0123	5.6624	-8.6805

Term	CaO*Li2O	CaO*Fe2O3	B2O3*MgO	B2O3*Na2O	K2O*K2O
Na2O	7.1486	9.7084	22.8696	-29.0184	-2.7077
P2O5	9.1275	-10.6784	-2.1734	7.2277	-4.3109
SiO2	4.6965	4.0376	10.8288	4.3856	-1.1330
ZrO2	11.8234	30.3392	-17.9346	4.3044	-21.3201
Others	4.2279	-0.8944	5.6599	2.0542	13.3522
CaO*Li2O	2181.7928	819.1763	810.6713	-25.9923	-398.1906
CaO*Fe2O3	819.1763	1633.1939	203.0666	-73.5093	-408.6876
B2O3*MgO	810.6713	203.0666	6060.0432	59.3798	202.3782
B2O3*Na2O	-25.9923	-73.5093	59.3798	361.3491	102.0262
K2O*K2O	-398.1906	-408.6876	202.3782	102.0262	6928.8404

Table A-9. Variance-Covariance Matrix for VHT Model

Term	Al2O3	B2O3	CaO	Fe2O3	K2O	Li2O
Al2O3	37.0274	-6.1959	-7.5969	0.8362	-3.8661	-21.7084
B2O3	-6.1959	35.0847	34.8292	1.0209	-6.1880	-37.0646
CaO	-7.5969	34.8292	89.2636	-12.8816	-23.1870	-31.9473
Fe2O3	0.8362	1.0209	-12.8816	22.3018	-11.4926	-19.7243
K2O	-3.8661	-6.1880	-23.1870	-11.4926	114.6504	11.3336
Li2O	-21.7084	-37.0646	-31.9473	-19.7243	11.3336	402.6862
MgO	-7.1062	-6.2560	-14.3315	-0.8794	33.6888	-3.1993
Na2O	-16.2542	6.5622	42.1681	-19.7161	-3.7296	150.0097
SiO2	0.7085	-7.7598	-12.6605	0.5479	0.5948	-14.3494
ZrO2	4.4076	-3.1717	-4.0153	5.4465	3.7883	-33.6196
Others	-2.6630	-0.3724	-11.9223	5.1363	-0.2410	-22.2422
(K2O)2*Na2O	771.0153	163.3330	859.1075	1630.2301	-10990.5144	-4461.2830
(Na2O)3	136.0406	-21.6663	-349.6870	195.3939	60.2046	-1792.6212
Li2O*Na2O*SiO2	276.5747	673.4985	310.5460	424.0416	230.0304	-6956.0025
B2O3*CaO*Na2O	640.1299	-3014.8798	-6657.9092	1204.3237	1358.4667	1732.9326

Term	MgO	Na2O	SiO2	ZrO2	Others
Al2O3	-7.1062	-16.2542	0.7085	4.4076	-2.6630
B2O3	-6.2560	6.5622	-7.7598	-3.1717	-0.3724
CaO	-14.3315	42.1681	-12.6605	-4.0153	-11.9223
Fe2O3	-0.8794	-19.7161	0.5479	5.4465	5.1363
K2O	33.6888	-3.7296	0.5948	3.7883	-0.2410
Li2O	-3.1993	150.0097	-14.3494	-33.6196	-22.2422
MgO	64.6618	-7.0818	-0.4710	2.6589	0.9723
Na2O	-7.0818	109.7369	-15.6511	-15.8112	-16.6912
SiO2	-0.4710	-15.6511	5.2310	0.3491	-0.6156
ZrO2	2.6589	-15.8112	0.3491	57.6249	-1.8627
Others	0.9723	-16.6912	-0.6156	-1.8627	28.6027
(K2O)2*Na2O	-2212.0420	-2639.7226	279.1963	-614.7721	786.0088
(Na2O)3	115.1066	-1302.7253	164.8064	112.1162	195.0451
Li2O*Na2O*SiO2	343.3545	-2825.3603	197.3669	368.3748	561.4452
B2O3*CaO*Na2O	1224.0790	-4182.2868	1064.2436	527.1768	927.7819

Term	(K2O)2*Na2O	(Na2O)3	Li2O*Na2O*SiO2	B2O3*CaO*Na2O
Al2O3	771.0153	136.0406	276.5747	640.1299
B2O3	163.3330	-21.6663	673.4985	-3014.8798
CaO	859.1075	-349.6870	310.5460	-6657.9092
Fe2O3	1630.2301	195.3939	424.0416	1204.3237
K2O	-10990.5144	60.2046	230.0304	1358.4667
Li2O	-4461.2830	-1792.6212	-6956.0025	1732.9326
MgO	-2212.0420	115.1066	343.3545	1224.0790
Na2O	-2639.7226	-1302.7253	-2825.3603	-4182.2868
SiO2	279.1963	164.8064	197.3669	1064.2436
ZrO2	-614.7721	112.1162	368.3748	527.1768
Others	786.0088	195.0451	561.4452	927.7819

Term	(K2O)2*Na2O	(Na2O)3	Li2O*Na2O*SiO2	B2O3*CaO*Na2O
(K2O)2*Na2O	1436442.3984	29221.3465	65274.7345	24923.3397
(Na2O)3	29221.3465	17067.2975	37209.8730	40016.3557
Li2O*Na2O*SiO2	65274.7345	37209.8730	150236.7297	-25688.2830
B2O3*CaO*Na2O	24923.3397	40016.3557	-25688.2830	598088.4681

Table A-10. Variance-Covariance Matrix for Viscosity Model

Term	Al2O3	B2O3	CaO	Fe2O3	K2O	Li2O
Al2O3	4.3931	-4.2122	-0.1233	-0.0843	0.0498	4.6732
B2O3	-4.2122	47.1379	-1.8275	-2.2280	-1.7454	-3.3764
CaO	-0.1233	-1.8275	0.9674	0.0108	0.1916	-0.7363
Fe2O3	-0.0843	-2.2280	0.0108	1.0795	0.0179	0.1230
K2O	0.0498	-1.7454	0.1916	0.0179	0.8756	0.2793
Li2O	4.6732	-3.3764	-0.7363	0.1230	0.2793	20.7045
MgO	0.6928	-20.4729	1.9764	1.2104	2.5447	-0.1117
Na2O	-0.1107	-1.9214	0.2159	0.0502	0.0852	0.7659
P2O5	-0.0789	-0.5171	0.2320	0.1245	0.2515	-0.3392
SiO2	-0.0429	-2.2502	-0.0453	0.0050	0.0266	-0.4024
ZrO2	-0.0615	-2.1771	0.2763	0.1063	-0.1280	-0.8618
Others	-0.2520	-1.2726	0.0602	0.2731	-0.0457	-1.0501
(B2O3)2	20.3262	-249.5197	9.9237	12.3605	9.4277	13.5252
(Li2O)2	0.0997	-12.1963	4.2240	-0.1684	-9.1920	-93.4991
Al2O3*Li2O	-75.9624	50.2923	2.8455	1.3714	5.7603	-190.3501
(MgO)2	-27.1251	390.6125	-33.5639	-21.9405	-44.4567	-8.3165
Al2O3/(T/1000)2	-2.7928	-0.0012	0.2130	0.2020	0.0001	0.0764
CaO/(T/1000)2	0.2113	-0.0023	-0.9869	0.1058	0.0003	0.4454
Fe2O3/(T/1000)2	0.2016	-0.0045	0.1043	-1.1063	-0.0008	-0.2253
Li2O/(T/1000)2	0.0822	0.0065	0.4475	-0.2271	-0.0005	-4.8829
MgO/(T/1000)2	0.5041	-0.0094	-0.2921	-0.0913	0.0014	-0.0124
Na2O/(T/1000)2	0.1874	0.0016	-0.1692	0.0557	-0.0009	-1.0799
P2O5/(T/1000)2	-0.0002	0.0554	-0.2028	-0.1564	-0.0020	-0.2204
SiO2/(T/1000)2	0.2305	0.0005	0.1368	0.1083	0.0001	0.3919
ZrO2/(T/1000)2	0.2824	0.0072	-0.3680	-0.0435	-0.0013	1.1774
Others/(T/1000)2	0.0521	-0.0081	0.0177	-0.1935	0.0019	0.2932

Term	MgO	Na2O	P2O5	SiO2	ZrO2	Others
Al2O3	0.6928	-0.1107	-0.0789	-0.0429	-0.0615	-0.2520
B2O3	-20.4729	-1.9214	-0.5171	-2.2502	-2.1771	-1.2726
CaO	1.9764	0.2159	0.2320	-0.0453	0.2763	0.0602
Fe2O3	1.2104	0.0502	0.1245	0.0050	0.1063	0.2731
K2O	2.5447	0.0852	0.2515	0.0266	-0.1280	-0.0457
Li2O	-0.1117	0.7659	-0.3392	-0.4024	-0.8618	-1.0501
MgO	30.4968	1.0138	0.2125	0.4123	-0.5144	0.5974
Na2O	1.0138	0.4543	0.0486	-0.0246	-0.1311	-0.0078
P2O5	0.2125	0.0486	8.2711	-0.0620	-0.2324	0.1048
SiO2	0.4123	-0.0246	-0.0620	0.2754	0.0220	-0.1523
ZrO2	-0.5144	-0.1311	-0.2324	0.0220	4.3076	-0.1032
Others	0.5974	-0.0078	0.1048	-0.1523	-0.1032	2.0486
(B2O3)2	107.9026	10.2913	2.7664	11.6977	11.0765	7.4392
(Li2O)2	-10.9375	-0.4836	4.7339	2.5586	0.1008	1.5422
Al2O3*Li2O	17.3764	3.3875	5.5647	-0.1315	-0.7979	11.7642
(MgO)2	-534.4482	-14.7794	-7.7473	-11.2139	21.0534	-15.3621
Al2O3/(T/1000)2	0.5136	0.1879	0.0040	0.2319	0.2772	0.0446
CaO/(T/1000)2	-0.2894	-0.1686	-0.2004	0.1368	-0.3660	0.0170
Fe2O3/(T/1000)2	-0.1139	0.0560	-0.1533	0.1090	-0.0387	-0.1942

Term	MgO	Na2O	P2O5	SiO2	ZrO2	Others
Li2O/(T/1000)2	-0.0575	-1.0790	-0.2152	0.3947	1.1620	0.2724
MgO/(T/1000)2	-4.2316	-0.2458	0.3431	0.2332	-0.5703	0.2492
Na2O/(T/1000)2	-0.2568	-0.4355	-0.0234	0.1449	0.2795	0.0955
P2O5/(T/1000)2	0.3159	-0.0256	-9.6661	0.1036	0.2737	-0.1465
SiO2/(T/1000)2	0.2358	0.1450	0.1060	-0.1768	0.1657	0.2560
ZrO2/(T/1000)2	-0.5962	0.2783	0.2752	0.1662	-4.7238	0.1832
Others/(T/1000)2	0.2725	0.0950	-0.1446	0.2553	0.1827	-2.2841

Term	(B2O3)2	(Li2O)2	Al2O3*Li2O	(MgO)2	Al2O3/(T/1000)2	CaO/(T/1000)2
Al2O3	20.3262	0.0997	-75.9624	-27.1251	-2.7928	0.2113
B2O3	-249.5197	-12.1963	50.2923	390.6125	-0.0012	-0.0023
CaO	9.9237	4.2240	2.8455	-33.5639	0.2130	-0.9869
Fe2O3	12.3605	-0.1684	1.3714	-21.9405	0.2020	0.1058
K2O	9.4277	-9.1920	5.7603	-44.4567	0.0001	0.0003
Li2O	13.5252	-93.4991	-190.3501	-8.3165	0.0764	0.4454
MgO	107.9026	-10.9375	17.3764	-534.4482	0.5136	-0.2894
Na2O	10.2913	-0.4836	3.3875	-14.7794	0.1879	-0.1686
P2O5	2.7664	4.7339	5.5647	-7.7473	0.0040	-0.2004
SiO2	11.6977	2.5586	-0.1315	-11.2139	0.2319	0.1368
ZrO2	11.0765	0.1008	-0.7979	21.0534	0.2772	-0.3660
Others	7.4392	1.5422	11.7642	-15.3621	0.0446	0.0170
(B2O3)2	1334.1445	61.0130	-199.7892	-2044.9113	-0.0209	0.0117
(Li2O)2	61.0130	1865.1464	-51.5337	113.7300	0.0292	-0.0295
Al2O3*Li2O	-199.7892	-51.5337	3142.4026	-64.0502	0.0986	0.0783
(MgO)2	-2044.9113	113.7300	-64.0502	10718.1194	-0.2344	-0.1081
Al2O3/(T/1000)2	-0.0209	0.0292	0.0986	-0.2344	5.1453	-0.3937
CaO/(T/1000)2	0.0117	-0.0295	0.0783	-0.1081	-0.3937	1.8219
Fe2O3/(T/1000)2	0.0219	-0.0963	0.0713	0.4542	-0.3688	-0.1946
Li2O/(T/1000)2	-0.0139	0.2143	-0.0200	0.8846	-0.1387	-0.8270
MgO/(T/1000)2	0.0437	-0.0437	-0.0298	-1.3377	-0.9292	0.5412
Na2O/(T/1000)2	0.0009	0.0233	-0.0073	0.2273	-0.3424	0.3119
P2O5/(T/1000)2	-0.3035	0.0376	0.0266	0.5350	-0.0127	0.3693
SiO2/(T/1000)2	-0.0007	0.0171	0.0282	-0.0353	-0.4263	-0.2516
ZrO2/(T/1000)2	-0.0509	-0.0321	-0.2577	0.6372	-0.5259	0.6740
Others/(T/1000)2	0.0410	-0.0521	-0.2877	-0.5317	-0.0898	-0.0334

Term	Fe2O3/(T/1000)2	Li2O/(T/1000)2	MgO/(T/1000)2	Na2O/(T/1000)2
Al2O3	0.2016	0.0822	0.5041	0.1874
B2O3	-0.0045	0.0065	-0.0094	0.0016
CaO	0.1043	0.4475	-0.2921	-0.1692
Fe2O3	-1.1063	-0.2271	-0.0913	0.0557
K2O	-0.0008	-0.0005	0.0014	-0.0009
Li2O	-0.2253	-4.8829	-0.0124	-1.0799
MgO	-0.1139	-0.0575	-4.2316	-0.2568
Na2O	0.0560	-1.0790	-0.2458	-0.4355
P2O5	-0.1533	-0.2152	0.3431	-0.0234

Term	Fe2O3/ (T/1000)2	Li2O/ (T/1000)2	MgO/ (T/1000)2	Na2O/ (T/1000)2
SiO2	0.1090	0.3947	0.2332	0.1449
ZrO2	-0.0387	1.1620	-0.5703	0.2795
Others	-0.1942	0.2724	0.2492	0.0955
(B2O3)2	0.0219	-0.0139	0.0437	0.0009
(Li2O)2	-0.0963	0.2143	-0.0437	0.0233
Al2O3*Li2O	0.0713	-0.0200	-0.0298	-0.0073
(MgO)2	0.4542	0.8846	-1.3377	0.2273
Al2O3/(T/1000)2	-0.3688	-0.1387	-0.9292	-0.3424
CaO/(T/1000)2	-0.1946	-0.8270	0.5412	0.3119
Fe2O3/(T/1000)2	2.0360	0.4119	0.1716	-0.1034
Li2O/(T/1000)2	0.4119	8.9724	0.0513	1.9851
MgO/(T/1000)2	0.1716	0.0513	7.9128	0.4583
Na2O/(T/1000)2	-0.1034	1.9851	0.4583	0.8025
P2O5/(T/1000)2	0.2845	0.3957	-0.6325	0.0422
SiO2/(T/1000)2	-0.2002	-0.7304	-0.4320	-0.2683
ZrO2/(T/1000)2	0.0786	-2.1333	1.0470	-0.5126
Others/(T/1000)2	0.3652	-0.4870	-0.4692	-0.1727

Term	P2O5/ (T/1000)2	SiO2/ (T/1000)2	ZrO2/ (T/1000)2	Others/ (T/1000)2
Al2O3	-0.0002	0.2305	0.2824	0.0521
B2O3	0.0554	0.0005	0.0072	-0.0081
CaO	-0.2028	0.1368	-0.3680	0.0177
Fe2O3	-0.1564	0.1083	-0.0435	-0.1935
K2O	-0.0020	0.0001	-0.0013	0.0019
Li2O	-0.2204	0.3919	1.1774	0.2932
MgO	0.3159	0.2358	-0.5962	0.2725
Na2O	-0.0256	0.1450	0.2783	0.0950
P2O5	-9.6661	0.1060	0.2752	-0.1446
SiO2	0.1036	-0.1768	0.1662	0.2553
ZrO2	0.2737	0.1657	-4.7238	0.1827
Others	-0.1465	0.2560	0.1832	-2.2841
(B2O3)2	-0.3035	-0.0007	-0.0509	0.0410
(Li2O)2	0.0376	0.0171	-0.0321	-0.0521
Al2O3*Li2O	0.0266	0.0282	-0.2577	-0.2877
(MgO)2	0.5350	-0.0353	0.6372	-0.5317
Al2O3/(T/1000)2	-0.0127	-0.4263	-0.5259	-0.0898
CaO/(T/1000)2	0.3693	-0.2516	0.6740	-0.0334
Fe2O3/(T/1000)2	0.2845	-0.2002	0.0786	0.3652
Li2O/(T/1000)2	0.3957	-0.7304	-2.1333	-0.4870
MgO/(T/1000)2	-0.6325	-0.4320	1.0470	-0.4692
Na2O/(T/1000)2	0.0422	-0.2683	-0.5126	-0.1727
P2O5/(T/1000)2	17.9128	-0.1942	-0.5139	0.2648
SiO2/(T/1000)2	-0.1942	0.3259	-0.3022	-0.4711
ZrO2/(T/1000)2	-0.5139	-0.3022	8.7153	-0.3605
Others/(T/1000)2	0.2648	-0.4711	-0.3605	4.2105

Table A-11. Variance-Covariance Matrix for Electrical Conductivity Model

Term	Al2O3	B2O3	CaO	Fe2O3	K2O	Li2O
Al2O3	6.4799	-0.7687	-0.5444	-0.6502	0.3336	0.1030
B2O3	-0.7687	3.0753	-0.2350	0.5775	0.2775	-1.2268
CaO	-0.5444	-0.2350	9.0967	-0.8749	-0.4213	4.9678
Fe2O3	-0.6502	0.5775	-0.8749	2.7741	-0.5565	-0.6301
K2O	0.3336	0.2775	-0.4213	-0.5565	4.7674	0.0410
Li2O	0.1030	-1.2268	4.9678	-0.6301	0.0410	25.2917
MgO	-0.9935	0.3064	-0.0479	0.1079	2.0530	-0.8496
Na2O	-0.3862	-0.2836	2.2997	-0.3634	-0.2676	4.5557
SiO2	-0.4047	-0.5409	-0.8098	-0.2683	-0.1665	-1.3387
ZrO2	-0.2125	-1.1722	0.7554	-0.0338	-0.4077	-2.5711
Others	-0.2443	0.5012	-1.0702	0.6758	-0.3242	-1.8311
CaO*Li2O	-1.2238	8.2817	-97.2024	10.3567	9.9114	-144.7756
CaO*Na2O	0.6257	2.6594	-37.2667	3.2215	4.5760	-23.1400
Li2O*Na2O	0.7076	0.4980	-3.8171	2.3793	1.5515	-49.3728
Al2O3/(T/1000)	-7.5254	0.8973	0.4993	0.7818	-0.3460	-0.2022
B2O3/(T/1000)	0.8936	-3.5307	-0.3263	-0.6165	-0.2495	0.8258
CaO/(T/1000)	0.5428	-0.3195	-2.6215	0.2754	-0.4498	1.2059
Fe2O3/(T/1000)	0.7772	-0.6154	0.2666	-3.1503	0.7529	-0.2586
K2O/(T/1000)	-0.3493	-0.2504	-0.4489	0.7530	-5.4297	-0.9151
Li2O/(T/1000)	-0.1538	0.8038	1.2660	-0.2552	-0.9205	-13.1967
MgO/(T/1000)	1.1952	-0.2491	-1.0073	-0.0067	-2.2522	-0.5340
Na2O/(T/1000)	0.3837	0.1629	-0.3799	0.1868	0.0067	-2.8888
SiO2/(T/1000)	0.4850	0.6685	0.4366	0.3658	0.2583	0.9848
ZrO2/(T/1000)	0.2397	1.3326	-0.8151	0.0439	0.4558	2.7148
Others/(T/1000)	0.3050	-0.4933	0.0014	-0.6695	0.5157	0.5978

Term	MgO	Na2O	SiO2	ZrO2	Others
Al2O3	-0.9935	-0.3862	-0.4047	-0.2125	-0.2443
B2O3	0.3064	-0.2836	-0.5409	-1.1722	0.5012
CaO	-0.0479	2.2997	-0.8098	0.7554	-1.0702
Fe2O3	0.1079	-0.3634	-0.2683	-0.0338	0.6758
K2O	2.0530	-0.2676	-0.1665	-0.4077	-0.3242
Li2O	-0.8496	4.5557	-1.3387	-2.5711	-1.8311
MgO	10.6342	0.2676	-0.5761	0.8667	-0.6353
Na2O	0.2676	1.6011	-0.4465	-0.5657	-0.4966
SiO2	-0.5761	-0.4465	0.5453	-0.1535	-0.4958
ZrO2	0.8667	-0.5657	-0.1535	11.0901	-0.5539
Others	-0.6353	-0.4966	-0.4958	-0.5539	4.5320
CaO*Li2O	15.5091	-27.7001	6.6834	0.0352	18.0251
CaO*Na2O	4.3607	-10.5266	2.2859	-0.5814	5.4664
Li2O*Na2O	3.0783	-4.2848	1.0436	2.1222	2.3364
Al2O3/(T/1000)	1.2016	0.3729	0.4873	0.2378	0.3140
B2O3/(T/1000)	-0.2525	0.1631	0.6690	1.3316	-0.4931
CaO/(T/1000)	-0.9684	-0.3947	0.4317	-0.8125	-0.0048
Fe2O3/(T/1000)	-0.0089	0.1873	0.3662	0.0427	-0.6668
K2O/(T/1000)	-2.2564	0.0078	0.2585	0.4556	0.5178
Li2O/(T/1000)	-0.5100	-2.8923	0.9836	2.7133	0.5798

Term	MgO	Na2O	SiO2	ZrO2	Others
MgO/(T/1000)	-12.2210	-0.6549	0.7407	-0.9862	0.9390
Na2O/(T/1000)	-0.6470	-1.1510	0.3650	0.6476	0.1982
SiO2/(T/1000)	0.7382	0.3665	-0.6023	0.1879	0.6645
ZrO2/(T/1000)	-0.9854	0.6460	0.1876	-12.9040	0.6778
Others/(T/1000)	0.9315	0.2048	0.6643	0.6765	-5.0739

Term	CaO*Li2O	CaO*Na2O	Li2O*Na2O	Al2O3/ (T/1000)	B2O3/ (T/1000)
Al2O3	-1.2238	0.6257	0.7076	-7.5254	0.8936
B2O3	8.2817	2.6594	0.4980	0.8973	-3.5307
CaO	-97.2024	-37.2667	-3.8171	0.4993	-0.3263
Fe2O3	10.3567	3.2215	2.3793	0.7818	-0.6165
K2O	9.9114	4.5760	1.5515	-0.3460	-0.2495
Li2O	-144.7756	-23.1400	-49.3728	-0.2022	0.8258
MgO	15.5091	4.3607	3.0783	1.2016	-0.2525
Na2O	-27.7001	-10.5266	-4.2848	0.3729	0.1631
SiO2	6.6834	2.2859	1.0436	0.4873	0.6690
ZrO2	0.0352	-0.5814	2.1222	0.2378	1.3316
Others	18.0251	5.4664	2.3364	0.3140	-0.4931
CaO*Li2O	1955.4791	445.9270	279.7517	0.8392	-0.0833
CaO*Na2O	445.9270	214.7187	-20.8270	0.2132	0.0547
Li2O*Na2O	279.7517	-20.8270	295.9502	-0.0160	-0.1174
Al2O3/(T/1000)	0.8392	0.2132	-0.0160	10.2181	-1.2142
B2O3/(T/1000)	-0.0833	0.0547	-0.1174	-1.2142	4.7895
CaO/(T/1000)	0.2714	0.0903	-0.0290	-0.7321	0.4311
Fe2O3/(T/1000)	0.2092	0.0305	-0.0398	-1.0621	0.8387
K2O/(T/1000)	-0.0760	-0.0100	0.0342	0.4675	0.3314
Li2O/(T/1000)	-0.8599	-0.2373	-0.0166	0.2379	-1.0927
MgO/(T/1000)	0.5694	0.1969	-0.0226	-1.6484	0.3250
Na2O/(T/1000)	-0.2141	-0.0500	-0.0316	-0.5099	-0.2228
SiO2/(T/1000)	-0.0733	-0.0355	0.0541	-0.6600	-0.9084
ZrO2/(T/1000)	-0.0523	0.0289	0.0110	-0.3207	-1.7838
Others/(T/1000)	-0.0016	-0.0585	-0.0907	-0.4295	0.6754

Term	CaO/ (T/1000)	Fe2O3/ (T/1000)	K2O/ (T/1000)	Li2O/ (T/1000)	MgO/ (T/1000)
Al2O3	0.5428	0.7772	-0.3493	-0.1538	1.1952
B2O3	-0.3195	-0.6154	-0.2504	0.8038	-0.2491
CaO	-2.6215	0.2666	-0.4489	1.2660	-1.0073
Fe2O3	0.2754	-3.1503	0.7530	-0.2552	-0.0067
K2O	-0.4498	0.7529	-5.4297	-0.9205	-2.2522
Li2O	1.2059	-0.2586	-0.9151	-13.1967	-0.5340
MgO	-0.9684	-0.0089	-2.2564	-0.5100	-12.2210
Na2O	-0.3947	0.1873	0.0078	-2.8923	-0.6549
SiO2	0.4317	0.3662	0.2585	0.9836	0.7407
ZrO2	-0.8125	0.0427	0.4556	2.7133	-0.9862
Others	-0.0048	-0.6668	0.5178	0.5798	0.9390
CaO*Li2O	0.2714	0.2092	-0.0760	-0.8599	0.5694
CaO*Na2O	0.0903	0.0305	-0.0100	-0.2373	0.1969

Term	CaO/ (T/1000)	Fe2O3/ (T/1000)	K2O/ (T/1000)	Li2O/ (T/1000)	MgO/ (T/1000)
Li2O*Na2O	-0.0290	-0.0398	0.0342	-0.0166	-0.0226
Al2O3/(T/1000)	-0.7321	-1.0621	0.4675	0.2379	-1.6484
B2O3/(T/1000)	0.4311	0.8387	0.3314	-1.0927	0.3250
CaO/(T/1000)	3.5331	-0.3723	0.6086	-1.6551	1.3049
Fe2O3/(T/1000)	-0.3723	4.2851	-1.0248	0.3279	0.0132
K2O/(T/1000)	0.6086	-1.0248	7.3644	1.2568	3.0460
Li2O/(T/1000)	-1.6551	0.3279	1.2568	17.9774	0.7249
MgO/(T/1000)	1.3049	0.0132	3.0460	0.7249	16.5800
Na2O/(T/1000)	0.5282	-0.2595	-0.0097	3.9412	0.8847
SiO2/(T/1000)	-0.5827	-0.4972	-0.3498	-1.3476	-0.9958
ZrO2/(T/1000)	1.1093	-0.0539	-0.6020	-3.6868	1.3306
Others/(T/1000)	0.0053	0.9181	-0.6959	-0.7680	-1.2733

Term	Na2O/ (T/1000)	SiO2/ (T/1000)	ZrO2/ (T/1000)	Others/ (T/1000)
Al2O3	0.3837	0.4850	0.2397	0.3050
B2O3	0.1629	0.6685	1.3326	-0.4933
CaO	-0.3799	0.4366	-0.8151	0.0014
Fe2O3	0.1868	0.3658	0.0439	-0.6695
K2O	0.0067	0.2583	0.4558	0.5157
Li2O	-2.8888	0.9848	2.7148	0.5978
MgO	-0.6470	0.7382	-0.9854	0.9315
Na2O	-1.1510	0.3665	0.6460	0.2048
SiO2	0.3650	-0.6023	0.1876	0.6643
ZrO2	0.6476	0.1879	-12.9040	0.6765
Others	0.1982	0.6645	0.6778	-5.0739
CaO*Li2O	-0.2141	-0.0733	-0.0523	-0.0016
CaO*Na2O	-0.0500	-0.0355	0.0289	-0.0585
Li2O*Na2O	-0.0316	0.0541	0.0110	-0.0907
Al2O3/(T/1000)	-0.5099	-0.6600	-0.3207	-0.4295
B2O3/(T/1000)	-0.2228	-0.9084	-1.7838	0.6754
CaO/(T/1000)	0.5282	-0.5827	1.1093	0.0053
Fe2O3/(T/1000)	-0.2595	-0.4972	-0.0539	0.9181
K2O/(T/1000)	-0.0097	-0.3498	-0.6020	-0.6959
Li2O/(T/1000)	3.9412	-1.3476	-3.6868	-0.7680
MgO/(T/1000)	0.8847	-0.9958	1.3306	-1.2733
Na2O/(T/1000)	1.5664	-0.4982	-0.8797	-0.2651
SiO2/(T/1000)	-0.4982	0.8185	-0.2568	-0.9051
ZrO2/(T/1000)	-0.8797	-0.2568	17.5140	-0.9500
Others/(T/1000)	-0.2651	-0.9051	-0.9500	6.8928

Table A-12. Particle Density of GFC and Sucrose

GFC or other additives^(a)	Particle density, g/L
Kyanite	3398.3
Boric Acid	1509.3
Wollastonite	2899.3
Hematite	4747.9
Lithium Carbonate	2109.6
Olivine	2948.2
Sodium Carbonate	2532.5
Silica	2649.5
Rutile	4647.8
Zincite	5596.9
Zircon	4701.4
Sucrose	1549.0

Appendix B—Results of Example Calculations

Table B-1. Composition of CRV Batches Used for Example Calculations in the Format as Reported by Analytical Laboratory

CRV Batch ID	A10	B10	A11	B11	A12	B12	A13	B13
Concentration of chemical elements, NOx, and TOC (mg/L)								
Ac								
Ag	3.2305E-01	3.1876E-01	3.1693E-01	3.1782E-01	3.1834E-01	3.1077E-01	2.9757E-01	2.8670E-01
Al	9.5241E+03	9.6281E+03	9.7247E+03	9.8076E+03	9.3131E+03	8.9359E+03	8.8641E+03	9.0613E+03
Am								
As	1.2149E+00	1.2002E+00	1.1706E+00	1.1495E+00	1.2373E+00	1.3507E+00	1.4016E+00	1.4023E+00
B	1.5902E+01	1.4783E+01	1.6770E+01	1.8207E+01	1.9934E+01	1.7651E+01	1.6987E+01	1.8055E+01
Ba	2.7294E-01	2.6936E-01	2.6287E-01	2.5781E-01	2.7820E-01	3.0466E-01	3.1690E-01	3.1742E-01
Be	5.1924E-01	5.1343E-01	5.1434E-01	5.2162E-01	4.9923E-01	4.5208E-01	4.0501E-01	3.7599E-01
Bi	4.7604E+00	4.7009E+00	4.5088E+00	4.3350E+00	5.0127E+00	5.9918E+00	6.5751E+00	6.7408E+00
Ca	3.4621E+01	3.4583E+01	3.5197E+01	3.6000E+01	3.6148E+01	3.6131E+01	3.5519E+01	3.4778E+01
Cd	8.0278E-01	7.9314E-01	7.9400E-01	8.0400E-01	7.7727E-01	7.1447E-01	6.4969E-01	6.0903E-01
Ce	2.5103E-01	2.4742E-01	2.3683E-01	2.2634E-01	2.6616E-01	3.2413E-01	3.5964E-01	3.7044E-01
Cl	2.7498E+03	2.7515E+03	2.7811E+03	2.8086E+03	2.8597E+03	2.8983E+03	2.9321E+03	2.9578E+03
Cm								
Co	3.9890E-01	3.9860E-01	4.0135E-01	4.0792E-01	4.0355E-01	3.8477E-01	3.6063E-01	3.4353E-01
Cr	6.4146E+02	6.3532E+02	6.1262E+02	5.9230E+02	6.7965E+02	8.0756E+02	8.8348E+02	9.0450E+02
Cs	3.3451E-03	3.2756E-03	3.2623E-03	3.2601E-03	3.5517E-03	3.7539E-03	3.8581E-03	3.8901E-03
Cu	7.6645E-01	7.5758E-01	7.5380E-01	7.5817E-01	7.4824E-01	7.1557E-01	6.7271E-01	6.4121E-01
Eu								
F	1.1429E+03	1.1056E+03	1.1532E+03	1.1946E+03	1.2303E+03	1.1409E+03	1.0823E+03	1.0780E+03
Fe	1.2554E+01	1.1624E+01	1.3181E+01	1.4209E+01	1.5952E+01	1.4716E+01	1.4614E+01	1.5634E+01
Gd	0.0000E+00	0.0000E+00	0.0000E+00	0.0000E+00	0.0000E+00	0.0000E+00	0.0000E+00	0.0000E+00
Hg	9.8536E-02	9.6952E-02	9.4184E-02	9.1371E-02	1.0619E-01	1.2554E-01	1.3778E-01	1.4235E-01
I								
K	1.3573E+04	1.3413E+04	1.3433E+04	1.3613E+04	1.3100E+04	1.1955E+04	1.0794E+04	1.0073E+04
La	3.6882E-01	3.6881E-01	3.6526E-01	3.6297E-01	3.9379E-01	4.3071E-01	4.4766E-01	4.4886E-01
Li	1.6135E-01	1.5949E-01	1.5850E-01	1.5924E-01	1.5790E-01	1.5222E-01	1.4405E-01	1.3779E-01
Mg	9.6546E+00	8.8701E+00	1.3066E+01	1.6327E+01	2.0030E+01	1.7710E+01	1.8632E+01	2.2824E+01
Mn	1.3040E+00	1.2564E+00	1.2967E+00	1.3170E+00	1.4302E+00	1.4517E+00	1.4757E+00	1.5099E+00
Mo	9.7705E+00	9.6510E+00	9.4758E+00	9.3783E+00	9.8362E+00	1.0339E+01	1.0458E+01	1.0344E+01
Na	1.5809E+05	1.5863E+05	1.5881E+05	1.5942E+05	1.5764E+05	1.5695E+05	1.5646E+05	1.5670E+05
Nb								
Nd	1.1961E+00	1.1823E+00	1.1758E+00	1.1821E+00	1.1691E+00	1.1220E+00	1.0578E+00	1.0098E+00
Ni	2.5738E+01	2.6017E+01	2.6535E+01	2.7270E+01	2.6996E+01	2.5584E+01	2.3845E+01	2.2669E+01
Np								
P	9.0542E+02	9.0200E+02	8.9007E+02	8.8407E+02	9.4110E+02	1.0127E+03	1.0406E+03	1.0363E+03
Pa								
Pb	3.2157E+01	3.2426E+01	3.2954E+01	3.3748E+01	3.3607E+01	3.2196E+01	3.0294E+01	2.8945E+01
Pd	7.3745E+00	7.2921E+00	7.3090E+00	7.4173E+00	7.0817E+00	6.3838E+00	5.6951E+00	5.2745E+00
Pr	1.0387E-02	1.0271E-02	1.0279E-02	1.0413E-02	1.0008E-02	9.1333E-03	8.2408E-03	7.6813E-03
Pu								
Ra								
Rb	1.5682E+00	1.5504E+00	1.5525E+00	1.5737E+00	1.5101E+00	1.3734E+00	1.2355E+00	1.1499E+00
Rh	3.0812E+00	3.0440E+00	3.0564E+00	3.1057E+00	2.9610E+00	2.6529E+00	2.3556E+00	2.1781E+00
Ru	1.3756E+01	1.3463E+01	1.3681E+01	1.3985E+01	1.3534E+01	1.2020E+01	1.0713E+01	1.0049E+01
S	1.6951E+03	1.6756E+03	1.6216E+03	1.5763E+03	1.7646E+03	2.0264E+03	2.1729E+03	2.2080E+03
Sb	3.3380E-01	3.3108E-01	3.1960E-01	3.0929E-01	3.5546E-01	4.2091E-01	4.5934E-01	4.6992E-01

CRV Batch ID	A10	B10	A11	B11	A12	B12	A13	B13
Se	2.2786E+00	2.2364E+00	2.2165E+00	2.2027E+00	2.3749E+00	2.5289E+00	2.6034E+00	2.6208E+00
Si	4.7632E+02	4.7764E+02	4.8740E+02	5.0008E+02	4.9956E+02	4.8809E+02	4.6999E+02	4.5543E+02
Sm								
Sn								
Sr	1.2933E-01	1.2797E-01	1.2313E-01	1.1877E-01	1.3684E-01	1.6270E-01	1.7799E-01	1.8226E-01
Ta	4.1030E-02	4.0572E-02	4.0675E-02	4.1288E-02	3.9381E-02	3.5437E-02	3.1560E-02	2.9201E-02
Tc								
Te	1.2404E-01	1.2235E-01	1.2303E-01	1.2506E-01	1.1982E-01	1.0766E-01	9.6045E-02	8.9215E-02
Th	4.1376E+00	4.1165E+00	3.9978E+00	3.8932E+00	4.4317E+00	5.1785E+00	5.6073E+00	5.7189E+00
Ti	2.6933E+00	2.4484E+00	2.9230E+00	3.2619E+00	3.6430E+00	3.1067E+00	2.9682E+00	3.2341E+00
Tl	1.0767E+00	1.0628E+00	1.0086E+00	9.5651E-01	1.1563E+00	1.4523E+00	1.6378E+00	1.6981E+00
U	3.7310E+01	3.6906E+01	3.6504E+01	3.6453E+01	3.7066E+01	3.7209E+01	3.6362E+01	3.5356E+01
V	3.8363E-01	3.7879E-01	3.7693E-01	3.7877E-01	3.7809E-01	3.6655E-01	3.4917E-01	3.3589E-01
W	1.1224E+01	1.1099E+01	1.1115E+01	1.1268E+01	1.0799E+01	9.8035E+00	8.8031E+00	8.1831E+00
Y	6.1252E-01	6.0565E-01	6.0673E-01	6.1531E-01	5.8896E-01	5.3341E-01	4.7795E-01	4.4376E-01
Zn	1.1381E+01	1.0442E+01	1.2223E+01	1.3509E+01	1.4864E+01	1.2703E+01	1.2055E+01	1.2989E+01
Zr	6.3441E+00	6.2069E+00	6.1977E+00	6.1875E+00	6.7302E+00	7.1512E+00	7.3830E+00	7.4774E+00
NO2	2.8881E+04	2.8526E+04	2.8022E+04	2.7747E+04	2.9067E+04	3.0489E+04	3.0796E+04	3.0443E+04
NO3	7.6201E+04	7.5263E+04	7.3888E+04	7.3111E+04	7.6831E+04	8.0948E+04	8.2017E+04	8.1195E+04
TOC	1.1578E+03	1.1487E+03	1.1372E+03	1.1358E+03	1.1678E+03	1.1905E+03	1.1769E+03	1.1511E+03
Activity of radionuclides (mCi/L)								
59Ni	3.8046E-04	3.8171E-04	3.8322E-04	3.8764E-04	3.9645E-04	3.9816E-04	3.8904E-04	3.7865E-04
60Co	6.2888E-04	6.2256E-04	6.1008E-04	6.0214E-04	6.4102E-04	6.8855E-04	7.0647E-04	7.0298E-04
63Ni	3.4696E-02	3.4803E-02	3.4938E-02	3.5339E-02	3.6122E-02	3.6249E-02	3.5396E-02	3.4439E-02
79Se	1.4871E-03	1.4641E-03	1.4329E-03	1.4040E-03	1.5876E-03	1.8106E-03	1.9459E-03	1.9941E-03
90Sr	6.2741E-01	6.2600E-01	6.2227E-01	6.2320E-01	6.4812E-01	6.6989E-01	6.6891E-01	6.5773E-01
90Y	6.0745E-01	6.0610E-01	6.0247E-01	6.0338E-01	6.2750E-01	6.4859E-01	6.4764E-01	6.3682E-01
93mNb	1.2991E+00	1.1706E+00	1.4223E+00	1.6005E+00	1.8069E+00	1.5322E+00	1.4694E+00	1.6178E+00
93Zr	9.5912E-03	9.4794E-03	9.3554E-03	9.3209E-03	9.5254E-03	9.6434E-03	9.4851E-03	9.2514E-03
99Tc	5.9927E-02	5.8829E-02	5.8025E-02	5.7282E-02	6.3615E-02	7.0395E-02	7.4422E-02	7.5932E-02
106Ru	5.6588E-07	5.5981E-07	5.3259E-07	5.0649E-07	6.1912E-07	7.7972E-07	8.8541E-07	9.1967E-07
113mCd	7.1317E-03	7.0379E-03	6.8724E-03	6.7596E-03	7.2140E-03	7.7831E-03	8.0136E-03	7.9892E-03
125Sb	1.7675E-03	1.7450E-03	1.6599E-03	1.5789E-03	1.8915E-03	2.3525E-03	2.6391E-03	2.7302E-03
126Sn	1.6010E-03	1.5875E-03	1.5700E-03	1.5663E-03	1.6133E-03	1.6497E-03	1.6347E-03	1.6006E-03
129I	1.1977E-04	1.1663E-04	1.1908E-04	1.2111E-04	1.2948E-04	1.3057E-04	1.3102E-04	1.3230E-04
134Cs	2.7949E-07	2.7328E-07	2.6649E-07	2.6351E-07	2.9898E-07	3.3508E-07	3.5423E-07	3.6111E-07
137mBa	1.0134E+02	9.9328E+01	9.8360E+01	9.7499E+01	1.0691E+02	1.1598E+02	1.2115E+02	1.2305E+02
137Cs	5.8453E-02	5.7245E-02	5.6786E-02	5.6532E-02	6.2455E-02	6.7283E-02	7.0018E-02	7.0961E-02
151Sm	1.8353E+00	1.8130E+00	1.7703E+00	1.7410E+00	1.8624E+00	2.0166E+00	2.0810E+00	2.0765E+00
152Eu	3.1269E-04	3.0974E-04	3.0069E-04	2.9325E-04	3.2652E-04	3.7222E-04	3.9703E-04	4.0214E-04
154Eu	6.1890E-03	6.2121E-03	6.2249E-03	6.2813E-03	6.4939E-03	6.6298E-03	6.5574E-03	6.4188E-03
155Eu	2.8626E-03	2.8431E-03	2.7833E-03	2.7405E-03	2.9790E-03	3.2869E-03	3.4331E-03	3.4448E-03
226Ra	4.9255E-06	4.8703E-06	4.8787E-06	4.9476E-06	4.7358E-06	4.2895E-06	3.8438E-06	3.5688E-06
227Ac	4.5478E-06	4.5060E-06	4.5182E-06	4.5843E-06	4.4161E-06	4.0416E-06	3.6568E-06	3.4160E-06
228Ra	1.9889E-06	1.9606E-06	1.8967E-06	1.8437E-06	2.0390E-06	2.3111E-06	2.4569E-06	2.4828E-06
229Th	2.1986E-07	2.1702E-07	2.0596E-07	1.9529E-07	2.3619E-07	2.9677E-07	3.3477E-07	3.4712E-07
231Pa	1.2617E-05	1.2476E-05	1.2495E-05	1.2668E-05	1.2139E-05	1.1017E-05	9.8907E-06	9.1930E-06
232Th	4.5355E-07	4.5126E-07	4.3819E-07	4.2668E-07	4.8569E-07	5.6766E-07	6.1470E-07	6.2691E-07
232U	6.2067E-07	6.1294E-07	5.9278E-07	5.7589E-07	6.4246E-07	7.3532E-07	7.8636E-07	7.9729E-07
233U	2.9000E-05	2.8656E-05	2.8130E-05	2.7844E-05	2.9132E-05	3.0557E-05	3.0847E-05	3.0468E-05

CRV Batch ID	A10	B10	A11	B11	A12	B12	A13	B13
234U	1.6670E-05	1.6479E-05	1.6319E-05	1.6323E-05	1.6451E-05	1.6288E-05	1.5749E-05	1.5231E-05
235U	6.2943E-07	6.2236E-07	6.1586E-07	6.1545E-07	6.2306E-07	6.2129E-07	6.0405E-07	5.8582E-07
236U	1.1561E-06	1.1428E-06	1.1349E-06	1.1392E-06	1.1329E-06	1.0975E-06	1.0428E-06	9.9951E-07
237Np	8.4642E-05	8.4020E-05	8.2274E-05	8.1046E-05	8.7794E-05	9.6441E-05	1.0047E-04	1.0072E-04
238Pu	4.4701E-05	4.4148E-05	4.2767E-05	4.1646E-05	4.6105E-05	5.2261E-05	5.5555E-05	5.6181E-05
238U	1.2434E-05	1.2299E-05	1.2165E-05	1.2148E-05	1.2353E-05	1.2402E-05	1.2120E-05	1.1785E-05
239Pu	5.2071E-04	5.1421E-04	4.9488E-04	4.7790E-04	5.4441E-04	6.3936E-04	6.9444E-04	7.0885E-04
240Pu	1.2698E-04	1.2539E-04	1.2057E-04	1.1631E-04	1.3298E-04	1.5686E-04	1.7081E-04	1.7454E-04
241Am	6.4277E-04	6.3463E-04	6.0647E-04	5.8034E-04	6.8138E-04	8.2887E-04	9.1864E-04	9.4567E-04
241Pu	1.4488E-03	1.4300E-03	1.3689E-03	1.3131E-03	1.5279E-03	1.8401E-03	2.0279E-03	2.0826E-03
242Cm	3.1290E-06	3.1172E-06	3.0237E-06	2.9365E-06	3.3395E-06	3.9002E-06	4.2271E-06	4.3068E-06
242Pu	1.4009E-08	1.3834E-08	1.3314E-08	1.2858E-08	1.4647E-08	1.7200E-08	1.8682E-08	1.9069E-08
243Am	1.0374E-07	1.0249E-07	9.9846E-08	9.7911E-08	1.0585E-07	1.1629E-07	1.2116E-07	1.2143E-07
243Cm	3.5947E-07	3.6007E-07	3.6058E-07	3.6185E-07	3.8048E-07	3.9835E-07	4.0151E-07	3.9678E-07
244Cm	7.3215E-06	7.3351E-06	7.3551E-06	7.3929E-06	7.7443E-06	8.0520E-06	8.0806E-06	7.9685E-06

Empty cells represent no data for components with radionuclides only

Table B-2. CRV Composition Converted to the Format Used in Glass Formulation for the 1st Transfer Waste Transferred from the A11th CRV

Component	Value	Component	Value
Glass oxide (mass fraction)		NOx and TOC concentration (g/L)	
Ac ₂ O ₃	2.6471E-13	NO ₂	2.7981E+01
Ag ₂ O	1.3045E-06	NO ₃	7.3780E+01
Al ₂ O ₃	7.0410E-02	TOC	1.1356E+00
Am ₂ O ₃	7.4775E-10	Radionuclide specific activity (mCi/g oxides)	
As ₂ O ₅	6.8805E-06	59Ni	1.4685E-06
B ₂ O ₃	2.0692E-04	60Co	2.3378E-06
BaO	1.1246E-06	63Ni	1.3388E-04
BeO	5.4699E-06	79Se	5.4909E-06
Bi ₂ O ₃	1.9262E-05	90Sr	2.3845E-03
CaO	1.8872E-04	90Y	2.3086E-03
CdO	3.4756E-06	93mNb	5.4502E-03
Ce ₂ O ₃	1.0629E-06	93Zr	3.5849E-05
Cl	1.0657E-02	99Tc	2.2235E-04
Cm ₂ O ₃	4.1731E-13	106Ru	2.0408E-09
CoO	1.9555E-06	113mCd	2.6335E-05
Cr ₂ O ₃	3.4310E-03	125Sb	6.3608E-06
Cs ₂ O	1.3254E-08	126Sn	6.0160E-06
CuO	3.6158E-06	129I	4.5629E-07
Eu ₂ O ₃	1.3553E-10	134Cs	1.0212E-09
F	4.4190E-03	137mBa	3.7691E-01
Fe ₂ O ₃	7.2215E-05	137Cs	2.1760E-04
Gd ₂ O ₃	0.0000E+00	151Sm	6.7836E-03
HgO	3.8970E-07	152Eu	1.1522E-06
I	2.5808E-06	154Eu	2.3853E-05
K ₂ O	6.2008E-02	155Eu	1.0666E-05
La ₂ O ₃	1.6415E-06	226Ra	1.8695E-08
Li ₂ O	1.3074E-06	227Ac	1.7313E-08
MgO	8.3024E-05	228Ra	7.2680E-09
MnO	6.4159E-06	229Th	7.8921E-10
MoO ₃	5.4477E-05	231Pa	4.7880E-08
Na ₂ O	8.2030E-01	232Th	1.6791E-09
Nb ₂ O ₅	3.2676E-08	232U	2.2715E-09
Nd ₂ O ₃	5.2552E-06	233U	1.0779E-07
NiO	1.2940E-04	234U	6.2532E-08
NpO ₂	5.0777E-07	235U	2.3599E-09
P ₂ O ₅	7.8152E-03	236U	4.3489E-09
Pa ₂ O ₅	1.1893E-09	237Np	3.1527E-07
PbO	1.3603E-04	238Pu	1.6388E-07
PdO	3.2219E-05	238U	4.6617E-08
Pr ₂ O ₃	4.6099E-08	239Pu	1.8964E-06
PuO ₂	3.7061E-08	240Pu	4.6204E-07
RaO	2.0280E-11	241Am	2.3240E-06
Rb ₂ O	6.5061E-06	241Pu	5.2457E-06
Rh ₂ O ₃	1.4443E-05	242Cm	1.1587E-08

Component	Value	Component	Value
RuO ₂	6.9023E-05	242Pu	5.1020E-11
SO ₃	1.5515E-02	243Am	3.8261E-10
Sb ₂ O ₃	1.4661E-06	243Cm	1.3817E-09
SeO ₂	1.1936E-05	244Cm	2.8185E-08
SiO ₂	3.9957E-03		
Sm ₂ O ₃	2.9870E-07		
SnO ₂	2.6572E-07		
SrO	5.5799E-07		
Ta ₂ O ₅	1.9032E-07		
Tc ₂ O ₇	2.0353E-05		
TeO ₂	5.8967E-07		
ThO ₂	1.7432E-05		
TiO ₂	1.8686E-05		
Tl ₂ O	4.0163E-06		
UO ₃	1.6809E-04		
V ₂ O ₅	2.5785E-06		
WO ₃	5.3711E-05		
Y ₂ O ₃	2.9525E-06		
ZnO	5.8300E-05		
ZrO ₂	3.2080E-05		
SUM	1.0000E+00		

Table B-3. Initial Composition, Adjusted Target Composition, Waste Contribution, and GFC Target Composition in the A101th MFPV Batch

Component	Initial target	Initial Waste contribution	Initial GFC target	Adjusted target	Adjusted Waste contribution	Adjusted GFC target
Ac ₂ O ₃	6.1720E-14	6.1720E-14		6.1720E-14	6.1720E-14	
Ag ₂ O	3.0417E-07	3.0417E-07		3.0417E-07	3.0417E-07	
Al ₂ O ₃	6.1000E-02	1.6417E-02	4.4583E-02	6.1000E-02	1.6417E-02	4.4583E-02
Am ₂ O ₃	1.7435E-10	1.7435E-10		1.7435E-10	1.7435E-10	
As ₂ O ₅	1.6043E-06	1.6043E-06		1.6043E-06	1.6043E-06	
B ₂ O ₃	1.0000E-01	4.8247E-05	9.9952E-02	1.0000E-01	4.8247E-05	9.9952E-02
BaO	2.6223E-07	2.6223E-07		2.6223E-07	2.6223E-07	
BeO	1.2754E-06	1.2754E-06		1.2754E-06	1.2754E-06	
Bi ₂ O ₃	4.4912E-06	4.4912E-06		4.4912E-06	4.4912E-06	
CaO	2.4706E-02	4.4002E-05	2.4662E-02	2.4706E-02	4.4002E-05	2.4662E-02
CdO	8.1040E-07	8.1040E-07		8.1040E-07	8.1040E-07	
Ce ₂ O ₃	2.4784E-07	2.4784E-07		2.4784E-07	2.4784E-07	
Cl	2.4848E-03	2.4848E-03		2.4848E-03	2.4848E-03	
Cm ₂ O ₃	9.7303E-14	9.7303E-14		9.7303E-14	9.7303E-14	
CoO	4.5595E-07	4.5595E-07		4.5595E-07	4.5595E-07	
Cr ₂ O ₃	8.0000E-04	8.0000E-04		8.0000E-04	8.0000E-04	
Cs ₂ O	3.0903E-09	3.0903E-09		3.0903E-09	3.0903E-09	
CuO	8.4308E-07	8.4308E-07		8.4308E-07	8.4308E-07	
Eu ₂ O ₃	3.1602E-11	3.1602E-11		3.1602E-11	3.1602E-11	
F	1.0304E-03	1.0304E-03		1.0304E-03	1.0304E-03	
Fe ₂ O ₃	5.5000E-02	1.6838E-05	5.4983E-02	5.5000E-02	1.6838E-05	5.4983E-02
Gd ₂ O ₃	0.0000E+00	0.0000E+00		0.0000E+00	0.0000E+00	
HgO	9.0864E-08	9.0864E-08		9.0864E-08	9.0864E-08	
I	6.0176E-07	6.0176E-07		6.0176E-07	6.0176E-07	
K ₂ O	1.4458E-02	1.4458E-02		1.4458E-02	1.4458E-02	
La ₂ O ₃	3.8274E-07	3.8274E-07		3.8274E-07	3.8274E-07	
Li ₂ O	3.0484E-07	3.0484E-07	0.0000E+00	1.9003E-03	3.0484E-07	1.9000E-03
MgO	1.4800E-02	1.9358E-05	1.4781E-02	1.4800E-02	1.9358E-05	1.4781E-02
MnO	1.4960E-06	1.4960E-06		1.4960E-06	1.4960E-06	
MoO ₃	1.2702E-05	1.2702E-05		1.2702E-05	1.2702E-05	
Na ₂ O	1.9127E-01	1.9127E-01	0.0000E+00	1.9127E-01	1.9127E-01	0.0000E+00
Nb ₂ O ₅	7.6190E-09	7.6190E-09		7.6190E-09	7.6190E-09	
Nd ₂ O ₃	1.2253E-06	1.2253E-06		1.2253E-06	1.2253E-06	
NiO	3.0172E-05	3.0172E-05		3.0172E-05	3.0172E-05	
NpO ₂	1.1839E-07	1.1839E-07		1.1839E-07	1.1839E-07	
P ₂ O ₅	1.8222E-03	1.8222E-03		1.8222E-03	1.8222E-03	
Pa ₂ O ₅	2.7729E-10	2.7729E-10		2.7729E-10	2.7729E-10	
PbO	3.1717E-05	3.1717E-05		3.1717E-05	3.1717E-05	
PdO	7.5123E-06	7.5123E-06		7.5123E-06	7.5123E-06	
Pr ₂ O ₃	1.0749E-08	1.0749E-08		1.0749E-08	1.0749E-08	
PuO ₂	8.6412E-09	8.6412E-09		8.6412E-09	8.6412E-09	
RaO	4.7286E-12	4.7286E-12		4.7286E-12	4.7286E-12	
Rb ₂ O	1.5170E-06	1.5170E-06		1.5170E-06	1.5170E-06	
Rh ₂ O ₃	3.3677E-06	3.3677E-06		3.3677E-06	3.3677E-06	
RuO ₂	1.6094E-05	1.6094E-05		1.6094E-05	1.6094E-05	
SO ₃	3.6176E-03	3.6176E-03		3.6176E-03	3.6176E-03	
Sb ₂ O ₃	3.4184E-07	3.4184E-07		3.4184E-07	3.4184E-07	
SeO ₂	2.7830E-06	2.7830E-06		2.7830E-06	2.7830E-06	

Component	Initial target	Initial Waste contribution	Initial GFC target	Adjusted target	Adjusted Waste contribution	Adjusted GFC target
SiO ₂	4.4983E-01	9.3165E-04	4.4890E-01	4.4793E-01	9.3165E-04	4.4700E-01
Sm ₂ O ₃	6.9647E-08	6.9647E-08		6.9647E-08	6.9647E-08	
SnO ₂	6.1957E-08	6.1957E-08		6.1957E-08	6.1957E-08	
SrO	1.3010E-07	1.3010E-07		1.3010E-07	1.3010E-07	
Ta ₂ O ₅	4.4375E-08	4.4375E-08		4.4375E-08	4.4375E-08	
Tc ₂ O ₇	4.7456E-06	4.7456E-06		4.7456E-06	4.7456E-06	
TeO ₂	1.3749E-07	1.3749E-07		1.3749E-07	1.3749E-07	
ThO ₂	4.0645E-06	4.0645E-06		4.0645E-06	4.0645E-06	
TiO ₂	1.4000E-02	4.3570E-06	1.3996E-02	1.4000E-02	4.3570E-06	1.3996E-02
Tl ₂ O	9.3647E-07	9.3647E-07		9.3647E-07	9.3647E-07	
UO ₃	3.9192E-05	3.9192E-05		3.9192E-05	3.9192E-05	
V ₂ O ₅	6.0121E-07	6.0121E-07		6.0121E-07	6.0121E-07	
WO ₃	1.2524E-05	1.2524E-05		1.2524E-05	1.2524E-05	
Y ₂ O ₃	6.8843E-07	6.8843E-07		6.8843E-07	6.8843E-07	
ZnO	3.5000E-02	1.3594E-05	3.4986E-02	3.5000E-02	1.3594E-05	3.4986E-02
ZrO ₂	3.0000E-02	7.4799E-06	2.9993E-02	3.0000E-02	7.4799E-06	2.9993E-02
SUM	1.00000	0.23317	0.76683	1.00000	0.23317	0.76683

Empty cells represent non-GFC components.

Li₂O and SiO₂ concentrations (in bold) are only changes after adjustment.

Table B-4a. Waste and Glass Compositions in Step 1 Calculation of the A101th MFPV Batch before Adjustment

Component	Waste Contribution	GFC Contribution	Combined Normalized	Glass After Retention	Final Glass Normalized
Ac ₂ O ₃	6.1720E-14		6.1659E-14	6.1487E-14	6.1852E-14
Ag ₂ O	3.0417E-07		3.0387E-07	2.9719E-07	2.9896E-07
Al ₂ O ₃	1.6417E-02	4.4583E-02	6.0940E-02	6.0871E-02	6.1232E-02
Am ₂ O ₃	1.7435E-10		1.7418E-10	1.7035E-10	1.7136E-10
As ₂ O ₅	1.6043E-06		1.6027E-06	1.2360E-06	1.2434E-06
B ₂ O ₃	4.8247E-05	9.9952E-02	9.9901E-02	9.8870E-02	9.9457E-02
BaO	2.6223E-07		2.6197E-07	2.6124E-07	2.6279E-07
BeO	1.2754E-06		1.2741E-06	1.2706E-06	1.2781E-06
Bi ₂ O ₃	4.4912E-06		4.4867E-06	4.3882E-06	4.4142E-06
CaO	4.4002E-05	2.4662E-02	2.4682E-02	2.4655E-02	2.4801E-02
CdO	8.1040E-07	3.5079E-06	4.3141E-06	4.3020E-06	4.3275E-06
Ce ₂ O ₃	2.4784E-07		2.4760E-07	2.4691E-07	2.4837E-07
Cl	2.4848E-03	0.0000E+00	2.4824E-03	1.3506E-03	1.3586E-03
Cm ₂ O ₃	9.7303E-14		9.7207E-14	9.6936E-14	9.7511E-14
CoO	4.5595E-07		4.5550E-07	4.5423E-07	4.5692E-07
Cr ₂ O ₃	8.0000E-04	9.9042E-05	8.9815E-04	8.5559E-04	8.6066E-04
Cs ₂ O	3.0903E-09		3.0872E-09	2.7137E-09	2.7298E-09
CuO	8.4308E-07		8.4224E-07	8.3989E-07	8.4487E-07
Eu ₂ O ₃	3.1602E-11		3.1570E-11	3.1482E-11	3.1669E-11
F	1.0304E-03		1.0293E-03	7.5126E-04	7.5572E-04
Fe ₂ O ₃	1.6838E-05	5.4983E-02	5.4946E-02	5.4862E-02	5.5187E-02
Gd ₂ O ₃	0.0000E+00		0.0000E+00	0.0000E+00	0.0000E+00
HgO	9.0864E-08		9.0774E-08	0.0000E+00	0.0000E+00
I	6.0176E-07		6.0116E-07	3.0636E-07	3.0818E-07
K ₂ O	1.4458E-02	2.0962E-05	1.4465E-02	1.3947E-02	1.4030E-02
La ₂ O ₃	3.8274E-07		3.8236E-07	3.8129E-07	3.8356E-07
Li ₂ O	3.0484E-07	0.0000E+00	3.0454E-07	3.0332E-07	3.0512E-07
MgO	1.9358E-05	1.4781E-02	1.4786E-02	1.4783E-02	1.4871E-02
MnO	1.4960E-06	1.3210E-04	1.3347E-04	1.3309E-04	1.3388E-04
MoO ₃	1.2702E-05		1.2690E-05	1.2411E-05	1.2484E-05
Na ₂ O	1.9127E-01	3.3154E-04	1.9141E-01	1.8975E-01	1.9088E-01
Nb ₂ O ₅	7.6190E-09		7.6115E-09	7.5902E-09	7.6353E-09
Nd ₂ O ₃	1.2253E-06		1.2241E-06	1.2207E-06	1.2279E-06
NiO	3.0172E-05	1.1299E-04	1.4302E-04	1.4186E-04	1.4270E-04
NpO ₂	1.1839E-07		1.1828E-07	1.1795E-07	1.1865E-07
P ₂ O ₅	1.8222E-03	1.6111E-04	1.9814E-03	1.9649E-03	1.9766E-03
Pa ₂ O ₅	2.7729E-10		2.7702E-10	2.7625E-10	2.7789E-10
PbO	3.1717E-05	5.8315E-07	3.2269E-05	3.1880E-05	3.2069E-05
PdO	7.5123E-06		7.5048E-06	7.4839E-06	7.5283E-06
Pr ₂ O ₃	1.0749E-08		1.0738E-08	1.0708E-08	1.0772E-08
PuO ₂	8.6412E-09		8.6327E-09	8.6086E-09	8.6597E-09
RaO	4.7286E-12		4.7239E-12	3.6431E-12	3.6647E-12
Rb ₂ O	1.5170E-06		1.5155E-06	1.4822E-06	1.4910E-06
Rh ₂ O ₃	3.3677E-06		3.3644E-06	3.3550E-06	3.3749E-06
RuO ₂	1.6094E-05		1.6078E-05	1.5725E-05	1.5818E-05
SO ₃	3.6176E-03	4.8607E-05	3.6626E-03	3.0777E-03	3.0960E-03
Sb ₂ O ₃	3.4184E-07		3.4150E-07	2.6337E-07	2.6493E-07
SeO ₂	2.7830E-06		2.7803E-06	2.1442E-06	2.1569E-06
SiO ₂	9.3165E-04	4.4890E-01	4.4939E-01	4.4905E-01	4.5172E-01

Component	Waste Contribution	GFC Contribution	Combined Normalized	Glass After Retention	Final Glass Normalized
Sm ₂ O ₃	6.9647E-08		6.9578E-08	6.9384E-08	6.9795E-08
SnO ₂	6.1957E-08		6.1896E-08	6.1723E-08	6.2090E-08
SrO	1.3010E-07		1.2997E-07	1.2961E-07	1.3038E-07
Ta ₂ O ₅	4.4375E-08		4.4331E-08	4.4208E-08	4.4470E-08
Tc ₂ O ₇	4.7456E-06		4.7409E-06	2.0409E-06	2.0530E-06
TeO ₂	1.3749E-07		1.3735E-07	1.0593E-07	1.0656E-07
ThO ₂	4.0645E-06		4.0605E-06	4.0492E-06	4.0732E-06
TiO ₂	4.3570E-06	1.3996E-02	1.3986E-02	1.3951E-02	1.4034E-02
Tl ₂ O	9.3647E-07		9.3554E-07	7.2150E-07	7.2578E-07
UO ₃	3.9192E-05	2.0287E-05	5.9420E-05	5.9254E-05	5.9606E-05
V ₂ O ₅	6.0121E-07	6.0333E-05	6.0874E-05	5.9536E-05	5.9890E-05
WO ₃	1.2524E-05		1.2511E-05	1.2476E-05	1.2550E-05
Y ₂ O ₃	6.8843E-07		6.8775E-07	6.8583E-07	6.8990E-07
ZnO	1.3594E-05	3.4986E-02	3.4965E-02	3.4886E-02	3.5093E-02
ZrO ₂	7.4799E-06	2.9993E-02	2.9970E-02	2.9965E-02	3.0143E-02
SUM	0.233165	0.767826	1.00000	0.99410	1.00000
Waste and GFC contributions		1.000991E+00			

Empty cells represent the components not present in any of the GFCs

Table B-4b. Waste and Glass Compositions in Step 1 Calculation of the A101th MFPV Batch after Adjustment

Component	Waste Contribution	GFC Contribution	Combined Normalized	Glass After Retention	Final Glass Normalized
Ac ₂ O ₃	6.1720E-14		6.1659E-14	6.1487E-14	6.1852E-14
Ag ₂ O	3.0417E-07		3.0387E-07	2.9719E-07	2.9896E-07
Al ₂ O ₃	1.6417E-02	4.4583E-02	6.0939E-02	6.0871E-02	6.1233E-02
Am ₂ O ₃	1.7435E-10		1.7418E-10	1.7035E-10	1.7136E-10
As ₂ O ₅	1.6043E-06		1.6027E-06	1.2360E-06	1.2434E-06
B ₂ O ₃	4.8247E-05	9.9952E-02	9.9900E-02	9.8869E-02	9.9457E-02
BaO	2.6223E-07		2.6197E-07	2.6124E-07	2.6279E-07
BeO	1.2754E-06		1.2741E-06	1.2706E-06	1.2781E-06
Bi ₂ O ₃	4.4912E-06		4.4867E-06	4.3881E-06	4.4142E-06
CaO	4.4002E-05	2.4662E-02	2.4682E-02	2.4655E-02	2.4801E-02
CdO	8.1040E-07	3.5079E-06	4.3140E-06	4.3020E-06	4.3275E-06
Ce ₂ O ₃	2.4784E-07		2.4759E-07	2.4690E-07	2.4837E-07
Cl	2.4848E-03	3.9337E-07	2.4827E-03	1.3508E-03	1.3588E-03
Cm ₂ O ₃	9.7303E-14		9.7206E-14	9.6935E-14	9.7511E-14
CoO	4.5595E-07		4.5549E-07	4.5422E-07	4.5692E-07
Cr ₂ O ₃	8.0000E-04	9.9514E-05	8.9862E-04	8.5603E-04	8.6112E-04
Cs ₂ O	3.0903E-09		3.0872E-09	2.7137E-09	2.7298E-09
CuO	8.4308E-07		8.4224E-07	8.3989E-07	8.4487E-07
Eu ₂ O ₃	3.1602E-11		3.1570E-11	3.1482E-11	3.1669E-11
F	1.0304E-03		1.0293E-03	7.5126E-04	7.5572E-04
Fe ₂ O ₃	1.6838E-05	5.4983E-02	5.4945E-02	5.4862E-02	5.5188E-02
Gd ₂ O ₃	0.0000E+00		0.0000E+00	0.0000E+00	0.0000E+00
HgO	9.0864E-08		9.0773E-08	0.0000E+00	0.0000E+00
I	6.0176E-07		6.0116E-07	3.0636E-07	3.0818E-07
K ₂ O	1.4458E-02	2.0978E-05	1.4465E-02	1.3947E-02	1.4030E-02
La ₂ O ₃	3.8274E-07		3.8236E-07	3.8129E-07	3.8356E-07
Li ₂ O	3.0484E-07	1.9000E-03	1.8984E-03	1.8908E-03	1.9021E-03
MgO	1.9358E-05	1.4781E-02	1.4786E-02	1.4783E-02	1.4871E-02

Component	Waste Contribution	GFC Contribution	Combined Normalized	Glass After Retention	Final Glass Normalized
MnO	1.4960E-06	1.3207E-04	1.3343E-04	1.3306E-04	1.3385E-04
MoO ₃	1.2702E-05		1.2689E-05	1.2411E-05	1.2484E-05
Na ₂ O	1.9127E-01	3.3462E-04	1.9141E-01	1.8976E-01	1.9088E-01
Nb ₂ O ₅	7.6190E-09		7.6114E-09	7.5902E-09	7.6353E-09
Nd ₂ O ₃	1.2253E-06		1.2241E-06	1.2207E-06	1.2279E-06
NiO	3.0172E-05	1.1299E-04	1.4302E-04	1.4186E-04	1.4270E-04
NpO ₂	1.1839E-07		1.1828E-07	1.1795E-07	1.1865E-07
P ₂ O ₅	1.8222E-03	1.6111E-04	1.9814E-03	1.9649E-03	1.9766E-03
Pa ₂ O ₅	2.7729E-10		2.7702E-10	2.7625E-10	2.7789E-10
PbO	3.1717E-05	5.8315E-07	3.2268E-05	3.1880E-05	3.2069E-05
PdO	7.5123E-06		7.5048E-06	7.4839E-06	7.5283E-06
Pr ₂ O ₃	1.0749E-08		1.0738E-08	1.0708E-08	1.0772E-08
PuO ₂	8.6412E-09		8.6326E-09	8.6085E-09	8.6597E-09
RaO	4.7286E-12		4.7239E-12	3.6431E-12	3.6647E-12
Rb ₂ O	1.5170E-06		1.5155E-06	1.4822E-06	1.4910E-06
Rh ₂ O ₃	3.3677E-06		3.3643E-06	3.3550E-06	3.3749E-06
RuO ₂	1.6094E-05		1.6078E-05	1.5725E-05	1.5818E-05
SO ₃	3.6176E-03	4.9866E-05	3.6638E-03	3.0788E-03	3.0971E-03
Sb ₂ O ₃	3.4184E-07		3.4150E-07	2.6336E-07	2.6493E-07
SeO ₂	2.7830E-06		2.7802E-06	2.1441E-06	2.1569E-06
SiO ₂	9.3165E-04	4.4700E-01	4.4748E-01	4.4715E-01	4.4981E-01
Sm ₂ O ₃	6.9647E-08		6.9577E-08	6.9383E-08	6.9795E-08
SnO ₂	6.1957E-08		6.1896E-08	6.1723E-08	6.2090E-08
SrO	1.3010E-07		1.2997E-07	1.2961E-07	1.3038E-07
Ta ₂ O ₅	4.4375E-08		4.4331E-08	4.4207E-08	4.4470E-08
Tc ₂ O ₇	4.7456E-06		4.7409E-06	2.0409E-06	2.0530E-06
TeO ₂	1.3749E-07		1.3735E-07	1.0593E-07	1.0656E-07
ThO ₂	4.0645E-06		4.0605E-06	4.0492E-06	4.0732E-06
TiO ₂	4.3570E-06	1.3996E-02	1.3986E-02	1.3951E-02	1.4034E-02
Tl ₂ O	9.3647E-07		9.3554E-07	7.2150E-07	7.2578E-07
UO ₃	3.9192E-05	2.0287E-05	5.9420E-05	5.9254E-05	5.9606E-05
V ₂ O ₅	6.0121E-07	6.0334E-05	6.0875E-05	5.9537E-05	5.9891E-05
WO ₃	1.2524E-05		1.2511E-05	1.2476E-05	1.2550E-05
Y ₂ O ₃	6.8843E-07		6.8774E-07	6.8583E-07	6.8990E-07
ZnO	1.3594E-05	3.4986E-02	3.4965E-02	3.4886E-02	3.5093E-02
ZrO ₂	7.4799E-06	2.9993E-02	2.9970E-02	2.9965E-02	3.0143E-02
SUM	0.233165	0.767831	1.00000	0.994096	1.000000
Waste and GFC contributions		1.000996E+00			

Empty cells represent the components not present in any of the GFCs

Table B-5a. Radionuclides Activities in Step 1 Calculation the A101th MFPV Batch before Adjustment

Radionuclide	Before Retention mCi/g glass	After Retention mCi/g glass	SD mCi/g glass
59Ni	3.42061E-07	3.41293E-07	2.44481E-08
60Co	5.44554E-07	5.46256E-07	2.81398E-08
63Ni	3.11851E-05	3.11150E-05	2.21133E-06
79Se	1.27903E-06	9.92253E-07	2.25001E-07
90Sr	5.55430E-04	5.57167E-04	2.87069E-05
90Y	5.37760E-04	5.39441E-04	2.78000E-05
93mNb	1.26953E-03	1.27350E-03	9.29833E-05
93Zr	8.35053E-06	8.39856E-06	6.02715E-07
99Tc	5.17932E-05	2.24287E-05	7.82282E-06
106Ru	4.75383E-10	4.67697E-10	4.60344E-11
113mCd	6.13426E-06	6.15343E-06	4.37393E-07
125Sb	1.48165E-06	1.14945E-06	2.53761E-07
126Sn	1.40134E-06	1.40573E-06	1.35855E-07
129I	1.06286E-07	5.44856E-08	1.94087E-08
134Cs	2.37865E-10	2.10328E-10	3.83314E-11
137mBa	8.77954E-02	8.80699E-02	4.59182E-03
137Cs	5.06870E-05	4.48192E-05	5.15875E-06
151Sm	1.58014E-03	1.58508E-03	1.97595E-04
152Eu	2.68392E-07	2.69231E-07	1.37499E-08
154Eu	5.55628E-06	5.57364E-06	2.87399E-07
155Eu	2.48438E-06	2.49215E-06	1.27901E-07
226Ra	4.35473E-09	3.37834E-09	8.70663E-10
227Ac	4.03288E-09	4.04549E-09	2.92393E-10
228Ra	1.69296E-09	1.31337E-09	4.91951E-10
229Th	1.83835E-10	1.84409E-10	5.41429E-11
231Pa	1.11528E-08	1.11877E-08	3.21593E-09
232Th	3.91129E-10	3.92351E-10	2.80536E-11
232U	5.29112E-10	5.30766E-10	2.75495E-11
233U	2.51086E-08	2.51871E-08	1.29041E-09
234U	1.45659E-08	1.46114E-08	7.45308E-10
235U	5.49713E-10	5.51431E-10	3.95082E-11
236U	1.01302E-09	1.01618E-09	5.20845E-11
237Np	7.34369E-08	7.36664E-08	3.83442E-09
238Pu	3.81740E-08	3.82933E-08	1.97530E-09
238U	1.08587E-08	1.08927E-08	7.68048E-10
239Pu	4.41730E-07	4.43110E-07	2.31630E-08
240Pu	1.07624E-07	1.07961E-07	7.76704E-09
241Am	5.41329E-07	5.32577E-07	4.01454E-08
241Pu	1.22191E-06	1.22573E-06	1.17456E-07
242Cm	2.69892E-09	2.70736E-09	1.96260E-10
242Pu	1.18844E-11	1.19216E-11	8.47851E-13
243Am	8.91223E-11	8.76813E-11	8.65084E-12
243Cm	3.21852E-10	3.22858E-10	3.12534E-11
244Cm	6.56516E-09	6.58568E-09	6.33379E-10
Total TRU ^(a)	1.20928E-06	1.20262E-06	4.71965E-08

(a) Total TRU measured by total alpha counting from LAW 1a sample will be used during plant operation. Sum of activities from TRU radionuclides is used in example calculation.

Table B-5b. Radionuclides Activities in Step 1 Calculation the A101th MFPV Batch after Adjustment

Radionuclide	Before Retention mCi/g glass	After Retention mCi/g glass	SD mCi/g glass
59Ni	3.42059E-07	3.41293E-07	2.43342E-08
60Co	5.44551E-07	5.46257E-07	2.80463E-08
63Ni	3.11849E-05	3.11151E-05	2.23726E-06
79Se	1.27902E-06	9.92254E-07	2.22039E-07
90Sr	5.55428E-04	5.57167E-04	2.90332E-05
90Y	5.37757E-04	5.39441E-04	2.77737E-05
93mNb	1.26952E-03	1.27350E-03	9.17426E-05
93Zr	8.35049E-06	8.39857E-06	6.04429E-07
99Tc	5.17929E-05	2.24288E-05	7.66743E-06
106Ru	4.75381E-10	4.67698E-10	4.62192E-11
113mCd	6.13423E-06	6.15344E-06	4.50918E-07
125Sb	1.48165E-06	1.14945E-06	2.48851E-07
126Sn	1.40134E-06	1.40573E-06	1.35899E-07
129I	1.06285E-07	5.44857E-08	1.89869E-08
134Cs	2.37863E-10	2.10328E-10	3.83694E-11
137mBa	8.77950E-02	8.80700E-02	4.54325E-03
137Cs	5.06867E-05	4.48192E-05	5.11592E-06
151Sm	1.58014E-03	1.58509E-03	1.95506E-04
152Eu	2.68391E-07	2.69232E-07	1.37589E-08
154Eu	5.55625E-06	5.57365E-06	2.89269E-07
155Eu	2.48437E-06	2.49215E-06	1.28703E-07
226Ra	4.35471E-09	3.37834E-09	8.99466E-10
227Ac	4.03286E-09	4.04549E-09	2.89147E-10
228Ra	1.69295E-09	1.31337E-09	4.86878E-10
229Th	1.83834E-10	1.84409E-10	5.31553E-11
231Pa	1.11527E-08	1.11877E-08	3.25948E-09
232Th	3.91127E-10	3.92352E-10	2.78769E-11
232U	5.29109E-10	5.30767E-10	2.75775E-11
233U	2.51085E-08	2.51871E-08	1.30522E-09
234U	1.45658E-08	1.46114E-08	7.46527E-10
235U	5.49710E-10	5.51432E-10	4.05786E-11
236U	1.01301E-09	1.01618E-09	5.20458E-11
237Np	7.34365E-08	7.36665E-08	3.81045E-09
238Pu	3.81738E-08	3.82934E-08	1.97868E-09
238U	1.08587E-08	1.08927E-08	7.68151E-10
239Pu	4.41727E-07	4.43111E-07	2.26847E-08
240Pu	1.07624E-07	1.07961E-07	7.61149E-09
241Am	5.41326E-07	5.32578E-07	3.99840E-08
241Pu	1.22190E-06	1.22573E-06	1.16798E-07
242Cm	2.69891E-09	2.70736E-09	1.95381E-10
242Pu	1.18843E-11	1.19216E-11	8.62480E-13
243Am	8.91218E-11	8.76815E-11	8.50568E-12
243Cm	3.21850E-10	3.22859E-10	3.09946E-11
244Cm	6.56513E-09	6.58569E-09	6.43148E-10
Total TRU ^(a)	1.20928E-06	1.20262E-06	4.67985E-08

(a) Total TRU measured by total alpha counting from LAW 1a sample will be used during plant operation. Sum of activities from TRU radionuclides is used in example calculation.

Table B-6. Waste and Glass Compositions in Step 3 Calculation the A101th MFPV Batch

Component	Waste contribution (Step 3)	GFC contribution (Step 3)	Combined normalized (Step 3)	After applying retention factors	Final normalized
Ac2O3	6.1658E-14		6.1658E-14	6.1486E-14	6.1851E-14
Ag2O	3.0386E-07		3.0386E-07	2.9719E-07	2.9895E-07
Al2O3	1.6401E-02	4.4555E-02	6.0956E-02	6.0887E-02	6.1249E-02
Am2O3	1.7417E-10		1.7417E-10	1.7035E-10	1.7136E-10
As2O5	1.6027E-06		1.6027E-06	1.2360E-06	1.2433E-06
B2O3	4.8198E-05	9.9834E-02	9.9883E-02	9.8852E-02	9.9439E-02
BaO	2.6197E-07		2.6197E-07	2.6123E-07	2.6279E-07
BeO	1.2741E-06		1.2741E-06	1.2706E-06	1.2781E-06
Bi2O3	4.4867E-06		4.4867E-06	4.3881E-06	4.4142E-06
CaO	4.3958E-05	2.4645E-02	2.4689E-02	2.4662E-02	2.4809E-02
CdO	8.0958E-07	3.5025E-06	4.3120E-06	4.3000E-06	4.3255E-06
Ce2O3	2.4759E-07		2.4759E-07	2.4690E-07	2.4837E-07
Cl	2.4823E-03	3.9374E-07	2.4827E-03	1.3508E-03	1.3588E-03
Cm2O3	9.7205E-14		9.7205E-14	9.6934E-14	9.7510E-14
CoO	4.5549E-07		4.5549E-07	4.5422E-07	4.5692E-07
Cr2O3	7.9919E-04	9.9401E-05	8.9860E-04	8.5601E-04	8.6109E-04
Cs2O	3.0872E-09		3.0872E-09	2.7137E-09	2.7298E-09
CuO	8.4223E-07		8.4223E-07	8.3988E-07	8.4486E-07
Eu2O3	3.1570E-11		3.1570E-11	3.1482E-11	3.1669E-11
F	1.0293E-03		1.0293E-03	7.5125E-04	7.5571E-04
Fe2O3	1.6821E-05	5.4913E-02	5.4930E-02	5.4847E-02	5.5172E-02
Gd2O3	0.0000E+00		0.0000E+00	0.0000E+00	0.0000E+00
HgO	9.0772E-08		9.0772E-08	0.0000E+00	0.0000E+00
I	6.0115E-07		6.0115E-07	3.0635E-07	3.0817E-07
K2O	1.4444E-02	2.0961E-05	1.4465E-02	1.3947E-02	1.4030E-02
La2O3	3.8235E-07		3.8235E-07	3.8129E-07	3.8355E-07
Li2O	3.0453E-07	1.9018E-03	1.9021E-03	1.8945E-03	1.9057E-03
MgO	1.9339E-05	1.4761E-02	1.4780E-02	1.4778E-02	1.4866E-02
MnO	1.4945E-06	1.3193E-04	1.3342E-04	1.3305E-04	1.3384E-04
MoO3	1.2689E-05		1.2689E-05	1.2411E-05	1.2484E-05
Na2O	1.9107E-01	3.3440E-04	1.9141E-01	1.8975E-01	1.9088E-01
Nb2O5	7.6113E-09		7.6113E-09	7.5901E-09	7.6352E-09
Nd2O3	1.2241E-06		1.2241E-06	1.2207E-06	1.2279E-06
NiO	3.0141E-05	1.1284E-04	1.4298E-04	1.4182E-04	1.4266E-04
NpO2	1.1828E-07		1.1828E-07	1.1795E-07	1.1865E-07
P2O5	1.8204E-03	1.6091E-04	1.9813E-03	1.9648E-03	1.9765E-03
Pa2O5	2.7702E-10		2.7702E-10	2.7624E-10	2.7788E-10
PbO	3.1686E-05	5.8224E-07	3.2268E-05	3.1879E-05	3.2069E-05
PdO	7.5047E-06		7.5047E-06	7.4838E-06	7.5282E-06
Pr2O3	1.0738E-08		1.0738E-08	1.0708E-08	1.0771E-08
PuO2	8.6325E-09		8.6325E-09	8.6084E-09	8.6596E-09
RaO	4.7238E-12		4.7238E-12	3.6430E-12	3.6647E-12
Rb2O	1.5155E-06		1.5155E-06	1.4822E-06	1.4910E-06
Rh2O3	3.3643E-06		3.3643E-06	3.3549E-06	3.3748E-06
RuO2	1.6078E-05		1.6078E-05	1.5724E-05	1.5818E-05
SO3	3.6140E-03	4.9807E-05	3.6638E-03	3.0787E-03	3.0970E-03
Sb2O3	3.4149E-07		3.4149E-07	2.6336E-07	2.6493E-07

Component	Waste contribution (Step 3)	GFC contribution (Step 3)	Combined normalized (Step 3)	After applying retention factors	Final normalized
SeO2	2.7802E-06		2.7802E-06	2.1441E-06	2.1569E-06
SiO2	9.3071E-04	4.4659E-01	4.4752E-01	4.4719E-01	4.4984E-01
Sm2O3	6.9576E-08		6.9576E-08	6.9382E-08	6.9794E-08
SnO2	6.1895E-08		6.1895E-08	6.1722E-08	6.2089E-08
SrO	1.2997E-07		1.2997E-07	1.2961E-07	1.3038E-07
Ta2O5	4.4330E-08		4.4330E-08	4.4207E-08	4.4469E-08
Tc2O7	4.7408E-06		4.7408E-06	2.0409E-06	2.0530E-06
TeO2	1.3735E-07		1.3735E-07	1.0593E-07	1.0656E-07
ThO2	4.0605E-06		4.0605E-06	4.0491E-06	4.0732E-06
TiO2	4.3526E-06	1.3986E-02	1.3990E-02	1.3955E-02	1.4038E-02
Tl2O	9.3553E-07		9.3553E-07	7.2149E-07	7.2577E-07
UO3	3.9153E-05	2.0263E-05	5.9415E-05	5.9250E-05	5.9602E-05
V2O5	6.0060E-07	6.0290E-05	6.0891E-05	5.9553E-05	5.9907E-05
WO3	1.2511E-05		1.2511E-05	1.2476E-05	1.2550E-05
Y2O3	6.8774E-07		6.8774E-07	6.8582E-07	6.8989E-07
ZnO	1.3580E-05	3.4932E-02	3.4945E-02	3.4866E-02	3.5073E-02
ZrO2	7.4724E-06	2.9957E-02	2.9965E-02	2.9959E-02	3.0137E-02
SUM	0.23293	0.76707	1.00000	0.99410	1.00000
Waste and GFC contributions		1.00000E+00			

Empty cells represent the components not present in any of the GFCs.

Table B-7. Radionuclides Activities in Step 3 Calculation the A101th MFPV Batch

Radionuclide	Before retention (Step 3) mCi/g glass	After retention (Step 3) mCi/g glass	SD mCi/g glass
59Ni	3.4205E-07	3.4129E-07	2.4466E-08
60Co	5.4454E-07	5.4625E-07	2.8064E-08
63Ni	3.1185E-05	3.1115E-05	2.2279E-06
79Se	1.2790E-06	9.9224E-07	2.1499E-07
90Sr	5.5542E-04	5.5716E-04	2.8693E-05
90Y	5.3775E-04	5.3943E-04	2.8171E-05
93mNb	1.2695E-03	1.2735E-03	9.0349E-05
93Zr	8.3504E-06	8.3985E-06	5.9083E-07
99Tc	5.1792E-05	2.2428E-05	7.5227E-06
106Ru	4.7537E-10	4.6769E-10	4.5578E-11
113mCd	6.1342E-06	6.1534E-06	4.4645E-07
125Sb	1.4816E-06	1.1494E-06	2.5101E-07
126Sn	1.4013E-06	1.4057E-06	1.3679E-07
129I	1.0628E-07	5.4485E-08	1.9243E-08
134Cs	2.3786E-10	2.1033E-10	3.8551E-11
137mBa	8.7794E-02	8.8069E-02	4.5725E-03
137Cs	5.0686E-05	4.4819E-05	5.0779E-06
151Sm	1.5801E-03	1.5851E-03	1.9667E-04
152Eu	2.6839E-07	2.6923E-07	1.3796E-08
154Eu	5.5562E-06	5.5736E-06	2.8811E-07
155Eu	2.4843E-06	2.4921E-06	1.2616E-07
226Ra	4.3547E-09	3.3783E-09	8.9244E-10
227Ac	4.0328E-09	4.0454E-09	2.9183E-10
228Ra	1.6929E-09	1.3134E-09	4.8513E-10
229Th	1.8383E-10	1.8441E-10	5.4186E-11
231Pa	1.1153E-08	1.1188E-08	3.3445E-09
232Th	3.9112E-10	3.9235E-10	2.8481E-11
232U	5.2910E-10	5.3076E-10	2.7295E-11
233U	2.5108E-08	2.5187E-08	1.2978E-09
234U	1.4566E-08	1.4611E-08	7.5277E-10
235U	5.4970E-10	5.5142E-10	3.9628E-11
236U	1.0130E-09	1.0162E-09	5.2242E-11
237Np	7.3436E-08	7.3666E-08	3.7579E-09
238Pu	3.8173E-08	3.8293E-08	1.9700E-09
238U	1.0859E-08	1.0893E-08	7.8669E-10
239Pu	4.4172E-07	4.4311E-07	2.3118E-08
240Pu	1.0762E-07	1.0796E-07	7.6493E-09
241Am	5.4132E-07	5.3257E-07	4.0675E-08
241Pu	1.2219E-06	1.2257E-06	1.1890E-07
242Cm	2.6989E-09	2.7073E-09	1.9515E-10
242Pu	1.1884E-11	1.1921E-11	8.4942E-13
243Am	8.9121E-11	8.7680E-11	8.6280E-12
243Cm	3.2185E-10	3.2285E-10	3.0759E-11
244Cm	6.5650E-09	6.5856E-09	6.3814E-10
Total TRU ^(a)	1.20926E-06	1.2026E-06	4.7601E-08

(a) Total TRU measured by total alpha counting from LAW 1a sample will be used during plant operation. Sum of activities from TRU radionuclides is used in example calculation.

Table B-8. Input and Results of Algorithm Calculations for 10 Example MFPV Batches

MFPV Batch	MFPV-A101	MFPV-B101	MFPV-A102	MFPV-B102
Input				
Source CRV (<i>d</i>)	CRV-A11	CRV-A11	CRV-A11	CRV-B11
CRV transfer # (<i>m</i>)	1	2	3	1
CRV volume before calculation, L	48709.0	39822.6	31002.5	48852.0
MFPV heel volume, L	6712	6651	6538	6443
Sampling line flush water volume, L	71.2	NA	NA	108.6
CRV-MFPV line flush water volume, L	NA	24.6	24.6	NA
Calculated dilution factor	0.99854	0.99792	0.99713	0.99778
Total mass of glass oxides in CRV waste, g/L	260.583	260.421	260.215	261.535
Step 1 Calculation				
Minimum Na ₂ O loading from formulation rules	19.13%	19.13%	19.13%	19.86%
Limiting rule or component	Cr2O3	Cr2O3	Cr2O3	Cr2O3
Initial waste loading	23.317%	23.317%	23.317%	24.223%
g oxides/L waste	1117.59	1116.89	1116.01	1079.70
g glass/L waste	1111.00	1110.30	1109.43	1073.17
Manual adjustment of GFC component	+0.19 wt% Li2O	+0.18 wt% Li2O	+0.21 wt% Li2O	None
Target waste transfer volume, L	8696.7	8671.3	8820.5	8955.6
GFC volume, L	3273.5	3261.2	3316.8	3211.4
Dust control water volume, L	330.2	329.0	334.6	323.9
Sucrose volume, L	200.8	200.1	203.4	204.4
CRV-MFPV line flush volume, L	37.5	66.2	37.5	40.5
Sampling line flush volume, L	175.3	247.2	175.3	247.2
Dilution water volume, L	0.0	0.0	0.0	0.0
Calculated MFPV working volume, L	19426.0	19426.0	19426.0	19426.0
Target Na Molarity, M	7.870	7.870	7.870	8.164
Dilution water volume, L	-1617.5	-1718.6	-1648.1	-1977.5
Na Molarity of CRV waste, M	6.898	6.893	6.888	6.919
(Target) Kyanite mass, kg	729.90	727.31	739.25	714.34
Boric Acid, kg	1718.73	1712.64	1740.75	1709.80
Wollastonite, kg	502.47	500.70	508.87	444.60
Hematite, kg	517.23	515.39	523.85	514.87
Li Carbonate, kg	45.93	43.36	50.51	0.00
Olivine, kg	296.51	295.46	300.31	294.98
Na Carbonate, kg	0.00	0.00	0.00	0.00
Silica, kg	3528.27	3516.74	3571.88	3507.22
Rutile, kg	137.92	137.43	139.69	137.33
Zincite, kg	340.67	339.47	345.04	338.90
Zircon, kg	438.13	436.58	443.74	435.87
Sucrose, kg	311.09	309.99	315.08	316.61
Total, kg	8566.83	8535.08	8678.96	8414.52
Glass mass per L feed before retention, g/L	765.2	758.9	764.6	745.5
Glass mass per L feed after retention, g/L	760.7	754.4	760.0	741.0
Final waste loading, before retention	23.293%	23.293%	23.293%	24.199%
Glass mass per batch, before retention, kg	9729.0	9694.5	9853.6	9678.9
Glass mass per batch, after retention, kg	9671.5	9637.3	9795.4	9620.3
Step 2 Calculation				
Actual waste transfer volume assumed, L	8957.6	8844.7	8908.7	9134.7
CRV-MFPV line flush volume, L	37.5	66.2	37.5	40.5
GFC volume, L	3371.8	3326.4	3349.9	3275.7

MFPV Batch	MFPV-A101	MFPV-B101	MFPV-A102	MFPV-B102
Dust control water volume, L	340.1	335.6	337.9	330.4
Sucrose volume, L	206.9	204.1	205.4	208.5
Sampling line flush volume, L	175.3	247.2	175.3	247.2
Dilution water volume, L	0.0	0.0	0.0	0.0
Calculated MFPV working volume, L	19801.1	19675.2	19552.7	19679.9
Difference in volume, L	375.1	249.2	126.7	253.9
Dilution water volume, L	-1659.7	-1746.7	-1662.4	-2011.3
(Calculated) Kyanite mass, kg	751.80	741.86	746.64	728.63
Boric Acid, kg	1770.30	1746.90	1758.15	1744.00
Wollastonite, kg	517.54	510.72	513.96	453.49
Hematite, kg	532.74	525.70	529.09	525.17
Li Carbonate, kg	47.31	44.23	51.02	0.00
Olivine, kg	305.40	301.37	303.31	300.88
Na Carbonate, kg	0.00	0.00	0.00	0.00
Silica, kg	3634.13	3587.08	3607.58	3577.37
Rutile, kg	142.06	140.18	141.09	140.08
Zincite, kg	350.89	346.26	348.49	345.68
Zircon, kg	451.28	445.31	448.18	444.59
Sucrose, kg	320.43	316.19	318.23	322.94
Total, kg	8823.88	8705.79	8765.71	8582.82
Step 3 Calculation				
(Assumed as actual) Kyanite mass, kg	752.1	742.0	747.1	728.7
Boric Acid, kg	1770.0	1747.1	1758.3	1744.1
Wollastonite, kg	517.7	510.7	514.1	453.2
Hematite, kg	532.6	525.6	529.1	525.2
Li Carbonate, kg	47.4	44.2	50.9	0.0
Olivine, kg	305.3	301.4	303.2	300.8
Na Carbonate, kg	0.0	0.0	0.0	0.0
Silica, kg	3634.4	3587.5	3607.3	3577.3
Rutile, kg	142.1	140.3	141.1	140.1
Zincite, kg	350.7	346.1	348.4	345.7
Zircon, kg	451.2	445.3	448.2	444.6
Sucrose, kg	320.3	316.2	318.3	322.5
Total, kg	8823.8	8706.4	8766.0	8582.2
Transfer waste volume, L	8957.6	8844.7	8908.7	9134.7
Dust control water volume, L	340.1	335.6	337.9	330.4
CRV-MFPV line flush volume, L	37.5	66.2	37.5	40.5
Sampling line flush volume, L	175.3	247.2	175.3	247.2
Dilution water volume, L	0.0	0.0	0.0	0.0
GFC volume, L	3371.7	3326.7	3350.0	3275.6
Sucrose volume, L	206.8	204.1	205.5	208.2
Calculated MFPV working volume, L	19801.0	19675.5	19552.8	19679.6
Glass mass per L feed before retention, g/L	765.6	759.3	764.7	745.8
Glass mass per L feed after retention, g/L	761.1	754.8	760.2	741.3
Mass of waste oxides per batch, kg	2,334.2	2,303.3	2,318.2	2,389.0
Mass of GFC oxides per batch, kg	7,686.8	7,585.6	7,634.1	7,483.2
Waste loading for Step 3	23.293%	23.292%	23.293%	24.200%
Mass of glass before retention, kg	10,021	9,889	9,952	9,872
Mass of glass after retention, kg	9,962	9,831	9,894	9,812

MFPV Batch	MFPV-A103	MFPV-B103	MFPV-A104	MFPV-B104
Input				
Source CRV (<i>d</i>)	CRV-B11	CRV-B11	CRV-A12	CRV-A12
CRV transfer # (<i>m</i>)	2	3	1	2
CRV volume before calculation, L	39825.9	30843.3	49049	40610.0
MFPV heel volume, L	6582	6488	6515	6441
Sampling line flush water volume, L	NA	NA	71.2	NA
CRV-MFPV line flush water volume, L	25.0	25.0	NA	24.6
Calculated dilution factor	0.99716	0.99635	0.99855	0.99795
Total mass of glass oxides in CRV waste, g/L	261.373	261.160	258.620	258.465
Step 1 Calculation				
Minimum Na ₂ O loading from formulation rules	19.86%	19.86%	17.11%	17.11%
Limiting rule or component	Cr2O3	Cr2O3	Cr2O3	Cr2O3
Initial waste loading	24.223%	24.223%	20.858%	20.858%
g oxides/L waste	1079.03	1078.16	1239.88	1239.14
g glass/L waste	1072.50	1071.63	1232.95	1232.21
Manual adjustment of GFC component	None	None	+0.22 wt% Li2O	+0.21 wt% Li2O
Target waste transfer volume, L	8918.4	8927.6	8467.8	8452.3
GFC volume, L	3196.1	3196.8	3657.4	3647.7
Dust control water volume, L	322.4	322.4	369.7	368.7
Sucrose volume, L	203.4	203.5	203.4	202.9
CRV-MFPV line flush volume, L	28.4	40.5	37.5	66.2
Sampling line flush volume, L	175.3	247.2	175.3	247.2
Dilution water volume, L	0.0	0.0	0.0	0.0
Calculated MFPV working volume, L	19426.0	19426.0	19426.0	19426.0
Target Na Molarity, M	8.164	8.164	7.061	7.061
Dilution water volume, L	-1890.9	-1982.6	-839.7	-943.9
Na Molarity of CRV waste, M	6.915	6.909	6.847	6.843
(Target) Kyanite mass, kg	710.93	711.09	829.17	827.15
Boric Acid, kg	1701.65	1702.02	1856.57	1852.06
Wollastonite, kg	442.48	442.57	793.31	791.40
Hematite, kg	512.42	512.53	557.42	556.07
Li Carbonate, kg	0.00	0.00	155.79	152.80
Olivine, kg	293.57	293.63	319.72	318.94
Na Carbonate, kg	0.00	0.00	0.00	0.00
Silica, kg	3490.50	3491.25	3740.06	3732.01
Rutile, kg	136.68	136.71	148.56	148.20
Zincite, kg	337.29	337.36	367.99	367.10
Zircon, kg	433.80	433.89	473.30	472.15
Sucrose, kg	315.10	315.16	314.99	314.23
Total, kg	8374.41	8376.21	9556.89	9532.10
Glass mass per L feed before retention, g/L	750.0	744.7	814.0	807.4
Glass mass per L feed after retention, g/L	745.4	740.2	809.5	802.9
Final Waste loading, before retention	24.199%	24.199%	20.837%	20.837%
Glass mass per batch, before retention, kg	9632.7	9634.8	10510.1	10484.5
Glass mass per batch, after retention, kg	9574.4	9576.5	10451.3	10425.9
Step 2 Calculation				
Actual waste transfer volume assumed, L	9007.6	8838.3	8510.2	8410.1
CRV-MFPV line flush volume, L	28.4	40.5	37.5	66.2
GFC volume, L	3228.1	3164.8	3675.7	3629.4
Dust control water volume, L	325.6	319.2	371.5	366.9

MFPV Batch	MFPV-A103	MFPV-B103	MFPV-A104	MFPV-B104
Sucrose volume, L	205.5	201.4	204.4	201.8
Sampling line flush volume, L	175.3	247.2	175.3	247.2
Dilution water volume, L	0.0	0.0	0.0	0.0
Calculated MFPV working volume, L	19552.4	19299.5	19489.5	19362.7
Difference in volume, L	126.4	-126.5	63.5	-63.3
Dilution water volume, L	-1907.8	-1965.6	-842.9	-940.7
(Calculated) Kyanite mass, kg	718.04	703.97	833.32	823.02
Boric Acid, kg	1718.67	1684.99	1865.86	1842.80
Wollastonite, kg	446.90	438.15	797.28	787.45
Hematite, kg	517.54	507.40	560.21	553.29
Li Carbonate, kg	0.00	0.00	156.57	152.04
Olivine, kg	296.51	290.70	321.32	317.35
Na Carbonate, kg	0.00	0.00	0.00	0.00
Silica, kg	3525.40	3456.33	3758.77	3713.37
Rutile, kg	138.04	135.34	149.30	147.46
Zincite, kg	340.66	333.99	369.83	365.27
Zircon, kg	438.13	429.55	475.67	469.79
Sucrose, kg	318.25	312.01	316.57	312.66
Total, kg	8458.14	8292.43	9604.70	9484.48
Step 3 Calculation				
(Assumed as actual) Kyanite mass, kg	718.1	703.7	833.1	822.9
Boric Acid, kg	1718.6	1685.0	1866.2	1842.6
Wollastonite, kg	446.5	437.9	797.3	787.3
Hematite, kg	517.5	507.3	560.1	553.3
Li Carbonate, kg	0.0	0.0	156.4	152.0
Olivine, kg	296.3	290.7	321.3	317.4
Na Carbonate, kg	0.0	0.0	0.0	0.0
Silica, kg	3524.9	3455.7	3758.9	3713.0
Rutile, kg	138.0	135.3	149.2	147.4
Zincite, kg	340.5	334.1	369.9	365.3
Zircon, kg	437.9	429.5	475.7	469.8
Sucrose, kg	318.6	312.0	316.4	312.4
Total, kg	8456.9	8291.2	9604.5	9483.4
Transfer waste volume, L	9007.6	8838.3	8510.2	8410.1
Dust control water volume, L	325.6	319.2	371.5	366.9
CRV-MFPV line flush volume, L	28.4	40.5	37.5	66.2
Sampling line flush volume, L	175.3	247.2	175.3	247.2
Dilution water volume, L	0.0	0.0	0.0	0.0
GFC volume, L	3227.6	3164.4	3675.8	3629.1
Sucrose volume, L	205.7	201.4	204.3	201.7
Calculated MFPV working volume, L	19552.1	19299.0	19489.5	19362.2
Glass mass per L feed before retention, g/L	750.0	744.5	814.1	807.3
Glass mass per L feed after retention, g/L	745.5	739.9	809.5	802.8
Mass of waste oxides per batch, kg	2,354.3	2,308.2	2,200.9	2,173.7
Mass of GFC oxides per batch, kg	7,373.1	7,229.0	8,361.7	8,257.7
Waste loading for Step 3	24.203%	24.202%	20.837%	20.838%
Mass of glass before retention, kg	9,727	9,537	10,563	10,431
Mass of glass after retention, kg	9,669	9,479	10,503	10,373

MFPV Batch	MFPV-A105	MFPV-B105
Input		
Source CRV (<i>d</i>)	CRV-A12	CRV-A12
CRV transfer # (<i>m</i>)	3	4
CRV volume before calculation, L	32224.5	23771.1
MFPV heel volume, L	6530	6405
Sampling line flush water volume, L	NA	NA
CRV-MFPV line flush water volume, L	24.6	24.6
Calculated dilution factor	0.99719	0.99615
Total mass of glass oxides in CRV waste, g/L	258.268	257.999
Step 1 Calculation		
Minimum Na ₂ O loading from formulation rules	17.11%	17.11%
Limiting rule or component	Cr2O3	Cr2O3
Initial waste loading	20.858%	20.858%
g oxides/L waste	1238.19	1236.90
g glass/L waste	1231.27	1229.99
Manual adjustment of GFC component	+0.23 wt% Li2O	+0.23 wt% Li2O
Target waste transfer volume, L	8461.1	8480.2
GFC volume, L	3650.3	3654.8
Dust control water volume, L	368.9	369.4
Sucrose volume, L	202.9	203.2
CRV-MFPV line flush volume, L	37.5	66.2
Sampling line flush volume, L	175.3	247.2
Dilution water volume, L	0.0	0.0
Calculated MFPV working volume, L	19426.0	19426.0
Target Na Molarity, M	7.061	7.061
Dilution water volume, L	-849.9	-960.3
Na Molarity of CRV waste, M	6.838	6.830
(Target) Kyanite mass, kg	827.38	828.39
Boric Acid, kg	1852.56	1854.82
Wollastonite, kg	791.58	792.54
Hematite, kg	556.22	556.90
Li Carbonate, kg	158.06	158.25
Olivine, kg	319.03	319.42
Na Carbonate, kg	0.00	0.00
Silica, kg	3730.94	3735.49
Rutile, kg	148.24	148.42
Zincite, kg	367.20	367.65
Zircon, kg	472.28	472.85
Sucrose, kg	314.31	314.70
Total, kg	9537.79	9549.42
Glass mass per L feed before retention, g/L	813.2	806.4
Glass mass per L feed after retention, g/L	808.7	801.9
Final Waste loading, before retention	20.837%	20.837%
Glass mass per batch, before retention, kg	10487.4	10500.2
Glass mass per batch, after retention, kg	10428.7	10441.4
Step 2 Calculation		
Actual waste transfer volume assumed, L	8478.0	8488.7
CRV-MFPV line flush volume, L	37.5	66.2
GFC volume, L	3657.6	3658.4
Dust control water volume, L	369.7	369.8

MFPV Batch	MFPV-A105	MFPV-B105
Sucrose volume, L	203.3	203.4
Sampling line flush volume, L	175.3	247.2
Dilution water volume, L	0.0	0.0
Calculated MFPV working volume, L	19451.4	19438.7
Difference in volume, L	25.4	12.7
Dilution water volume, L	-851.2	-960.9
(Calculated) Kyanite mass, kg	829.04	829.22
Boric Acid, kg	1856.27	1856.67
Wollastonite, kg	793.16	793.33
Hematite, kg	557.33	557.45
Li Carbonate, kg	158.37	158.41
Olivine, kg	319.67	319.74
Na Carbonate, kg	0.00	0.00
Silica, kg	3738.41	3739.22
Rutile, kg	148.53	148.57
Zincite, kg	367.93	368.01
Zircon, kg	473.22	473.32
Sucrose, kg	314.94	315.01
Total, kg	9556.87	9558.96
Step 3 Calculation		
(Assumed as actual) Kyanite mass, kg	829.4	829.3
Boric Acid, kg	1855.9	1856.7
Wollastonite, kg	793.3	793.4
Hematite, kg	557.2	557.5
Li Carbonate, kg	158.3	158.3
Olivine, kg	319.8	319.8
Na Carbonate, kg	0.0	0.0
Silica, kg	3738.7	3739.3
Rutile, kg	148.6	148.6
Zincite, kg	367.8	368.0
Zircon, kg	473.2	473.2
Sucrose, kg	315.0	315.1
Total, kg	9557.2	9559.2
Transfer waste volume, L	8478.0	8488.7
Dust control water volume, L	369.7	369.8
CRV-MFPV line flush volume, L	37.5	66.2
Sampling line flush volume, L	175.3	247.2
Dilution water volume, L	0.0	0.0
GFC volume, L	3657.6	3658.5
Sucrose volume, L	203.4	203.4
Calculated MFPV working volume, L	19451.4	19438.8
Glass mass per L feed before retention, g/L	813.3	806.4
Glass mass per L feed after retention, g/L	808.7	801.9
Mass of waste oxides per batch, kg	2,189.6	2,190.1
Mass of GFC oxides per batch, kg	8,319.2	8,320.8
Waste loading for Step 3	20.836%	20.836%
Mass of glass before retention, kg	10,509	10,511
Mass of glass after retention, kg	10,450	10,452

Table B-9. Waste and Final Glass Compositions and SD for Glass Composition in 10 Example MFPV Batches

Batch	MFPV-A101			MFPV-B101		
	Waste	Glass	Glass SD	Waste	Glass	Glass SD
Ac2O3	2.6471E-13	6.1851E-14	4.4618E-15	2.6471E-13	6.1849E-14	4.4677E-15
Ag2O	1.3045E-06	2.9895E-07	3.6975E-08	1.3045E-06	2.9894E-07	3.7303E-08
Al2O3	7.0410E-02	6.1249E-02	1.1848E-03	7.0410E-02	6.1238E-02	1.2159E-03
Am2O3	7.4775E-10	1.7136E-10	1.3066E-11	7.4775E-10	1.7135E-10	1.2692E-11
As2O5	6.8805E-06	1.2433E-06	3.2541E-07	6.8805E-06	1.2433E-06	3.2158E-07
B2O3	2.0692E-04	9.9439E-02	1.6440E-03	2.0692E-04	9.9463E-02	1.6529E-03
BaO	1.1246E-06	2.6279E-07	2.5200E-08	1.1246E-06	2.6278E-07	2.5305E-08
BeO	5.4699E-06	1.2781E-06	6.6004E-08	5.4699E-06	1.2780E-06	6.5164E-08
Bi2O3	1.9262E-05	4.4142E-06	3.2805E-07	1.9262E-05	4.4140E-06	4.2971E-07
CaO	1.8872E-04	2.4809E-02	6.6487E-04	1.8872E-04	2.4799E-02	6.5394E-04
CdO	3.4756E-06	4.3255E-06	1.3246E-06	3.4756E-06	4.3257E-06	1.3349E-06
Ce2O3	1.0629E-06	2.4837E-07	3.6910E-08	1.0629E-06	2.4836E-07	3.6792E-08
Cl	1.0657E-02	1.3588E-03	3.7987E-04	1.0657E-02	1.3587E-03	3.8397E-04
Cm2O3	4.1731E-13	9.7510E-14	8.8478E-15	4.1731E-13	9.7506E-14	8.6969E-15
CoO	1.9555E-06	4.5692E-07	6.8675E-08	1.9555E-06	4.5690E-07	6.9227E-08
Cr2O3	3.4310E-03	8.6109E-04	6.3918E-05	3.4310E-03	8.6108E-04	6.2643E-05
Cs2O	1.3254E-08	2.7298E-09	3.8148E-10	1.3254E-08	2.7297E-09	3.8097E-10
CuO	3.6158E-06	8.4486E-07	1.2826E-07	3.6158E-06	8.4483E-07	1.2615E-07
Eu2O3	1.3553E-10	3.1669E-11	1.5183E-12	1.3553E-10	3.1667E-11	1.5058E-12
F	4.4190E-03	7.5571E-04	1.3883E-04	4.4190E-03	7.5568E-04	1.3835E-04
Fe2O3	7.2215E-05	5.5172E-02	9.7216E-04	7.2215E-05	5.5175E-02	9.7787E-04
Gd2O3	0.0000E+00	0.0000E+00	0.0000E+00	0.0000E+00	0.0000E+00	0.0000E+00
HgO	3.8970E-07	0.0000E+00	0.0000E+00	3.8970E-07	0.0000E+00	0.0000E+00
I	2.5808E-06	3.0817E-07	1.0885E-07	2.5808E-06	3.0816E-07	1.0893E-07
K2O	6.2008E-02	1.4030E-02	7.8322E-04	6.2008E-02	1.4029E-02	7.9140E-04
La2O3	1.6415E-06	3.8355E-07	2.7446E-08	1.6415E-06	3.8354E-07	2.7598E-08
Li2O	1.3074E-06	1.9057E-03	3.1946E-05	1.3074E-06	1.8008E-03	3.0298E-05
MgO	8.3024E-05	1.4866E-02	2.9267E-04	8.3024E-05	1.4872E-02	2.9269E-04
MnO	6.4159E-06	1.3384E-04	3.4375E-05	6.4159E-06	1.3382E-04	3.4246E-05
MoO3	5.4477E-05	1.2484E-05	9.3488E-07	5.4477E-05	1.2484E-05	9.3213E-07
Na2O	8.2030E-01	1.9088E-01	1.1599E-02	8.2030E-01	1.9087E-01	1.1644E-02
Nb2O5	3.2676E-08	7.6352E-09	5.4174E-10	3.2676E-08	7.6349E-09	5.4752E-10
Nd2O3	5.2552E-06	1.2279E-06	1.2103E-07	5.2552E-06	1.2279E-06	1.2054E-07
NiO	1.2940E-04	1.4266E-04	1.7514E-05	1.2940E-04	1.4270E-04	1.7210E-05
NpO2	5.0777E-07	1.1865E-07	6.0525E-09	5.0777E-07	1.1864E-07	5.9732E-09
P2O5	7.8152E-03	1.9765E-03	1.3468E-04	7.8152E-03	1.9764E-03	1.3627E-04
Pa2O5	1.1893E-09	2.7788E-10	8.3073E-11	1.1893E-09	2.7787E-10	8.1826E-11
PbO	1.3603E-04	3.2069E-05	3.1069E-06	1.3603E-04	3.2067E-05	3.0737E-06
PdO	3.2219E-05	7.5282E-06	7.2562E-07	3.2219E-05	7.5279E-06	7.2577E-07
Pr2O3	4.6099E-08	1.0771E-08	1.0262E-09	4.6099E-08	1.0771E-08	1.0562E-09
PuO2	3.7061E-08	8.6596E-09	4.4231E-10	3.7061E-08	8.6592E-09	4.4179E-10
RaO	2.0280E-11	3.6647E-12	9.6776E-13	2.0280E-11	3.6645E-12	9.6176E-13
Rb2O	6.5061E-06	1.4910E-06	2.2412E-07	6.5061E-06	1.4909E-06	2.2499E-07
Rh2O3	1.4443E-05	3.3748E-06	1.7223E-07	1.4443E-05	3.3747E-06	1.7546E-07
RuO2	6.9023E-05	1.5818E-05	8.8424E-07	6.9023E-05	1.5817E-05	8.7594E-07
SO3	1.5515E-02	3.0970E-03	3.3241E-04	1.5515E-02	3.0968E-03	3.2700E-04
Sb2O3	1.4661E-06	2.6493E-07	7.0143E-08	1.4661E-06	2.6491E-07	6.8393E-08

Batch	MFPV-A101			MFPV-B101		
SeO2	1.1936E-05	2.1569E-06	5.4927E-07	1.1936E-05	2.1568E-06	5.6620E-07
SiO2	3.9957E-03	4.4984E-01	7.2343E-03	3.9957E-03	4.4993E-01	7.2505E-03
Sm2O3	2.9870E-07	6.9794E-08	8.6608E-09	2.9870E-07	6.9792E-08	8.5223E-09
SnO2	2.6572E-07	6.2089E-08	6.0421E-09	2.6572E-07	6.2086E-08	5.9870E-09
SrO	5.5799E-07	1.3038E-07	6.7076E-09	5.5799E-07	1.3037E-07	6.6832E-09
Ta2O5	1.9032E-07	4.4469E-08	4.2870E-09	1.9032E-07	4.4468E-08	4.2755E-09
Tc2O7	2.0353E-05	2.0530E-06	6.8859E-07	2.0353E-05	2.0529E-06	7.0596E-07
TeO2	5.8967E-07	1.0656E-07	2.7969E-08	5.8967E-07	1.0655E-07	2.8249E-08
ThO2	1.7432E-05	4.0732E-06	6.1610E-07	1.7432E-05	4.0730E-06	6.0225E-07
TiO2	1.8686E-05	1.4038E-02	2.7022E-04	1.8686E-05	1.4045E-02	2.7154E-04
Tl2O	4.0163E-06	7.2577E-07	1.6305E-07	4.0163E-06	7.2574E-07	1.6131E-07
UO3	1.6809E-04	5.9602E-05	4.3474E-06	1.6809E-04	5.9602E-05	4.3436E-06
V2O5	2.5785E-06	5.9907E-05	1.9505E-05	2.5785E-06	5.9937E-05	1.9800E-05
WO3	5.3711E-05	1.2550E-05	6.4042E-07	5.3711E-05	1.2550E-05	6.4478E-07
Y2O3	2.9525E-06	6.8989E-07	1.0319E-07	2.9525E-06	6.8986E-07	1.0619E-07
ZnO	5.8300E-05	3.5073E-02	5.6709E-04	5.8300E-05	3.5075E-02	5.7030E-04
ZrO2	3.2080E-05	3.0137E-02	5.1482E-04	3.2080E-05	3.0141E-02	5.1925E-04
SUM	1.0000E+00	1.0000E+00	NA	1.0000E+00	1.0000E+00	NA
Rad	mCi/g oxides	mCi/g glass	mCi/g glass	mCi/g oxides	mCi/g glass	mCi/g glass
59Ni	1.4685E-06	3.4129E-07	2.4466E-08	1.4685E-06	3.4128E-07	2.4552E-08
60Co	2.3378E-06	5.4625E-07	2.8064E-08	2.3378E-06	5.4623E-07	2.8103E-08
63Ni	1.3388E-04	3.1115E-05	2.2279E-06	1.3388E-04	3.1113E-05	2.2151E-06
79Se	5.4909E-06	9.9224E-07	2.1499E-07	5.4909E-06	9.9220E-07	2.2354E-07
90Sr	2.3845E-03	5.5716E-04	2.8693E-05	2.3845E-03	5.5714E-04	2.8694E-05
90Y	2.3086E-03	5.3943E-04	2.8171E-05	2.3086E-03	5.3941E-04	2.7870E-05
93mNb	5.4502E-03	1.2735E-03	9.0349E-05	5.4502E-03	1.2734E-03	9.1322E-05
93Zr	3.5849E-05	8.3985E-06	5.9083E-07	3.5849E-05	8.3981E-06	6.0551E-07
99Tc	2.2235E-04	2.2428E-05	7.5227E-06	2.2235E-04	2.2428E-05	7.7125E-06
106Ru	2.0408E-09	4.6769E-10	4.5578E-11	2.0408E-09	4.6767E-10	4.6015E-11
113mCd	2.6335E-05	6.1534E-06	4.4645E-07	2.6335E-05	6.1531E-06	4.4787E-07
125Sb	6.3608E-06	1.1494E-06	2.5101E-07	6.3608E-06	1.1494E-06	2.4814E-07
126Sn	6.0160E-06	1.4057E-06	1.3679E-07	6.0160E-06	1.4057E-06	1.3555E-07
129I	4.5629E-07	5.4485E-08	1.9243E-08	4.5629E-07	5.4483E-08	1.9260E-08
134Cs	1.0212E-09	2.1033E-10	3.8551E-11	1.0212E-09	2.1032E-10	3.8364E-11
137mBa	3.7691E-01	8.8069E-02	4.5725E-03	3.7691E-01	8.8065E-02	4.5349E-03
137Cs	2.1760E-04	4.4819E-05	5.0779E-06	2.1760E-04	4.4817E-05	5.0869E-06
151Sm	6.7836E-03	1.5851E-03	1.9667E-04	6.7836E-03	1.5850E-03	1.9355E-04
152Eu	1.1522E-06	2.6923E-07	1.3796E-08	1.1522E-06	2.6922E-07	1.3696E-08
154Eu	2.3853E-05	5.5736E-06	2.8811E-07	2.3853E-05	5.5734E-06	2.8500E-07
155Eu	1.0666E-05	2.4921E-06	1.2616E-07	1.0666E-05	2.4920E-06	1.2843E-07
226Ra	1.8695E-08	3.3783E-09	8.9244E-10	1.8695E-08	3.3782E-09	8.8703E-10
227Ac	1.7313E-08	4.0454E-09	2.9183E-10	1.7313E-08	4.0453E-09	2.9222E-10
228Ra	7.2680E-09	1.3134E-09	4.8513E-10	7.2680E-09	1.3133E-09	4.6909E-10
229Th	7.8921E-10	1.8441E-10	5.4186E-11	7.8921E-10	1.8440E-10	5.4131E-11
231Pa	4.7880E-08	1.1188E-08	3.3445E-09	4.7880E-08	1.1187E-08	3.2943E-09
232Th	1.6791E-09	3.9235E-10	2.8481E-11	1.6791E-09	3.9233E-10	2.7921E-11
232U	2.2715E-09	5.3076E-10	2.7295E-11	2.2715E-09	5.3074E-10	2.7301E-11
233U	1.0779E-07	2.5187E-08	1.2978E-09	1.0779E-07	2.5186E-08	1.3053E-09
234U	6.2532E-08	1.4611E-08	7.5277E-10	6.2532E-08	1.4611E-08	7.5550E-10
235U	2.3599E-09	5.5142E-10	3.9628E-11	2.3599E-09	5.5140E-10	3.8998E-11

Batch	MFPV-A101			MFPV-B101		
236U	4.3489E-09	1.0162E-09	5.2242E-11	4.3489E-09	1.0161E-09	5.1606E-11
237Np	3.1527E-07	7.3666E-08	3.7579E-09	3.1527E-07	7.3663E-08	3.7087E-09
238Pu	1.6388E-07	3.8293E-08	1.9700E-09	1.6388E-07	3.8291E-08	1.9492E-09
238U	4.6617E-08	1.0893E-08	7.8669E-10	4.6617E-08	1.0892E-08	7.8698E-10
239Pu	1.8964E-06	4.4311E-07	2.3118E-08	1.8964E-06	4.4309E-07	2.3021E-08
240Pu	4.6204E-07	1.0796E-07	7.6493E-09	4.6204E-07	1.0796E-07	7.8820E-09
241Am	2.3240E-06	5.3257E-07	4.0675E-08	2.3240E-06	5.3255E-07	3.9518E-08
241Pu	5.2457E-06	1.2257E-06	1.1890E-07	5.2457E-06	1.2257E-06	1.1808E-07
242Cm	1.1587E-08	2.7073E-09	1.9515E-10	1.1587E-08	2.7072E-09	1.9353E-10
242Pu	5.1020E-11	1.1921E-11	8.4942E-13	5.1020E-11	1.1921E-11	8.4990E-13
243Am	3.8261E-10	8.7680E-11	8.6280E-12	3.8261E-10	8.7677E-11	8.5247E-12
243Cm	1.3817E-09	3.2285E-10	3.0759E-11	1.3817E-09	3.2284E-10	3.1243E-11
244Cm	2.8185E-08	6.5856E-09	6.3814E-10	2.8185E-08	6.5853E-09	6.2770E-10
TRU ^(a)	5.1915E-06	1.2026E-06	4.7601E-08	5.1915E-06	1.2026E-06	4.6602E-08

Batch	MFPV-A102			MFPV-B102		
Comp	Waste	Glass	Glass SD	Waste	Glass	Glass SD
Ac2O3	2.6471E-13	6.1851E-14	4.4240E-15	2.6740E-13	6.4922E-14	4.6356E-15
Ag2O	1.3045E-06	2.9895E-07	3.6630E-08	1.3024E-06	3.1013E-07	3.8242E-08
Al2O3	7.0410E-02	6.1258E-02	1.1936E-03	7.0698E-02	6.1248E-02	1.2034E-03
Am2O3	7.4775E-10	1.7136E-10	1.2879E-11	7.1244E-10	1.6965E-10	1.2354E-11
As2O5	6.8805E-06	1.2433E-06	3.2701E-07	6.7267E-06	1.2631E-06	3.2675E-07
B2O3	2.0692E-04	9.9463E-02	1.6993E-03	2.2365E-04	9.9481E-02	1.6928E-03
BaO	1.1246E-06	2.6278E-07	2.5250E-08	1.0982E-06	2.6663E-07	2.5366E-08
BeO	5.4699E-06	1.2781E-06	6.5620E-08	5.5230E-06	1.3409E-06	6.7622E-08
Bi2O3	1.9262E-05	4.4141E-06	4.3670E-07	1.8438E-05	4.3904E-06	4.3051E-07
CaO	1.8872E-04	2.4808E-02	6.6220E-04	1.9217E-04	2.2049E-02	5.9266E-04
CdO	3.4756E-06	4.3266E-06	1.3389E-06	3.5039E-06	4.3668E-06	1.3459E-06
Ce2O3	1.0629E-06	2.4836E-07	3.7648E-08	1.0114E-06	2.4556E-07	3.7339E-08
Cl	1.0657E-02	1.3588E-03	3.7904E-04	1.0715E-02	1.4194E-03	3.9320E-04
Cm2O3	4.1731E-13	9.7509E-14	8.7175E-15	4.1743E-13	1.0135E-13	9.0067E-15
CoO	1.9555E-06	4.5691E-07	6.9188E-08	1.9787E-06	4.8042E-07	7.3463E-08
Cr2O3	3.4310E-03	8.6112E-04	6.2236E-05	3.3027E-03	8.6084E-04	6.2073E-05
Cs2O	1.3254E-08	2.7298E-09	3.9018E-10	1.3186E-08	2.8220E-09	3.9365E-10
CuO	3.6158E-06	8.4486E-07	1.2772E-07	3.6207E-06	8.7908E-07	1.3050E-07
Eu2O3	1.3553E-10	3.1668E-11	1.5164E-12	1.3527E-10	3.2843E-11	1.5164E-12
F	4.4190E-03	7.5570E-04	1.4036E-04	4.5576E-03	8.0986E-04	1.4457E-04
Fe2O3	7.2215E-05	5.5187E-02	1.0094E-03	7.7503E-05	5.5200E-02	9.9525E-04
Gd2O3	0.0000E+00	0.0000E+00	0.0000E+00	0.0000E+00	0.0000E+00	0.0000E+00
HgO	3.8970E-07	0.0000E+00	0.0000E+00	3.7639E-07	0.0000E+00	0.0000E+00
I	2.5808E-06	3.0817E-07	1.0769E-07	2.6133E-06	3.2425E-07	1.1542E-07
K2O	6.2008E-02	1.4030E-02	7.8154E-04	6.2561E-02	1.4707E-02	7.9214E-04
La2O3	1.6415E-06	3.8355E-07	2.7083E-08	1.6240E-06	3.9429E-07	2.8096E-08
Li2O	1.3074E-06	2.0606E-03	2.9626E-08	1.3077E-06	3.1711E-07	3.0795E-08
MgO	8.3024E-05	1.4865E-02	3.1126E-04	1.0329E-04	1.4870E-02	2.9847E-04
MnO	6.4159E-06	1.3386E-04	3.3890E-05	6.4877E-06	1.2824E-04	3.4054E-05
MoO3	5.4477E-05	1.2484E-05	9.2987E-07	5.3679E-05	1.2782E-05	9.3840E-07
Na2O	8.2030E-01	1.9088E-01	1.1898E-02	8.1983E-01	1.9821E-01	1.1843E-02
Nb2O5	3.2676E-08	7.6351E-09	5.4216E-10	3.6608E-08	8.8881E-09	6.2388E-10
Nd2O3	5.2552E-06	1.2279E-06	1.1623E-07	5.2602E-06	1.2771E-06	1.2297E-07

Batch	MFPV-A102			MFPV-B102		
	Waste	Glass	Glass SD	Waste	Glass	Glass SD
NiO	1.2940E-04	1.4265E-04	1.7495E-05	1.3240E-04	1.4459E-04	1.7361E-05
NpO2	5.0777E-07	1.1864E-07	6.1051E-09	4.9799E-07	1.2091E-07	6.0622E-09
P2O5	7.8152E-03	1.9765E-03	1.3206E-04	7.7283E-03	2.0267E-03	1.3424E-04
Pa2O5	1.1893E-09	2.7788E-10	8.0908E-11	1.2004E-09	2.9145E-10	8.6102E-11
PbO	1.3603E-04	3.2068E-05	3.0726E-06	1.3869E-04	3.3940E-05	3.1635E-06
PdO	3.2219E-05	7.5281E-06	7.1533E-07	3.2552E-05	7.9033E-06	7.5353E-07
Pr2O3	4.6099E-08	1.0771E-08	1.0426E-09	4.6495E-08	1.1289E-08	1.0893E-09
PuO2	3.7061E-08	8.6595E-09	4.3550E-10	3.5629E-08	8.6503E-09	4.3045E-10
RaO	2.0280E-11	3.6646E-12	9.4955E-13	2.0474E-11	3.8444E-12	9.9596E-13
Rb2O	6.5061E-06	1.4910E-06	2.2768E-07	6.5656E-06	1.5634E-06	2.3705E-07
Rh2O3	1.4443E-05	3.3748E-06	1.7150E-07	1.4612E-05	3.5476E-06	1.7370E-07
RuO2	6.9023E-05	1.5818E-05	8.7436E-07	7.0248E-05	1.6728E-05	9.0363E-07
SO3	1.5515E-02	3.0971E-03	3.2703E-04	1.5015E-02	3.1131E-03	3.2978E-04
Sb2O3	1.4661E-06	2.6492E-07	6.9841E-08	1.4126E-06	2.6523E-07	6.9954E-08
SeO2	1.1936E-05	2.1568E-06	5.5768E-07	1.1809E-05	2.2173E-06	5.8492E-07
SiO2	3.9957E-03	4.4963E-01	7.4306E-03	4.0816E-03	4.4621E-01	7.3342E-03
Sm2O3	2.9870E-07	6.9794E-08	8.6323E-09	2.9247E-07	7.1008E-08	8.8608E-09
SnO2	2.6572E-07	6.2088E-08	5.9532E-09	2.6393E-07	6.4080E-08	6.0201E-09
SrO	5.5799E-07	1.3038E-07	6.6736E-09	5.3587E-07	1.3011E-07	6.4827E-09
Ta2O5	1.9032E-07	4.4469E-08	4.3624E-09	1.9233E-07	4.6697E-08	4.5210E-09
Tc2O7	2.0353E-05	2.0530E-06	7.0272E-07	2.0004E-05	2.0966E-06	7.2215E-07
TeO2	5.8967E-07	1.0655E-07	2.7582E-08	5.9678E-07	1.1206E-07	2.9476E-08
ThO2	1.7432E-05	4.0731E-06	6.1216E-07	1.6901E-05	4.1035E-06	6.2896E-07
TiO2	1.8686E-05	1.4036E-02	2.9117E-04	2.0761E-05	1.4039E-02	2.7890E-04
Tl2O	4.0163E-06	7.2576E-07	1.6314E-07	3.7920E-06	7.1201E-07	1.5873E-07
UO3	1.6809E-04	5.9605E-05	4.3369E-06	1.6711E-04	6.0908E-05	4.3598E-06
V2O5	2.5785E-06	5.9896E-05	1.9533E-05	2.5796E-06	5.9985E-05	1.9858E-05
WO3	5.3711E-05	1.2550E-05	6.3908E-07	5.4213E-05	1.3163E-05	6.5499E-07
Y2O3	2.9525E-06	6.8988E-07	1.0333E-07	2.9811E-06	7.2380E-07	1.0962E-07
ZnO	5.8300E-05	3.5084E-02	6.0051E-04	6.4149E-05	3.5101E-02	5.8286E-04
ZrO2	3.2080E-05	3.0144E-02	5.3508E-04	3.1886E-05	3.0149E-02	5.2964E-04
SUM	1.0000E+00	1.0000E+00	NA	1.0000E+00	1.0000E+00	NA
Rad	mCi/g oxides	mCi/g glass	mCi/g glass	mCi/g oxides	mCi/g glass	mCi/g glass
59Ni	1.4685E-06	3.4129E-07	2.4381E-08	1.4789E-06	3.5714E-07	2.5044E-08
60Co	2.3378E-06	5.4625E-07	2.7714E-08	2.2972E-06	5.5775E-07	2.7855E-08
63Ni	1.3388E-04	3.1114E-05	2.2207E-06	1.3482E-04	3.2558E-05	2.3334E-06
79Se	5.4909E-06	9.9223E-07	2.1759E-07	5.3564E-06	1.0058E-06	2.2629E-07
90Sr	2.3845E-03	5.5716E-04	2.8511E-05	2.3776E-03	5.7725E-04	2.8863E-05
90Y	2.3086E-03	5.3943E-04	2.7343E-05	2.3019E-03	5.5889E-04	2.7862E-05
93mNb	5.4502E-03	1.2735E-03	9.0429E-05	6.1059E-03	1.4825E-03	1.0405E-04
93Zr	3.5849E-05	8.3984E-06	6.0061E-07	3.5560E-05	8.6562E-06	6.1624E-07
99Tc	2.2235E-04	2.2428E-05	7.6771E-06	2.1854E-04	2.2905E-05	7.8893E-06
106Ru	2.0408E-09	4.6769E-10	4.5622E-11	1.9323E-09	4.6012E-10	4.5378E-11
113mCd	2.6335E-05	6.1533E-06	4.3848E-07	2.5788E-05	6.2612E-06	4.4408E-07
125Sb	6.3608E-06	1.1494E-06	2.4858E-07	6.0235E-06	1.1310E-06	2.4590E-07
126Sn	6.0160E-06	1.4057E-06	1.3478E-07	5.9755E-06	1.4508E-06	1.3630E-07
129I	4.5629E-07	5.4485E-08	1.9040E-08	4.6203E-07	5.7327E-08	2.0405E-08
134Cs	1.0212E-09	2.1032E-10	3.8400E-11	1.0053E-09	2.1515E-10	3.8679E-11
137mBa	3.7691E-01	8.8068E-02	4.5095E-03	3.7197E-01	9.0310E-02	4.5263E-03

Batch	MFPV-A102			MFPV-B102		
	Waste	Glass	Glass SD	Waste	Glass	Glass SD
137Cs	2.1760E-04	4.4818E-05	5.1433E-06	2.1567E-04	4.6158E-05	5.2306E-06
151Sm	6.7836E-03	1.5851E-03	1.9604E-04	6.6420E-03	1.6126E-03	2.0123E-04
152Eu	1.1522E-06	2.6923E-07	1.3818E-08	1.1188E-06	2.7163E-07	1.3429E-08
154Eu	2.3853E-05	5.5735E-06	2.8692E-07	2.3964E-05	5.8182E-06	2.8938E-07
155Eu	1.0666E-05	2.4921E-06	1.2826E-07	1.0455E-05	2.5385E-06	1.2765E-07
226Ra	1.8695E-08	3.3783E-09	8.7573E-10	1.8876E-08	3.5442E-09	9.1856E-10
227Ac	1.7313E-08	4.0454E-09	2.8936E-10	1.7489E-08	4.2463E-09	3.0319E-10
228Ra	7.2680E-09	1.3133E-09	4.8118E-10	7.0340E-09	1.3208E-09	4.8744E-10
229Th	7.8921E-10	1.8441E-10	5.4340E-11	7.4506E-10	1.8089E-10	5.3882E-11
231Pa	4.7880E-08	1.1187E-08	3.2573E-09	4.8329E-08	1.1734E-08	3.4665E-09
232Th	1.6791E-09	3.9234E-10	2.8064E-11	1.6278E-09	3.9522E-10	2.7719E-11
232U	2.2715E-09	5.3075E-10	2.6793E-11	2.1971E-09	5.3343E-10	2.6865E-11
233U	1.0779E-07	2.5187E-08	1.2873E-09	1.0623E-07	2.5791E-08	1.2837E-09
234U	6.2532E-08	1.4611E-08	7.4307E-10	6.2275E-08	1.5120E-08	7.4798E-10
235U	2.3599E-09	5.5142E-10	3.9166E-11	2.3480E-09	5.7007E-10	4.0122E-11
236U	4.3489E-09	1.0162E-09	5.1979E-11	4.3462E-09	1.0552E-09	5.3158E-11
237Np	3.1527E-07	7.3665E-08	3.7906E-09	3.0920E-07	7.5070E-08	3.7639E-09
238Pu	1.6388E-07	3.8293E-08	1.9529E-09	1.5888E-07	3.8575E-08	1.9345E-09
238U	4.6617E-08	1.0892E-08	7.7040E-10	4.6347E-08	1.1253E-08	7.8816E-10
239Pu	1.8964E-06	4.4310E-07	2.2728E-08	1.8232E-06	4.4266E-07	2.2485E-08
240Pu	4.6204E-07	1.0796E-07	7.7615E-09	4.4373E-07	1.0773E-07	7.5949E-09
241Am	2.3240E-06	5.3257E-07	4.0096E-08	2.2141E-06	5.2721E-07	3.8456E-08
241Pu	5.2457E-06	1.2257E-06	1.1761E-07	5.0095E-06	1.2163E-06	1.1734E-07
242Cm	1.1587E-08	2.7073E-09	1.9200E-10	1.1203E-08	2.7200E-09	1.9226E-10
242Pu	5.1020E-11	1.1921E-11	8.6059E-13	4.9053E-11	1.1910E-11	8.4938E-13
243Am	3.8261E-10	8.7680E-11	8.5834E-12	3.7354E-10	8.8948E-11	8.6311E-12
243Cm	1.3817E-09	3.2285E-10	3.0922E-11	1.3805E-09	3.3517E-10	3.1916E-11
244Cm	2.8185E-08	6.5855E-09	6.2971E-10	2.8205E-08	6.8478E-09	6.5068E-10
TRU ^(a)	5.1915E-06	1.2026E-06	4.6937E-08	4.9791E-06	1.1985E-06	4.5392E-08

Batch	MFPV-A103			MFPV-B103		
	Waste	Glass	Glass SD	Waste	Glass	Glass SD
Ac2O3	2.6740E-13	6.4931E-14	4.5957E-15	2.6740E-13	6.4929E-14	4.6407E-15
Ag2O	1.3024E-06	3.1018E-07	3.7915E-08	1.3024E-06	3.1017E-07	3.7954E-08
Al2O3	7.0698E-02	6.1256E-02	1.1870E-03	7.0698E-02	6.1234E-02	1.1977E-03
Am2O3	7.1244E-10	1.6967E-10	1.2511E-11	7.1244E-10	1.6966E-10	1.2443E-11
As2O5	6.7267E-06	1.2632E-06	3.3367E-07	6.7267E-06	1.2632E-06	3.3067E-07
B2O3	2.2365E-04	9.9485E-02	1.7345E-03	2.2365E-04	9.9486E-02	1.7133E-03
BaO	1.0982E-06	2.6666E-07	2.5723E-08	1.0982E-06	2.6665E-07	2.5114E-08
BeO	5.5230E-06	1.3411E-06	6.8656E-08	5.5230E-06	1.3411E-06	6.7289E-08
Bi2O3	1.8438E-05	4.3910E-06	4.3178E-07	1.8438E-05	4.3909E-06	4.3376E-07
CaO	1.9217E-04	2.2047E-02	6.1012E-04	1.9217E-04	2.2053E-02	5.8708E-04
CdO	3.5039E-06	4.3655E-06	1.3183E-06	3.5039E-06	4.3682E-06	1.3274E-06
Ce2O3	1.0114E-06	2.4560E-07	3.6437E-08	1.0114E-06	2.4559E-07	3.6668E-08
Cl	1.0715E-02	1.4196E-03	3.9952E-04	1.0715E-02	1.4195E-03	4.0160E-04
Cm2O3	4.1743E-13	1.0136E-13	9.2382E-15	4.1743E-13	1.0136E-13	8.9366E-15
CoO	1.9787E-06	4.8049E-07	7.1121E-08	1.9787E-06	4.8047E-07	7.2648E-08
Cr2O3	3.3027E-03	8.6092E-04	6.2664E-05	3.3027E-03	8.6093E-04	6.2423E-05
Cs2O	1.3186E-08	2.8224E-09	3.8786E-10	1.3186E-08	2.8223E-09	3.9286E-10

Batch	MFPV-A103			MFPV-B103		
	Waste	Glass	Glass SD	Waste	Glass	Glass SD
CuO	3.6207E-06	8.7920E-07	1.3222E-07	3.6207E-06	8.7917E-07	1.3366E-07
Eu2O3	1.3527E-10	3.2847E-11	1.5411E-12	1.3527E-10	3.2846E-11	1.5343E-12
F	4.5576E-03	8.0997E-04	1.4885E-04	4.5576E-03	8.0995E-04	1.5030E-04
Fe2O3	7.7503E-05	5.5200E-02	1.0275E-03	7.7503E-05	5.5193E-02	9.9704E-04
Gd2O3	0.0000E+00	0.0000E+00	0.0000E+00	0.0000E+00	0.0000E+00	0.0000E+00
HgO	3.7639E-07	0.0000E+00	0.0000E+00	3.7639E-07	0.0000E+00	0.0000E+00
I	2.6133E-06	3.2429E-07	1.1365E-07	2.6133E-06	3.2428E-07	1.1332E-07
K2O	6.2561E-02	1.4709E-02	8.0871E-04	6.2561E-02	1.4708E-02	8.1803E-04
La2O3	1.6240E-06	3.9435E-07	2.7943E-08	1.6240E-06	3.9433E-07	2.7730E-08
Li2O	1.3077E-06	3.1715E-07	3.0378E-08	1.3077E-06	3.1714E-07	3.0504E-08
MgO	1.0329E-04	1.4865E-02	3.1747E-04	1.0329E-04	1.4875E-02	2.9831E-04
MnO	6.4877E-06	1.2823E-04	3.4265E-05	6.4877E-06	1.2824E-04	3.4467E-05
MoO3	5.3679E-05	1.2784E-05	9.4620E-07	5.3679E-05	1.2784E-05	9.4419E-07
Na2O	8.1983E-01	1.9823E-01	1.2101E-02	8.1983E-01	1.9823E-01	1.1902E-02
Nb2O5	3.6608E-08	8.8893E-09	6.3816E-10	3.6608E-08	8.8890E-09	6.1775E-10
Nd2O3	5.2602E-06	1.2773E-06	1.2272E-07	5.2602E-06	1.2773E-06	1.2300E-07
NiO	1.3240E-04	1.4456E-04	1.7411E-05	1.3240E-04	1.4463E-04	1.7633E-05
NpO2	4.9799E-07	1.2092E-07	6.0096E-09	4.9799E-07	1.2092E-07	6.0643E-09
P2O5	7.7283E-03	2.0269E-03	1.3736E-04	7.7283E-03	2.0268E-03	1.3494E-04
Pa2O5	1.2004E-09	2.9149E-10	8.5504E-11	1.2004E-09	2.9148E-10	8.4903E-11
PbO	1.3869E-04	3.3944E-05	3.2233E-06	1.3869E-04	3.3944E-05	3.2462E-06
PdO	3.2552E-05	7.9044E-06	7.5982E-07	3.2552E-05	7.9042E-06	7.6054E-07
Pr2O3	4.6495E-08	1.1290E-08	1.0692E-09	4.6495E-08	1.1290E-08	1.0884E-09
PuO2	3.5629E-08	8.6515E-09	4.2148E-10	3.5629E-08	8.6512E-09	4.3118E-10
RaO	2.0474E-11	3.8449E-12	9.8428E-13	2.0474E-11	3.8448E-12	1.0113E-12
Rb2O	6.5656E-06	1.5636E-06	2.3321E-07	6.5656E-06	1.5636E-06	2.3411E-07
Rh2O3	1.4612E-05	3.5481E-06	1.7823E-07	1.4612E-05	3.5479E-06	1.7806E-07
RuO2	7.0248E-05	1.6730E-05	8.9515E-07	7.0248E-05	1.6729E-05	8.9104E-07
SO3	1.5015E-02	3.1135E-03	3.2608E-04	1.5015E-02	3.1134E-03	3.3010E-04
Sb2O3	1.4126E-06	2.6527E-07	6.9087E-08	1.4126E-06	2.6526E-07	6.9581E-08
SeO2	1.1809E-05	2.2176E-06	5.9038E-07	1.1809E-05	2.2175E-06	5.7091E-07
SiO2	4.0816E-03	4.4620E-01	7.5408E-03	4.0816E-03	4.4618E-01	7.4256E-03
Sm2O3	2.9247E-07	7.1018E-08	8.7455E-09	2.9247E-07	7.1015E-08	8.7248E-09
SnO2	2.6393E-07	6.4089E-08	6.2305E-09	2.6393E-07	6.4087E-08	6.1163E-09
SrO	5.3587E-07	1.3012E-07	6.6038E-09	5.3587E-07	1.3012E-07	6.5344E-09
Ta2O5	1.9233E-07	4.6704E-08	4.5199E-09	1.9233E-07	4.6702E-08	4.5111E-09
Tc2O7	2.0004E-05	2.0969E-06	7.2888E-07	2.0004E-05	2.0968E-06	7.2127E-07
TeO2	5.9678E-07	1.1207E-07	2.9351E-08	5.9678E-07	1.1207E-07	2.8946E-08
ThO2	1.6901E-05	4.1040E-06	6.1329E-07	1.6901E-05	4.1039E-06	6.1137E-07
TiO2	2.0761E-05	1.4035E-02	2.9892E-04	2.0761E-05	1.4034E-02	2.7812E-04
Tl2O	3.7920E-06	7.1211E-07	1.5700E-07	3.7920E-06	7.1209E-07	1.6042E-07
UO3	1.6711E-04	6.0905E-05	4.3418E-06	1.6711E-04	6.0911E-05	4.4644E-06
V2O5	2.5796E-06	5.9966E-05	1.9328E-05	2.5796E-06	5.9965E-05	1.9830E-05
WO3	5.4213E-05	1.3164E-05	6.5957E-07	5.4213E-05	1.3164E-05	6.5170E-07
Y2O3	2.9811E-06	7.2390E-07	1.0969E-07	2.9811E-06	7.2387E-07	1.0888E-07
ZnO	6.4149E-05	3.5088E-02	6.1239E-04	6.4149E-05	3.5115E-02	5.8989E-04
ZrO2	3.1886E-05	3.0136E-02	5.5535E-04	3.1886E-05	3.0148E-02	5.3327E-04
SUM	1.0000E+00	1.0000E+00	NA	1.0000E+00	1.0000E+00	NA
--	--	--	--	--	--	--

Batch	MFPV-A103			MFPV-B103		
	Waste	Glass	Glass SD	Waste	Glass	Glass SD
	Rad	mCi/g oxides	mCi/g glass	mCi/g oxides	mCi/g glass	mCi/g glass
59Ni	1.4789E-06	3.5718E-07	2.4950E-08	1.4789E-06	3.5717E-07	2.5943E-08
60Co	2.2972E-06	5.5782E-07	2.7979E-08	2.2972E-06	5.5781E-07	2.7968E-08
63Ni	1.3482E-04	3.2563E-05	2.3171E-06	1.3482E-04	3.2561E-05	2.3373E-06
79Se	5.3564E-06	1.0059E-06	2.3292E-07	5.3564E-06	1.0059E-06	2.2122E-07
90Sr	2.3776E-03	5.7733E-04	2.9206E-05	2.3776E-03	5.7731E-04	2.8873E-05
90Y	2.3019E-03	5.5897E-04	2.8412E-05	2.3019E-03	5.5895E-04	2.8005E-05
93mNb	6.1059E-03	1.4827E-03	1.0644E-04	6.1059E-03	1.4826E-03	1.0304E-04
93Zr	3.5560E-05	8.6574E-06	6.2592E-07	3.5560E-05	8.6571E-06	6.0974E-07
99Tc	2.1854E-04	2.2908E-05	7.9628E-06	2.1854E-04	2.2908E-05	7.8797E-06
106Ru	1.9323E-09	4.6018E-10	4.5902E-11	1.9323E-09	4.6017E-10	4.5806E-11
113mCd	2.5788E-05	6.2620E-06	4.4870E-07	2.5788E-05	6.2618E-06	4.4687E-07
125Sb	6.0235E-06	1.1312E-06	2.4573E-07	6.0235E-06	1.1311E-06	2.4545E-07
126Sn	5.9755E-06	1.4510E-06	1.4106E-07	5.9755E-06	1.4509E-06	1.3847E-07
129I	4.6203E-07	5.7335E-08	2.0094E-08	4.6203E-07	5.7333E-08	2.0034E-08
134Cs	1.0053E-09	2.1518E-10	3.8947E-11	1.0053E-09	2.1518E-10	3.8712E-11
137mBa	3.7197E-01	9.0323E-02	4.5793E-03	3.7197E-01	9.0320E-02	4.5024E-03
137Cs	2.1567E-04	4.6164E-05	5.1394E-06	2.1567E-04	4.6162E-05	5.1760E-06
151Sm	6.6420E-03	1.6128E-03	1.9861E-04	6.6420E-03	1.6128E-03	1.9814E-04
152Eu	1.1188E-06	2.7167E-07	1.3676E-08	1.1188E-06	2.7166E-07	1.3574E-08
154Eu	2.3964E-05	5.8190E-06	2.9357E-07	2.3964E-05	5.8188E-06	2.9317E-07
155Eu	1.0455E-05	2.5388E-06	1.2894E-07	1.0455E-05	2.5387E-06	1.2730E-07
226Ra	1.8876E-08	3.5447E-09	9.0779E-10	1.8876E-08	3.5446E-09	9.3277E-10
227Ac	1.7489E-08	4.2468E-09	3.0058E-10	1.7489E-08	4.2467E-09	3.0353E-10
228Ra	7.0340E-09	1.3209E-09	4.8487E-10	7.0340E-09	1.3209E-09	4.7817E-10
229Th	7.4506E-10	1.8092E-10	5.3394E-11	7.4506E-10	1.8091E-10	5.2534E-11
231Pa	4.8329E-08	1.1735E-08	3.4424E-09	4.8329E-08	1.1735E-08	3.4182E-09
232Th	1.6278E-09	3.9528E-10	2.8214E-11	1.6278E-09	3.9527E-10	2.8149E-11
232U	2.1971E-09	5.3350E-10	2.6588E-11	2.1971E-09	5.3348E-10	2.6529E-11
233U	1.0623E-07	2.5794E-08	1.3004E-09	1.0623E-07	2.5793E-08	1.3111E-09
234U	6.2275E-08	1.5122E-08	7.5314E-10	6.2275E-08	1.5121E-08	7.5846E-10
235U	2.3480E-09	5.7015E-10	4.0290E-11	2.3480E-09	5.7013E-10	4.0075E-11
236U	4.3462E-09	1.0554E-09	5.3087E-11	4.3462E-09	1.0553E-09	5.3930E-11
237Np	3.0920E-07	7.5081E-08	3.7313E-09	3.0920E-07	7.5078E-08	3.7653E-09
238Pu	1.5888E-07	3.8580E-08	1.9520E-09	1.5888E-07	3.8579E-08	1.9337E-09
238U	4.6347E-08	1.1254E-08	8.0587E-10	4.6347E-08	1.1254E-08	8.0691E-10
239Pu	1.8232E-06	4.4273E-07	2.1979E-08	1.8232E-06	4.4271E-07	2.2474E-08
240Pu	4.4373E-07	1.0775E-07	7.6832E-09	4.4373E-07	1.0775E-07	7.7549E-09
241Am	2.2141E-06	5.2729E-07	3.8954E-08	2.2141E-06	5.2727E-07	3.8737E-08
241Pu	5.0095E-06	1.2164E-06	1.1569E-07	5.0095E-06	1.2164E-06	1.1718E-07
242Cm	1.1203E-08	2.7204E-09	1.9353E-10	1.1203E-08	2.7203E-09	1.9470E-10
242Pu	4.9053E-11	1.1911E-11	8.4618E-13	4.9053E-11	1.1911E-11	8.3352E-13
243Am	3.7354E-10	8.8960E-11	8.5566E-12	3.7354E-10	8.8957E-11	8.7726E-12
243Cm	1.3805E-09	3.3522E-10	3.2252E-11	1.3805E-09	3.3521E-10	3.2275E-11
244Cm	2.8205E-08	6.8487E-09	6.6742E-10	2.8205E-08	6.8485E-09	6.4471E-10
TRU ^(a)	4.9791E-06	1.1987E-06	4.5582E-08	4.9791E-06	1.1987E-06	4.5652E-08

Batch	MFPV-A104			MFPV-B104		
	Waste	Glass	Glass SD	Waste	Glass	Glass SD
Ac2O3	2.6069E-13	5.4473E-14	3.9173E-15	2.6069E-13	5.4476E-14	3.9660E-15
Ag2O	1.3203E-06	2.7058E-07	3.4282E-08	1.3203E-06	2.7059E-07	3.4365E-08
Al2O3	6.7942E-02	6.1199E-02	1.1292E-03	6.7942E-02	6.1208E-02	1.1380E-03
Am2O3	8.4636E-10	1.7345E-10	1.2992E-11	8.4636E-10	1.7346E-10	1.3061E-11
As2O5	7.3276E-06	1.1841E-06	3.1191E-07	7.3276E-06	1.1842E-06	3.0992E-07
B2O3	2.4782E-04	9.9440E-02	1.5195E-03	2.4782E-04	9.9417E-02	1.5210E-03
BaO	1.1993E-06	2.5060E-07	2.4631E-08	1.1993E-06	2.5062E-07	2.4463E-08
BeO	5.3496E-06	1.1178E-06	5.8228E-08	5.3496E-06	1.1179E-06	5.8997E-08
Bi2O3	2.1577E-05	4.4219E-06	3.3355E-07	2.1577E-05	4.4222E-06	3.3314E-07
CaO	1.9529E-04	3.6204E-02	9.1150E-04	1.9529E-04	3.6199E-02	9.2816E-04
CdO	3.4282E-06	4.2310E-06	1.3141E-06	3.4282E-06	4.2310E-06	1.3038E-06
Ce2O3	1.2037E-06	2.5151E-07	3.8542E-08	1.2037E-06	2.5153E-07	3.7404E-08
Cl	1.1041E-02	1.2594E-03	3.5262E-04	1.1041E-02	1.2595E-03	3.6159E-04
Cm2O3	4.4300E-13	9.2568E-14	8.4361E-15	4.4300E-13	9.2574E-14	8.4852E-15
CoO	1.9811E-06	4.1397E-07	6.2376E-08	1.9811E-06	4.1400E-07	6.2922E-08
Cr2O3	3.8354E-03	8.6155E-04	6.3488E-05	3.8354E-03	8.6161E-04	6.3665E-05
Cs2O	1.4539E-08	2.6779E-09	3.7874E-10	1.4539E-08	2.6781E-09	3.7880E-10
CuO	3.6164E-06	7.5567E-07	1.1419E-07	3.6164E-06	7.5572E-07	1.1277E-07
Eu2O3	1.4350E-10	2.9985E-11	1.4790E-12	1.4350E-10	2.9987E-11	1.4922E-12
F	4.7503E-03	7.2647E-04	1.3278E-04	4.7503E-03	7.2651E-04	1.3171E-04
Fe2O3	8.8061E-05	5.5158E-02	8.9652E-04	8.8061E-05	5.5173E-02	8.9744E-04
Gd2O3	0.0000E+00	0.0000E+00	0.0000E+00	0.0000E+00	0.0000E+00	0.0000E+00
HgO	4.4272E-07	0.0000E+00	0.0000E+00	4.4272E-07	0.0000E+00	0.0000E+00
I	2.8276E-06	3.0194E-07	1.0638E-07	2.8276E-06	3.0196E-07	1.0607E-07
K2O	6.0931E-02	1.2332E-02	7.0467E-04	6.0931E-02	1.2332E-02	7.0837E-04
La2O3	1.7831E-06	3.7260E-07	2.7248E-08	1.7831E-06	3.7262E-07	2.7227E-08
Li2O	1.3123E-06	5.9632E-03	9.0520E-05	1.3123E-06	5.8683E-03	8.9571E-05
MgO	1.2825E-04	1.4867E-02	2.8001E-04	1.2825E-04	1.4871E-02	2.8223E-04
MnO	7.1305E-06	1.5750E-04	3.4441E-05	7.1305E-06	1.5751E-04	3.4185E-05
MoO3	5.6978E-05	1.1677E-05	8.7961E-07	5.6978E-05	1.1678E-05	8.8018E-07
Na2O	8.2044E-01	1.7078E-01	1.0814E-02	8.2044E-01	1.7079E-01	1.0880E-02
Nb2O5	4.1829E-08	8.7404E-09	6.3346E-10	4.1829E-08	8.7410E-09	6.4170E-10
Nd2O3	5.2652E-06	1.1002E-06	1.0792E-07	5.2652E-06	1.1003E-06	1.0654E-07
NiO	1.3264E-04	1.3994E-04	1.7382E-05	1.3264E-04	1.3998E-04	1.7624E-05
NpO2	5.4596E-07	1.1408E-07	5.9200E-09	5.4596E-07	1.1409E-07	6.0532E-09
P2O5	8.3260E-03	1.8902E-03	1.3047E-04	8.3260E-03	1.8904E-03	1.3017E-04
Pa2O5	1.1641E-09	2.4326E-10	7.0643E-11	1.1641E-09	2.4327E-10	7.1190E-11
PbO	1.3978E-04	2.9515E-05	2.8390E-06	1.3978E-04	2.9517E-05	2.8714E-06
PdO	3.1454E-05	6.5724E-06	6.3309E-07	3.1454E-05	6.5728E-06	6.4007E-07
Pr2O3	4.5224E-08	9.4499E-09	9.1880E-10	4.5224E-08	9.4504E-09	9.4052E-10
PuO2	4.1086E-08	8.5853E-09	4.4880E-10	4.1086E-08	8.5858E-09	4.4680E-10
RaO	1.9838E-11	3.2059E-12	8.5059E-13	1.9838E-11	3.2061E-12	8.4421E-13
Rb2O	6.3763E-06	1.3067E-06	2.0005E-07	6.3763E-06	1.3068E-06	1.9951E-07
Rh2O3	1.4099E-05	2.9461E-06	1.5848E-07	1.4099E-05	2.9462E-06	1.5591E-07
RuO2	6.8799E-05	1.4100E-05	7.9094E-07	6.8799E-05	1.4100E-05	7.9690E-07
SO3	1.7012E-02	3.0397E-03	3.2351E-04	1.7012E-02	3.0398E-03	3.2952E-04
Sb2O3	1.6430E-06	2.6550E-07	6.9311E-08	1.6430E-06	2.6552E-07	7.0728E-08
SeO2	1.2886E-05	2.0823E-06	5.4779E-07	1.2886E-05	2.0824E-06	5.4606E-07
SiO2	4.1264E-03	4.5652E-01	6.7067E-03	4.1264E-03	4.5660E-01	6.7079E-03
Sm2O3	3.1663E-07	6.6162E-08	8.2984E-09	3.1663E-07	6.6166E-08	8.2202E-09
SnO2	2.7513E-07	5.7491E-08	5.6494E-09	2.7513E-07	5.7494E-08	5.6208E-09
SrO	6.2482E-07	1.3056E-07	6.9338E-09	6.2482E-07	1.3057E-07	6.9003E-09

Batch	MFPV-A104			MFPV-B104		
	Waste	Glass	Glass SD	Waste	Glass	Glass SD
Ta2O5	1.8567E-07	3.8796E-08	3.7549E-09	1.8567E-07	3.8799E-08	3.7709E-09
Tc2O7	2.2483E-05	2.0281E-06	6.9992E-07	2.2483E-05	2.0282E-06	6.8930E-07
TeO2	5.7866E-07	9.3511E-08	2.4345E-08	5.7866E-07	9.3517E-08	2.4833E-08
ThO2	1.9471E-05	4.0685E-06	6.1222E-07	1.9471E-05	4.0688E-06	6.1981E-07
TiO2	2.3466E-05	1.4020E-02	2.6267E-04	2.3466E-05	1.4025E-02	2.6294E-04
Tl2O	4.6394E-06	7.4974E-07	1.6795E-07	4.6394E-06	7.4978E-07	1.7196E-07
UO3	1.7197E-04	5.6260E-05	4.3158E-06	1.7197E-04	5.6263E-05	4.3535E-06
V2O5	2.6061E-06	5.9602E-05	1.9535E-05	2.6061E-06	5.9623E-05	1.9444E-05
WO3	5.2582E-05	1.0987E-05	5.7995E-07	5.2582E-05	1.0988E-05	5.8282E-07
Y2O3	2.8879E-06	6.0344E-07	9.2608E-08	2.8879E-06	6.0348E-07	8.9960E-08
ZnO	7.1434E-05	3.5087E-02	5.1791E-04	7.1434E-05	3.5086E-02	5.2092E-04
ZrO2	3.5101E-05	3.0134E-02	4.7472E-04	3.5101E-05	3.0135E-02	4.7826E-04
SUM	1.0000E+00	1.0000E+00	NA	1.0000E+00	1.0000E+00	NA
Rad	mCi/g oxides	mCi/g glass	mCi/g glass	mCi/g oxides	mCi/g glass	mCi/g glass
59Ni	1.5307E-06	3.1814E-07	2.3301E-08	1.5307E-06	3.1816E-07	2.2969E-08
60Co	2.4750E-06	5.1717E-07	2.7427E-08	2.4750E-06	5.1720E-07	2.7062E-08
63Ni	1.3947E-04	2.8987E-05	2.1038E-06	1.3947E-04	2.8988E-05	2.1027E-06
79Se	6.1299E-06	9.9059E-07	2.2389E-07	6.1299E-06	9.9065E-07	2.1825E-07
90Sr	2.5024E-03	5.2290E-04	2.7580E-05	2.5024E-03	5.2293E-04	2.7240E-05
90Y	2.4228E-03	5.0627E-04	2.6566E-05	2.4228E-03	5.0630E-04	2.6690E-05
93mNb	6.9767E-03	1.4578E-03	1.0566E-04	6.9767E-03	1.4579E-03	1.0702E-04
93Zr	3.6778E-05	7.7052E-06	5.5564E-07	3.6778E-05	7.7057E-06	5.5761E-07
99Tc	2.4562E-04	2.2156E-05	7.6464E-06	2.4562E-04	2.2158E-05	7.5305E-06
106Ru	2.3905E-09	4.8990E-10	4.8430E-11	2.3905E-09	4.8993E-10	4.8072E-11
113mCd	2.7854E-05	5.8202E-06	4.1964E-07	2.7854E-05	5.8206E-06	4.2743E-07
125Sb	7.3031E-06	1.1802E-06	2.5729E-07	7.3031E-06	1.1803E-06	2.6495E-07
126Sn	6.2291E-06	1.3016E-06	1.2789E-07	6.2291E-06	1.3017E-06	1.2726E-07
129I	4.9991E-07	5.3383E-08	1.8805E-08	4.9991E-07	5.3386E-08	1.8752E-08
134Cs	1.1544E-09	2.1263E-10	3.9233E-11	1.1544E-09	2.1264E-10	3.8682E-11
137mBa	4.1280E-01	8.6257E-02	4.5805E-03	4.1280E-01	8.6262E-02	4.5056E-03
137Cs	2.4114E-04	4.4416E-05	5.1322E-06	2.4114E-04	4.4419E-05	5.1507E-06
151Sm	7.1909E-03	1.5026E-03	1.8846E-04	7.1909E-03	1.5027E-03	1.8668E-04
152Eu	1.2607E-06	2.6343E-07	1.3825E-08	1.2607E-06	2.6345E-07	1.3933E-08
154Eu	2.5073E-05	5.2393E-06	2.7680E-07	2.5073E-05	5.2396E-06	2.8035E-07
155Eu	1.1502E-05	2.4035E-06	1.2720E-07	1.1502E-05	2.4036E-06	1.2751E-07
226Ra	1.8285E-08	2.9549E-09	7.8436E-10	1.8285E-08	2.9551E-09	7.7849E-10
227Ac	1.7051E-08	3.5629E-09	2.5624E-10	1.7051E-08	3.5631E-09	2.5940E-10
228Ra	7.8728E-09	1.2723E-09	4.6811E-10	7.8728E-09	1.2723E-09	4.6840E-10
229Th	9.1195E-10	1.9056E-10	5.5717E-11	9.1195E-10	1.9057E-10	5.6504E-11
231Pa	4.6868E-08	9.7935E-09	2.8441E-09	4.6868E-08	9.7941E-09	2.8661E-09
232Th	1.8753E-09	3.9186E-10	2.8661E-11	1.8753E-09	3.9188E-10	2.8805E-11
232U	2.4806E-09	5.1834E-10	2.7752E-11	2.4806E-09	5.1837E-10	2.7158E-11
233U	1.1248E-07	2.3503E-08	1.2553E-09	1.1248E-07	2.3505E-08	1.2484E-09
234U	6.3517E-08	1.3272E-08	6.9921E-10	6.3517E-08	1.3273E-08	6.8822E-10
235U	2.4057E-09	5.0268E-10	3.6360E-11	2.4057E-09	5.0271E-10	3.6928E-11
236U	4.3742E-09	9.1402E-10	4.8272E-11	4.3742E-09	9.1408E-10	4.8524E-11
237Np	3.3898E-07	7.0831E-08	3.6757E-09	3.3898E-07	7.0836E-08	3.7583E-09
238Pu	1.7801E-07	3.7197E-08	1.9659E-09	1.7801E-07	3.7200E-08	1.9699E-09
238U	4.7697E-08	9.9666E-09	7.2863E-10	4.7697E-08	9.9672E-09	7.1880E-10
239Pu	2.1020E-06	4.3923E-07	2.3404E-08	2.1020E-06	4.3925E-07	2.3308E-08
240Pu	5.1345E-07	1.0729E-07	7.8636E-09	5.1345E-07	1.0729E-07	7.7731E-09
241Am	2.6309E-06	5.3916E-07	4.0444E-08	2.6309E-06	5.3919E-07	4.0661E-08
241Pu	5.8995E-06	1.2327E-06	1.2178E-07	5.8995E-06	1.2328E-06	1.1882E-07

Batch	MFPV-A104			MFPV-B104		
	Waste	Glass	Glass SD	Waste	Glass	Glass SD
242Cm	1.2894E-08	2.6943E-09	1.9515E-10	1.2894E-08	2.6945E-09	1.9644E-10
242Pu	5.6551E-11	1.1817E-11	8.5003E-13	5.6551E-11	1.1817E-11	8.4354E-13
243Am	4.0871E-10	8.3760E-11	8.2557E-12	4.0871E-10	8.3765E-11	8.3359E-12
243Cm	1.4691E-09	3.0697E-10	3.0467E-11	1.4691E-09	3.0699E-10	2.9851E-11
244Cm	2.9901E-08	6.2480E-09	6.0807E-10	2.9901E-08	6.2484E-09	6.1139E-10
TRU ^(a)	5.7951E-06	1.2004E-06	4.7572E-08	5.7951E-06	1.2004E-06	4.7701E-08

Batch	MFPV-A105			MFPV-B105		
	Waste	Glass	Glass SD	Waste	Glass	Glass SD
Ac2O3	2.6069E-13	5.4470E-14	3.8698E-15	2.6069E-13	5.4472E-14	4.0206E-15
Ag2O	1.3203E-06	2.7056E-07	3.3173E-08	1.3203E-06	2.7057E-07	3.3327E-08
Al2O3	6.7942E-02	6.1228E-02	1.1549E-03	6.7942E-02	6.1214E-02	1.1615E-03
Am2O3	8.4636E-10	1.7344E-10	1.3385E-11	8.4636E-10	1.7345E-10	1.3194E-11
As2O5	7.3276E-06	1.1841E-06	3.1191E-07	7.3276E-06	1.1841E-06	3.0656E-07
B2O3	2.4782E-04	9.9397E-02	1.5247E-03	2.4782E-04	9.9421E-02	1.5328E-03
BaO	1.1993E-06	2.5059E-07	2.4581E-08	1.1993E-06	2.5060E-07	2.4512E-08
BeO	5.3496E-06	1.1178E-06	5.9319E-08	5.3496E-06	1.1178E-06	5.8426E-08
Bi2O3	2.1577E-05	4.4217E-06	3.3662E-07	2.1577E-05	4.4218E-06	3.3860E-07
CaO	1.9529E-04	3.6208E-02	9.2537E-04	1.9529E-04	3.6205E-02	9.1751E-04
CdO	3.4282E-06	4.2289E-06	1.3071E-06	3.4282E-06	4.2302E-06	1.3551E-06
Ce2O3	1.2037E-06	2.5150E-07	3.7919E-08	1.2037E-06	2.5151E-07	3.7441E-08
Cl	1.1041E-02	1.2594E-03	3.5639E-04	1.1041E-02	1.2594E-03	3.5059E-04
Cm2O3	4.4300E-13	9.2563E-14	8.4632E-15	4.4300E-13	9.2566E-14	8.4016E-15
CoO	1.9811E-06	4.1395E-07	6.2749E-08	1.9811E-06	4.1396E-07	6.2742E-08
Cr2O3	3.8354E-03	8.6160E-04	6.4201E-05	3.8354E-03	8.6160E-04	6.4330E-05
Cs2O	1.4539E-08	2.6778E-09	3.7663E-10	1.4539E-08	2.6778E-09	3.7761E-10
CuO	3.6164E-06	7.5563E-07	1.1425E-07	3.6164E-06	7.5565E-07	1.1423E-07
Eu2O3	1.4350E-10	2.9984E-11	1.4957E-12	1.4350E-10	2.9985E-11	1.4914E-12
F	4.7503E-03	7.2643E-04	1.3079E-04	4.7503E-03	7.2645E-04	1.3488E-04
Fe2O3	8.8061E-05	5.5155E-02	9.0840E-04	8.8061E-05	5.5172E-02	9.0906E-04
Gd2O3	0.0000E+00	0.0000E+00	0.0000E+00	0.0000E+00	0.0000E+00	0.0000E+00
HgO	4.4272E-07	0.0000E+00	0.0000E+00	4.4272E-07	0.0000E+00	0.0000E+00
I	2.8276E-06	3.0192E-07	1.0656E-07	2.8276E-06	3.0193E-07	1.0759E-07
K2O	6.0931E-02	1.2331E-02	7.1516E-04	6.0931E-02	1.2331E-02	7.0908E-04
La2O3	1.7831E-06	3.7258E-07	2.7474E-08	1.7831E-06	3.7259E-07	2.7217E-08
Li2O	1.3123E-06	6.0665E-03	9.3054E-05	1.3123E-06	6.0654E-03	9.3042E-05
MgO	1.2825E-04	1.4873E-02	2.8018E-04	1.2825E-04	1.4870E-02	2.8561E-04
MnO	7.1305E-06	1.5750E-04	3.4488E-05	7.1305E-06	1.5752E-04	3.3935E-05
MoO3	5.6978E-05	1.1676E-05	8.7802E-07	5.6978E-05	1.1677E-05	8.9308E-07
Na2O	8.2044E-01	1.7077E-01	1.0974E-02	8.2044E-01	1.7078E-01	1.0920E-02
Nb2O5	4.1829E-08	8.7400E-09	6.3905E-10	4.1829E-08	8.7402E-09	6.2807E-10
Nd2O3	5.2652E-06	1.1001E-06	1.0730E-07	5.2652E-06	1.1002E-06	1.0774E-07
NiO	1.3264E-04	1.3999E-04	1.7159E-05	1.3264E-04	1.3997E-04	1.7483E-05
NpO2	5.4596E-07	1.1408E-07	6.0724E-09	5.4596E-07	1.1408E-07	6.0258E-09
P2O5	8.3260E-03	1.8901E-03	1.3173E-04	8.3260E-03	1.8902E-03	1.3071E-04
Pa2O5	1.1641E-09	2.4324E-10	7.0953E-11	1.1641E-09	2.4325E-10	6.9884E-11
PbO	1.3978E-04	2.9513E-05	2.8883E-06	1.3978E-04	2.9514E-05	2.8464E-06
PdO	3.1454E-05	6.5721E-06	6.4438E-07	3.1454E-05	6.5723E-06	6.5060E-07
Pr2O3	4.5224E-08	9.4494E-09	9.1877E-10	4.5224E-08	9.4496E-09	9.2966E-10
PuO2	4.1086E-08	8.5848E-09	4.5169E-10	4.1086E-08	8.5850E-09	4.5051E-10
RaO	1.9838E-11	3.2057E-12	8.4332E-13	1.9838E-11	3.2058E-12	8.3855E-13
Rb2O	6.3763E-06	1.3067E-06	2.0310E-07	6.3763E-06	1.3067E-06	2.0269E-07
Rh2O3	1.4099E-05	2.9459E-06	1.5751E-07	1.4099E-05	2.9460E-06	1.5599E-07

Batch	MFPV-A105			MFPV-B105		
RuO2	6.8799E-05	1.4099E-05	8.0260E-07	6.8799E-05	1.4099E-05	7.9533E-07
SO3	1.7012E-02	3.0396E-03	3.3040E-04	1.7012E-02	3.0397E-03	3.2811E-04
Sb2O3	1.6430E-06	2.6549E-07	6.8122E-08	1.6430E-06	2.6550E-07	6.9184E-08
SeO2	1.2886E-05	2.0822E-06	5.4109E-07	1.2886E-05	2.0823E-06	5.4847E-07
SiO2	4.1264E-03	4.5645E-01	6.8064E-03	4.1264E-03	4.5642E-01	6.7679E-03
Sm2O3	3.1663E-07	6.6159E-08	8.2170E-09	3.1663E-07	6.6161E-08	8.2647E-09
SnO2	2.7513E-07	5.7488E-08	5.6875E-09	2.7513E-07	5.7489E-08	5.4666E-09
SrO	6.2482E-07	1.3055E-07	6.9183E-09	6.2482E-07	1.3056E-07	7.0290E-09
Ta2O5	1.8567E-07	3.8794E-08	3.7738E-09	1.8567E-07	3.8795E-08	3.7724E-09
Tc2O7	2.2483E-05	2.0280E-06	7.0237E-07	2.2483E-05	2.0280E-06	7.1015E-07
TeO2	5.7866E-07	9.3506E-08	2.4451E-08	5.7866E-07	9.3508E-08	2.4459E-08
ThO2	1.9471E-05	4.0683E-06	6.2478E-07	1.9471E-05	4.0684E-06	6.1782E-07
TiO2	2.3466E-05	1.4035E-02	2.6315E-04	2.3466E-05	1.4032E-02	2.6081E-04
Tl2O	4.6394E-06	7.4970E-07	1.7091E-07	4.6394E-06	7.4972E-07	1.7009E-07
UO3	1.7197E-04	5.6255E-05	4.2621E-06	1.7197E-04	5.6252E-05	4.4123E-06
V2O5	2.6061E-06	5.9665E-05	1.9326E-05	2.6061E-06	5.9654E-05	1.9310E-05
WO3	5.2582E-05	1.0987E-05	5.8697E-07	5.2582E-05	1.0987E-05	5.8396E-07
Y2O3	2.8879E-06	6.0341E-07	9.2319E-08	2.8879E-06	6.0342E-07	9.1466E-08
ZnO	7.1434E-05	3.5066E-02	5.2701E-04	7.1434E-05	3.5078E-02	5.2460E-04
ZrO2	3.5101E-05	3.0129E-02	4.8220E-04	3.5101E-05	3.0124E-02	4.8240E-04
SUM	1.0000E+00	1.0000E+00	NA	1.0000E+00	1.0000E+00	NA
Rad	mCi/g oxides	mCi/g glass	mCi/g glass	mCi/g oxides	mCi/g glass	mCi/g glass
59Ni	1.5307E-06	3.1813E-07	2.3048E-08	1.5307E-06	3.1813E-07	2.2984E-08
60Co	2.4750E-06	5.1714E-07	2.7714E-08	2.4750E-06	5.1715E-07	2.7558E-08
63Ni	1.3947E-04	2.8985E-05	2.1300E-06	1.3947E-04	2.8986E-05	2.1102E-06
79Se	6.1299E-06	9.9054E-07	2.2134E-07	6.1299E-06	9.9056E-07	2.2394E-07
90Sr	2.5024E-03	5.2287E-04	2.8170E-05	2.5024E-03	5.2289E-04	2.7653E-05
90Y	2.4228E-03	5.0624E-04	2.6755E-05	2.4228E-03	5.0625E-04	2.6853E-05
93mNb	6.9767E-03	1.4578E-03	1.0659E-04	6.9767E-03	1.4578E-03	1.0476E-04
93Zr	3.6778E-05	7.7048E-06	5.6813E-07	3.6778E-05	7.7050E-06	5.6191E-07
99Tc	2.4562E-04	2.2155E-05	7.6732E-06	2.4562E-04	2.2156E-05	7.7583E-06
106Ru	2.3905E-09	4.8987E-10	4.9403E-11	2.3905E-09	4.8988E-10	4.8736E-11
113mCd	2.7854E-05	5.8199E-06	4.2593E-07	2.7854E-05	5.8200E-06	4.2591E-07
125Sb	7.3031E-06	1.1801E-06	2.5570E-07	7.3031E-06	1.1802E-06	2.5894E-07
126Sn	6.2291E-06	1.3015E-06	1.2877E-07	6.2291E-06	1.3016E-06	1.2377E-07
129I	4.9991E-07	5.3380E-08	1.8839E-08	4.9991E-07	5.3381E-08	1.9022E-08
134Cs	1.1544E-09	2.1262E-10	3.8515E-11	1.1544E-09	2.1262E-10	3.8517E-11
137mBa	4.1280E-01	8.6253E-02	4.5871E-03	4.1280E-01	8.6255E-02	4.6330E-03
137Cs	2.4114E-04	4.4414E-05	5.1120E-06	2.4114E-04	4.4415E-05	5.0396E-06
151Sm	7.1909E-03	1.5025E-03	1.8661E-04	7.1909E-03	1.5025E-03	1.8770E-04
152Eu	1.2607E-06	2.6342E-07	1.4145E-08	1.2607E-06	2.6342E-07	1.3848E-08
154Eu	2.5073E-05	5.2390E-06	2.8045E-07	2.5073E-05	5.2391E-06	2.7930E-07
155Eu	1.1502E-05	2.4033E-06	1.2771E-07	1.1502E-05	2.4034E-06	1.2741E-07
226Ra	1.8285E-08	2.9547E-09	7.7770E-10	1.8285E-08	2.9548E-09	7.7328E-10
227Ac	1.7051E-08	3.5627E-09	2.5311E-10	1.7051E-08	3.5628E-09	2.6297E-10
228Ra	7.8728E-09	1.2722E-09	4.6196E-10	7.8728E-09	1.2722E-09	4.6660E-10
229Th	9.1195E-10	1.9055E-10	5.6422E-11	9.1195E-10	1.9055E-10	5.5476E-11
231Pa	4.6868E-08	9.7930E-09	2.8566E-09	4.6868E-08	9.7932E-09	2.8135E-09
232Th	1.8753E-09	3.9184E-10	2.8498E-11	1.8753E-09	3.9185E-10	2.8900E-11
232U	2.4806E-09	5.1831E-10	2.7431E-11	2.4806E-09	5.1832E-10	2.7885E-11
233U	1.1248E-07	2.3502E-08	1.2426E-09	1.1248E-07	2.3503E-08	1.2553E-09
234U	6.3517E-08	1.3272E-08	7.0281E-10	6.3517E-08	1.3272E-08	7.0440E-10
235U	2.4057E-09	5.0266E-10	3.6747E-11	2.4057E-09	5.0267E-10	3.7005E-11
236U	4.3742E-09	9.1398E-10	4.9163E-11	4.3742E-09	9.1400E-10	4.8761E-11

Batch	MFPV-A105			MFPV-B105		
237Np	3.3898E-07	7.0828E-08	3.7703E-09	3.3898E-07	7.0830E-08	3.7413E-09
238Pu	1.7801E-07	3.7195E-08	1.9758E-09	1.7801E-07	3.7196E-08	1.9527E-09
238U	4.7697E-08	9.9661E-09	7.2694E-10	4.7697E-08	9.9663E-09	7.3322E-10
239Pu	2.1020E-06	4.3920E-07	2.3563E-08	2.1020E-06	4.3921E-07	2.3466E-08
240Pu	5.1345E-07	1.0728E-07	7.8167E-09	5.1345E-07	1.0728E-07	8.0058E-09
241Am	2.6309E-06	5.3913E-07	4.1673E-08	2.6309E-06	5.3915E-07	4.1075E-08
241Pu	5.8995E-06	1.2327E-06	1.2064E-07	5.8995E-06	1.2327E-06	1.1828E-07
242Cm	1.2894E-08	2.6942E-09	1.9468E-10	1.2894E-08	2.6942E-09	1.9477E-10
242Pu	5.6551E-11	1.1816E-11	8.6061E-13	5.6551E-11	1.1816E-11	8.5975E-13
243Am	4.0871E-10	8.3755E-11	8.3714E-12	4.0871E-10	8.3757E-11	8.4701E-12
243Cm	1.4691E-09	3.0695E-10	3.0239E-11	1.4691E-09	3.0696E-10	3.0187E-11
244Cm	2.9901E-08	6.2477E-09	6.1082E-10	2.9901E-08	6.2479E-09	6.0591E-10
TRU ^(a)	5.7951E-06	1.2003E-06	4.8698E-08	5.7951E-06	1.2003E-06	4.8167E-08

Table B-10. Results of Glass Properties and Constraint Quantities for 10 Example MFPV Batches

Properties/Constraints	MFPV-A101	MFPV-B101	MFPV-A102	MFPV-B102	MFPV-A103
<i>P^{prop}</i>					
ln(<i>r_B</i>)	0.0540	0.0492	0.0634	0.1408	0.1412
ln(<i>r_{Na}</i>)	-0.0579	-0.0618	-0.0506	0.0009	0.0012
ln(<i>D</i>)	2.6105	2.5922	2.6358	2.8623	2.8656
ln(<i>η₁₁₀₀</i>), <i>u</i>	4.6076	4.6131	4.5985	4.5922	4.5920
ln(<i>η₁₁₅₀</i>), <i>l</i>	4.1117	4.1168	4.1032	4.0990	4.0987
ln(<i>η₁₁₅₀</i>), <i>u</i>	4.1117	4.1168	4.1032	4.0990	4.0987
ln(<i>ε₁₁₀₀</i>), <i>l</i>	-1.0551	-1.0561	-1.0537	-0.9829	-0.9826
ln(<i>ε₁₂₀₀</i>), <i>u</i>	-0.7026	-0.7033	-0.7014	-0.6374	-0.6371
<i>U^{prop}_{pred}</i>					
ln(<i>r_B</i>)	0.1537	0.1545	0.1526	0.1640	0.1640
ln(<i>r_{Na}</i>)	0.1651	0.1656	0.1643	0.1765	0.1765
ln(<i>D</i>)	0.6303	0.6339	0.6250	0.6563	0.6562
ln(<i>η₁₁₀₀</i>), <i>u</i>	0.0326	0.0327	0.0324	0.0353	0.0353
ln(<i>η₁₁₅₀</i>), <i>l</i>	0.0328	0.0329	0.0326	0.0355	0.0355
ln(<i>η₁₁₅₀</i>), <i>u</i>	0.0328	0.0329	0.0326	0.0355	0.0355
ln(<i>ε₁₁₀₀</i>), <i>l</i>	0.0321	0.0322	0.0320	0.0353	0.0354
ln(<i>ε₁₂₀₀</i>), <i>u</i>	0.0327	0.0328	0.0325	0.0359	0.0359
<i>U^{prop}_{comp}</i>					
ln(<i>r_B</i>)	0.3366	0.3516	0.3458	0.3496	0.3745
ln(<i>r_{Na}</i>)	0.2852	0.2982	0.2944	0.2895	0.3088
ln(<i>D</i>)	1.2035	1.2679	1.2219	1.3583	1.4372
ln(<i>η₁₁₀₀</i>), <i>u</i>	0.2523	0.2409	0.2618	0.2573	0.2597
ln(<i>η₁₁₅₀</i>), <i>l</i>	0.2254	0.2348	0.2337	0.2327	0.2467
ln(<i>η₁₁₅₀</i>), <i>u</i>	0.2333	0.2224	0.2415	0.2375	0.2396
ln(<i>ε₁₁₀₀</i>), <i>l</i>	0.1766	0.1689	0.1865	0.1788	0.1814
ln(<i>ε₁₂₀₀</i>), <i>u</i>	0.1528	0.1606	0.1618	0.1564	0.1686
<i>B^{prop}_{ucci,lcci}</i>					
ln(<i>r_B</i>)	0.5443	0.5553	0.5619	0.6544	0.6796
ln(<i>r_{Na}</i>)	0.3924	0.4020	0.4081	0.4669	0.4865
ln(<i>D</i>)	4.4442	4.4940	4.4828	4.8770	4.9590
ln(<i>η₁₁₀₀</i>), <i>u</i>	4.8925	4.8867	4.8927	4.8848	4.8869
ln(<i>η₁₁₅₀</i>), <i>l</i>	3.8536	3.8491	3.8369	3.8308	3.8166
ln(<i>η₁₁₅₀</i>), <i>u</i>	4.3779	4.3721	4.3773	4.3720	4.3738
ln(<i>ε₁₁₀₀</i>), <i>l</i>	-1.2638	-1.2572	-1.2722	-1.1971	-1.1993
ln(<i>ε₁₂₀₀</i>), <i>u</i>	-0.5172	-0.5099	-0.5071	-0.4451	-0.4327
Model validity single component constraints					
Al ₂ O ₃	0.06125	0.06124	0.06126	0.06125	0.06126
Cl	0.00136	0.00136	0.00136	0.00142	0.00142
Cr ₂ O ₃	0.00086	0.00086	0.00086	0.00086	0.00086
F	0.00076	0.00076	0.00076	0.00081	0.00081
P ₂ O ₅	0.00198	0.00198	0.00198	0.00203	0.00203
SiO ₂	0.44984	0.44993	0.44963	0.44621	0.44620

Properties/Constraints	MFPV-A101	MFPV-B101	MFPV-A102	MFPV-B102	MFPV-A103
Sum of Minors	0.00051	0.00051	0.00051	0.00051	0.00051
Model validity PCT constraints					
P^{pctB} (ln[g/L])	0.0540	0.0492	0.0634	0.1408	0.1412
P^{pctNa} (ln[g/L])	-0.0579	-0.0618	-0.0506	0.0009	0.0012
Model validity multiple component constraints					
Li ₂ O	0.00191	0.00180	0.00206	0.00000	0.00000
Cr ₂ O ₃	0.00086	0.00086	0.00086	0.00086	0.00086
Na ₂ O	0.19088	0.19087	0.19088	0.19821	0.19823
Li ₂ O	0.00191	0.00180	0.00206	0.00000	0.00000
Na ₂ O	0.19088	0.19087	0.19088	0.19821	0.19823
Li ₂ O	0.00191	0.00180	0.00206	0.00000	0.00000
Na ₂ O	0.19088	0.19087	0.19088	0.19821	0.19823
Lower limit					
function of Na ₂ O	-0.05336	-0.05336	-0.05336	-0.05720	-0.05722
function of P ₂ O ₅	-0.00138	-0.00138	-0.00138	-0.00137	-0.00137
function of CaO	0.08877	0.08878	0.08877	0.09292	0.09292
function of CaO	0.00000	0.00000	0.00000	0.00000	0.00000
function of SO ₃	0.03645	0.03645	0.03645	0.03615	0.03614
function of SO ₃	-0.02079	-0.02079	-0.02079	-0.02068	-0.02068
function of SiO ₂	0.00469	0.00457	0.00498	0.00952	0.00953
Upper limit					
function of Na ₂ O	0.02851	0.02851	0.02851	0.02643	0.02642
function of P ₂ O ₅	0.00234	0.00234	0.00234	0.00235	0.00235
function of CaO	0.28177	0.28178	0.28177	0.28592	0.28592
function of CaO	0.03953	0.03952	0.03952	0.03827	0.03826
function of SO ₃	0.25785	0.25785	0.25785	0.25755	0.25754
function of SO ₃	0.05081	0.05081	0.05081	0.05092	0.05092
function of SiO ₂	0.20729	0.20717	0.20758	0.21212	0.21213
Waste Na₂O loading constraint					
$\hat{g}_{Na_2O(w),j}^{oxide\ in\ MFPV,Step3\ (a)}$	0.181	0.181	0.181	0.188	0.188
Radionuclide Concentration Constraints					
$\hat{a}_{137Cs,j}^{rad\ in\ MFPV,Step3} + k^{rad} \hat{s}_{137Cs,j}^{rad\ in\ MFPV,Step3}$ (Ci/m ³)	0.150	0.150	0.150	0.155	0.154
$SF_{LL,j}^{rad\ in\ MFPV,Step3} + k^{rad} S_{LL,j}^{radSF\ in\ MFPV,Step3}$ (Ci/m ³)	1.678	1.678	1.677	1.733	1.736
$SF_{LL,j}^{rad\ in\ MFPV,Step3} + k^{rad} S_{LL,j}^{radSF\ in\ MFPV,Step3}$	0.04843	0.04877	0.04871	0.04959	0.04972
$SF_{SL,j}^{rad\ in\ MFPV,Step3} + k^{rad} S_{SL,j}^{radSF\ in\ MFPV,Step3}$	0.00039	0.00039	0.00039	0.00041	0.00041

Properties/Constraints	MFPV-B103	MFPV-A104	MFPV-B104	MFPV-A105	MFPV-B105
P^{prop}					
ln(r_B)	0.1422	-0.1863	-0.1915	-0.1829	-0.1819
ln(r_{Na})	0.0021	-0.2200	-0.2241	-0.2170	-0.2163

Properties/Constraints	MFPV-B103	MFPV-A104	MFPV-B104	MFPV-A105	MFPV-B105
$\ln(D)$	2.8639	1.9768	1.9632	1.9922	1.9923
$\ln(\eta_{1100}), u$	4.5914	4.6402	4.6453	4.6356	4.6349
$\ln(\eta_{1150}), l$	4.0982	4.1344	4.1391	4.1301	4.1294
$\ln(\eta_{1150}), u$	4.0982	4.1344	4.1391	4.1301	4.1294
$\ln(\varepsilon_{1100}), l$	-0.9826	-1.2526	-1.2538	-1.2515	-1.2514
$\ln(\varepsilon_{1200}), u$	-0.6371	-0.8745	-0.8755	-0.8736	-0.8734
U_{pred}^{prop}					
$\ln(r_B)$	0.1640	0.1478	0.1482	0.1472	0.1471
$\ln(r_{Na})$	0.1765	0.1510	0.1513	0.1505	0.1505
$\ln(D)$	0.6562	0.6211	0.6240	0.6179	0.6178
$\ln(\eta_{1100}), u$	0.0353	0.0293	0.0294	0.0292	0.0292
$\ln(\eta_{1150}), l$	0.0355	0.0295	0.0296	0.0294	0.0294
$\ln(\eta_{1150}), u$	0.0355	0.0295	0.0296	0.0294	0.0294
$\ln(\varepsilon_{1100}), l$	0.0353	0.0298	0.0299	0.0297	0.0297
$\ln(\varepsilon_{1200}), u$	0.0359	0.0303	0.0304	0.0302	0.0302
U_{comp}^{prop}					
$\ln(r_B)$	0.3660	0.2941	0.3012	0.3048	0.2973
$\ln(r_{Na})$	0.3023	0.2658	0.2724	0.2751	0.2689
$\ln(D)$	1.4159	0.8537	0.8734	0.8787	0.8667
$\ln(\eta_{1100}), u$	0.2575	0.2319	0.2221	0.2282	0.2352
$\ln(\eta_{1150}), l$	0.2425	0.2084	0.2123	0.2148	0.2101
$\ln(\eta_{1150}), u$	0.2378	0.2131	0.2052	0.2098	0.2168
$\ln(\varepsilon_{1100}), l$	0.1789	0.1701	0.1641	0.1689	0.1719
$\ln(\varepsilon_{1200}), u$	0.1645	0.1480	0.1521	0.1539	0.1519
$B_{ucci,lcci}^{prop}$					
$\ln(r_B)$	0.6722	0.2556	0.2579	0.2690	0.2626
$\ln(r_{Na})$	0.4809	0.1967	0.1996	0.2086	0.2030
$\ln(D)$	4.9359	3.4515	3.4606	3.4888	3.4768
$\ln(\eta_{1100}), u$	4.8841	4.9014	4.8968	4.8931	4.8993
$\ln(\eta_{1150}), l$	3.8202	3.8964	3.8973	3.8859	3.8899
$\ln(\eta_{1150}), u$	4.3715	4.3770	4.3739	4.3694	4.3757
$\ln(\varepsilon_{1100}), l$	-1.1969	-1.4526	-1.4478	-1.4501	-1.4529
$\ln(\varepsilon_{1200}), u$	-0.4367	-0.6962	-0.6929	-0.6895	-0.6913
Model validity single component constraints					
Al_2O_3	0.06123	0.06120	0.06121	0.06123	0.06121
Cl	0.00142	0.00126	0.00126	0.00126	0.00126
Cr_2O_3	0.00086	0.00086	0.00086	0.00086	0.00086
F	0.00081	0.00073	0.00073	0.00073	0.00073
P_2O_5	0.00203	0.00189	0.00189	0.00189	0.00189
SiO_2	0.44618	0.45652	0.45660	0.45645	0.45642
Sum of Minors	0.00051	0.00052	0.00052	0.00052	0.00052
Model validity PCT constraints					
$P^{pctB} (\ln[g/L])$	0.1422	-0.1863	-0.1915	-0.1829	-0.1819
$P^{pctNa} (\ln[g/L])$	0.0021	-0.2200	-0.2241	-0.2170	-0.2163

Properties/Constraints	MFPV-B103	MFPV-A104	MFPV-B104	MFPV-A105	MFPV-B105
Model validity multiple component constraints					
Li ₂ O	0.00000	0.00596	0.00587	0.00607	0.00607
Cr ₂ O ₃	0.00086	0.00086	0.00086	0.00086	0.00086
Na ₂ O	0.19823	0.17078	0.17079	0.17077	0.17078
Li ₂ O	0.00000	0.00596	0.00587	0.00607	0.00607
Na ₂ O	0.19823	0.17078	0.17079	0.17077	0.17078
Li ₂ O	0.00000	0.00596	0.00587	0.00607	0.00607
Na ₂ O	0.19823	0.17078	0.17079	0.17077	0.17078
Lower limit					
function of Na ₂ O	-0.05721	-0.04284	-0.04284	-0.04283	-0.04284
function of P ₂ O ₅	-0.00137	-0.00140	-0.00140	-0.00140	-0.00140
function of CaO	0.09291	0.07162	0.07163	0.07161	0.07162
function of CaO	0.00000	0.00000	0.00000	0.00000	0.00000
function of SO ₃	0.03614	0.03753	0.03752	0.03753	0.03753
function of SO ₃	-0.02068	-0.02116	-0.02116	-0.02116	-0.02116
function of SiO ₂	0.00955	-0.00418	-0.00428	-0.00408	-0.00404
Upper limit					
function of Na ₂ O	0.02642	0.03421	0.03421	0.03422	0.03422
function of P ₂ O ₅	0.00235	0.00231	0.00231	0.00231	0.00231
function of CaO	0.28591	0.26462	0.26463	0.26461	0.26462
function of CaO	0.03827	0.04473	0.04472	0.04473	0.04473
function of SO ₃	0.25754	0.25893	0.25892	0.25893	0.25893
function of SO ₃	0.05092	0.05044	0.05044	0.05044	0.05044
function of SiO ₂	0.21215	0.19842	0.19832	0.19852	0.19856
Waste Na₂O loading constraint					
$\hat{g}_{Na_2O(w),j}^{oxide\ in\ MFPV,Step3\ (a)}$	0.188	0.162	0.162	0.162	0.162
Radionuclide Concentration Constraints					
$\hat{a}_{137Cs,j}^{rad\ in\ MFPV,Step3} + k^{rad} \hat{s}_{137Cs,j}^{rad\ in\ MFPV,Step3}$ (Ci/m ³)	0.154	0.149	0.149	0.149	0.149
$SF_{LL,j}^{rad\ in\ MFPV,Step3} + k^{rad} S_{LL,j}^{radSF\ in\ MFPV,Step3}$ (Ci/m ³)	1.734	1.578	1.576	1.581	1.578
$SF_{LL,j}^{rad\ in\ MFPV,Step3} + k^{rad} S_{LL,j}^{radSF\ in\ MFPV,Step3}$	0.04957	0.04835	0.04814	0.04840	0.04855
$SF_{SL,j}^{rad\ in\ MFPV,Step3} + k^{rad} S_{SL,j}^{radSF\ in\ MFPV,Step3}$	0.00041	0.00037	0.00037	0.00037	0.00037

(a) It was assumed that the waste in the A11th, B11th, and A12th CRV were designated as Envelope A and had the fraction of sodium that is classified as waste sodium (ω_{A11}) was 95%.

Appendix C–Summary of Data Requirements

Table C-1. Assumptions to be Reviewed Before Final Algorithm is Complete

Description	Current Assumptions	Status
1. Glass property models	Models for PCT, VHT, viscosity, and electrical conductivity are from Piepel et al. 2007. Model coefficients are listed in Tables 5 through 8. Model forms are given by Equations (19), (22), (23), and (24). Model variance-covariance matrices are in Tables A-7 through A-11 and glass component concentration and property ranges for model validity are given in Tables 11 through 13.	No specific verification or testing needs are associated with the use of these models.
2. GFC composition, uncertainty in GFC composition, and GFC particle density	The minimum, most likely, and maximum component mass fraction values are given in Table A-4. Particle densities are given in Table A-12. Data listed in Table A-4 were used to define the uncertainty for the GFC composition based on PERT distribution. The nominal GFC composition in Table A-5 was obtained by Monte Carlo simulations and used for nominal glass composition calculation. These data are based on the initial GFC vendor certifications obtained during characterization testing (Schumacher 2003).	Eventually the algorithm will use data for the specific materials used in each MFPV batch. A decision needs be made on how to obtain these data for each material. Two possible options are: (1) use the vendor certifications supplied by the vendors for each material, or (2) measure the composition and particle density at WTP.
3. Melter retention factors and uncertainty of melt retention factors	Table A-3 lists the preliminary melter retention factors expressed as ln(DF) in terms of minimum, most likely, and maximum values for uncertainty expression by PERT distribution (24590-LAW-RPT-RT-11-001, Rev 0).	The melter retention factors and recycle effects should be updated as more data become available and may need to be expressed as a function of glass and feed compositions for selected components.
4. RSD in chemical and radiological analyses of CRV batches	Table A-2 lists constants and uncertainty values used in the calculations showing how the algorithm works. These values were based on CCN 111456. Other assumptions for components not listed in CCN 111456 are summarized in Table A-2.	A plan should be developed and implemented to establish a maximum acceptable analytical uncertainty before methods validation in order to demonstrate that the methods meet an established requirement.
5. RSD in mixing/sampling and RSD for bias correction of mixing and sampling in CRV batches	RSD in mixing/sampling is assumed as 1.47% for all components (Table A-2) without bias correction as recommended by 24590-LAW-RPT-RT-11-001, Rev 0.	A plan should be developed and implemented to establish a maximum acceptable mixing/sampling uncertainty before methods validation in order to demonstrate that the methods meet an established requirement.
6. CRV and MFPV volumes	CRV volumes are from 24590-LAW-M6C-LCP-00001, Rev 1 and MFPV volumes are from 24590-LAW-M6C-LFP-00001, Rev 1 as given in Table 1.	The vessel volumes will be updated upon any design change.

Description	Current Assumptions	Status
7. SD in GFC mass measurement	Appendix E discusses the method obtaining the SD values based on the load cell data and weigh hopper information. For the purpose of this preliminary algorithm it was assumed that the Mettler Toledo's Centerlign Weigh Module model 744 (for 250 lb capacity) and 745 (for 500 lb capacity) are used.	The calculation process should be updated as necessary once the equipments are finalized.
8. SD in waste transfer volume measurement	Appendix D discusses the approach taken to obtain the SD values for waste transfer volume measurement based on a recommended value of 1.41 inches for the level measurement uncertainty given in 24590-LAW-RPT-RT-11-001, Rev 0.	The level measurement uncertainty used in the algorithm should be compared to the uncertainty from actual plant equipment to verify proper representation in the algorithm.
9. Dust control water volume estimate	Equation (58) specifies 4 wt% water addition based on 24590-LAW-M4C-20-00002, Rev 0.	The validity of the Equation (58) may need to be tested to meet engineering requirements.
10. Line flush water volumes	Line flush and wash water volumes applicable to ILAW algorithm are summarized in Table 14. These values are based on project line flush volume guidance.	Line flush volumes will be updated as relevant engineering documents and operating procedures are modified.
11. Sucrose volume calculation	Equation (34) prescribes the amount of sucrose to add to HLW and LAW melter feed based on the concentrations of organic carbon, nitrate, and nitrite in the feed. This relationship was empirically derived from pilot melter testing and is used to avoid melter upsets due to over oxidation of multivalent elements (Matlack 2005). No attempt to optimize reductant addition to improve melting parameters (such as volatility, metal reduction, and feed processing rate) has yet been performed.	No testing or verification is required until optimization is needed.
12. Confidence level in satisfying various constraints	90% confidence level is used for all properties as discussed in Section 4.3.4.	No testing or verification is required. Values may need to be updated by project management decision.
13. Software for implementing the algorithm described in this report	The calculations described in this report have been demonstrated using an Excel™ with a RiskAMP™ add-in. However, the use of that system will likely not suit the requirements of plant operation. No software has yet been developed.	Software development, validation, and verification will be required prior to implementation of this algorithm.

Description	Current Assumptions	Status
15. Methods/software to be used for statistical process control (SPC)	Statistical process control is a useful tool that should be incorporated into the formulation decision making as described in Sections 5.2, 6.2, and 6.4. As SPC software to meet the highlighted purposes is a common, of the shelf, product and it was not developed as part of the algorithm equations. However, to meet the functions described, such software must be selected and integrated into the algorithm.	No testing or verification is envisioned outside of software selection, validation, and verification activities. The notification values will be set by management decision.

Table C-2. Data and Inputs Required During Operations: 1. Inputs Required on an Every Batch Basis

Symbol	Brief Description	Anticipated Source
$c_{id}^{element\ in\ CRV}$	Concentration of the i^{th} analyte in the d^{th} CRV batch (mg/L)	Analytical laboratory
$M_{kj}^{GFC\ in\ MFPV,\ measured}$	Measured mass of k^{th} GFC added to the j^{th} MFPV batch (g)	LAW operator
$V_j^{heel\ MFPV}$	MFPV heel volume in the j^{th} MFPV batch (L)	LAW operator
$V_j^{waste\ MFPV}$	volume of waste transferred from CRV to the j^{th} MFPV (L)	LAW operator
$V_j^{dust\ MFPV,\ measured}$	measured volume of water added to control GFC dusting in the j^{th} MFPV batch (L)	LAW operator
$V_j^{transflush\ MFPV,\ measured}$	measured volume of water used to flush the CRV-MFPV transfer line in the j^{th} MFPV batch (L)	LAW operator
$V_j^{sampflush\ MFPV,\ measured}$	measured volume of water used to flush the MFPV sampling line in the j^{th} MFPV batch (L)	LAW operator
$V_j^{dilute\ MFPV,\ measured}$	measured volume of dilution water added to maintain satisfactory melter-feed rheological properties in the j^{th} MFPV batch (L)	LAW operator
Envelop	Type of LAW, A, B, or C	LAW operator
ω_d	Fraction of the sodium in the d^{th} CRV batch that is classified as waste sodium (unitless)	LAW operator

Table C-3. Data and Inputs Required During Operations: 2. Inputs Required Only When Process Changes are Made

Symbol	Brief Description	Anticipated Source
No symbol	Parameters for statistical process monitoring	LAW operations manager
$V_j^{dust\ MFPV}$	volume of water added to control GFC dusting in the j^{th} MFPV batch (L)	LAW operations manager
$m_{ik}^{oxides\ in\ GFC}$	Mass fraction of the i^{th} glass oxide in the k^{th} GFC (g oxide per g GFC including volatiles)	GFC vendor or analytical laboratory
$V_j^{transflush\ MFPV}$	Volume of water used to flush the CRV-MFPV transfer line in the j^{th} MFPV batch (L)	LAW operations manager
$V_j^{sampflush\ MFPV}$	Volume of water used to flush the MFPV sampling line in the j^{th} MFPV batch (L)	LAW operations manager
CL%=100(1- α)	Level of confidence in meeting predicted property constraints, may be different for different properties	LAW operations manager
RSD in $c_{id}^{element\ in\ CRV}$	RSD in concentration of the i^{th} analyte in the d^{th} CRV batch (mg/L)	LAW operations manager

Appendix D—Uncertainties for Waste Transfer Volume Measurements

Appendix D–Uncertainties for Waste Transfer Volume Measurements

The MFPV and CRV vessel volumes will be obtained from the radar level measurements. The volume of waste transferred from CRV to MFPV ($V_j^{waste\ MFPV}$) is determined based on the volume change in MFPV (24590-LAW-3YD-LFP-00001, Rev 2), i.e.,

$$V_j^{waste\ MFPV} = \Delta V_j^{MFPV} \tag{D-1}$$

where $V_j^{waste\ MFPV}$ = measured volume of the waste transferred from the CRV to the j^{th} MFPV (L).

ΔV_j^{MFPV} = volume change in the j^{th} MFPV after waste transfer from the CRV (L)

The SD for MFPV volume measurement is calculated from the SD for MFPV level measurement:

$$s^{MFPV\ V} = \pi \left(\frac{D^{MFPV}}{2} \right)^2 s^{MFPV\ level} \tag{D-2}$$

where $s^{MFPV\ V}$ = SD for MFPV volume measurement (L)

D^{MFPV} = inside diameter of MFPV vessel (cm)

$s^{MFPV\ level}$ = SD for MFPV level measurement (L)

The SD for waste transfer is calculated from error propagation of two volume measurements:

$$s_j^{waste\ MFPV} = \sqrt{2} s^{MFPV\ V} \tag{D-3}$$

where $s_j^{waste\ MFPV}$ is SD for measured volume of the waste transferred from the CRV to the j^{th} MFPV (L), which is a constant for all MFPV batches.

Table D-1 summarizes the calculation of SD for MFPV volume change. Table D-1 also includes the results of the same calculation for CRV volume for reference.

Table D-1. Calculation of SD for MFPV and CRV Volume Changes

Item	MFPV	CRV	Notes
Inside diameter of vessel, ft	11 (335.28 cm)	14 (426.72 cm)	24590-LAW-M6C-LFP-00001, Rev. 1 24590-LAW-M6C-LCP-00001, Rev. 1
Level measurement SD, inch	1.41 (3.581 cm)	1.41 (3.581 cm)	24590-LAW-RPT-RT-11-001, Rev 0
Volume measurement SD, L	316.2	512.2	Calculated from level measurement SD
Volume change SD, L	447.2	724.3	Corresponding to two volume measurements

Appendix E—Uncertainties for GFC Mass Measurements

Appendix E–Uncertainties for GFC Mass Measurements

Measurements of GFC masses will be done using the load cells in the weigh hopper. According to 24590-BOF-3YD-GFR-00001, Rev 0, the weighing of GFCs will be done in 5 weigh hoppers. Four of these 5 weigh hoppers have a capacity of 10 ft³ and one hopper 3 ft³. As summarized in Table E-1 four GFCs (hematite, olivine, rutile, and zircon) use 3 ft³ hopper and the rest uses the 10 ft³ hopper.

The exact models for load cells are not finalized, but the product from one of the candidate vendors was assumed for the purpose of this preliminary algorithm. The calculation process should be updated as necessary once the equipments are finalized. The mass capacity that can be measured in each hopper depends on bulk density of each GFC. Table E-2 summarizes the bulk density of GFC for ILAW production, which was obtained from Schumacher (2003). Based on volume capacity of each hopper and average and maximum density of GFC, the mass of each GFC per each hopper measurement is calculated in Table E-1. Table E-1 shows that the maximum expected mass is 1011 lb for the 10 ft³ hopper (Kyanite) and 465 lb for 3 ft³ hopper (Zircon). Each weigh hopper consists of three load cells of equal capacity and the final mass of each measurement is obtained by summing up three load cell readings. Then, based on maximum weight capacity reacquired given in Table E-1 and the models available for the selected candidate vendor assumed in this report, it was assumed that the 10 ft³ hopper uses three 500 lb capacity load cell models and 3 ft³ hopper three 250 lb models to provide 1500 and 750 lb capacity weigh hoppers as summarized in Table E-1.⁽¹⁹⁾

Table E-1. Weight Capacity of Weigh Hoppers

GFC/Sucrose	Weigh hopper volume, ft ³	Weight capacity (Average bulk density base), lb	Max Weight capacity (Maximum bulk density base), lb	Assumed weight capacity of weigh hopper, lb
Kyanite	10	886.5	1011	1500
Boric Acid	10	569.0	590	1500
Wollastonite	10	676.5	768	1500
Hematite	3	377.3	422.7	750
Li Carbonate	10	670.0	722	1500
Olivine	3	288.6	293.7	750
Na Carbonate	10	669.0	675	1500
Silica	10	790.0	889	1500
Rutile	3	368.3	405.6	750
Zincite	10	543.0	661	1500
Zircon	3	415.2	464.7	750
Sucrose	10	550.5	559	1500

Table E-2. Bulk Density of GFCs and Sucrose

GFC/Sucrose	Min	Max	Average
Kyanite	76.2	101.1	88.65
Boric Acid	54.8	59	56.9
Wollastonite	58.5	76.8	67.65

⁽¹⁹⁾ For the purpose of this preliminary algorithm it was assumed that the Mettler Toledo’s Centerlign Weigh Module model 744 (for 250 lb capacity) and 745 (for 500 lb capacity) are used.

GFC/Sucrose	Min	Max	Average
Hematite	110.6	140.9	125.75
Li Carbonate	61.8	72.2	67
Olivine	94.5	97.9	96.2
Na Carbonate	66.3	67.5	66.9
Silica	69.1	88.9	79
Rutile	110.3	135.2	122.75
Zincite	42.5	66.1	54.3
Zircon	121.9	154.9	138.4
Sucrose	54.2	55.9	55.05

A brief review of the example MFPV batch formulations shows that the required mass of most GFCs would require multiple measurements to measure each GFC for a single MFPV batch. Therefore, the uncertainty related to the mass of each GFC added to the MFPV are calculated using the error propagation method described in Piepel et al. (2005) (Section 3.4.1.1).

First the SD is calculated for each weigh hopper using⁽²⁰⁾:

$$s_{weigh}^{WH} = \sqrt{3 \left(\frac{2}{3} SPC_{CE}^2 + SPC_{NR}^2 \right)} \tag{E-1}$$

where s_{weigh}^{WH} = standard deviation for weigh hopper weight measurement (kg)
 SPC_{CE} = specification for combined error (CE) as given in the data sheet for each load cell. Includes linearity and hysteresis errors. (kg)
 SPC_{NR} = specification for non-repeatability (NR) as given in the data sheet for each load cell (kg)

The SPC_{CE} and SPC_{NR} values are obtained by multiplying the combined error or non-repeatability error given in percent of full scale output (%FSO) by the full scale of each load cell.

The SD for weighing each GFC depends on the number of weighing required for each MFPV batch. For Step 3 of glass formulation algorithm, the SD for weighing is given as:

$$s_k^{GFC\ mass\ MFPV} = \sqrt{n_{kj}^{GFC\ weigh} \left[(s_{weigh}^{WH})^2 + (s_{control}^{WH})^2 \right]} \text{ for Step 1} \tag{E-2}$$

$$s_k^{GFC\ mass\ MFPV} = s_{weigh}^{WH} \sqrt{n_{kj}^{GFC\ weigh}} \text{ for Step 3} \tag{E-3}$$

where $s_{kj}^{GFC\ mass\ MFPV}$ = standard deviation of weighing the k^{th} GFC in the j^{th} MFPV batch
 $n_{kj}^{GFC\ weigh\ MFPV}$ = number of weighing required for the k^{th} GFC in the j^{th} MFPV batch

⁽²⁰⁾ Reichmuth A. 2000. *Estimating Weighing Uncertainty from Balance Data Sheet Specifications*, Mettler Toledo, Columbus, OH. (available at www.mt.com)

S_{weigh}^{WH} = standard deviation for weigh hopper weight measurement (kg)
 $S_{control}^{WH}$ = standard deviation for target mass control in weigh hopper weight measurement (kg) (to be obtained after testing the plant equipment installed)

For Step 3, the $n_{kj}^{GFC\ weigh\ MFPV}$ is the actual number, however, for Step 1 the number of weighing is calculated based on the weighing mass capacity of weigh hopper as below:

$$n_{kj}^{GFC\ weigh\ MFPV} = \text{truncate} \left(\frac{M_{kj}^{GFC\ in\ MFPV, target, Step1}}{M_k^{WH\ capa}} \right) + 1 \tag{E-4}$$

where $n_{kj}^{GFC\ weigh\ MFPV}$ = number of weighing required for the k^{th} GFC in the j^{th} MFPV batch
 $M_{kj}^{GFC\ in\ MFPV, target, Step1}$ = target mass of k^{th} GFC to add to the j^{th} MFPV batch resulted from algorithm calculation Step 1 (g)
 $M_k^{GFC\ mass\ WH\ capa}$ = mass capacity of the weigh hopper for the k^{th} GFC

Appendix F–GFC and Sucrose Volume Contributions

Appendix F–GFC and Sucrose Volume Contributions

The calculation of volume contribution from GFCs in Equation (56) assumes ideal mixing between waste slurry and GFC particles, i.e.

$$V^{slurry} = V^{water} + \sum_{k=1}^n \frac{M_k^{GFC}}{\rho_k^{GFC}} \quad (F-1)$$

where V^{slurry} = calculated volume of slurry (L)
 V^{water} = volume of water (L)
 M_k^{GFC} = mass of the k^{th} GFC (g)
 ρ_k^{GFC} = density of the k^{th} GFC (g/L) (Table F-1)

However, the actual slurry volume will be different from that calculated based on ideal mixing because: (1) dissolution of water soluble materials tends to decrease the volume of slurry and (2) entrapment of small bubbles on the surface of solid particles would increase the slurry volume.

To evaluate the difference between calculated and actual slurry volumes, existing data on measured density of slurry feeds was evaluated. Table F-2 includes the feed recipes for GFCs, sucrose, and spiking chemicals in terms of added masses per 1 liter of waste simulant and target density of waste simulant and measured density of slurry feed. The waste oxide loading in glass for each feed is also included in Table F-2 for information. The target density of waste simulant and measured density of slurry feed data are used to obtain the “measured” volume of slurry feed.

$$V_{meas}^{slurry} = \frac{\rho^{waste\ simul} \times 1\ L + \sum_{k=1}^n M_k^{additives}}{\rho^{feed}} \quad (F-2)$$

The “calculated” volume of slurry feed is from Equation (F-1).

$$V_{calc}^{slurry} = 1\ L\ (waste\ simul) + \sum_{k=1}^n \frac{M_k^{additives}}{\rho_k} \quad (F-3)$$

where V_{meas}^{slurry} = “measured” slurry volume obtained from target density of waste simulant and measured density of slurry feed (L)
 $\rho^{waste\ simul}$ = target density of waste simulant (g/L)
 $M_k^{additives}$ = mass of the k^{th} additive (GFCs, sucrose, and spiking chemicals) per 1 L of waste simulant (g)
 ρ^{feed} = measured density of slurry feed (g/L)
 V_{calc}^{slurry} = “calculated” slurry volume based on ideal mixing between waste simulant and additives (L)
 ρ_k = density of the k^{th} additive (GFCs, sucrose, and spiking chemicals) (g/L) (Table F-1)

Table F-2 shows the “measured” and “calculated” volumes of slurry feed and their relative percent difference for each feed. The difference ranged from -1.5% (underestimation) to 3.3 % (overestimation) with more feeds overestimating, which suggest that within limited data the deviation of calculated slurry feed volume from actual is relatively small. As discussed in Section 5.2, the allowable volume increase before the “High Operator Response” was 3,331 L. A half of this 3,331 L was used for allowable feed volume increase caused by accidentally increased waste transfer volume leaving the room for calculation errors. The GFC volume contribution is expected to be the main source of error in calculating the total feed volume. The room of 1,666 L corresponds to 12.9 % of the MFPV batch volume (12,870 L), which sufficiently higher than the range of differences between -1.5 and 3.3 %.

Table F-1. Particle Density of GFCs, Sucrose and Spiking Chemicals

GFC or other additives^(a)	Particle density, g/L
Kyanite	3398.3
Boric Acid	1509.3
Wollastonite	2899.3
Hematite	4747.9
Lithium Carbonate	2109.6
Olivine	2948.2
Sodium Carbonate	2532.5
Silica	2649.5
Rutile	4647.8
Zincite	5596.9
Zircon	4701.4
Sucrose	1549.0
Na ₂ SO ₄ (spiking chemical)	2680.0
NaCl (spiking chemical)	2165.0
NaF (spiking chemical)	2780.0
KI (spiking chemical)	3670.0

(a) Densities of GFCs and sucrose are as given in Table A-12. Densities of spiking chemicals were obtained from Alfa Aesar® brochure.

Table F-2. Data Collected for Various Slurry Feeds and Estimated Slurry Feed Volumes

Feed ID	3M Na LAW	8 M Na NaNO ₃	Envelope A1	Envelope C1	Envelope A2	Envelope B1	Envelope B2	Envelope A3	Envelope C2
GFC and other chemicals ^(a) Data source	Eibling et al. 2003		Matlack et al. 2003a		Matlack et al. 2003b		Matlack et al. 2003c	Matlack et al. 2003d	
Kyanite	35.67	95.12	35.84	145.92	99.98	156.10	148.9	67.53	128.48
Boric Acid	87.65	233.74	200.17	233.04	238.52	282.85	252.9	233.43	224.71
Wollastonite	21.16	56.42	52.48	138.63	59.77	236.73	211.7	139.26	205.71
Fe ₂ O ₃	27.21	72.55	81.90	63.38	72.18	75.82	67.9	66.79	43.65
Li Carbonate	-	-	-	80.79	-	170.61	152.4	80.93	107.74
Olivine	15.50	41.33	52.09	40.98	41.46	95.57	85.2	38.29	41.53
Na Carbonate	-	-	-	-	-	-	61.1	-	-
SiO ₂	183.63	489.68	470.39	431.63	490.66	516.51	460.2	465.38	427.26
Rutile	10.52	28.05	25.95	15.51	28.82	23.52	21.0	15.46	14.79
ZnO	14.99	39.97	36.88	39.61	40.18	76.96	69.0	39.85	53.00
ZrSiO ₄	22.67	60.45	55.63	58.50	61.07	75.89	68.0	58.88	59.64
Sucrose	-	-	78.50	4.65	83.66	24.55	8.0	63.85	23.66
Na ₂ SO ₄ (spiking chemical)	-	-	0.85	1.74	1.47	5.60	5.0	1.30	2.25
NaCl (spiking chemical)	-	-	12.93	1.54	5.08	0.24	0.1	9.01	4.51
NaF (spiking chemical)	-	-	0.02	1.55	1.71	0.46	0.1	0.30	0.54
KI (spiking chemical)	-	-	-	-	1.78	2.08	1.9	1.69	1.72
Target density of waste simulant, g/L	1157.6	1390	1358.94	1256.95	1381.06	1125.48	1065.09	1292.43	1245.07
Measured density of slurry feed, g/L	1382.0	1713.0	1714.3	1673.3	1730.0	1705.0	1690.0 ^(b)	1692.5	1692.5
Waste oxide loading in glass, wt%	-	-	26.04	15.62	24.54	6.71	4.01	18.84	13.95
Estimated Slurry Volumes									
Based on measured slurry density, L	1.141	1.466	1.436	1.503	1.507	1.683	1.585	1.521	1.527
Calculated from GFCs/chemicals densities, L	1.166	1.442	1.455	1.501	1.507	1.693	1.637	1.533	1.537
RPD between “measured” and “calculated”, %	2.2	-1.5	1.3	-0.1	0.0	0.6	3.3	0.8	0.7

“-” represents empty data field

RPD: relative percent difference, $([\text{calculated}] - [\text{measured}])/[\text{measured}]$

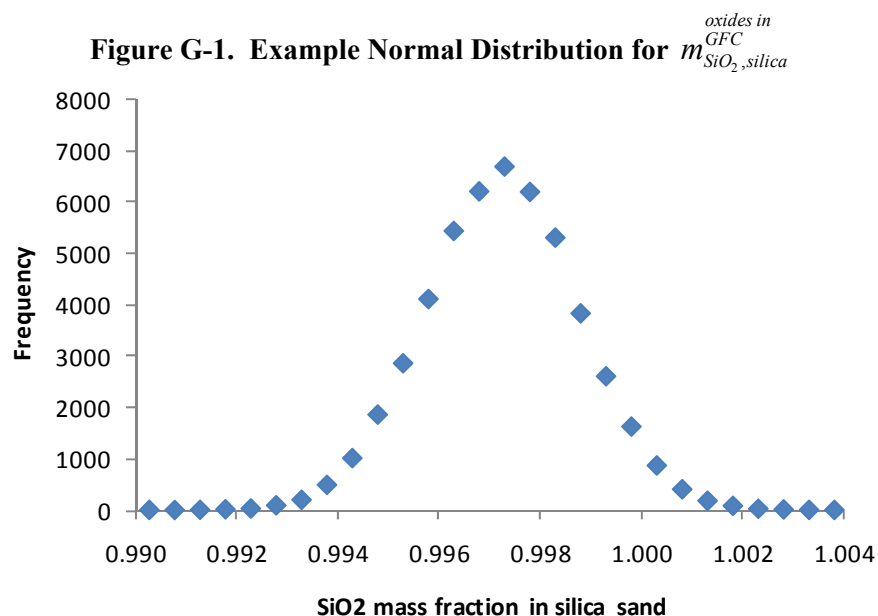
(a) Given as g per 1 L waste simulant for GFC, sucrose, and spiking chemicals.

(b) For Envelop B2 feed, target value is given because measured data is not available.

Appendix G—PERT Distribution

Appendix G—PERT Distribution

For GFC composition ($m_{ik}^{oxides\ in\ GFC}$), values outside of 0 and 1 are not physically meaningful. This precludes the use of normal distribution for some GFC compositions which can yield a significant fraction of the distribution outside of this range. As an example, silica sand has a most likely (or mean) SiO₂ concentration of 0.997, minimum of 0.992, and maximum of 0.999 (Table A-4). The SD value was estimated as 0.0015 as described in Piepel et al. (2005). Figure G-1 shows an example normal distribution (for $m_{SiO_2, silica}^{oxides\ in\ GFC}$) that yields a fraction of the data greater than 1. In addition, the normal distribution gives a symmetric distribution for skewed data.



To address these concerns a PERT distribution was selected for use in the formulation algorithm. Figure G-2 shows an example PERT distribution for $m_{SiO_2, silica}^{oxides\ in\ GFC}$. PERT distribution was also applied to ln(DF) to calculate the retention factor (v_i).

The following description borrowed heavily from RiskAmp[®] software; exact quotes are italicized in this section. *The PERT distribution uses the minimum, most likely, maximum, and potentially a scale parameter. Depending on the values provided, the PERT distribution can provide a close fit to the normal or lognormal distributions. Like the triangular distribution, the PERT distribution emphasizes the "most likely" value over the minimum and maximum estimates. However, unlike the triangular distribution the PERT distribution constructs a smooth curve which places progressively more emphasis on values around (near) the most likely value, in favor of values around the edges.* Figure G-3 shows examples of the PERT distribution with symmetric and asymmetric “most likely” or median values.

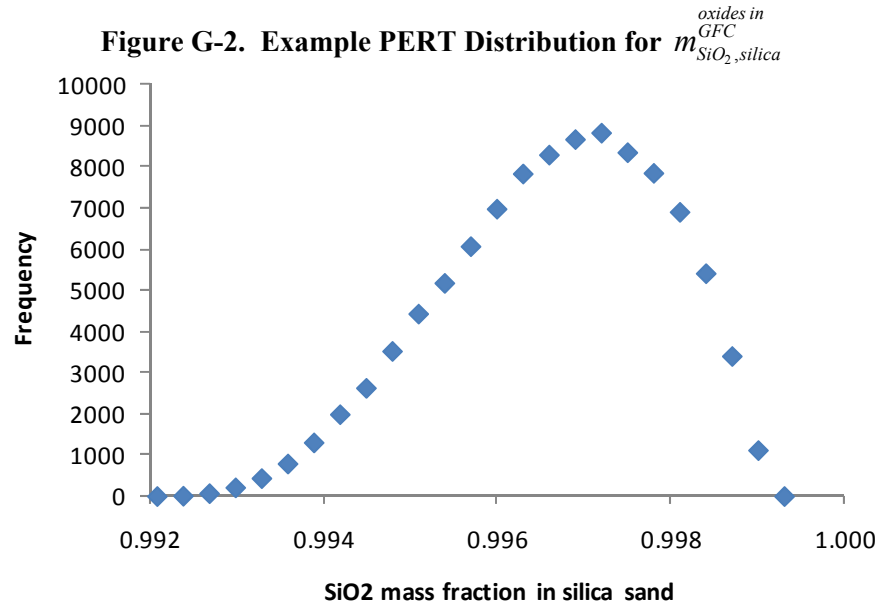
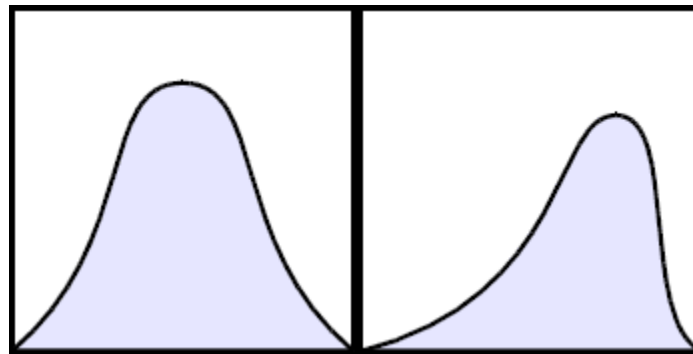


Figure G-3. Examples of the PERT distribution



The PERT distribution is given by the following function:

$$F(x) = \begin{cases} B_x(v, w) / B(v, w) & \rightarrow 0 \leq x \leq 1 \\ 0 & \rightarrow otherwise \end{cases} \quad (G-1)$$

where

$$B(v, w) \equiv \int_0^1 t^{v-1} (1-t)^{w-1} dt \text{ and } B_x(v, w) \equiv \int_0^x t^{v-1} (1-t)^{w-1} dt. \quad (G-2)$$

The PERT distribution uses the mode or most likely parameter to generate the shape parameters v and w . An additional scale parameter λ scales the height of the distribution; the default value for this parameter is 4.

In the PERT distribution, the mean (μ) is calculated

$$\mu = \frac{x_{\min} + x_{\max} + \lambda x_{\text{mode}}}{\lambda + 2} \quad (\text{G-3})$$

and used to calculate the v and w shape parameters

$$v = \frac{(\mu - x_{\min})(2x_{\text{mode}} - x_{\min} - x_{\max})}{(x_{\text{mode}} - \mu)(x_{\max} - x_{\min})} \quad \text{and} \quad w = \frac{v(x_{\max} - \mu)}{\mu - x_{\min}} \quad (\text{G-4})$$

which are used, with the minimum and maximum scale parameters, to sample the beta distribution. For more information and a more detailed analysis, see for example, Vose 2000. The PERT distribution gives realistic responses that strongly favor the “expected value” and smoothly vary to the range of measured values without exceeding the minimum or maximum. In order to implement the PERT distribution the required values are the minimum, maximum, and most likely value (or mode). The scaling factor (λ) can be used to adjust the height to width of the distribution, but, are not used in this report and will not be discussed in this context.